THE UNIVERSITY
of EDINBURGH

Modulation of innate cells by helminth infection and helminth derived products

Fumi K. Varyani

Thesis submitted for degree of Doctor of Philosophy

The University of Edinburgh

2018

Declaration

I am aware of and understand the university's policy to plagiarism. I declare that this thesis has been composed by myself, describes my own work except where indicated and that the work has not been submitted towards any other degree.

Some paragraphs and tables outlined in Chapter 3 has been previously published as a review in AJP of the "Helminths in the gastrointestinal tract as modulators of immunity and pathology" authored by F Varyani, J Fleming and R Maizels (Varyani et al., 2017).

Additional contributions include help from my colleagues in the Maizels' lab: Dr S Loeser has conducted many of the experiments alongside myself and has taken all BAL and lung samples; Dr M White has undertaken fluorescent electronic sorting and IVs in a rescue experiment; Dr C Druery has undertaken the organoid experiments mentioned in the thesis; Ms N Britton has done some of the qRT-PCR work. CXCR2-deficient mice have been obtained from Professor Gerry Graham at the University of Glasgow, the s100a9-deficient mice have been obtained from Dr Robert Gray at the University of Edinburgh. Initial *N.brasiliensis* parasitology in MIF-deficient mice has been performed by Ms Y Harcus. Figure 4.2.1 has been obtained from Dr K.Filbey's thesis and provides context to the subsequent experiments performed. I would also like to mention Dr F Gerbe from the Jay group in Montpellier who has performed much of the epithelial cell stainings. I declare that I have contributed to a large proportion of the work outlined, designed all the experiments and have performed all of the analysis of the experimental data.

Acknowledgements

This thesis is dedicated to my beloved daughter, Nina. Thanks to Rick Maizels' entire lab, for supporting me through my 3 year PhD, providing detailed guidance and support throughout all my experiments. In particular thanks to Dr Stephan Loeser, who has taught me how to drill down the important questions required for a scientific story, as well as providing much practical help.

Thesis Abstract

Helminth infection affects around a quarter of people worldwide, with no effective vaccines available. Future vaccines against helminth infection will require a more precise understanding of the cellular and molecular basis of protective immunity. In addition, it is notable that the prevalence of allergic and autoimmune diseases has increased, whilst that of helminths infections has reduced. This suggested that immune responses are dampened through direct immunomodulation by helminths infections or their excretory secretory products.

Based on initial observations that *Heligmosomoides polygyrus* excretory secretory products (HES) can improve disease scores in a chronic T cell induced colitis, we explored the role of (HES) in an innate RAG-/- CD40 colitis. We found that HES did not affect inflammatory scores and disease activity in this model of colitis, however reduced the infiltration of inflammatory cells into the peritoneum.

Immunity to intestinal helminth *Nippostrongylus brasiliensis* and *H. polygyrus* requires innate and adaptive mechanisms co-ordinated through the Type 2 IL-4R/STAT6-dependent pathway. We have now found that macrophage migration inhibitory factor (MIF) is also essential for development of immunity

to infection. MIF-deficient mice are slower to expel *N. brasiliensis*, while in wildtype animals, the expression of MIF is upregulated in macrophages in response to infection.

Cellular analyses in the MIF-deficient mice demonstrate reduced recruitment of innate lymphoid cells, eosinophils and alternatively activated macrophages. Type 2 epithelial responses were reduced in the mice showing reduced tuft cell hyperplasia and almost absent RELM-ß protein in goblet cells.

In order to assess if this was a developmental abnormality, we administered 4-IPP, an inhibitor of MIF to infected wild type mice. Mice receiving 4-IPP were unable to expel parasites and demonstrated similar cellular and epithelial responses as the MIF-deficient mice. IL-25 has been shown to accelerate expulsion of *N.brasiliensis* via the recruitment of ILC2s. Administration of rIL-25 is able to completely rescue the MIF-deficient cellular and epithelial cell phenotype. The ligands for MIF are hypothesised to be CXCR2, CXCR4 and CD74. We demonstrate that ILCs and macrophages express CXCR4. CXCR2-deficiency did not result in the epithelial cell phenotype, therefore it is unlikely that MIF is acting via CXCR2 in the gut. A deficiency of CXCR2 however, altered the immune response to *N. brasiliensis* in the lung with reduced alternative activation of macrophages.

In parallel, we assessed the immune responses in *H. polygyrus*. From previous work, we know that MIF-deficient mice are less able to expel *H. polygyrus* primary infection, and in addition, do not mount protective secondary immune responses or protective responses to immunisation with HES. We found no difference in the percentage of Foxp3 positive T regulatory cells or HES specific antibody levels. As in the *N. brasiliensis* model, MIF-deficient mice produced fewer alternatively activated macrophages confirming a defect in the innate immune compartment. A microarray had previously been performed comparing BALB/c and MIF-

deficient duodenum, finding genes *arl2bp*, *phc2* and *s100a8* being downregulated in the MIF-deficient mice. In order to assess the role of S100A8 deficiency in helminths infections, we infected s100a9-/- mice in which the A8/A9 complex cannot form. We found no difference in the primary or secondary clearance of *H. polygyrus* suggesting that S100A8 is not important in the pathogenesis of helminths infection. ARL2BP is known to be important for STAT3 nuclear retention. We assessed STAT6 and STAT3 phosphorylation and found no difference between the BALB/c and MIF-deficient mice in phosphorylation of STAT3/6.

We conclude that in Type 2 infection, MIF plays an important role in the protective Type 2 response, potentially at two levels: firstly in activation of ILCs in a manner which is upstream of, and rescued by, IL-25; and secondly in promoting alternative activation of macrophages in synergy with IL-4.

Lay Abstract

Infection with worms affects approximately a quarter of the world population. There are no effective vaccines to treat worm infections. In order to be able to develop vaccines, we need to better understand how the immune system reacts to help get eliminate the worms. There has also been a marked increase in auto-immune diseases (where the body's immune system reacts to itself), whilst improved sanitation has resulted in reduced worm infections. This may be because the worm itself is able to reduce the immune response towards it by secreting a cocktail of molecules that can directly act on immune cells.

We first assessed a mouse model of inflammatory bowel disease, to assess if the helminth secreted products can modify the immune system. Inflammatory Bowel Disease is a condition that results in the immune system attacking the guts/intestine resulting in pain in the stomach, diarrhoea, loss of weight and low blood count. We found giving products of the worm *Heligmosomoides polygyrus* (HES) (which commonly affects wild mice) was able to reduce the number of immune cells during a model of inflammatory bowel disease, however it did not affect the severity of the disease or the damage to the tissues generated during the inflammatory bowel disease process.

We looked at how a molecule called *Macrophage Migration Inhibitory Factor* (*MIF*) affects the immune response to worms. *MIF* is called a signalling molecule that attracts cells to the site of damage caused by the worms. We infected mice that do not produce the *MIF* molecule with two types of worm models that closely ressemble human hookworms called *Heligmosomoides polygyrus* and *Nippostrongylus brasiliensis*. We found that the mice that do not have *MIF* cannot get rid of the parasites. These mice also do not produce

an important arm of the immune system which are the first responders to infection and are called innate lymphoid cells, macrophages and eosinophils. The lining of the gut is also important in creating an adverse environment for the worms to live for example by increasing mucus production, by pushing the worms out of the gut and by making molecules that bind the parasite directly and reduce nutrient supply. We found that the lining of the gut does not respond appropriately in the mice that do not have *MIF*. We looked at the lining of the gut alone in the mouse that does not produce *MIF*, and found that it responded normally to appropriate levels of alarm signals that are produced by immune cells suggesting that there is not enough alarm signal produced in the mice that do not produce MIF. Overall, this suggests that *MIF* is most important to start the immune responses that eventually get rid of the worms

Abbreviations

AM- Alveolar macrophage

APC- Antigen Presenting Cell

Arg-1- arginase-1

ARL2BP- ADP Ribosylation Factor Like GTPase 2 Binding Protein

CXCR2- C-X-C Motif Chemokine Receptor 2

CXCR4- C-X-C Motif Chemokine Receptor 4

CD11b- Integrin alpha M

CD11c- Integrin alpha X

CD74- HLA class II histocompatibility antigen gamma chain

DC- dendritic cell

DCLK1- double cortin like kinase 1

ELISA- enzyme-linked immunosorbent assay

ES- excretory-secretory products

Foxp3- Forkhead box P3

GATA-3- GATA3 binding protein 3

HRP- horseradish peroxidase

HES- *H.polygyrus* ES

ICOS- inducible T cell costimulator

ILC- innate lymphoid cell

IM- interstitial macrophage

i.p.- intra-peritoneal

i.v.- intra-venous

Lin- lineage markers e.g.CD3, Ly6C/G, CD11b, CD45R/B220, TER-119

LP- lamina propria

LPS- lipopolysaccharide

MIF- Macrophage migration inhibitory factor

MLN- mesenteric lymph node

PEC- peritoneal exudate cells

PHC2- polyhomeotic homolog 2

p.i. post infeciton

Pou2f3- Pou domain class 2, transcription factor 3

RNA- ribonucleic acid

ST2- Interleukin 1 receptor-related protein

S100a8- s100 calcium binding protein A8

TNF- Tumor necrosis Factor

Treg- T regulatory cell

Figures

Table

Chapter 1-Introduction

1.1 Helminths and the Hygiene Hypothesis

Parasitic worms infect around a quarter of the people in the world (Hotez et al., 2008) and would have inhabited most humans in historic times. Many helminths establish long lasting chronic infections and are the cause of approximately 4.98 million years lived with disability (YLD) attributable to soil transmitted helminths (Pullan et al., 2014). In children they cause stunting of growth, and learning (Hotez et al., 2008).

Helminths achieve chronic infestation by causing downregulation of the host immune response. Therefore, an understanding of the immune mechanisms elicited towards helminth infections can lead to a better understanding of how to clear the infections. *Heligmosomoides polygyrus* and *Nippostrongylus brasiliensis* are rodent parasites related to the human hookworms which are widely used to model human helminths diseases.

Strachan established the Hygiene Hypothesis based on an epidemiological survey of family size and birth order in British school children with allergic conditions (Strachan, 1989). He found the prevalence of allergy was much reduced in younger siblings of larger families and thus proposed that early childhood infections may be protective to the later development of allergic/autoimmune disease. Improved hygiene and less crowding have lead to the elimination of helminths. However, there has been an association with increased prevalence of autoimmune diseases such as IBD and diabetes (2016; Molodecky et al., 2012). One hypothesis is that helminths and their immunomodulatory molecules directly modulate the immune system to allow them to establish long lasting infections. This may provide an opportunity to study the parasites for potential molecules that may help modulate autoimmune disease.

The hygiene hypothesis has been elaborated by many other authors and initially was suggested to be a balance between TH1 and TH2 arms of the immune system, in which TH1-driving microbes inhibited TH2-mediated allergy. However many other inflammatory conditions are themselves TH1 (and/or TH17) therefore would not be blocked by TH1/17-activating microbes. With the observation that Tregulatory cells are also greatly expanded in helminth infections, the hygiene hypothesis was refined to that of immunosuppressive regulatory cells which could be a means by which infections could dampen both TH2 allergies and TH1/17 autoimmunity

1.2 Helminth models of infection

1.2.1. *H. polygyrus*

H. polygyrus is a natural parasite of wild mice. Infective *H. polygyrus* can enter the GI tract orally and start to invade the intestinal mucosa in 24 hours. The helminth passes though two larval stages before emerging as adults in the intestine. *H. polygyrus* is so called as it winds tightly round the villus. The adult worms coil around the small intestinal villi and produce eggs that are excreted in faeces. The eggs hatch in the environment undergoing two moults to become L3 larvae. The means of transmission in the wild is through the faecal-oral route, however, in the lab the larvae can be gavaged directly into the stomach (Reynolds et al., 2012). The infection can be assessed by counting the number of eggs per gram faeces, and by counting the number of adult worms remaining in the small intestine. There is variation in the different strains of mice to expel the *H.polygyrus* parasite. Slow responder strains that take over 20 weeks to expel worms include the CBA, C3H, and A/J mice; intermediately responsive strains which expel mice within 20 weeks include the C57BL/6 and 129/J mice; mice capable of rapidly expelling the parasite are the BALB/c, NIH , SJL and SWR strains (Reynolds

et al., 2012). There is also considerable variation in the corresponding immune response in these various strains of mice (Filbey et al., 2014).

At the site at which the larvae of *H. polygyrus* invade, granulomas form. In general these are more abundant in resistant strains. Granuloma formation is dependent on IL4Rα signalling. Granulomas in primary infection have neutrophils, macrophages, DCs and eosinophils, whereas in secondary infection they are predominantly composed of $CD4^+$ TH2 cells and alternatively activated macrophages (Anthony et al., 2006; Patel et al., 2009).

The mammalian stages of the worm can also be cultured in vitro to produce *H. polygyrus* excretory-secretory antigens (Hewitson et al., 2011). Proteomic analysis has found 374 HES proteins that were different to those in the somatic extract of the worm. The major products were the part of the venom allergen like family (Hewitson et al., 2011). These products have been fractionated by the Maizels lab and specific proteins have been found including a TGFβ mimic (Johnston et al., 2017) and HpARI which binds and inhibits IL-33 (Osbourn et al., 2017). A more detailed explanation of the production of HES is in the methods section and in a JOVE video (Johnston et al., 2015).

1.2.2. *N.brasiliensis*

Larvae of *N. brasiliensis* enter through the skin, migrate to the blood vessels and travel to the lung. The larvae moult once within the lung and then migrate to the airways within 48 hours where they are coughed up and swallowed, thereby reaching the GI tract. *N. brasiliensis* is very rapidly expelled in mice within 2 weeks, and is hence a model of an acute helminth infection (Camberis et al., 2003). The adult worms mature in the duodenum where they mate and produce eggs. Faecal egg burdens, and worm counts in the gut can be used to assess the immune response. Adult worms are believed to feed on host intestinal tissue (Bansemir and Sukhdeo, 2001).

H. polygyrus remains in the intestine chronically, whereas *N. brasiliensis* is very rapidly expelled. One way in which *N. brasiliensis* more closely represents the human hookworms *Ancylostoma duodenale* and *Necator americanus* is by having a migratory phase through the lung tissue. This results in long term emphysematous damage (Marsland et al., 2008). Importantly, *N. brasiliensis* is a natural rat parasite that most mouse strains can expel within 7-9 days, while *H. polygyrus* is a natural mouse parasite able to modulate host immunity and establish longer-term infection in a strain-dependent manner. Thus, by comparing both models we are able to establish the importance of MIF in immunity during acute (*N.brasiliensis*) and chronic infection (*H.polygyrus*). In addition, we were also able to assess the lung phase of infection with *N.brasiliensis* which is absent from *H. polygyrus* which always remains within the gastrointestinal tract..

Most of the papers described below administer parasites as a bolus, however, in the natural environment there will be repeated low inoculum infections, which may well contribute to a different dynamic response.

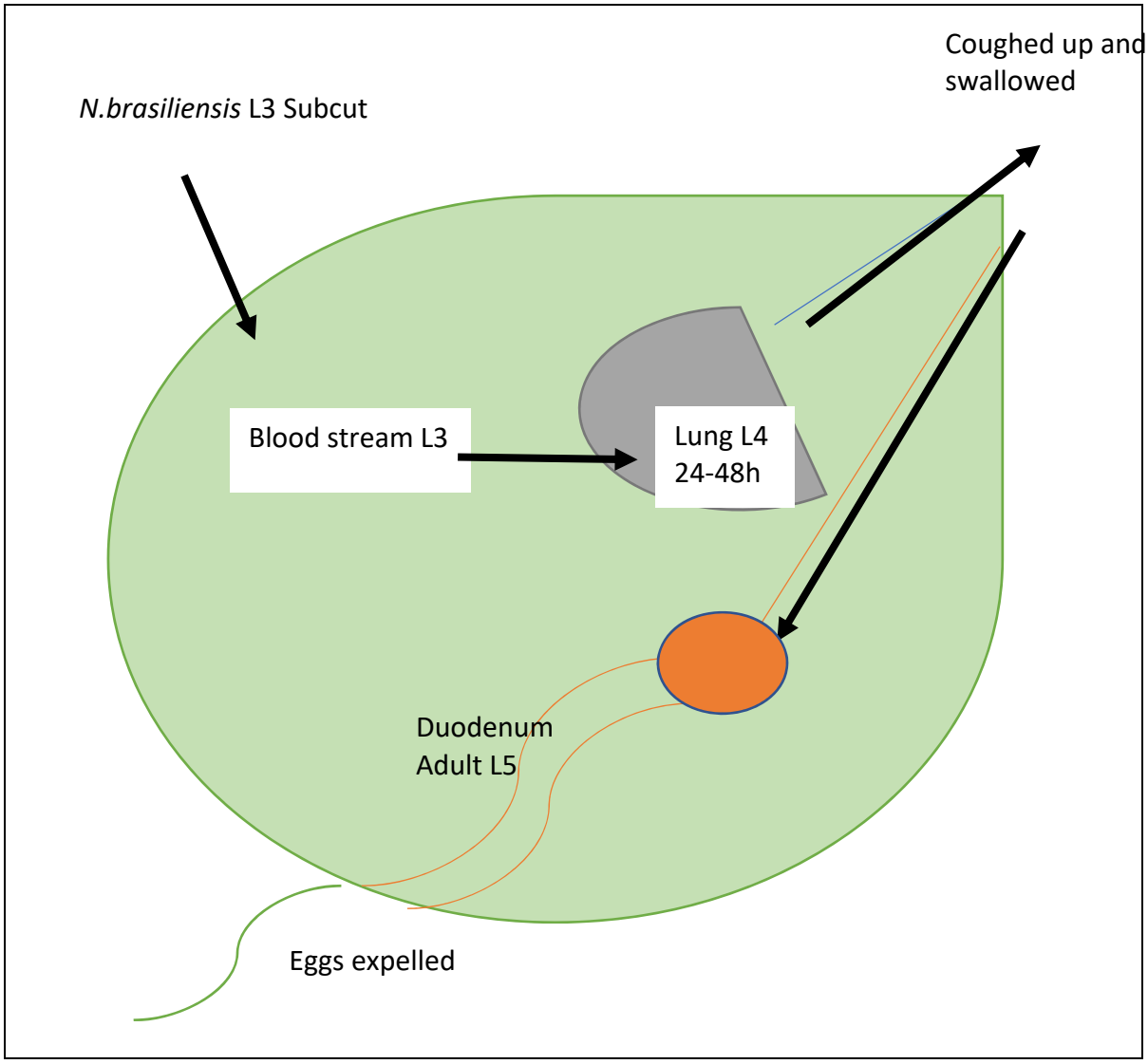

Figure1.1 Lifecycle of *N.brasiliensis*

The larval stages infect the host through the skin between 0-6 hours. Within the lung the larvae moult from L3 to L4 stages (18-72 hours) causing tissue damage. The L4 emerge in the alveoli and are transported to the pharynx where they are coughed and swallowed. The L4 larvae arrive in the duodenum, moult into adult worms, and mate producing eggs that are excreted (adapted from Allen et al 2014(Allen and Sutherland, 2014)).

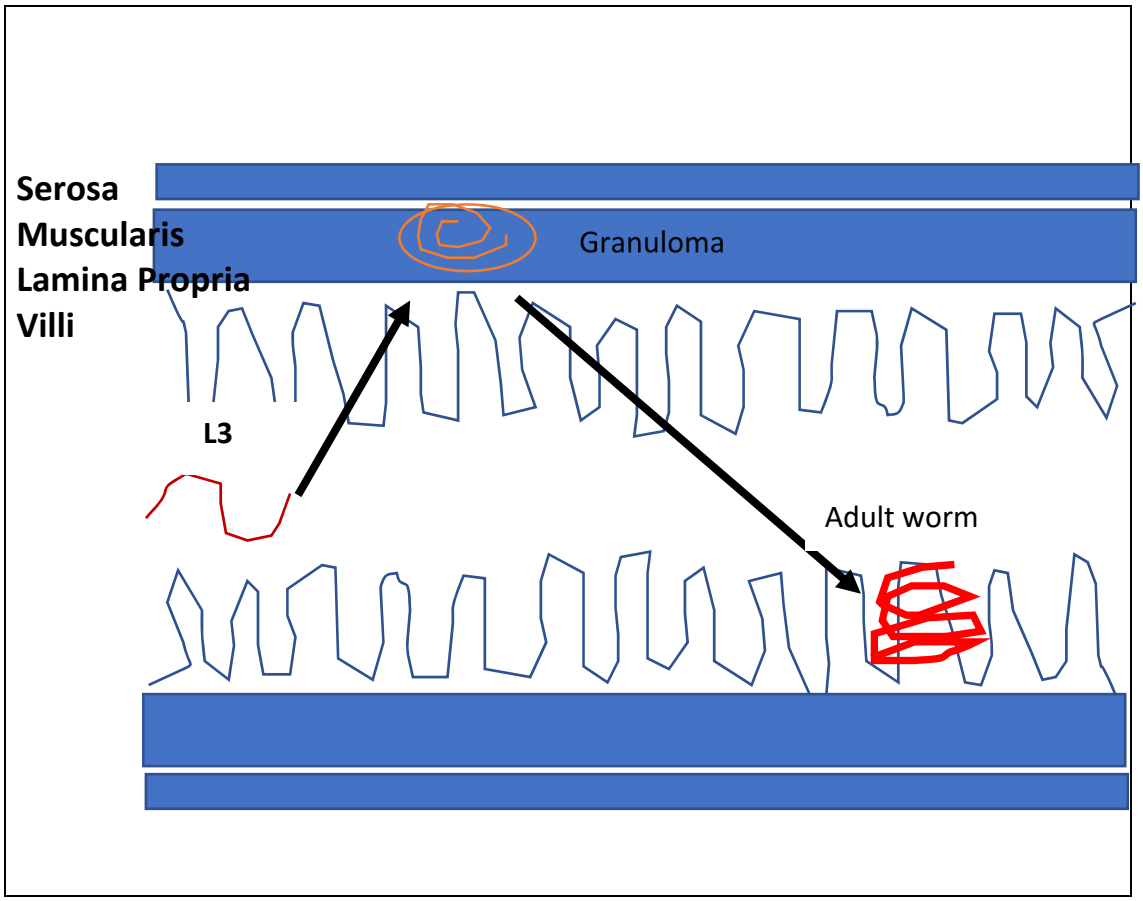

Figure1.2 Lifecycle of *H.polygyrus*

The larvae are ingested orally. In 24 hours they have penetrated through the wall of the small intestine to the submucosa where they undergo two molts. On the 10th day the adult worms have emerged through the submucosa into the gut lumen. The adult worms mate and produce eggs that are excreted in the faeces. (Adapted from Reynolds et al 2012 (Reynolds et al., 2012)).

1.3 Immune responses to helminths

1.3.1 T cell responses

$CD4^+$ T helper cells can be subdivided into TH1, TH2, TH17 and T regulatory cells. $CD4^+$ T helper cells are important for immunity. Antigen-presenting cells (APC) present MHC-bound peptide antigen that activates the T cell via the T cell receptor (TCR); costimulatory molecules present on the T cell and APC stabilise the MHCII-TCR interaction. Following this a third signal is mediated by cytokines secreted by the APC and help polarise the T cell to the appropriate phenotype (Gutcher and Becher, 2007). TH1 cells are primed by IL-12, produce cytokines IFNγ and are under control of the master transcription factor T-bet. TH2 cells are controlled by GATA3 and produce IL-4, -5, -9 and -13. TH17 are under the control of master transcription factor RORα and produce IL-17. T regulatory cells are under the control of master transcription factor forkhead box protein 3 or Foxp3, and are able to produce TGFβ and IL-10. Blocking all $CD4^+$ T cell responses by administering an antibody to CD4 resulted in ablation of protective immunity to *H. polygyrus* (Urban et al., 1991) and to *Trichuris muris* (Koyama et al., 1995). $CD8^+$ T helper cell depletion had no effect on immunity to *H.polygyrus* or *T.muris* (Koyama et al., 1995; Urban et al., 1991).

The co-stimulatory signal is also essential for the development of immunity to *H. polygyrus*- CD86 deficiency resulted in greater egg production in *H.polygyrus* infection (Greenwald et al., 1999).

TH2 responses are essential for immunity to helminths, however, overactivation of TH2 responses can lead to fibrosis. Primary *H. polygyrus* infection induces TH2 cytokine expression in cells from both the mesenteric lymph nodes and Peyer's patches (Svetic et al., 1993). Culturing mesenteric lymph node cells with helminth-derived antigens results in secretion of IL-4, -5, -13 protein, confirming that the TH2 response is parasite antigen-specific (Rausch et al., 2008; Reynolds et al., 2012). The Th2 response is controlled by master transcription factor GATA3 (Hoyler et al., 2012), which leads to TH2 cell commitment and blocks TH1 development (Ouyang et al., 1998). GATA3 increases expression of several IL-4 enhancer regions (HSS, IE, HSS-IL/4P-IE) in TH2 cells (Lee et al., 2001). In helminth infection, TH2 cells produce the cytokines IL-4 and IL-13 that directly result in proliferation of leucocytes, and affects epithelial cells and myenteric neurones that express IL-4Ra. TH2 respones contribute to the weep and sweep responses (Anthony et al., 2007).

Although helminth infections predominantly elicit the TH2 response, there is evidence of other T helper subset involvement. TH17 cells for example, are most effective at controlling bacterial, fungal and anti-helminth responses (Sutherland et al., 2014). These cells produce IL-17 and upregulate neutrophil migration. In *S .mansoni*, the neutralisation of IL-17 dampens down granulomatous inflammation(Zhang et al., 2012).

In human helminth infections, a state of T cell hyporesponsiveness or anergy is frequently observed, that can be reversed by drug-mediated removal of parasites (Taylor et al., 2012). Hyporesponsiveness is elicited by the T regulatory cell population. In humans, T regulatory cells (Treg) increase after helminth therapy, especially in hosts that develop immune dependent pathologies during filarial infections such as elephantiasis (Maizels and McSorley, 2016). Inducible T regulatory cells (iTregs) develop from naïve T cells and produce TGFβ and IL-10. Helminth infections induce regulatory T

cells (Grainger et al., 2010; McSorley et al., 2008) and these Tregs allow the helminths to survive in its host. Boosting Tregs in a *H.polygyrus* model by administration of rIL-2: anti-IL-2C increases worm survival although it was shown that low level Treg activity is also required as complete ablation of Foxp3 cells paradoxically increases worm burden through creation of a incoherent cytokine storm (Smith et al., 2016) .

1.3.2 B cells and humoral immunity in helminth infections

In primary infections, μMT mice (in which B cells do not develop) had similar *H. polygyrus* infection kinetics to wild-type mice; however, they were unable to expel parasites as rapidly as wild type mice in a secondary infection model in which drug-mediated clearance of parasites is followed by a challenge infection (Wojciechowski et al., 2009). However μMT mice also have defects in lymphoid tissue organogenesis, so in order to assess if it is the specific deficiency of B cells that is important, μMT were sublethally irradiated and reconstituted with bone marrow from C57BL/6 or μMT mice. Mice that were reconstituted with C57BL/6 bone marrow were able to expel *H. polygyrus,* confirming that it was indeed the B cell compartment that is essential for immunity to challenge (Wojciechowski et al., 2009). Furthermore, the production of high-affinity antibodies is critical to the immunity that B cells afford, as AID-deficient mice, which have B cells and IgM-secreting plasma cells but cannot undergo isotype class switch or somatic hypermutation are not able to mount a protective response to secondary *H.polygyrus* infection (McCoy et al., 2008).

B cells are not only capable of antibody production but also can produce cytokines depending on which T helper cell subset they are primed with. B cells primed by TH1 cells make IFNγ and IL-12. IL-4 from T cells promotes B cell class switching to IgE and IgG1. IgE activates mast cells and basophils, however IgE does not have a role in *H.polygyrus* or *N.brasilienis* infection (Harris and Gause, 2011).

1.3.3 Innate Lymphoid Cells

The TH2 cells of the adaptive immune system are not the only source of the IL-13 and IL-4 cytokines. Group 2 innate lymphoid cells were originally discovered using reporter mice for IL-13 and IL-4 as a distinct population of $CD45^{+}$ cells that had none of the classical lineage markers (T, B, NK, myeloid or DC-associated) that produce Th2 cytokines on stimulation with IL-25 and IL-33. ILC2 are involved not only in expulsion of helminths but are also involved in allergic disease (Nausch and Mutapi, 2018). Human ILC2s have been similarly described as not having lineage markers, being CD45 and CD127 positive (Nausch and Mutapi, 2018).

Innate lymphoid have similar cytokine secreting profiles as TH1/2 and 3 (Innate lymphoid cells can be divided into ILC1/2/3). The ILC2 population produce type 2 cytokines IL-5, IL-9, IL-13 and amphiregulin. ILC2s also express GATA3 in addition to TH2 cells (Hoyler et al., 2012). ILC2 differentiation depends on RORα (Wong et al., 2012), T-cell factor 1 and GFI1 (Nausch and Mutapi, 2018).

ILC2s are the major responsive cells to epithelial alarmins IL-25, IL-33 and TSLP. Initial studies demonstrated that the RAG-/- mouse, which does not have T cells produces IL-4 and IL-13 to expel *N.brasiliensis* (Voehringer et al., 2006). Fallon (Fallon et al., 2006) found that a population of cells produced IL-5 and IL-13 in *N.brasiliensis* and this was in response to IL-25. The ILCs responsive to IL-25 expressed KLRG1, whereas those responding to IL-33 produced ST2. IL-4/13 production from innate cells and T cells is responsible for epithelial cell responses such as goblet cell hyperplasia and secretion of Mucin5ac and RELMβ in the small intestine(Oeser et al., 2015).

There is evidence of cross talk between ILC2 and TH2 cells. Group 2 ILCs secrete IL-4 and differentiate T cells to TH2 (Pelly et al., 2016). ILCs have been reported to express MHCII, and experimental deletion of the MHCII on IL-13 expressing ILCs showed that T cell responses are amplified by ILC2s in an MHCII-dependent manner. Human ILC2s also expressed MHCII with costimulatory molecules and presented antigen to T cells (Oliphant et al., 2014). In addition, PD-L1 expression by ILC2s stimulated GATA3 and production of IL-13 by TH2 cells, with a conditional ILC2 PD-L1 deletion impairing TH2 polarisation (Schwartz et al., 2017).

The nervous system is also involved in a newly described circuit between ILC2s and epithelial cells. The release of the peptide Neuromedin U by neurons was found to be a fast and potent regulator of type 2 lymphoid cells via the neuromedin U receptor 1 (Nmur1) on ILC2s in both the lung and small intestine (Cardoso et al., 2017; Klose et al., 2017; Loser and Maizels, 2018). The same receptor is also expressed on human ILC2s, and its importance emphasised by the finding that NMUR1-deficient mice had increased *N.brasiliensis* burdens (Klose et al., 2017).

1.3.4 Alternatively Activated Macrophages

The intestine has the largest population of macrophages in the body. Constantly exposed to pathogens and foreign antigens, cells must discriminate pathogenic from harmless stimuli in order to mount protective responses and avoid pathogenic insults. A feature of intestinal macrophages is that exposure to bacteria does not automatically trigger a proinflammatory response. They do however express low levels of IL-10 and TNFα in steady state (Bain and Mowat, 2014).

In the context of TH2 cytokines, tissue resident macrophages develop an alternatively activated (M2) phenotype (Jenkins et a., 2013). Macrophages of the M2 phenotype express high levels of Arginase1, RELM-α and YM1. Using these markers, it was found that M2 macrophage percentages are increased in the more resistant SJL and BALB/c strains of mice during *H. polygyrus* infection (Filbey et al., 2014). In both *H. polygyrus* and *N. brasiliensis* infection, depletion of macrophages using clodronate liposomes increased susceptibility(Filbey et al., 2014; Zhao et al., 2008). Arginase inhibition results in diminished immunity to *N. brasiliensis* (Zhao et al., 2008) although the role of Relmα and YM1 are less clear.

They can be tissue resident or derived from blood as monocytes. The resident macrophages of the small intestine are $CD4^+$ $TIM4^+$ (Shaw et al., 2018). Interestingly, ddifferent tissue environments have recently been found to express specific amplifiers for AAMs. Surfactant protein A enhances AAM proliferation in the lung, while in the peritoneal cavity C1q amplifies AAMs (Minutti et al., 2017b). IL-33 induces macrophage population to proliferate in the peritoneal cavity (Jackson-Jones et al., 2016). In addition, AAms can be a source or retinoic acid and can expand T regulatory cells (Broadhurst 2012). Depletion of macrophages via clodronate reduces the hypercontractility response to helminths (Zhao et al., 2008). Inhibiting arginase by use of its inhibitor BEC (S-(2-boronoethyl)-1-cysteine) impaired intestinal smooth muscle contractility (Zhao et al., 2008).

From our laboratory experience, preparations of live cell suspensions from the lamina propria for flow cytometry are difficult to obtain from helminth-infected mice due to high levels of apoptosis and mucus secretion, Therefore, the peritoneal cavity is utilized to assess immune responses to helminth infections.

1.3.5 Dendritic cells

Another subset of antigen presenting cell include the dendritic cells (DCs). Intestinal DCs are classified into three distinct subsets dependant on expression of Cd11b and CD103 as well as interferon regulatory factor 4 or 8 (IRF4 or IRF8) for development and/or survival (Tamura et al., 2005). The three different subtypes are $CD103^{-}Cd11b^{-}$, $CD103^{+}Cd11b^{-}$,Cd103-$CD11b^{+}$) and one minor $CD103^{-}Cd11b^{-}$ subset. All four subtypes are found in the migratory compartment of intestinal lymph nodes (Joeris et al., 2017).

TH2-inducing DCs are generated by exposure to helminths, TSLP and innocuous allergens (Liu et al., 2007). These TH2 inducing DCs are dependent on the transcription factor IRF4 (interferon regulatory factor 4)(Gao et al., 2013) and are $CD11b^{+}CD103^{-}$ (Mayer et al., 2017). IRF8 positive DCs promote TH1 immune responses. Therefore it may be that different subsets are capable of driving TH2 immunity in different directions (Sorobetea et al., 2018).

DCs recognise microbial pathogens through ligands of the innate Toll-like receptors (TLRs) such as LPS and CpG. Simultaneously DCs up-regulate costimulatory molecules CD40, CD80 and CD86 and then also release IL-12 to direct T cell polarisation towards TH1 (MacDonald and Maizels, 2008). DC production of RELMα primes TH2 responses and controls TH1 responses (Cook et al., 2012).

1.3.6 Eosinophils

Eosinophils, basophils and mast cells develop from a GATA1^{+} granulocyte-monocyte precursor (GMP) that is distinct from the GATA1^{-} GMP that gives rise to neutrophils, monocytes and macrophages (Weller and Spencer, 2017). Eosinophils contain granules of cationic proteins, and therefore stain with acidic dyes such as eosin. Eosinophils can be recognised in mice as Siglec-F^{+} and SSC^{hi} although the exact markers depends on the tissue sites. The cationic granules can degranulate and kill helminths *in vitro*. Initially, eosinophil differentiation and recruitment is dependent on the cytokine IL-5 secreted predominantly by ILC2s (Nussbaum et al., 2013).

The role of eosinophils in helminth infection can vary according to the helminth in question. In vitro studies have shown that eosinophils are able to bind to and kill *N.braslliensis* larvae (Shin et al., 2001).In filarial infection models, eosinophils are required for clearing *B. malayi* microfilariae in primary but not secondary challenge infection (Cadman et al., 2014)

1.3.7 Neutrophils

Neutrophils are also granulocytes, which have recently also been found to be important effectors of Type 2 immunity. They are present in the nodules formed around *L. sigmodontis*, and in the *H. polygyrus* granulomas (Allen et al., 2015). Neutrophils act with macrophages to kill *S.stercoralis* larval forms in vitro (Bonne-Annee et al., 2013), they prime an effector macrophage phenotype that can expel *N.brasiliensis* (Chen et al., 2014), and they are important in primary immunity to *H. polygyrus* (Hewitson et al., 2015; Pentilla et al., 1985). Sutherland et al. describe an N2 phenotype emerging in the lung of mice infected with *N.brasiliensis*, and in this setting neutrophils mediate IL-17 dependent larval killing (Sutherland et al., 2014)

1.3.8 Immune cell cytokines and effectors

The cells of the type 2 immune system use cytokines and effector molecules to enhance helminth expulsion. IL-4 is essential for effective immunity to *H.polygyrus* (Urban et al., 1998), as well as to *T. muris*, (Bancroft et al., 1998); however it is not required for immunity to *N. brasiliensis* (Urban et al., 1998). IL-13 is required to expel *N. brasiliensis* (Urban et al., 1998) and *T. muris*. (Bancroft et al., 1998). IL-13 supports DC migration. There is some redundancy between IL-4 and IL-13 because they share the IL4Rα subunit. IL4Rα expression is not required on immune cells to provide immunity to *T. spiralis*, and IL4Rα expression on non bone marrow cells was required to expel *N. brasiliensis* (Urban et al., 2001). Therefore, it is likely to be the non-immune cell compartment that ultimately responds to IL-4/13.

IL-5 is crucial for eosinophil recruitment and differentiation. In *N. brasiliensis* infections, mice overexpressing IL-5 had reduced worm burden during secondary infection but primary infection is unaffected by the absence of eosinophils. In secondary infection, the larvae are intercepted en route to the lung and this interception is eosinophil mediated (Knott et al., 2007). IL-5 was not required to clear *S. mansoni, T. spiralis* or *T muris* (Allen and Sutherland, 2014; Betts and Else, 1999; Herndon and Kayes, 1992; Sher et al., 1990).

IL-9 recruits mast cells, and IL-9 overexpression results in expulsion of *T. spiralis* (Faulkner et al., 1997), adoptive transfer of TH9 cells results in expulsion of *N.brasiliensis* (Licona-Limon et al., 2013). T helper cells and ILC2s are largely responsible for producing IL-9 (Licona-Limon et al., 2013). Mast cells themselves can secrete IL-9 and IL-13 in response to *IL-33* and mast cell protease 1 (Chen et al., 2015).

Arginase 1 is produced by alternatively activated macrophages, and is an enzyme in the urea cycle. It functions to convert arginine to ornithine and urea and is under the control of IL-4, IL-10, IL-13 via STAT3/6 (Vasquez-Dunddel et al., 2013). The ornithine produced is converted to polyamines required for cell proliferation and prolines required for the synthesis of collagen (Rodriguez et al., 2017). Arginase competes with iNOS for arginine, thereby reducing NO-mediated activation of the classically activated macrophage (Allen and Sutherland, 2014). Arginase1 dependent depletion of arginase from the environment also arrests T cell development (Van de Velde et al., 2017). The inhibiton of arginase by BEC-1 resulted in impaired secondary immunity to *H. polygyrus* (Anthony et al., 2006). Arginase-deficient macrophages were found to have increased fibrosis in the liver (Pesce et al., 2009a) but unaltered inflammatory responses in the lung (Barron et al., 2013). Antibodies from *H. polygyrus*-challenged mice induced adherence of macrophages to larvae in vitro, immobilising them, while macrophages that did not express Arginase-1 had reduced larval trapping in vitro (Esser-von Bieren et al., 2013). Arginase-1 expressing macrophages are important in healing after infection (Maizels and McSorley, 2016).

YM1 is also produced by alternatively activated macrophages, and belongs to a family of Chitinase-like proteins (CLPs). These are part of a family that includes chitotriosidase and acidic mammalian chitinase (AMCase) that cleaves and therefore provides defences against chitin in arthropods, parasites and fungi. In mice there are three CLPs: YM1, YM2 and BRP-39. YM1 was found to be the dominant CLP in the Lung (Sutherland et al., 2014), and its overexpression increases neutrophil recruitment in the lung. Conversely, neutralising YM1 reduces the accumulation of neutrophils and IL-17. The source of the IL-17 was found to be the gamma-delta T cells (Sutherland et al., 2014).

The RELM family, are made up of RELM-α, RELM-β, RELM-γ. They are similar to resistin, which is an adipocyte-secreted factor regulating response to insulin(Nair et al., 2006). RELMα is expressed in bronchial epithelial cells and the wall of the intestine, but it is also expressed by macrophages in a STAT6 dependent fashion (Stutz et al., 2003). RELMα production is upregulated by IL-4/13 (Munitz et al., 2012) and Resistin like alpha (Retlna-/-) deficient mice had higher levels of IL-4,5 and 13 producing $CD4^+$ T cells and exacerbated lung inflammation in *S. mansoni* infection (Nair et al., 2009; Pesce et al., 2009b). RELMα was found to upregulate pro-inflammatory IL-6, TNFα secretion compared with LPS alone(Munitz et al., 2008).

Amphiregulin is an EGF-receptor ligand that is expressed by epithelial and mesenchymal cell types but also immune cells including ILC2s, eosinophils, and TH2 cells (Zaiss et al., 2015). Amphiregulin is produced by lung ILCs and restores lung function and tissue remodelling after influenza virus and nematode-induced lung damage (Monticelli et al., 2011; Turner et al., 2013). AREG-deficient mice had reduced proliferation of gut epithelial cells and did not expel *T. muris* (Zaiss et al., 2006). EGF expression by $CD4^+$ cells results in resistance to *H. polygyrus* and *N.brasiliensis* (Minutti et al., 2017a).

1.3.10 Final mechanisms in helminths expulsion

Type 2 immune responses (TH2 cells, ILC2s, M2 macrophage, eosinophils, basophils and mast cells) are activated upon tissue damage caused by helminth infections. The pathways lead not only to helminth expulsion, but also a wound healing response. M2 macrophage products result in myofibroblast activation and tissue repair. Eosinophils release material that can also contribute to wound healing responses (Gause et al., 2013).

The final common pathway that results in helminth expulsion from the gut occurs in the intestinal epithelial cells themselves. The release of cytokines by the epithelium and immune cells results in a series of cascading events that eventually lead to intestinal peristalisis and epithelial fluid egress resulting in a “weep and sweep” model of expulsion. IL-13 signalling increases epithelial cell electrolyte secretion and permeabililty, to increase the intestinal epithelial cell turnover (Cliffe et al., 2005), and to change the production of mucins from MUC2 to a less degradable Muc5ac (Hasnain et al., 2011); mast cell proteases degrade tight junctions allowing the fluid to leak into the lumen (McDermott et al., 2003). The epithelial cells upregulate their turnover to produce an epithelial escalator to dislodge the worms (Cliffe et al., 2005). Infection with many species of intestinal nematode also induces changes in the muscle contractility. The hypercontractile response is dependent on the IL-4 STAT6 pathway (Zhao et al., 2003). The epithelial cell subtypes, their functions and alarmin signals will be explored further in the following section.

The lung is another epithelial site which primes immune protection to secondary infections in *N.brasiliensis*. Lung-restricted infection was sufficient to generate protective immunity against tissue-migrating parasites, as immunity to secondary infection could be achieved when primary infection only occurred in the lung (Harvie et al., 2010).

1.4 Immune mechanisms in the GI tract

1.4.1 Gut Mucosa

The gut mucosa is central to the mechanism by which the host senses the invasion by a large multicellular organism and finally by which it attempts to expel the pathogen as explained by the “weep and sweep” hypothesis. It is likely that tissue damage initiated by multicellular helminths is the initial stimulus from which TH2 immunity is driven in helminth infection. The damage results in secretion of alarmin cytokines IL-25, IL-33, TSLP and various other molecules ((Gause et al., 2013). These molecules communicate with immune cells such as the ILC2s that secrete cytokines e.g. IL-13 leading to multiple processes that expel the worms. The gut mucosa both senses pathogen and allows for physical removal of multicellular organisms (Figure 3).

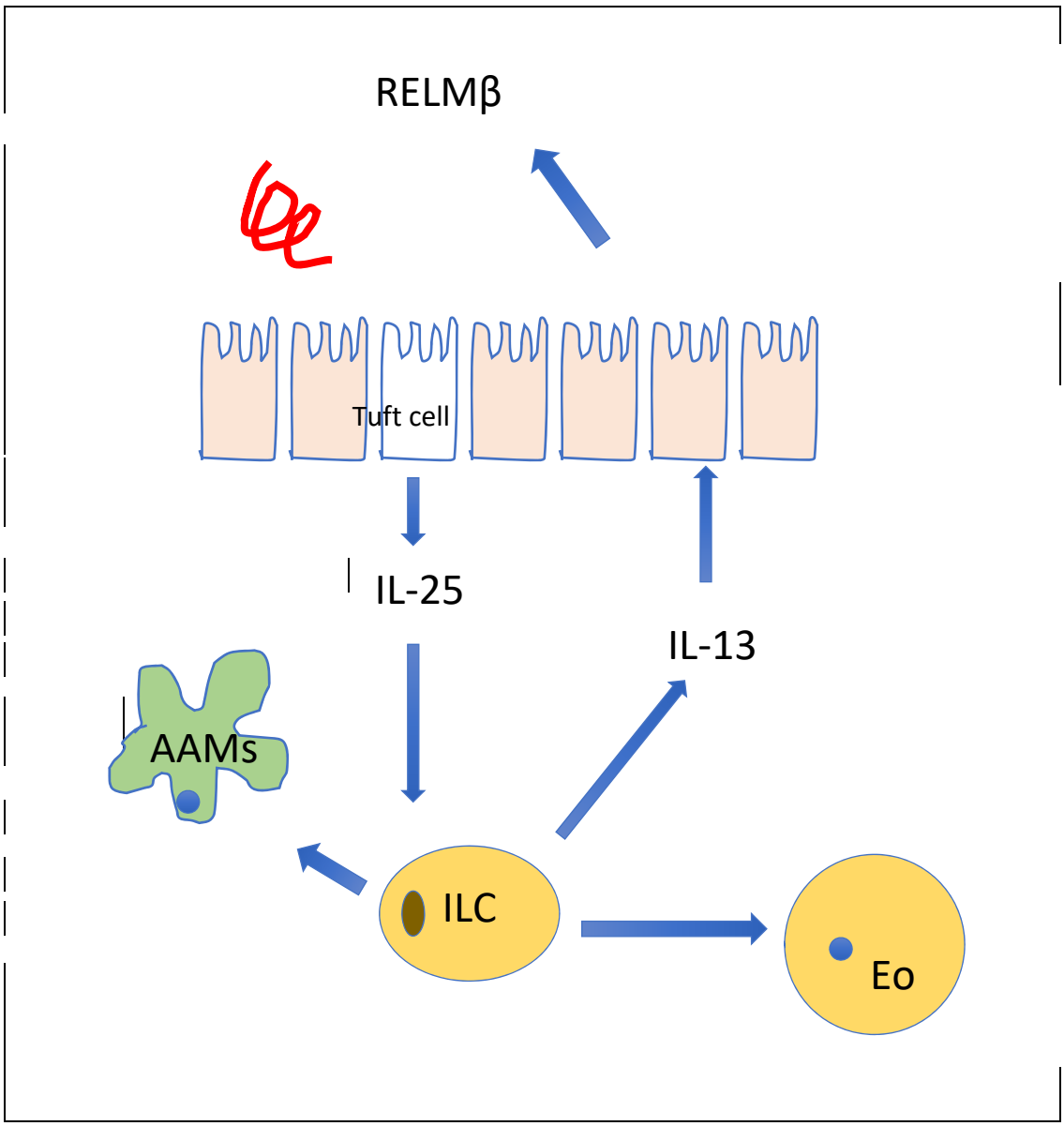

Figure1.3 Intestinal immune response in helminth infection

Tuft cells sense invading worms and release IL-25 which recruits ILCs to the site of infection. The ILCs secrete IL-13 which starts a cascade of events that results in worm expulsion but also proliferation of intestinal tuft cells in a positive feedback loop. ILC derived IL-5 also recruits eosinophils and alternatively activated macrophages which themselves secrete further cytokines and mediate anti-helminth immunity.

The intestine is a barrier surface that both protects the host from pathogens and obtains nutrition. The epithelial layer must be able to discriminate between harmful and protective stimuli. The epithelium consists of the epithelial monolayer, the basement membrane and the lamina propria.

The intestinal immune cells reside within the gut-associated lymphoid tissue (GALT) consisting of lymphocytes which are present throughout the epithelium and lamina propria, but also in areas of organised tissues. These organised tissues are the Peyer's patches, mesenteric lymph nodes and isolated lymphoid follicles. Overlying the Peyer's patch is an area of follicle-associated epithelium (FAE) and the subepithelial dome (SED). This epithelium has microfold (M) cells which lack surface microvilli or a mucus layer, and are available to bind pathogens and antigens. The M cells function to pass on molecules to antigen presenting cells in the epithelium or the SED. They then present to T cells in the Peyer's patch or travel to the MLN to present antigen.

The cells of the epithelial monolayer are formed by enterocytes, goblet cells, neuroendocrine cells, paneth and tuft cells. The epithelium releases alarmins in response to pathogenic stimulus. In helminth infections, three cell types are of interest: these are the goblet cells, paneth and tuft cells.

Goblet cells are responsible for synthesising secretory mucin glycoproteins (MUC2) and epithelial membrane bound mucins (MUC1, MUC3, MUC17), trefoil factor peptides (TFF) and resistin-like molecule B (RELMβ). The mucus layer formed by the mucins forms a gel-like structure which acts as a defence against injury from trauma or chemical injury (Kim and Ho, 2010).

The intestinal epithelium is divided into finger like projections called villi, and invaginations called crypts. Paneth cells reside in the base of the intestinal crypts and contribute to first line defence by secreting granules of lysozyme, phospholipase A2, defencins and REGIIIγ. After differentiation, the Paneth

cells remain in the crypts, however, the other cells migrate to the villi (Martinez Rodriguez et al., 2012).

Tuft cells have been described in 1956 (Jarvi and Keyrilainen, 1956; Rhodin and Dalhamn, 1956), in the trachea and the gastro-intestinal tract by electron microscopy because of their morphology. They had a tuft of long and thick microvilli projecting into the lumen (Gerbe and Jay, 2016). Although little was known about their function (Grencis and Worthington, 2016) they were thought to be chemosensory in nature. In 2016 three groups found these to be the epithelial cell producers of IL-25. Gerbe et al (Gerbe and Jay, 2016; Gerbe et al., 2016) found that in the absence of Pou doumain, class2, transcription factor 3 or POU2F3, mice were unable to make tuft cells and did not express *IL-25*. Organoid cultures demonstrated that IL-4/13 was able to induce the production of Tuft cells in wild type organoids, therefore likely part of an epithelial cell feedback loop. Moltke et al (von Moltke et al., 2016) also found via the use of an IL-25 reporter mouse that the tuft cells were the source of the IL-25. Tuft cells express double-cortin like kinase 1 (DCLK1) and transient potential receptor cation channel subfamily M, member 5 (TRMP5). They are upregulated 8.5 fold on infection with *N.brasiliensis*. I

1.4.2 Epithelial cell alarmins and their functions

The epithelium produces several alarmin cytokines in response to the physical damage caused by helminths that amplify the effective T cell responses required to eventually expel the invading pathogens.

IL-25 is part of the IL-17 cytokine family. IL-25-deficient mice are unable to expel *N. brasiliensis* (Fallon et al., 2006). The major cell type thought to be responsive to IL-25 is the innate lymphoid cell (Price et al., 2010): injection of wild type ILCs but not IL-13-deficient ILCs into IL-17Br-/- mice restored IL-25 responsiveness and leads to expulsion (Neill et al., 2010). IL-25-deficient mice also fail to eradicate *T. muris* (Owyang et al., 2006). In the lung, IL-25 is responsible for allergic responses and fibrosis (Hams et al., 2014).

IL-33 is a member of the IL-1 family. IL-33 induces IL-13 producing ILCs or nuocytes. IL-33 can also promote TH2 cells to secrete IL-13 (Guo Nature Immunology 2015). The IL-33 receptor is expressed on T cells, macrophages, endothelial cells, epithelial cells and ILC2s on all of which it binds the ST2 receptor (Cayrol and Girard, 2018). IL-33 is released from the nucleus in necrosis, however, during apoptosis Il-33 is inactivated by caspase cleavage. A deficiency of IL-33 or its receptor results in susceptibility to several helminths (Coakley et al., 2017),

Mice that do not have IL-33 or its receptor (ST2) are unable to mount a type 2 immune response to *N. brasiliensis* (Hung et al., 2013). IL-33 may have a critical time window when it is active, as administering *rIL-33* early promotes immunity to *T muris*, whereas when given in chronic *T muris* infection, it has little effect and is unable to redirect already polarised TH1 cell responses (Humphreys et al., 2008). Recently Osbourn (Osbourn et al., 2017) et al have discovered an *H. polygyrus* derived molecule HpARI which suppressed IL-33

while extracellular vesicles secreted by *H. polygyrus* are able to suppress expression of the IL-33 receptor (Buck et al.).

Thymic stromal lymphopoietin (TSLP) is a member of the IL-2 cytokine family (Ziegler et al., 2013). The major responsive cells are the myeloid derived dendritic cells but it also affects monocytes, T cells and B cells (Ziegler and Artis, 2010). ILC2 activation in the skin is dependent on TSLP (Kim et al., 2013). *N brasiliensis* and *H.polygyrus* develop normally in TSLP-deficient mice (Harris and Loke, 2017). In *T. muris* however, TSLP blockade made resistant mice susceptible (Taylor et al., 2009) via suppression of IL-12p40 on dendritic cells. A hypothesis as to why TSLP deficient makes no difference to *N.brasiliensis* or *H polygyrus* is because these parasites secrete molecules that inhibit host IL-12p40 directly (Massacand et al., 2009). Another reason may be that TSLP is expressed in the large intestine rather than the small intestinal niche of these parasites (Taylor et al., 2009).

Mucins trap the parasite *T. muris*, and deficiency of mucins delays the expulsion of the worm (Hasnain et al., 2010). In the normal intestine MUC2 is the major mucin forming the gel-layer whereas Muc5A is normally expressed in diseased states such as ulcerative colitis and in parasitic infections (Forgue-Lafitte et al., 2007). Muc5A is expressed in the caecum of mice resistant to *T. muris* in an IL-13 dependant manner and associated with worm expulsion. Muc5A deficient mice have delay in expulsion of *T. spiralis* and *N. brasiliensis* (Hasnain et al., 2011).

RELMβ is a protein which is part of a family of resistin-like cytokine molecules. It is produced by the goblet cells and secreted into the lumen. It is upregulated during helminth infections. RELMβ directly binds the parasite and interferes with its access to nutrients (Artis et al., 2004). The RELMβ deficient mouse found to be resistant to chronic *T. muris* inflammation and failed to acquire a chronic infection (Nair et al., 2008). In the context of *H. polygyrus* and *N. brasiliensis* however, intestinal RELMβ was important for

worm expulsion and IL4Rα expression was required on intestinal epithelial cells for the production of RELMβ (Herbert et al., 2009).

1.5 Macrophage migration inhibitor factor (MIF) in helminth infections

The main focus of this thesis is on the cytokine Macrophage migration inhibitory factor (MIF) and its role in helminth infections. MIF is a cytokine first discovered in the 1960s as a product of activated T cells (Bloom and Bennett, 1966; David, 1966). Since then it has been found to be constitutively expressed by many tissues especially at mucosal sites and by a large number of immune cells with multiple functions (Calandra and Roger, 2003).

69% of the mouse and human gene sequence is identical (Kozak et al., 1995), and numerous homologues of MIF have been found in all members of the animal kingdom including helminths and in fishes (Prieto-Lafuente et al., 2009; Sato et al., 2003). Defects in the MIF gene have been found in human diseases such as inflammatory bowel disease (Zhang et al., 2013) and autoimmune hepatitis (Assis et al., 2014). MIF can be strongly pro-inflammatory (Bernhagen et al., 1998; Calandra et al., 1994), and high levels in septic shock are associated with poorer outcomes (Chuang et al., 2014). MIF more broadly regulates immune responses in inflammation. MIF activates the ERK1/ERK2/MAPK (Lue et al., 2006) pathways, the NF-KB pathway (Kim et al., 2017) and up-regulates the expression of Toll-like receptor 4 that recognises endotoxin-expressing bacteria.

The receptors for MIF have been reported as CXCR2 and CXCR4 (Bernhagen et al., 2007), with CD74 (Leng et al., 2003) being a co-receptor for MIF (Calandra and Roger, 2003). MIF is responsible for mononuclear arrest at site of human aortic endothelial cells, and this arrest is abrogated with the addition of anti-CXCR2 (Bernhagen et al., 2007). MIF has also been found to bind CXCR2 through a pseudo-ELR motif (Weber et al., 2008). This cytokine has also been found to have enzymatic activities incuding D-

dopachrome tautomerase, phenylpyruvate keto-enol isomerase and thiol-protein oxidoreducase activity. However, it is not clear if the enzyme activity is important for the in vivo biological effects of MIF (Calandra and Roger, 2003).

The level of MIF needs to regulated in order to achieve a balanced immune response towards a pathogen (Calandra and Roger, 2003). A low dose of pathogen in a MIF-deficient environment results in mice succumbing to infection as in the *S.typhimurium* model (Koebernick et al., 2002) whereas wildtype animals do not. However, in septic shock models where the wildtype mice die of lethal sepsis, MIF deficiency was protective (Calandra et al., 2000): this was found in several models including lipopolysaccharide (Bozza et al., 1999), *E. coli*, caecal ligation & puncture (Calandra et al., 2000) and staphylococcal toxic-shock syndrome toxin 1 models of sepsis.

MIF has been studied previously in the context of helminth infections. Rodriguez-Sosa et al (Rodriguez-Sosa et al., 2003) found that MIF-deficient mouse have impaired immunity to the helminth *Taenia crassiceps*. In a *Schistosoma mansoni* infection model, the MIF-deficient mice had smaller granulomas and fewer eosinophils (Magalhaes et al., 2009). A recent paper by Damle et al 2017 (Damle et al., 2017) found MIF-deficient mice to be able to clear *N.brasiliensis* infection more easily than wild type mice, however, much of the focus was on the parasitological responses and the work was predominantly done on a C57BL/6 background of mouse. Bezencon discovered that MIF is expressed in tuft cells approximately two fold above the levels in the remaining intestinal epithelial cell population (Bezencon et al., 2008). Recently, Haber et al discovered that MIF is upregulated specifically in enterendocrine cells in the third day of *H. polygyrus* infection (Haber et al., 2017).

In contrast to the older literature indicating that MIF drives classical inflammatory pathways, more recent data point to its ability to promote

alternative activation of macrophages, often termed M2 cells. Our group previously reported that murine MIF and *Brugia malayi* MIF (a homologue of MIF found in the filarial nematode *B. malayi*) synergised with IL-4 to induce bone marrow derived macrophages to upregulate the alternatively activated products Arginase-1, RELMα and Ym-1 (Prieto-Lafuente et al., 2009). MIF was also found to be important in alternative activation of tumour associated macrophages (Yaddanapudi et al., 2013). As M2 macrophages are implicated as key effectors of immunity to helminth parasites (Anthony et al., 2006; Filbey et al., 2014), the question arose of whether MIF contributes to protective immunity to helminth infection.

1.6 Inflammatory Bowel Disease and Helminths

Ulcerative Colitis (UC) and Crohn's disease (CD) are both inflammatory bowel diseases (IBD) resulting in significant long term morbidity and mortality (Molodecky et al., 2012). IBD is a chronic relapsing remitting disease of the GI tract. In the case of Crohns' disease it can lead to fistulation, abscess formation, and over the long term increases the risk of neoplasia.

Potent anti-TNF treatments are available, however, contraindications, primary non-response, loss of response and intolerance occur often. Consequently, IBD is associated with a high economic impact, not only from hospitalisation and surgery but also loss of productivity at work (van der Valk et al., 2014). In adults, the incidence has risen to 24.3/100000/yr for UC and 12.7/100000/yr for CD in Europe (Molodecky et al., 2012). There is strong epidemiological evidence of the role of the environment in IBD phenotype (as is the case for smoking in CD).

1.6.1 Role of helminth derived products in Inflammatory Bowel Disease (IBD).

Helminths are multicellular parasites that have co-evolved with humans for many millennia and have adopted mechanisms to down-modulate inflammation. Several studies have evaluated the role of helminths in managing inflammatory diseases-such as IBD- these are referred to directly in Chapter 3. As part of the thesis, we wanted to investigate if helminth infection modifies the innate immune responses in TH1/17 predominant models of infection such as IBD.

1.6.2 T regulatory cells in IBD

T regulatory cells play a role in IBD disease development (Powrie et al., 1993; Salas and Panes, 2015). Mutation of the Foxp3 gene results in a syndrome of diabetes, enteropathy and endocrinopathy (IPEX) (Wildin et al., 2001). Regulatory Treg development represents an antigen-specific mechanism to inhbit harmful autoreactive responses. The cells can be thymus-derived (tTreg) or peripherally-derived pTreg).

T reg cell administration is currently being evaluated to treat patients with several autoimmune disease such as graft-versus-host disease (GVHD), type 1 DM, organ transplants. Canavan et al (Canavan et al., 2016) demonstrated that T regs count be expanded in vitro, and are stable enough not to convert to TH17 cells that are proinflammatory, they also express integrins and home to the gut. The only trial to date showed a short term response in the CDAI in patients infused T regulatory cells (Desreumaux et al., 2012). Measures to further the use of T regulatory cells have been limited because of a lack of knowledge of the self antigens involved, and the short lived life span of T regulatory cells in vivo (Salas and Panes, 2015). There is therefore potential to use therapies that expand and stabilise Foxp3 T regulatory cells. For some time, we have been aware that helminth secretions induce de novo T cell FOXP3 expression via the TGFβ pathway(Grainger et al., 2010), and recently a novel helminth molecule with TGFβ activity has been found that can be used to reduce rejection in skin

grafts (Johnston et al., 2017). Foxp3 positive T regulatory cells induced *by H. polygyrus* infection have been used to supress pathology in a T cell model of colitis (Hang et al., 2013).

TH17 cytokines are elevated in human IBD (Fujino et al., 2003). TH17 cells were distinguished as a different subset from TH1 and TH2 cells in 2005, as a phenotype which produced IL-17 but not IFNγ or IL-4 (Bouchery et al., 2014). These cells are pro-inflammatory and express IL-17, IL-22 IL-5 and TGFβ under the control of RORγt.

TH17-derived IL-17 in the T cell transfer model of colitis increases the severity of colitis and was associated with upregulated IFNγ in the colon. IL12 and IL23 are secreted by DCs, and polymorphisms of IL23R were associated with IBD risk. IL-23 blocade reduced the colitis in a RAG-/- CD40 model of colitis.

ILC3 in the *Helicobacter hepaticus* RAG-/- model of colitis ($Thy1^+$ $Rorgt^+$ve $SCA1^+$ve cells) produce IL-23 mediated gut inflammation (Buonocore et al., 2010). These cells are also implicated in human IBD. The different human ILCs closely resemble the T cell lineages, as is also the case for mouse ILCs. ILC1s accumulate in the terminal ileum of patients with Crohn's disease (Bernink et al., 2013). IL-22 is also produced by TH17 cells and may protect against colitis, but may have context dependent effects: $IL22^+$T cells in Crohn's disease increased expression of cytokines in the subepithelial myofibroblasts, but in UC were associated with amelioration of symptoms (Broadhurst, Sci Trans Med 2010).

A positive consequence of the TH2 and T regulatory cell skew by helminths (away from TH1 and TH17 immunity) can modify autoimmune disease such as IBD.

1.6.3 Innate cell populations in IBD and IL-10

Alterations to innate cell populations e.g. macrophages can result in autoimmunity: macrophages lacking IL10R caused spontaneous colitis in mice and pediatric mutations in IL10R result in more pro-inflammatory macrophages and an IBD type phenotype in mice and in a pediatric cohort (Zigmond et al., 2014).

T cell transfer models depleted of macrophage populations have less severe colitis (Kanai et al., 2006), as do mice in which innate lymphoid cells are depleted with anti-Thy1 antibody (Buonocore et al., 2010). Another important gene locus is NOD2, as the odds ratio for a carrier of two susceptibility alleles of NOD2 is 17.1 for Crohn's disease (95% CI 10.7-27.2) (Economou et al., 2004) and this is heavily expressed in macrophages (Forrest et al., 2014).

1.6.4 Microbiota and IBD

Alterations in the composition of microbiota may play a role in the pathogenesis of IBD. Short chain fatty acids produced by fermentation by some Clostridial spp can upregulate T regulatory cells. Bile salt hydrolase enzymes from bacteria within the intestinal tract contribute to the enterohepatic circuit, and these are reduced during flares of IBD (Ni et al., 2017). This suggests that microbiota may be a key target for novel therapies in IBD (Ni et al., 2017).

1.7 Thesis rationale

MIF is a cytokine with wide ranging effects: it has been explored extensively in the context of type 1 infections with data focusing on macrophages.

Little data are available in type 2 responses, and the mechanisms by which MIF mediates type 2 immunity. MIF-deficient mice were compared with wild type mice to explore the differences in innate immune cells such as macrophages, eosinophils and innate lymphoid cells. In addition the epithelial phenotype (crucial in expelling *N. brasiliensis*) was assessed. The importance of MIF in organogenesis, led us to look at inhibiting MIF during the infection through 4-IPP as well as using the MIF-deficient mouse. We assessed the ability of rIL-25 to rescue the MIF phenotype due to the importance of MIF in recruiting innate lymphoid cells. The ligands of MIF are known to be CXCR2. CXCR4 and CD74. We finally assess the MIF ligand CXCR2 and how a deficiency of CXCR2 affects the immune responses to *N.brasiliensis*. We explored the response to primary infection (using *N. brasiliensis* and *H. polygyrus*), and secondary infection (using *H. polygyrus*).

Work in our laboratory is being conducted into the effects of HES on pathology generated in 3 different models of colitis, evoked by T cell transfer, DSS in drinking water, and anti-CD40 antibody treatment. The T cell transfer model involves infusion of the CD45RBhi subpopulation of CD4+ cells from normal BALB/c mice into recombination activating gene (RAG) deficient mice (Powrie et al., 1993), DSS-mediated colitis induces a chemical colitis from damage to the epithelial layer(Kiesler et al., 2015). The anti CD40 model of colitis involves injection of anti-CD40 which subsequently activates CD40+ APCs. In RAG deficient mice, this results in a systemic inflammatory response that results in weight loss and diarrhoea that is mediated by the innate immune system (Uhlig et al., 2006). Therefore, in order to explore the effect of HES specifically on the innate system we used the anti-CD40 model of colitis (Chapter 3). When assessing the effect of recombinant molecules, few previous studies have utilised modified recombinant proteins as controls. We aimed to further the work with HES by exploring recombinant proteins shown to modify other immune models such as TGM.

Chapter 2: General Methods

2.1 Mouse strains

BALB/c, C57BL/6, MIF-/-, RAG1-/- STAT3LysMCre , F1 (C57BL/6 x CBA) mice were bred in-house in Edinburgh and Glasgow. The MIF-/- mice were obtained by Rick Maizels from Dr Abhay Satoskar, Ohio State University in July 2006 and are on a BALB/c background (Bozza et al., 1999). The RAG1-/- mice were acquired from Professor David Gray, and are on a C57BL/6 background (Mombaerts et al., 1992). The STAT3LysMCre were obtained from Dr Susanne Nylen at the Karolinska institute. These were housed in individually ventilated cages (IVCs) according to UK Home Office guidelines.

MIF-/- have a neo cassette disrupting 2-3 exons of the MIF gene abolishing gene expression: this was electroporated into 129S4/SvJae-derived J1 embryonic stem (ES) cells injected into C57BL/6 blastocysts. The chimeras were backcrossed to BALB/cAnNTac mice for a minimum of 6 generations (Jax.org).

2.2 Cell isolation and culture

2.2.1 L929 culture (M-CSF)

The L929 fibroblast cell line was grown in cDMEM and incubated at 37°C with 5% CO2 in T75 flasks. Supernatants were harvested 3 days later when

cells were confluent and passed through a 0.22µm filter. The supernatant was stored at -20°C until it was required for macrophage growth. For L929 cell line passage, cells were dissociated with trypsin and resuspended in cDMEM.

2.2.2 Bone marrow macrophages

Approximately 10 million bone marrow derived cells were obtained from the tibia and femurs per mouse(Wagner et al., 2014). A single cell suspension was formed in 10mls of PBS by passing through a 23g needle. This was filtered through a 100µm nylon cell strainer. Cells were plated at a density of 6 x 10^6 cells/ plate on 90mm petri dishes (Fisher 11309283) in 10ml cDMEM with 20% L929 media as a source of M-CSF and incubated at 37°C with 5% CO2. A further 5ml of cDMEM with 20% L929 was added on day 3. Macrophages were harvested on day 7 using 3mM EDTA/10mM glucose in PBS. Cells were washed in PBS, resuspended in cDMEM and plated at 2 x 10^5 cells/ well in 96 well plates for stimulation.

2.2.3 Anti-CD40 antibody purification

The FGK45 hybridoma cell line was gifted to the laboratory by Dr David Gray (Edinburgh): it produces an IgG2a anti-CD40 antibody. It was grown up initially in T25 cRPMI before resuspending at 5 x 10^5 cells in cRPMI with low IgG FCS. Supernatants were collected 7 days later, when the cells were confluent, and sterile filtered. 100mls of supernatant was then applied to a HiTrap Protein G 5ml column in binding buffer (2x PBS). The immunoglobulin was then eluted in 0.1M glycine-HCL (pH 2.7) either using the AKTA chromatography system or manual elution with a minipuls pump. Samples were collected in 120µl 1M Tris-HCL pH9.0 for each 2ml fraction to be collected.

3mls of eluted antibody was then dialysed 3 times in 5 litres of PBS at 4°C. This was then sterile filtered through a 0.22µl filter, and protein concentration was measured on a Nanodrop instrument. The antibody was then diluted to 1 mg/ml PBS for use in vivo, with mice receiving 200 µg in 200 µl. An isotype control antibody was used as a comparator in experiments (ThermoFisher Catalogue no. 10700).

2.3 Ex vivo techniques

2.3.1. Peritoneal lavage

Five ml of ice cold cDMEM was instilled into the peritoneal cavity of mice. This was then gently shaken in order to dislodge any cells. Up to 5 ml was then aspirated out of the peritoneal cavity. This process was repeated once more and samples pooled for each mouse. Fluid was then taken for CBA and ELISA, cells were taken for flow cytometry analysis and qPCR. The cells were spun down and then resuspended in 1 ml of red blood cell lysis buffer (11814389001 Roche) for 3 minutes at room temperature. The cells were then resuspended in 3 ml cDMEM for counting on Nexelecom cellometer.

2.3.2 Mesenteric lymph node single cell suspension

Mesenteric lymph nodes were retrieved from the abdominal cavity of mice and placed in cRPMI on ice. These were then mashed through a 70 µm cell strainer and resuspended in 10 ml of cRPMI for cell counting manually using the Trypan blue assay or through the Nexelecom cellometer.

2.3.3 Peritoneal populations isolation

Peritoneal lavage was obtained from mice by flushing two 5ml washes of ice-cold cDMEM into the peritoneal cavity to obtain peritoneal exudate cells (PEC). The samples for each mouse were placed on ice till the following step. The cells were spun down at 350g for 5 minutes at 4°C (this was for every spin step) and counted using a Nexelecom cellometer. The cells were processed using the Miltynei macrophage isolation kit (peritoneum), mouse (Cat 130 110 434) as follow. First, the cell suspension was centrifuged at 300g at 4°C for 20 minutes, and the supernatant discarded, pelleted cells were resuspended in 36 µl of PBS with 0.5% BSA. Following this, 10µl of Macrophage Biotin-Antibody Cocktail were added per 10^7 cells and incubated for 10 minutes at 4°C. Cells were then washed in Automacs buffer and then resuspended in 80 µl of PBS with 0.5% BSA with 20 µl of Anti-Biotin Microbeads. These were incubated for 15 minutes at 4°C and washed in 1ml of Automacs buffer, spun at 300g at 4°C for 10mins, then resuspended in 500µl of PBS with 0.5% BSA. Magnetic separation was performed with the autoMACS Pro Separator using the **deplete** operation. Cells were then resuspended in Trizol for RNA extraction downstream. The full protocol is available as below:

(http://www.miltenyibiotec.com/en/products-and-services/macs-cell-separation/cell-separation-reagents/monocytes-and-macrophages/macrophage-isolation-kit-peritoneum--mouse.aspx)

In order to assess which of the immune cells in the peritoneum expressed MIF during *N.brasiliensis* infect, peritoneal exudate cells were isolated from BALB/c infected and uninfected mice for cell sorting by Dr Maddie White. These were surface stained with AF647 Siglec F, FITC CD19, PercpCy5.5 CD4, PB Cd11b and PeCy7 F4/80 as per protocol in 2.5.1. The cells were

then sorted on a FACS ARIA directly into Qiagen RLT buffer (Qiagen: 79216) at a ratio of 100µl of volume into 300µl of RLT buffer.

2.4 Helminth Infection

2.4.1 *Nippostrongylus brasiliensis* infection

N. brasiliensis was maintained by serial passage through Wistar or Sprague-Dawley rats following a protocol similar to that described by(Camberis et al., 2003). Third stage larvae (L3) were washed three times in sterile PBS and then injected subcutaneously with a 23G needle into the back of the mice. Mice were infected with 250-400L3 of *N. brasiliensis* on D0 in 200µl PBS.

2.4.2 *Heligmosomoides polygyrus* infection model

H. polygyrus were maintained by serial passage through male CBAxC57BL/6 F1 mice(Johnston et al., 2015). The third stage larvae (L3) were obtained from charcoal larvae plates and were washed three times in distilled water. Mice were gavaged with 200 L3 in 200 µl of distilled water.

2.4.3 Egg and Worm counts

For faecal egg counts, two faecal pellets were obtained per mouse and weighed, then suspended in 1 ml of distilled water; 1 ml of f saturated salt solution was added just before counting in a McMaster egg counting

chamber. Egg counts were adjusted to represent eggs per gram of faeces. For adult worm burdens, the small intestine was removed and sliced longitudinally, and worms were counted as they were manually removed from the intestinal lumen.

2.4.4 Secondary *Heligmosomoides polygyrus* infection

For a secondary infection, we followed previously published protocols (Hewitson et al., 2011). Mice were infected with 200 L3 *H. polygyrus* for 28 days, following which they were administered 2 doses of 2.5mg pyrantel embonate (Strongid-p paste) dissolved in 200µl of distilled water on day 28 and day 29. Mice were then re-infected with 200 L3 and levels of parasite infection evaluated 14 days later.

2.4.5 Production of HES

The collection of HES is described in (Johnston et al., 2015) In brief, 8 week old F1 mice are gavaged with 400L3 of *H polygyrus* in 200ul of distilled water. On the 14th day of infection, 20cm of proximal intestine that has the adult worms is removed and placed in a petri dish with 5mls of Hanks' solution in 30°C. The inside of the gut lining is scraped and worms removed with a glass slide. The worms from two petri dishes are then placed in a muslin bag and then funnel in Hanks' solution at 37°C for 1-2 hours. The worms are then washed six times with Hanks solution. The worms are subsequently moved to a laminar flow hood and washed in RPMI supplemented with supplemented with 1.2% glucose, 5U/ml penicillin, 5µg/ml streptomycin, 2mM of L-glutamine and 1% gentamycin. The worms are aliquoted into vented T25 flasks, with approximately 1000 worms in 15ml of *H.polygyrus* media per flask and placed in 37°C at 5% CO2 for 3 weeks.

HES is collected from *H. polygyrus* cultured in the above parasite media for 21 days, centrifuged at 400g for 10 minutes to remove eggs and then concentrated over a 3000 MW cut-off membrane in an Amicon Diafiltration pressue cell (Millipore). Approximately 1L of media was concentrated to 5ml, sterile filtered through a syringe-tip 0.2µm filter (Millipore) and frozen at -80°C.

2.4.6. Anti-CD40 colitis

RAG1-/- mice on a C57BL/6 background were injected with 200µg in 200µl of anti-CD40 antibody or a Rat IgG isotype on D0 intraperitoneally. Mice were also given 10µg HES i.p. daily in 200µl PBS or 200 µl PBS daily from D-1 to D6. The mice were then scored using a disease activity score (Table 2.4.1) for 7 days. Mice which reached severity threshold or lost greater than 25% body weight were culled prior to the intended end of the experiment. Mice were harvested at D7 and intestine embedded in paraffin for histology. Tissues were also taken for flow cytometry and qPCR. These mice were scored via a disease activity score (adapted by Dr Danielle Smyth from the David Artis lab) and a global histology score devised by Professor Mark Arends (Edinburgh) as presented in Table 2.4.2. The experiment was not blinded for disease activity score assessment and weights. However, the histology was blinded and was assessed by two independent histopathologists.

Parameter	Score
Body weight	**0** No weight loss
	1 1-5%
	2 5-10%
	3 10-20%
	4 >20%
Blood in stool	**0** No blood
	1 Blood present in/on faeces
	2 Visible blood in rectum
	3 Visible blood on fur
Stool consistency	**0** Well formed/normal
	1 Pasty/semi-formed
	2 Pasty/some blood
	3 Diarrhoea that does not adhere to anus
	4 Diarrhoea that adheres to anus
General appearance	**0** Normal
	1 Piloerection only
	2 Lethargy, piloerection
	4 Motionless, sickly, sunken-eyes, ataxic

Table 2.4.1 Anti CD40 colitis disease activity scoring

Histological parameter
1 **Degree of Crypt loss**
2 **Ulceration**
3 **Crypt abscesses**
4 **Goblet cell loss**
5 **Mucosal inflammatory infiltration**
6 **Sub-mucosal inflammatory infiltration**

Table 2.4.2 Histology score

2.5 Flow Cytometric analysis

2.5.1 Surface staining for flow cytometry

PEC were plated at 1 x 10^6 cells/well in 96 well round bottom plates (Corning). Cells were washed in PBS (all washes are performed at 350g for 5 minutes in 4°C) and then incubated in 200µl of live/dead stain, followed by 10 minutes in CD16/32 Fc block (eBioscience) and then surface stained in a 30 µl master mix of FACS buffer, at concentrations shown in table 2.5.1 . Fixation was performed by incubating in 200 µl of eBioscience (Foxp3) fix perm solution (diluted 1 part to 3 parts of the provided diluent) (ThermoFisher 00-5523-00) for 45 minutes if transcription factor analysis was required..

Where staining of intracellular proteins (such as Arg1, RELMα and Ym1) was required, surface fixation was performed using 200µl of eBioscience intracellular fixation buffer (Cat 00-8222-49) for 20 minutes. This surface staining method retained the forward side scatter properties of the cells better than the Foxp3 fix perm solution. Fluorescence minus one (FMO) controls were used for each experiment. Spare samples were pooled from both infected and uninfected mice, and these were stained with a cocktail that included all the stains but one. FMO controls were performed for each stain used.

2.5.2 Intracellular staining

For either transcription factor analysis or for intracellular proteins, cells were permeabilised using eBioscience Perm buffer and incubated for 20 minutes, followed by intracellular staining. Primary antibody for RELMα or Ym1 was applied for 20 minutes followed by secondary antibody for 20 minutes. The cells were then left in FACS buffer and acquired on BD LSRII, Fortessa or

Celesta. Between each step two washes were performed, in PBS (for the extracellular stains) or in Perm buffer for the intracellular staining steps. Single stains were performed on ebioscience compensation beads. Cells were filtered through a 100µm mesh prior to acquisition.

2.5.3 Phosflow

In order to assess differences in phosphorylation of signal transducer and activation of transcription factors (STATs), the fixation is performed at specific time points, with any surface and intracellular staining performed afterwards. This is because phosphorylation of the STATs occurs early. Accurately stopping further reactions by fixation terminates further changes in phosphoration and allows for accurate comparisons.

The phosphorylations is performed as per the BD Perm buffer IV protocol. 50ml of 10x BD Lyse/Fix Buffer (Cat No. 558049) was diluted to 1x in distilled water and prewarmed to 37°C at prior to use. Cells were stimulated in FACS tubes and kept in a 37°C incubator between stimulation periods. Stimulations were performed in a 200µl maximum volume, at the end of stimulus 2 ml of prewarmed Lyse/Fix buffer was added to end any reactions. Following a final incubation at 37°C for 15 minutes, cells were centrifuged at 400 g at 4°C for 10 minutes and supernatant discarded. The fixed leukocytes were washed once in PBS, and pelleted at 400g for 10 minutes at 4°C. 1ml of 1.0x BD perm buffer IV (Cat 560746) was added dropwise to each tube and incubated at room temperature for a total of 15 minutes. This was then centrifuged at 400g for 10 minutes at 4°C. Cells were washed twice in FACS buffer and then incubated in both intracellular and extracellular antibodies overnight at 4°C. Cells were washed twice and data then acquired on BD Fortessa/Celesta instruments.

2.5.4. Lung digestion

Mouse lung was collected in 5ml of PBS. Liberase TL was made up in water at 13U/ml of Liberase in water (Sigma: 054010200001). A digest mix was made using HBSS with calcium and magnesium and 1% Penicillin/Streptomycin. 2U/ml of Liberase and 160 units/ml of DNAse added to this digest mix. The lung from each mouse was snipped into 2mm pieces and subsequently transferred into 1 ml of digest mix with liberase and DNAse. The bijoux are transferred into a 37°C shaking incubator (at around 200rpm) for approximately 35 minutes. After incubation in the shaking incubator, the solution is topped with 5ml of cRPMI and mashed through a 70µm cell strainer. The solution was spun at 400g for 5minutes at 4°C and red cell lysis was performed as previously described.

2.5.5. Lamina propria preparation

Lamina propria preparations followed the protocol set out for the lamina propria dissociation kit by Miltynei biotech (Cat 130-0970410). First, enzymes A, D and R (provided in the miltynei lamina propria kit) were reconstituted in HBSS (w) (HBSS with calcium and magnesium) as per protocol. Small intestine from 6-10 week old mice were flushed with PBS and then placed in a petri dish in HBSS (w/o) (HBSS without calcium and magnesium). Residual fat and peyer's patches were removed and discarded. This is as residual fat is known to lead to less viability in the prep and inclusion of immune cells peyer's patches will contaminate the lamina propria sample. The intestine was cut into 3cm pieces and then transferred into 50ml Falcon tubes containing 20ml predigestion solution (1x HBSS (w/o) containing 5mM EDTA, 5% FBS, 1mM DTT). The sample was incubated for 20 minutes at 37° C under continuous rotation using the MACSmix Tube Rotator. The contents were then applied to a 100 µm smart strainer and transferred into a new 50ml tube containing 20 ml of fresh predigestion solution. This process was

repeated twice. The samples were then incubated for 20 minutes in HBSS (w/o) and then placed in the digestion solution (1x HBSS (w) containing 5% FBS) in "Gentle MACS" C tubes on programme 37_m_LPDK_1. After the programme has run the sample is resuspended in PBS with 1% BSA. Full protocol details and buffers are available at http://www.miltenyibiotec.com/en/products-and-services/macs-sample-preparation/tissue-dissociation-kits/lamina-propria-dissociation-kit-mouse.aspx.

2.5.6. Gating Strategy

In Gating strategy 2.5.6.1, the flow cytometric analysis of peritoneal macrophages is described. In the top row from left to right, we first gate Side scatter against forward scatter to capture the majority of the cells in the lavage, going right we gate out the doublets by plotting FSC-H against FSC-A. Next we gate out any cells that are positive for live dead stain (and therefore are alive). The last gate is Siglec-F against Cd11b, we gate out the cells that are Siglec-F positive and thus exclude eosinophils from the macrophage gate. In the next row we proceed then look at F4/80 vs Cd11b and this gate- we define the F4/80, Cd11b high populations as the macrophages in the peritoneal cavity. The next plots demonstrate the percentages of macrophages that are positive for Ym1 and RELMα and the isotype controls.

In gating strategy 2.5.6.2, the gating for mesenteric lymph node innate lymphoid cells and TH2 cells is described. On the top line from left to right we gate out any duplicates by plotting FSC-A vs FSC-H, in the next plot we exclude dead cells, and cells that are beyond the expected FSC-A and SSC-A subset. On the next line we include CD45 positive cells, and split these into those that are positive for CD4, and those that are negative for CD4. We calculate the percentage of TH2 cells by gating the GATA3 positive

population of CD4 cells. We then go on to gate the CD4 negative cells and choose the cells that are negative for lineage markers but positive for ICOS. We have used the GATA3 staining to confirm the percentages of ICS2s (defined here as $CD45^+$ $CD4^-$ Lin- $ICOS^+$ $GATA3^+$ cells). These are compared to their FMOs.

In gating strategy 2.5.6.3, the gating strategy of peritoneal macrophages is described. In 2.5.6.3-1 from left to right we gate FSC-H against FSC-A to obtain single cells, then we gate the live population of cells by gating Live/Dead vs FSC-A. Then we gate out eosinophils as Cd11c int and Siglec F positive cells. In figure 2.5.6.3-2 we gate Cd11b vs Cd11c. Those populations that are positive for Cd11c and negative for Cd11b are gated against Siglec F. The population of cells that are positive for Siglec F are labelled alveolar macrophages. The population of cells that are Cd11b positive and F4/80 positive are labelled as interstitial macrophages.

In gating strategy 2.5.6.4, the gating strategy of MLN FoxP3 positive CD4 cells is described. From left to right in the top figures we gate single, live CD45 positive cells. We then gate on CD3 and CD4 positve cells which are described as T cells. We then choose those CD4+ T cells that are positive for FoxP3. We also include CD25 as a separate marker, although this is not used in the analysis.

2.5.6.1 Gating Strategy- Peritoneal Lavage Macrophages (Alternatively Activated) /Eosinophils

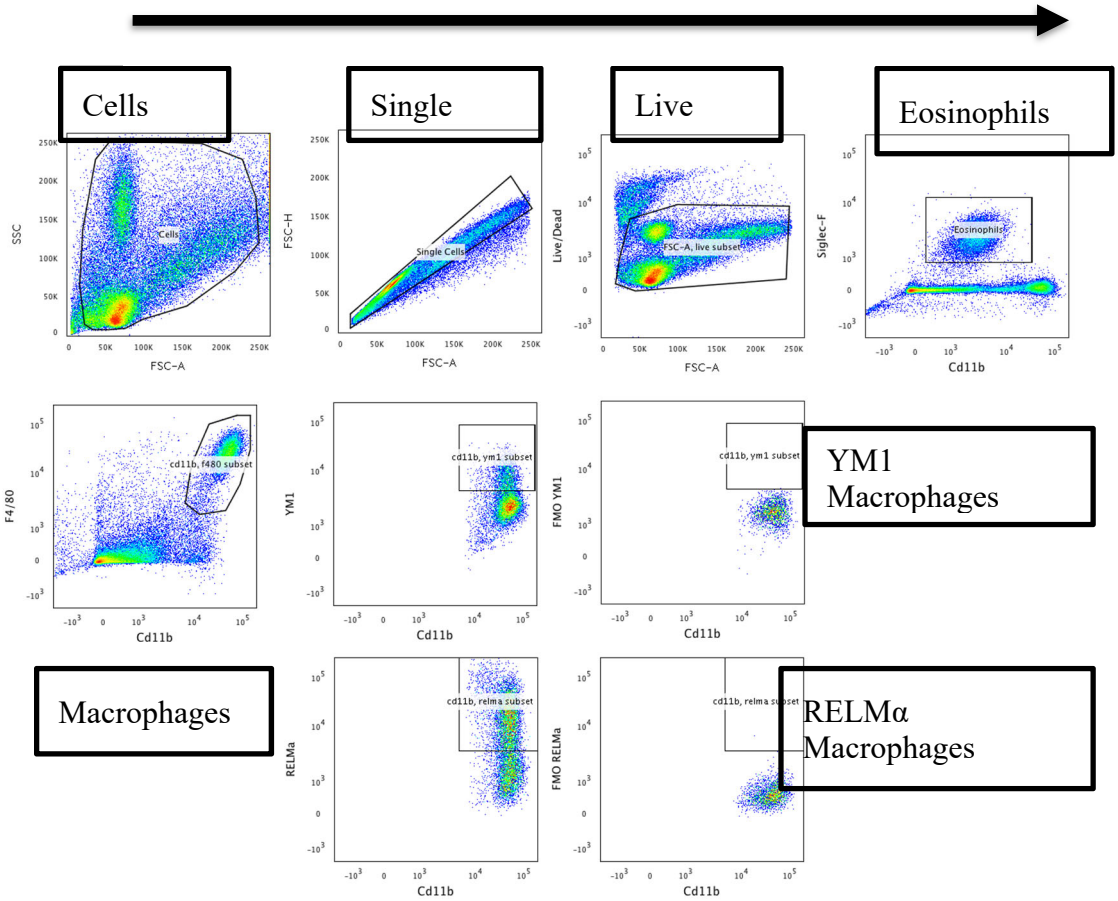

Figure 2.5.6.1 Peritoneal lavage gating strategy

2.5.6.2 Gating Strategy- MLN ILCs and TH2

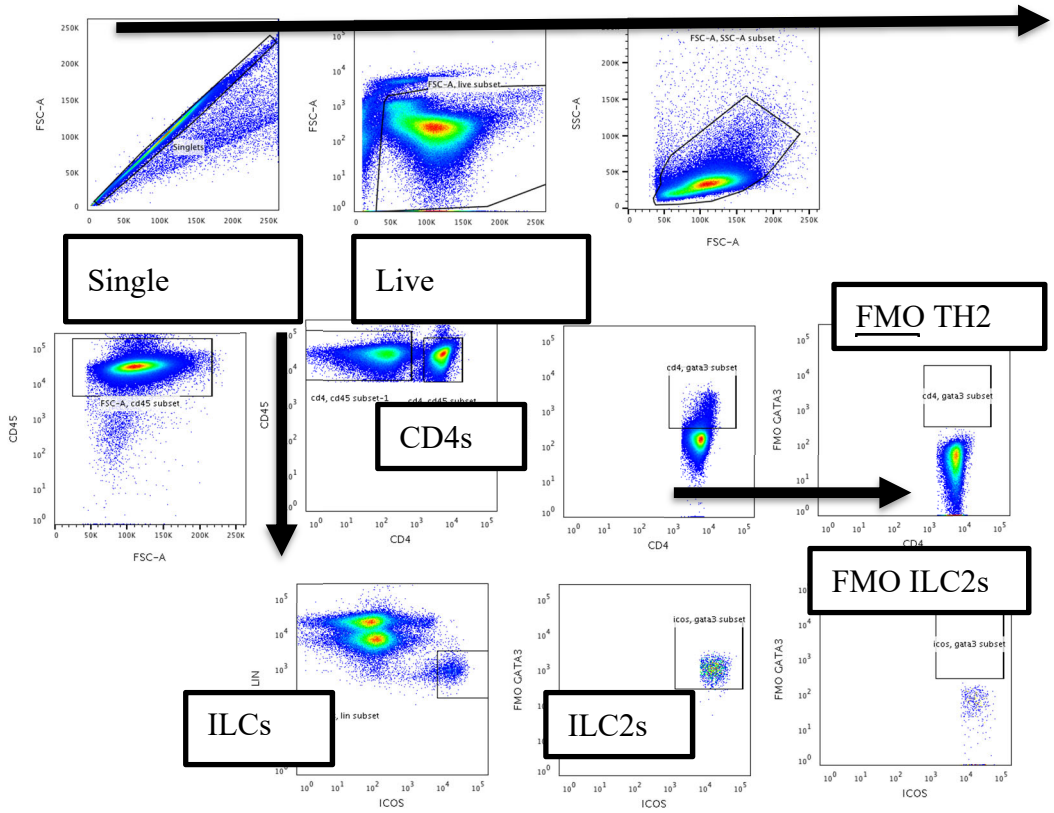

Figure 2.5.6.2 Gating Strategy MLN ILCs/TH2

2.5.6.3 Lung Macrophages Gating Strategy-1

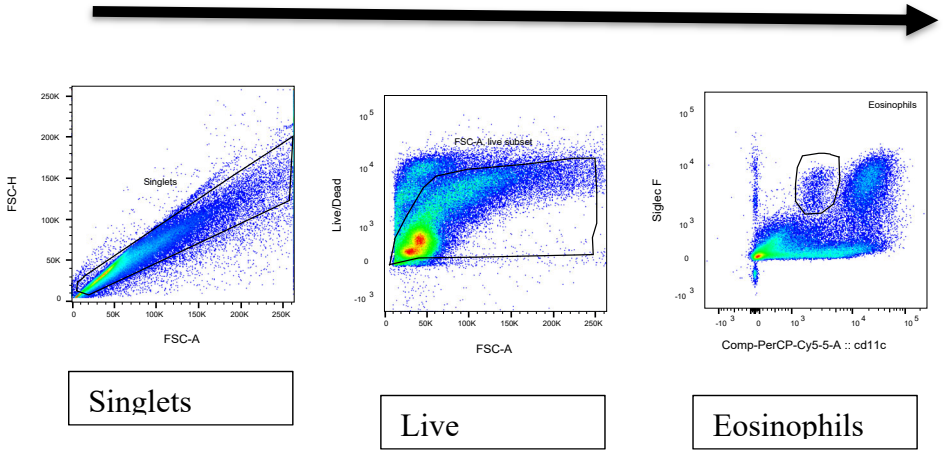

Singlets

Live

Eosinophils

2.5.6.3 Lung Macrophages Gating Strategy-2

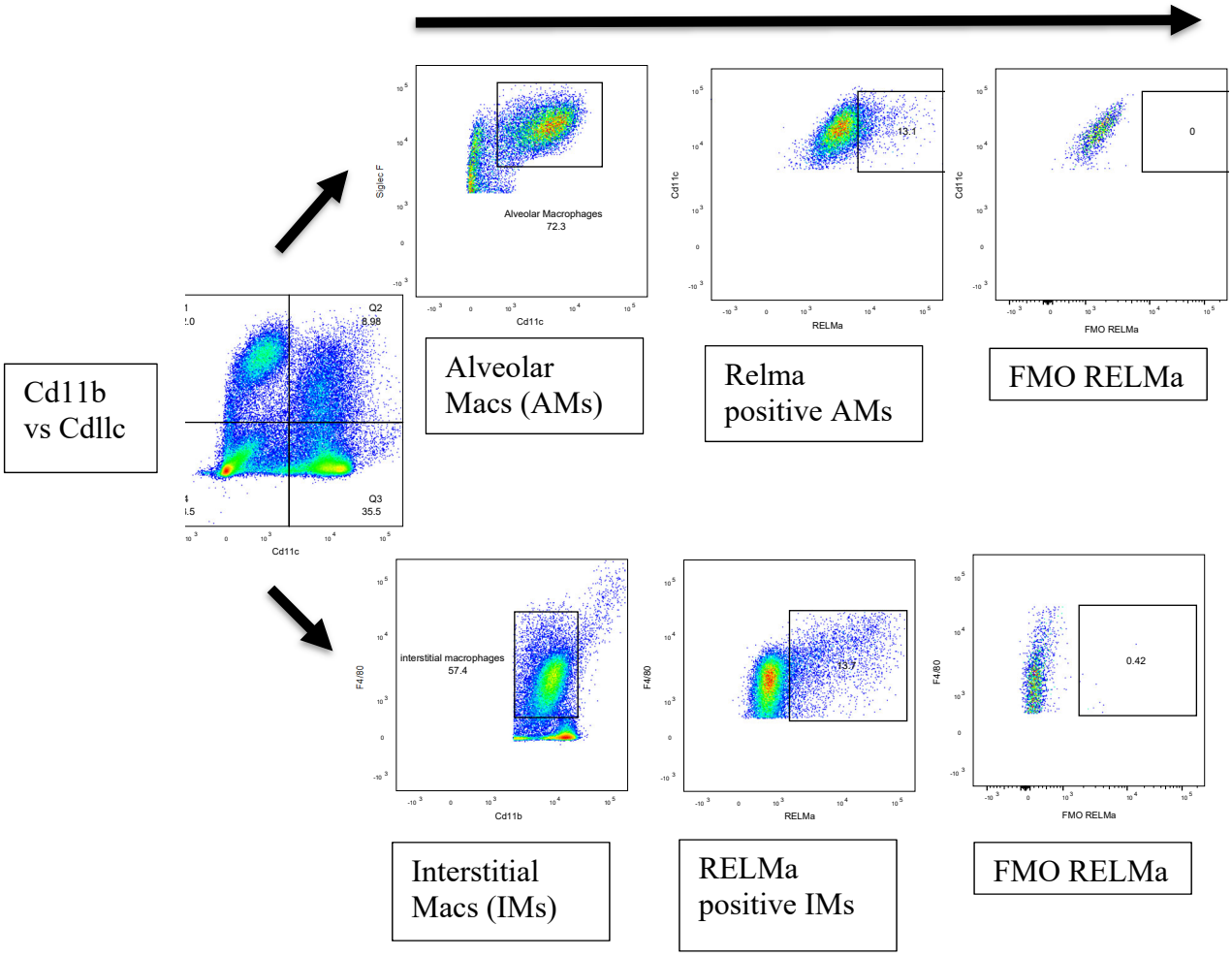

Figure 2.5.6. 3 Lung Macrophages Gating Strategy-2

2.5.6.4 MLN FOXP3 gating strategy

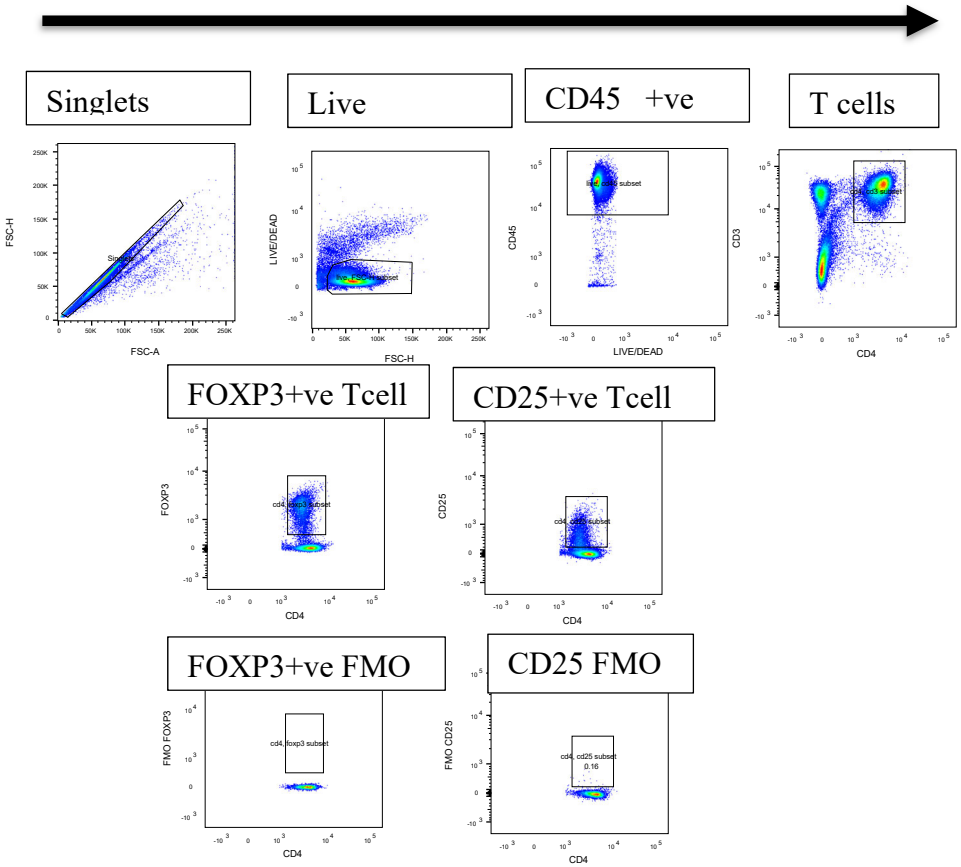

Figure 2.5.6.4 MLN FOXP3 gating strategy

Table 2.5.1 Antibodies used for flow cytometry						
Specificity	**Flurochrome**	**Clone**	**Manufacturer**	**Dilution**	**Isotype**	**Catalogue Number**
Live Dead stain						
Live/dead	Ef506		ebioscience	1/1000		65-0866-14
FC receptor block						
CD16/32 (Fc block)	-	93	ebioscience	1/100	-	16-0161-82
Macrophage Panel						
Cd11b	PB	M1/70	Biolegend	1/200	Rat IgG2b, k	101224
F4/80	PerCpCy5.5 PeCy7	BM8 BM8	Biolegend Biolegend	1/200 1/100		123128 123114
Arginase1	PE	Polyclonal	R&D systems	1/100		IC5868P
RELMα	Uncoupled	Polyclonal	Preprotech	1/100 of 100µg/ml		500-P214
Ym1	uncoupled	Polyclonal	R&D systems	1/25		BAF2446
Zenon AF488/AF647 Rabbit IgG	AF488, AF647	Polyclonal	Life technologies	1/200		Z25302 (AF488), A20186 (AF647)
CD206	BV711 AF647	15-2	Biolegend	1/400		141727 141712
pSTAT3	PE	pY705	BD	5µl per test	IgG2a, K	562072
pSTAT6	AF647	pY641	BD	5µl per test		558242
Siglec F/CD170	PE BUV395	E50-2440 E50-2440	BD BD	1/200 1/100		552126 740280
Ly6G	APC	1A8	Biolegend	1/100		127614
ILC/T cell Panel						
KLRG1	BUV395	2F1	BD	1/100		740279
CD45	PERCPCy5.5	30-F11	Biolegend	1/100		103132
GATA3	AF488	16£10A23	Biolegend	5µl/test		653806
LIN	BV421	17A2/RB6-8C5/RA3-6B2/Ter-119/M1/70	Biolegend	1/20		133311
CD4	PE	GK 1.5	Biolegend	1/100		100408
FOXP3 T regulatory cell panel						
CD25	FITC	3C7	Biolegend	1/100		101908
CD4	PerpCy5.5	GK1.5	Biolengend	1/100		100432
CD45	PeCy7	I3/2.3	Biolegend	1/100		103114
CD3e	PE	145-2C11	Biolegend	1/100		100308
FOXP3	Ef450	FJK-15s	ThermoFisher	1/100		653808
MIF Receptor Panel						
CD74	FITC			1/100		
CXCR2/CD182	AF647	SA044G4	Biolegend	1/100		149306
CXCR4	BV711	L276F12	Biolegend	1/100		146517

Table 2.5.1 FACS Antibodies

2.6 RNA isolation and qPCR

2.6.1 RNA isolation

To isolate mRNA from whole tissue, samples were first immersed in Trizol (Qiagen) and stored at -80°C until processing. The, samples were lysed for 2 minutes in 1ml of Trizol in Qiagen. Samples were then spun down in centrifuge and supernatant aspirated, the supernatant from each sample was then placed in labelled RNA free tubes. Samples were isolated with Qiagen mRNA easy kits (Qiagen: 74106). If cell sorting of single cells was performed, these were sorted directly into RLT buffer and stored at -80°C until analysis.

The following steps are part of the mRNA easy protocol (Qiagen). 140µl of chloroform was added to each tube and shaken vigorously for 15 seconds. Tubes were then stood on the benchtop at room temperature for 5 minutes. Samples were then centrifuged for 15 minutes at 12000g at 4°C. The upper aqueous phase was transferred to a new collection tube without interrupting the white phase between the two layers. 1.5 volumes of 100% ethanol were added, mixing thoroughly by pipetting and up and down several times. Up to 700µl was placed in RNeasy spin columns and centrifuged 8000g for one minute at room temperature. 350µl of Buffer RW1 (which contains ethanol, RWT for the microRNA kit) was added onto the columns and centrifuged at 8000g for 1 minute. Then, 10µl of DNase1 was added to 70µl of RDD buffer, and the 80µl mixed volume was placed onto spin columns and incubated for 15 minutes. A further 350µl of Buffer RW1 was added and centrifuged again at 8000g for 1 minute. 500µl of Buffer RPE was added, before centrifuging again at 8000g for 1 minute. A second aliquot of 500µl of Buffer RPE was

added onto spin columns and spun for 2 minutes at 8000g. The spin columns are transferred into new collection tubes and centrifuged at >1000g to remove the excess ethanol. These spin columns were then placed in RNA free tubes. Add 40µl of RNAse-free water to column (wait 2 minutes) and then centrifuge >8000g. The water will then elute RNA from sample and thereby you will have the final RNA in water.

2.6.2 cDNA production with qScript (Quiagen)

The cDNA synthesis kit includes oligo-DT which binds the 3' end of the mRNA, a reverse transcriptase which makes the cDNA from template RNA and dNTPs. The RNA concentration and purity measured using a NanDrop 2000 (Thermo Scientific). 1 µl of oligo-DT primer was added to 1µg RNA in 15µl RNase free water and incubated for 10minutes at 70°C, after which the sample was cooled son ice for 5 minutes. 8µl of cDNA master mix was added before following the manufacturer's protocol (Table 2.5.1)

MasterMix	Volume	Protocol	Time
5xqSript Reaction Mix	4µl	22°C	5min
qScript RT	1 µl	42 °C	30min
RNA 250-500ng	15µl	85 °C	5 min
		4 °C	hold

Table 2.6.2.1 cDNA synthesis

2.6.3 Real time PCR

Primers used (synthesized by Eurofins or Sigma). Lyophylised primers were reconstituted at 100μM in RNA free water and stored in -20°C. 10μM working stocks were generated by dilution of primers in RNA free water.

cDNA was diluted 1/5 and a 1μl of each sample pooled for use as a top standard. Standards were serially diluted ¼ to obtain at least 6 standards. 2μl of standard was added to 4μl of master mix and added to a 384 well plate. qPCR runs were performed using the Applied Bioscience Quantstudioflex 7. Analysis was performed by a delta-delta Ct method.

Programme	Cycles	Target	Hold
Pre-incubation	1	95°C	2-3 minutes
Amplification	40	95°C 60°C	15 seconds 1 minute
Melting curve	1	95°C 65°C 97°C	5 60 continuous

Table 2.6.3.1 qPCR cycling conditions

Primer	Protein	Primer sequence
Arg1	Arginase 1	F: GTC TGT GGG GAA AGC CAA T R: GCT TCC AAC TGC CAG ACT GT
ARL2BP	ADP-ribosylation factor-like binding protein	F: CGTATCCCAGGCTTCAACA R: TGTGAGCAGCATGTCAAAGA
CXCR2	C-X-C motif chemokine receptor 2	F: CTACTGCAGGATTAAGTTT R: GACGTATATTACAACCACA
CHAT	Choline Acetyl Transferase	F: TCCTCTTAAAAGACTCCACC R: GACTTGTCATACCAACGATTC
DCLK1	Doublecortin-like kinase 1	F: CAGCCTGGACGAGCTGGTGG R: TGACCAGTTGGGGTTCACAT
GAPDH	Glyceraldehyde-3-phosphate dehydrogenase	F: ATGACATCAAGAAGG R: CATACCAGGAAATGAAAATGAGTTG
GATA3	Transacting T-cell-specific transcription factor GATA-3	F: GGG TTC GGA TGT AAG TCG AG R:CCA CAG TGG GGT AGA GGT TG
HPRT	Hypoxanthine phosphoribosyltransferase 1	F: AGGGATTTGAATCACGTTTG R: TTTACTGGCAACATCAACAG
IL-25	Interleukin 25	F: TGG AGC TCT GCA TCT GTG TC R: CGA TTC AAG TCC CTG TCC A
IL-5	Interleukin 5	F: ACA TTG ACC GCC AAA AAG AG R: ATC CAG GAA CTG CCT CGT
IFNG	Interferon gamma	F: TGAGTATTGCCAAGTTTGAG R: CTTATTGGGACAATCTCTTCC
MIF	Macrophage migration inhibitory factor	F: ACA GCA TCG GCA AGA TCG R: GGC CAC ACA GCA GCT TAC T
PGDS	Prostaglandin-D synthase	F: TTCAACAAGACAAGTTCCTG R: GAAGGTAGAGGTGAGATTGAG
PHC2	Polyhomeotic 2	F: CCC ACA AAA TGG AAT GTA GAG G R: ACT CCT CCG CGA TCT CCT
RETLNA	Resistin-like alpha	F: TAT GAA CAG ATG GGC CTC CT R: GGC AGT TGC AAG TAT CTC CAC
RETLNB	Resistin-like beta protein	F: CGT CTC CCT TTT CCC ACT G R: CAG GAG ATC GTC TTA GGC TCT
S100a8	S100 calcium binding protein A8 (calgranulin A)	F: TCCTTGCGATGGTGATAAAA R: GGCCAGAAGCTCTGCTACTC
YM1/ Chil3	Chitinase-like 3	F: TCA CAG GTC TGG CAA TTC TTC TG R: TTG TCC TTA GGA GGG CTT CCT C

Table 2.6.3.2 Table of primers utilized for qPCR

2.7 Histology

2.7.1. Swiss rolls

Gut tissue from mouse models were removed intact, the intestines were washed in PBS and then everted onto a bamboo skewer. These were fixed for 4 hours in 10% NBF, then cut and rolled into the swiss roll structure. The rolls were stored in double height cassettes in 10% NBF overnight and then in 70% ethanol before paraffin fixation and cutting. The Swiss rolls were H&E stained by the Histopathology Department in Edinburgh Royal Infirmary and in the Sir Graeme Davies Building in Glasgow by Ms Nicola Britton.

2.7.2. Periodic Acid Schiff Goblet cell staining and quantifications

Slides were first de-paraffinised and rehydrated as follows. Slides were heated in an oven at 60°C for 20 minutes. The slides were washed and then immersed in Xylene 2 x 5 minutes, 100% ethanol 2 x 5 minutes, 100% ethanol 2 x 3 minutes, 90% ethanol 2 x 3 minutes, 70% ethanol 2 x 3 minutes and then rinsed in tap water for 3 minutes. They had a final rinse in distilled water. Following this the slides were stained in Alcian blue (pH 2.5) for 10 minutes, washed in distilled water for 3-5 minutes and then treated with periodic acid 1% solution for 10 minutes. Slides were then washed and then stained in Haemalum Mayer for 30 seconds, followed by rinsing in running tap water. Excess stain was removed in running water. Slides were then dehydrated, cleared and mounted as follows: 70% ethanol 2 x 3 minutes, 90% ethanol 2 x 3 minutes, 100% ethanol 2 x 3 minutes, xylene 2 x 3 minutes. Slides were covered with a coverslip and mounting media and allow to dry.

Quantification was performed by counting the number of goblet cells per villus and crypt unit and taking an average of 100 counts per sample.

2.7.3 DCLK1 and RELMß staining

Slides were deparaffinised as above in the PAS staining protocol. The slides were placed for 8 minutes in hot 10 mM sodium citrate buffer (pH 6.0) in a microwave (high setting) and then left to cool down for 15 minutes. Slides were then placed in a bucket with running tap water. The slides were washed twice for 15 minutes in TBS and 0.1% Triton X-100. Samples were then circled with a wax pen, following which block (10% donkey serum in 0.1% Triton-X100/TBS) was applied for 1 hour at room temperature. 200µl DCLK1 primary (abcam ab31704) was applied at a dilution of 1/1000 in TBS with 1% BSA and 0.1% Trition X-100. This was incubated overnight at 4°C. The next day the slides were rinsed twice for 5 minutes in TBS with 0.1% Triton X-100 and then apply 200 µl of secondary antibody (1:1000 donkey anti-rabbit AF555 ab150062; Abcam) in TBS with 0.1% Triton X-100. The slides were incubated for 40 minutes at room temperature. The slides were rinsed three times for 5minutes and then mount with mounting media containing DAPI.

2.8 CBA and ELISA

2.8.1 ELISA

On day 1 of the ELISA protocol, carbonate buffer was made up at appropriate dilutions. 96 well NUNC plate were coated with with 5 ml of coating antibody per plate, wrapped in clingfilm and placed in 4 °C overnight. On the second day of the protocol ELISA block buffer was made. The coating

antibody was thrown off and the plate washed in buffer four times. 150µl per well of block buffer was added to all plates and the plates were then wrapped in cling film. The plates were incubated for 2 hours at 37°C. Standards of the relevant cytokine were made up (these are the cytokines given at a certain concentration, that are doubling diluted down in order to give a standard curve against which the OD of our samples can be compared against) in PBS double diluted. After blocking, the plates were washed four times in TBS-T. 40µl of sample and 40 µl of standard was added to 96 well NUNC plate. These plates were wrapped in cling film and incubated at 4°C overnight. On the third day of the protocol, the plates were washed 6 times in TBST and detection antibody was made up in block buffer at the appropriate dilution. The plates were wrapped in cling film and incubated at 37°C for one hour. The plates were washed 4 times in TBST. The plates had 50µl of extravadin-AP added per well and were incubated at 37°C for one hour (Sigma E2636). They were then washed in TBST and dH2O. SIGMAFAST p-Nitrophenyl phosphate tablets (Sigma: 224-246-5) in dH20. 100 µl per well of detection reagent was added to the plates Plates were placed in a dark drawer for a couple of hours or overnight (depending on strength of signal) before reading on an Emax precision microplate reader (Molecular Devices) and concentrations extrapolated from standard curves determined by SoftMax Pro software (Molecular Devices).

Specificity	Capture Ab	Conc	Top standard conc	Detection Ab	Conc
RELMα (Peprotech)	Anti-RELMα (500-P214)	250ng/ml	100ng/ml	Biotinylated anti-murine RELMα (500-P214BT)	250ng/ml
Ym1 (R&D)	Anti-Ym1 (DY2446)	2880ng/ml	10000pg/ml	Biotinylated anti-murine YM1 (DY2446)	36µg/ml

Table 2.8.1 ELISA reagents and concentrations

2.8.2 Cytokine Bead Assays

Make up standards at top dilution of 2500pg/ml. Double dilute standards for 11 dilutions in CBA buffer (in a 96 well round bottomed plate-leave the first well as a blank). Add 50µl of sample into a 96-well round bottom plate. Make up capture beads master mix of each cytokine bead at 1/250 dilution and add 50µl of this master mix to each of the standards, samples and blank. Wrap in foil and leave at room temperature for one hour. Make up detection antibody master mix at 1/250 dilution. Add 50µl per well and leave at room temperature for one hour. Wash the plate in 100 µl and then 200 µl per well of CBA buffer spinning at 2000rpm for 5 minutes. Acquire sample on MasQUANT. In order to calculate the concentration of cytokine in supernatants, the PE MFI of each bead population was extrapolated to a standard curve generated from standards.

Capture Bead	Bead Coordinate	BD Flextest catalogue number
IL4	A7	558298
IL5	A6	558302
IL13	B8	558349

Table 2.8.2 CBA concentrations and reagents

Automacs buffer	PBS 0.5% BSA 2mM EDTA
Carbonate Bufffer for ELISA	45.3ml sol. A (8.5g $NaHCO_3$ in 100ml dH20) 18.2ml sol. B (10.6g $NaCO_3$ in 100ml dH20) 936.5ml dH20 pH 9.6 10µl of a 5% sodium Azide solution
cDMEM	500ml DMEM 50ml FCS 5ml L-Glutamine 5ml Penicillin/Streptomycin (Gibco)
cRPMI (low IgG)	500ml RPMI 50ml FCS (Low IgG for hybdridoma culture) 5ml L-Glutamine 5ml Penicillin/Streptomycin
CBA Buffer	PBS 0.5% BSA 0.05% Sodium Azide
ELISA blocking buffer	TBS 0.05% Tween 20 10% FCS or 1% BSA for Ym1 and RELMα ELISAs.
ELISA Washing Buffer	5 L TBS 2.5 ml Tween 20
FACS buffer	PBS 0.5% BSA
Macrophage dissociation media	PBS 10 mM Glucose 3 mM EDTA

Table 2.8.3 Buffers and Media

Chapter 4: Role of MIF in *H.polygyrus* infection.

3.1 Introduction to MIF in *H.polygyrus*

MIF has long been known to be important in amplifying Type 1 immune response (Calandra et al., 2000; Calandra and Roger, 2003). However, there is evidence that MIF may have a very context specific role. Current literature demonstrates that MIF is upregulated in the small intestinal epithelial cells at D3 of H.polygyrus infection (Haber et al., 2017), which requires Type 2 immune responses to expel the parasite. Previous results from the laboratory have indicated that MIF-deficient mice have impaired immunity to *H.Polygyrus* both in primary and secondary infection.

The chronicity of *H.polygyrus* is in many ways more representative of human helminths infection with *N.americanus* and *A.duodenale*. There is clear literatures describing the immunophenotype of the innate type 2 immune response, the T regulatory cell responses and the adaptive TH2 and B cell humoral response to *H.Polygyrus.* Therefore the *H.polygyrus* parasite was used to assess the role if MIF in polarisation to the TH2 immune response.

H.polygyrus is a model organism, a natural parasite of wild mice (Reynolds et al., 2012). It can persist for many months in certain strains of mice. Slow responding strains include the CBA, C3H, SL and A/J strains which take over 20 weeks to expel worms. Intermediately responsive animals include the C57BL/6 strain (which can take between 20-8 weeks to clear infection). The fast responsive strains include BALB/c (which can clear infection in 6-8 weeks). The SJL can clear parasites in 4-6 weeks and are amongst the most rapid at clearance (Reynolds et al., 2012). The more resistant strains produce a higher titre of antibody, produce macrophage rich granulomas, and upregulate the markers of alternative activation (Filbey et al., 2014).

The BALB/c background strain that we use here, results in expulsion of the parasite within 6-8 weeks (Filbey et al., 2014; Reynolds et al., 2012). Normally the primary infection can be cleared by antihelminthic treatment with pyrantel pamoate or ivermecin, subsequently the mouse develops an effective memory response clearing the infection the second time more rapidly. BALB/c mice are particularly able to mount an effective immune response post secondary infection, as are all strains of mice.

Strains that produce high levels of antibody result in level of IgG1 and IgE to HES is associated with reduced worm survival after a primary worm infection (Reynolds et al., 2012). B cells produce antibodies, cytokines and costimulatory molecules that amplify the T cell response. In *N.brasiliensis*, however, the TH2 response develops independently of the B cell responses(Liu et al., 2010). μMT mice lacking B cells cannot clear *H.polygyrus*. Therefore, *H.Polygyrus* is a useful model in which to assess antibody responses to infection.

Foxp3 expressing T cells are immunoregulatory and are important in reducing immune-mediated pathology. T regulatory cells can be grouped into natural Tregs, and induced Tregs (which were Foxp3 negative) –these are converted to Foxp3 expressing cells through exposure to TGF-β and IL-10. T regulatory cells expand in the lamina propria and the MLN of infected mice (Smith et al., 2016). The kinetics of Foxp3+ cells are complicated: partially depleting Foxp3+ T regulatory cells with anti CD25 antibody results in stronger TH2 responses and parasite clearance. Complete depletion in DEREG mice causes a cytokine store, high levels of IFNγ in response to bacterial translocation during parasite migration, and inhibition of the Th2 response, hence parasite survival (Smith et al., 2016).

3.2 Results: MIF in *H.polygyrus*

3.2.1 MIF deficiency impairs immunity *to H. polygyrus* in primary and secondary infection

At the outset of this thesis work, it had been found that MIF-deficient mice are significantly impaired in their ability to expel *H. polygyrus*. These data are presented in Figure 3.1 to provide context for the further experiments described in this chapter. In primary infection with *H. polygyrus*, BALB/c mice sharply reduce adult worm production (Fig3.2.1A) and egg (Fig3.2.1B) between day 14 and day 28. In contrast, the MIF deficient mice show higher egg counts, which like adult worm numbers show little reduction at day 28. In the context of a secondary infection, by D21 the MIF-deficient mouse is unable to expel the adult worm (Fig3.2.1C) whereas the wild type has expelled most of the adult *H.polygyrus* worms. The MIF-deficient is also unable to mount an effective immune response after immunisation with secreted parasite antigens (HES) with a regimen that drives sterile immunity in the wildtype animals (Fig 3.2.1 D). As MIF is likely to be important in the development of the immune system, experiments were conducted in wild type animals with an inhibitor of MIF, 4-IPP. Burdens of both eggs (Fig 3.2.1 E) and adult worms (Fig 3.2.1 F) at D28 were significantly elevated in the group administered 4-IPP.

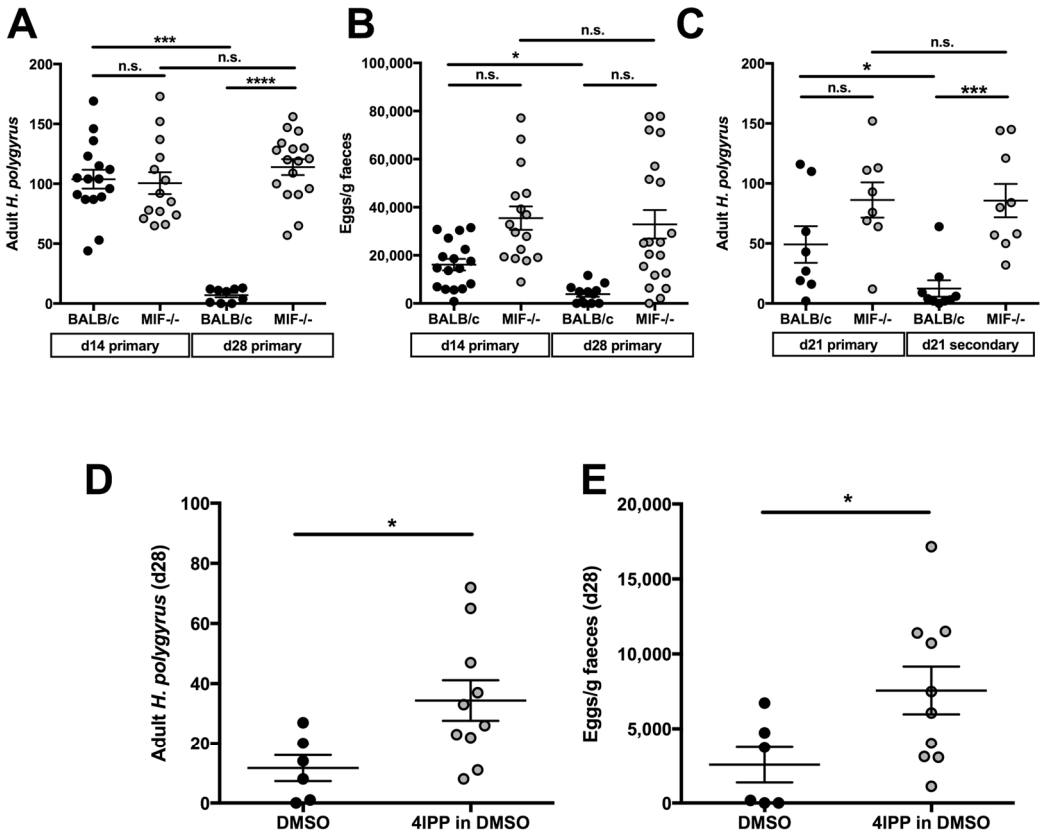

Figure 3.2.1 A-E MIF-deficient mice have increased worm burden in primary and secondary infection

A,B. Immunity in a primary infection. BALB/c and MIF$^{-/-}$ mice were infected with 200 *H.polygyrus* L3 larvae by oral gavage in a primary infection. Adult worm burden **(A)** and egg counts **(B)** enumerated at d14 and d28 of a primary infection.
C. Immunity in a secondary infection. At d28 following a primary infection with 200L3 *H.Polygyrus*, BALB/c and MIF$^{-/-}$ administered 2.5mg of pyrantel embonate in 200µl of water. At d21 after infection, adult worm counts were enumerated.
D,E. The MIF inhibitor 4-iodo-6-phenylpyrimidine (4-IPP) inhibits immunity in BALB/c mice infected with 200 L3 of *H.polygyrus*. 1mg of 4-IPP was injected i.p. at d -1,-2,4 and 6 of infection. Adult worms **(D)** and egg counts **(E)** taken at d28 p.i.
Data analysed by one-way ANOVA, and corrected for multiple comparisons by a Sidak's test. All experiments performed on one occasion. For all panels, * = $p<0.05$, ** = $p<0.01$, *** $p<0.001$. Experiments part of K.Filbey's thesis.

3.2.2 MIF-deficient mice have impaired cell expansion in the peritoneal cavity during *H.polygyrus* infection

BALB/c and MIF-deficient mice were infected for 3 and 6 days, the peritoneal exudate cells were harvested to compare the myeloid compartments as previously the Maizels' lab has demonstrated that MIF synergises with IL-4 to upregulate the products of alternative activation in bone marrow derived macrophages (Prieto-Lafuente et al., 2009). *H. polygyrus* infection induces a significant cellular expansion in the peritoneal cavity, including a strong alternatively activated macrophage population (Jenkins et al., 2013). It was observed that MIF-deficient mice have reduced cellular responses in the peritoneal cavity during *H. polygyrus* infection at d3 and d6 (Fig3.2.2A). By D6, there is almost a two-fold increase in the number of cells in the peritoneal lavage of the wild type mice, with a mean yield of over 3 x 10^6 cells; in contrast, the MIF deficient mice averaged 1.4 x 10^6 cells. Some of this increase can be accounted for by a greater expansion in macrophage numbers in the BALB/c than the MIF-deficient mice. At d0 there is an average of 0.28 x 10^6 $CD11b^+$ $F4/80^+$ population in the peritoneal cavity of BALB/c mice; this increases to 0.59 x 10^6 in D6 BALB/c infected mice. In the MIF-deficient mice the naïve mice have 0.31 x 10^6 $CD11b^+$ $F4/80^+$ cells and the D6 infected mice have 0.40 x 10^6. At d6 the total numbers of $CD11b^+$ $F4/80^+$ peritoneal macrophages are greater in the BALB/c infected mice than in the MIF-deficient mice, but this is not significantly (Fig3.2.2B). Strikingly, however, there is a marked difference in the total numbers of Siglec F^+ eosinophils in the peritoneal cavity at d6 of *H. polygyrus* infection (Fig3.2.2C). The BALB/c mice have 0.5 x 10^6 Siglec F^+ eosinophils in the lavage, 5-fold greater than in naive wildtype animals (p=0.001), whereas the MIF-deficient mice have only 0.02 x 10^6 SiglecF^+ eosinophils, not significantly higher than the baseline in uninfected animals.

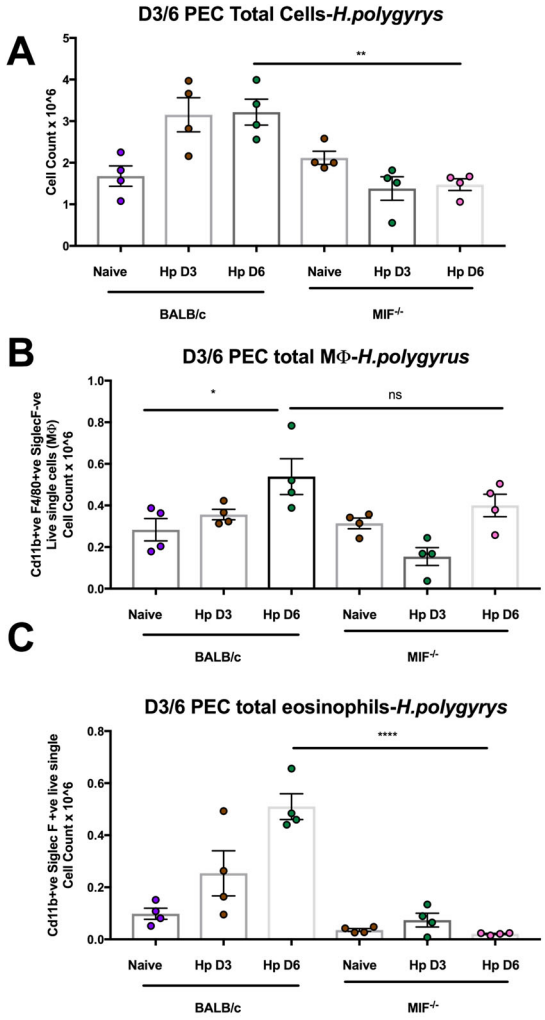

Figure 3.2.2 A-C MIF-deficient mice have impaired cell infiltration in the peritoneal cavity during *H.polygyrus* infection

BALB/c and MIF$^{-/-}$ mice were infected with 200 *H.polygyrus* L3 larvae by oral gavage. Peritoneal exudate cells were taken at d3 and d6 p.i. Cells were stained for analysis by flow cytometry.
(A) Total cells in peritoneal lavage at d3 and d6 p.i in BALB/c and MIF$^{-/-}$ mice.
(B) Total numbers of macrophages (Mφ) in the peritoneal cavity during *H.polygyrus* infection, determined as CD11b^{+} F4/80^{+} cells at d3 and d6 p.i in BALB/c and MIF$^{-/-}$ mice.
(C) Total numbers of eosinophils in the peritoneal cavity during *H.polygyrys* infection determined as CD11b^{+} SigF^{+} cells at d3 and d6 p.i in BALB/c and MIF$^{-/-}$ mice. Experiment completed once. Data analysed by one-way ANOVA, and corrected for multiple comparisons by a Sidak's test. For all panels, * = $p<0.05$, ** = $p<0.01$, *** $p<0.001$.

3.2.3 MIF-deficient mice have impaired type 2 alternative activation of macrophages in the peritoneal cavity during *H. polygyrus* infection

Alternatively activated macrophages and their products are correlated with resistance to *H. polygyrus* infection (Anthony et al., 2007; Filbey et al., 2014). In Fig3.1 we infected BALB/c and MIF-deficient mice for 3 and 6 days with 200L3 of *H.polygyrus* by oral gavage. Peritoneal lavage was taken to assess the peritoneal exudate cells by flow cytometry. Peritoneal macrophages were therefore evaluated for alternative activation in wildtype and MIF-deficient mice. The M2 marker Arginase-1 was highly expressed by peritoneal macrophages by D3, with 32.9% positive in the BALB/c mice but only 7.9% in the MIF-deficient mouse (Fig3.2.3A). Similar results were found with two other M2 markers, RELMα and YM1, which while not significantly increased by D3, did show substantial expression by D6, with 49.3 and 14.0% positive macrophages respectively in BALB/c infected mice (Fig 3.2.3B,D). In comparison, the percentage of peritoneal macrophages that are positive for RELMα and YM1 at d6 were 28.7% and 2.5% in the MIF-deficient mice. Consistent with this pattern of macrophage expression, soluble RELMα (Fig3.2.3D) and YM1 (Fig3.2.3E) protein could be recovered in peritoneal lavage fluid of wildtype mice, while MIF-deficient animals showed reduced RELMα and absence of Ym1.RELMα seems to be least affected by the deficiency of MIF.

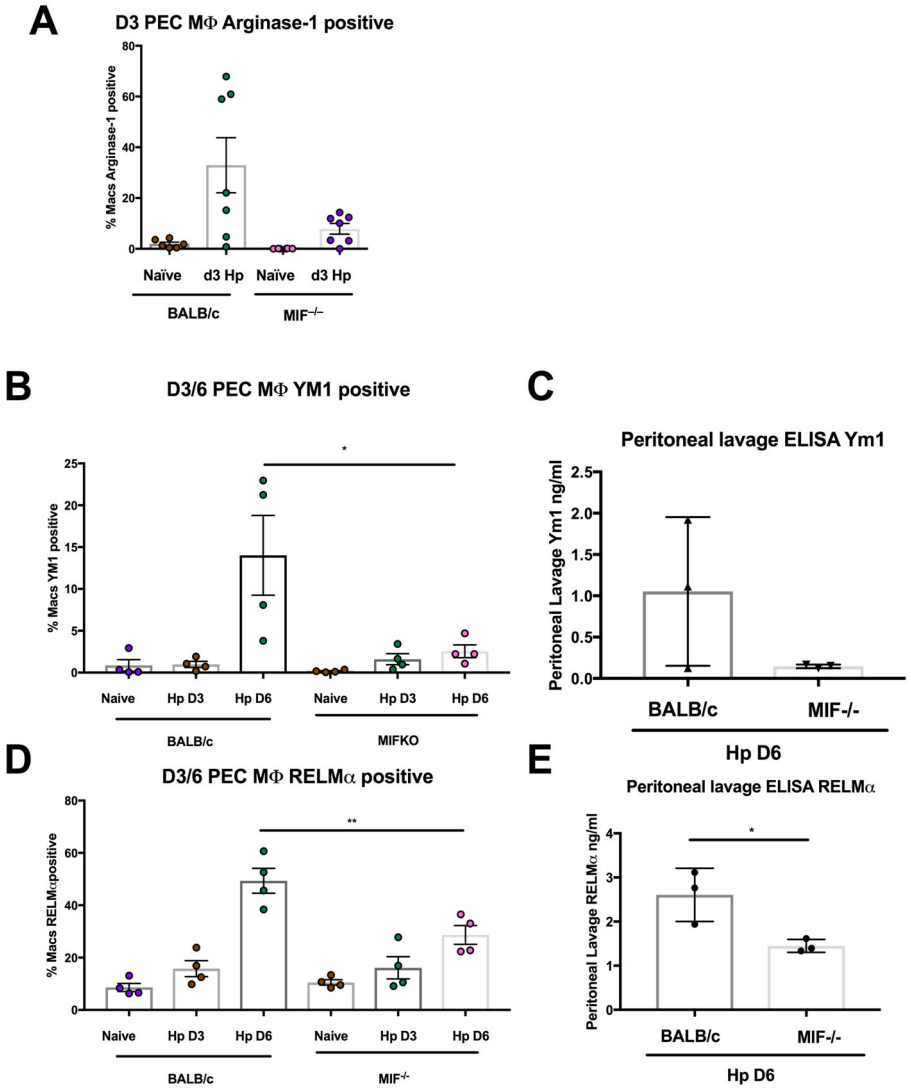

Figure 3.2.3 A-D MIF-deficient mice have impaired type 2 alternative activation in the peritoneal cavity during *H.polygyrus* infection

BALB/c and MIF$^{-/-}$ mice were infected with 200 *H.polygyrus* L3 larvae by oral gavage. Peritoneal exudate cells were taken at d3 and d6 p.i. Cells were stained for analysis by flow cytometry

A Reduction in percentage of CD11b+ F4/80+ Arg1+ cells at d3 post infection. Data in **A** is pooled from two experiments

B,D Percentage of CD11b^{+} F4/80^{+} YM1+ **(B)** and RELMα^{+} **(D)** cells in peritoneal cavity at d3 and d6 post infection.

C,E Levels of YM1 **(C)** and RELMα **(E)** in peritoneal lavage at d6 p.i.

Data in B-E obtained from one experiment

Data analysed by one-way ANOVA, and corrected for multiple comparisons by a Sidak's test. For all panels, * = $p<0.05$, ** = $p<0.01$, *** $p<0.001$.

3.2.4 MIF-deficient mice have reduced numbers of $CD4^+Foxp3^+$ cells in the MLN at D28 of infection

Because T regulatory cells are known to control susceptibility to *H. polygyrus* (Smith et al., 2016), we evaluated levels of $CD4^+Foxp3^+$ Tregs in the mesenteric lymph nodes of BALB/c and MIF-deficient mice. T regulatory cells are known to increase 28 days after infection with *H.polygyrus* (Finney et al., 2007). We infected BALB/c and MIF-deficient mice with 200L3 *H.polygyrus* for 28 and 14 days to compare the MLN $CD4^+$ $Foxp3^+$ populations. The overall cell numbers in the mesenteric lymph nodes was much greater in wild type mice with 28.3 X 10^6 at day 28, whereas the MIF deficient mouse had 7.5 x 10^6 cells recovered at day 28, although the data did not attain statistical significance.

It was found that the frequency of $Foxp3^+$ cells in the MLN did not differ between wild type and MIF deficient mice. In general, there was a trend towards a higher percentage of $CD4^+Foxp3^+$ cells in the MLN of both groups (Fig3.2.4B), increasing between naïve mice to d28 infected mice from 10.8 to 14.5% of all $CD4^+$ MLN cells in BALB/c, and 7.3 to 13.5% in MIF-deficient mice.

Because of the marked difference in MLN cellularity between the two strains, there are much greater total numbers of $CD4^+Foxp3^+$ cells in the MLN of BALB/c mice at d28 of infection, compared to the MIF deficient mice., with 2.1 x 10^6 $CD4^+Foxp3^+$ cells of the wildtype, but only 0.37 x 10^6 cells in the MIF-deficient animals (Fig3.2.4C).

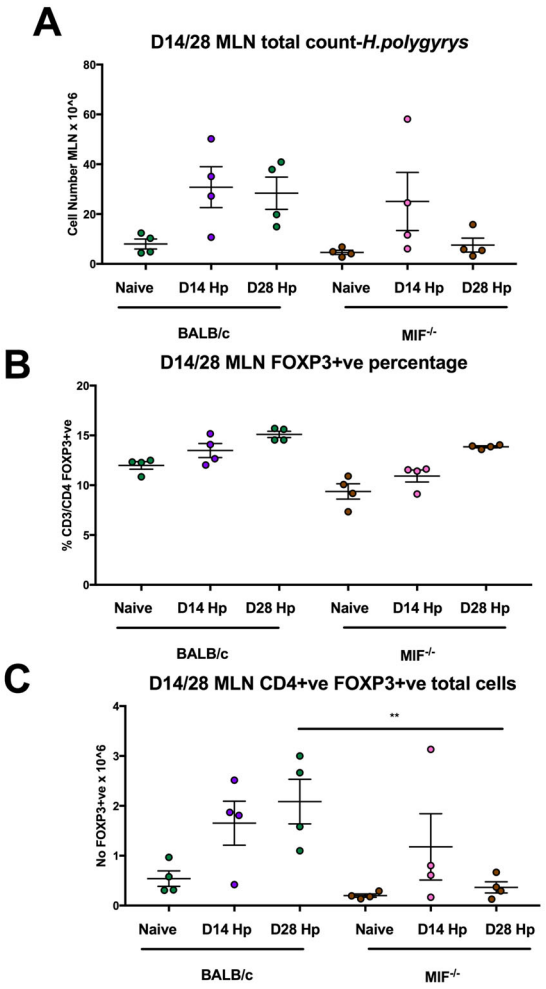

Figure 3.2.4 A-C MIF-deficient mice have reduced numbers of CD4+ FoxP3+ cells in the MLN at d28 of *H.polygyrus* infection.

BALB/c and MIF$^{-/-}$ mice were infected with 200 *H.polygyrys* L3 larvae by oral gavage for 14 and 28 days: analysis of MLN by flow cytometry.
A. Total numbers of cells in the MLN at d14 and 28 p.i. with *H.polygyrus* in BALB/c and MIF$^{-/-}$ mice.
B. Percentages of CD4^{+} FOXP3^{+}cells at d14 and 28 p.i. with *H.polygyrus* in BALB/c and MIF$^{-/-}$ mice.
C. Numbers of CD4^{+} FOXP3^{+}cells at d14 and 28 p.i. with *H.polygyrus* in BALB/c and MIF$^{-/-}$ mice.
Experiments conducted once, data analysed by one-way ANOVA, and corrected for multiple comparisons by a Sidak's test. For all panels, * = $p<0.05$, ** = $p<0.01$, *** $p<0.001$.

3.2.5-6 MIF-deficient mice have intact antibody responses to parasite antigens

B cell and antibody responses are essential for the expulsion of *H.polygyrus,* with the IgG1 isotype regarded as the most important. We assessed the HES specific antibody responses in BALB/c and MIF deficient mice by ELISA, and determined the dilution curves, overall the MIF-deficient mice have intact IgG1 antibody responses (Fig 3.2.5A), however, IgA (Fig 3.2.6A) is much higher in the MIF-deficient mice.

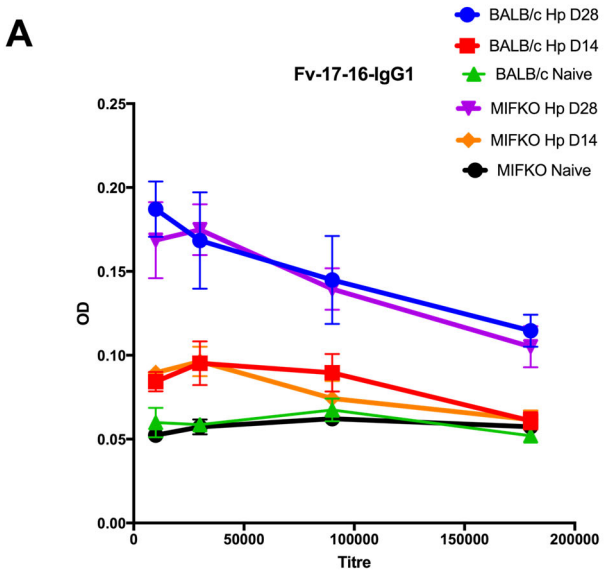

Figure 3.2.5 A MIF-deficient mice have intact IgG1 antibody responses

BALB/c and MIF$^{-/-}$ mice were infected with 200 *H.polygyrus* L3 larvae by oral gavage: and sera serially diluted to determine titre.
A. Standard curve created of dilution titre for IgG1.
Experiment completed once.

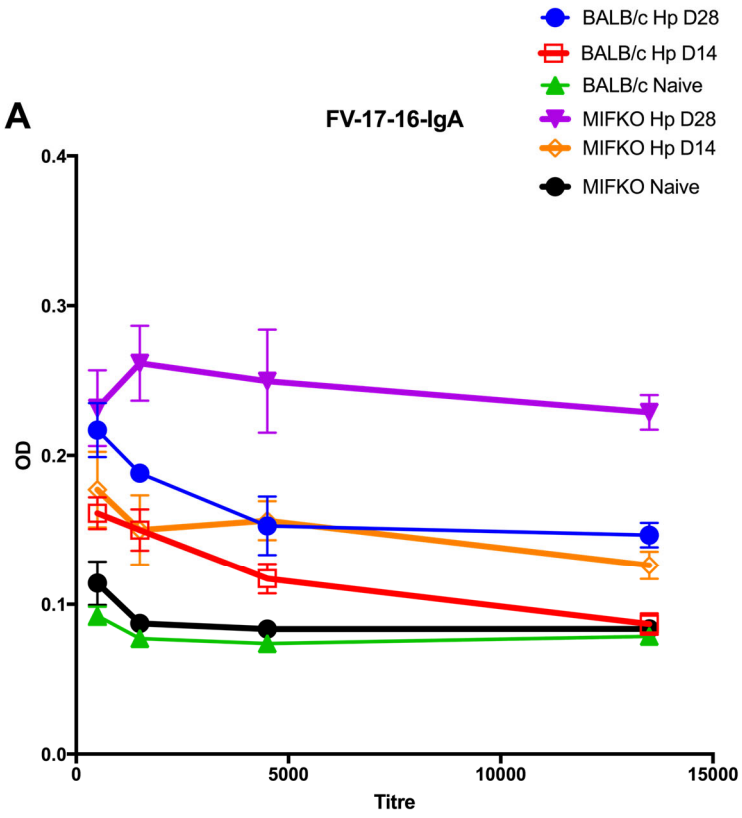

Figure 3.2.6 A MIF-deficient mice have intact IgA antibody responses.

BALB/c and MIF$^{-/-}$ mice were infected with 200 *H.polygyrus* L3 larvae by oral gavage: and sera serially diluted to determine titre.
A. Standard curve created of dilution titre for IgA.
Experiment completed once.
.

3.2.7 Gene expression comparison of whole duodenum comparing d3 infected BALB/c and MIF$^{-/-}$ mice

MIF has so far been shown to slow expulsion of *H.Polygyrus* in primary infection, and induce innate cell M2 polarisation along with eosinophilia. The mechanism by which this phenotype occurs is not understood. Therefore, in order to better understand how MIF may lead to altered early immunity to *H.Polygyrus*, we undertook a microarray analysis of whole duodenum. BALB/c and MIF-deficient mice were infected for 3 and 7 days with 200 L3 *H.polygyrus*, whole duodenum and MLN from the infected and uninfected mice was homogenized for RNA extraction. The RNA extraction was performed by Dr D J Smyth, sent for analysis at Edinburgh Bioinformatics and analysis by Dr Al Ivens using the using R package lumi.

Figure 3.2.7 is a volcano plot comparing BALB/c and MIF-deficient duodenum at D5 of an *H. polygyrus* infection. Of the top 10 sequences found to be differentially upregulated at d5 in the BALB/c mouse compared to the MIF deficient mouse are *MIF, ARL2BP, PHC2*. Other genes did not reach the statistical threshold for multiple testing or the effect size was not above two fold different, however *s100a8* was of borderline significance and therefore we choose to look at this in some further detail.

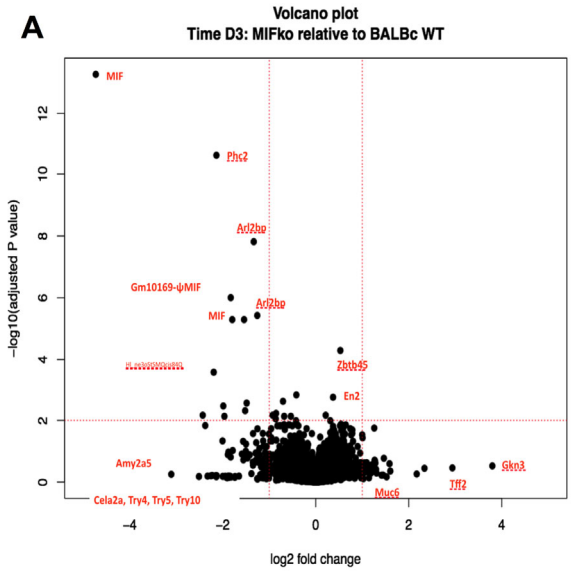

Figure 3.2.7 A Gene Expression comparison of whole duodenum comparing BALB/c and MIF$^{-/-}$ mice infected with *H.polygyrus* for 3 days.

BALB/c and MIF$^{-/-}$ mice were infected with 200 *H.polygyrus* L3 larvae s.c. for 3 days: analysis of whole duodenum.
A. Volcano plot of gene expression comparing d3 BALB/c and MIF-/- infected duodenum. Contributions: RNA extraction by K.Filbey, analysis by Dr A Ivens, $p<0.05$ after correction.

3.2.8 qPCR validation of targets found in microarray in 3.7

In Figure 3.2.8, we next validated the targets found on microarray by qPCR of the RNA extracted from 3.7. We found that the levels of *s100a8* (Fig 3.2.8A) *ARL2BP* (Fig 3.8B), *PHC2*, (Fig 3.2.8C) were upregulated by 11, 2.5 and 6 fold respectively in the proximal duodenum of BALB/c infected mouse compared to the MIF deficient mouse at d5 of *H.polygyrus* infection. S100a8 and s100a9 are calcium binding proteins that are important in neutrophil migration and are released in inflammatory states as damage associated molecular signals. ARL2BP is important in STAT3 nuclear localisation and PHC2 is important in skeletal organogenesis and in immunity.

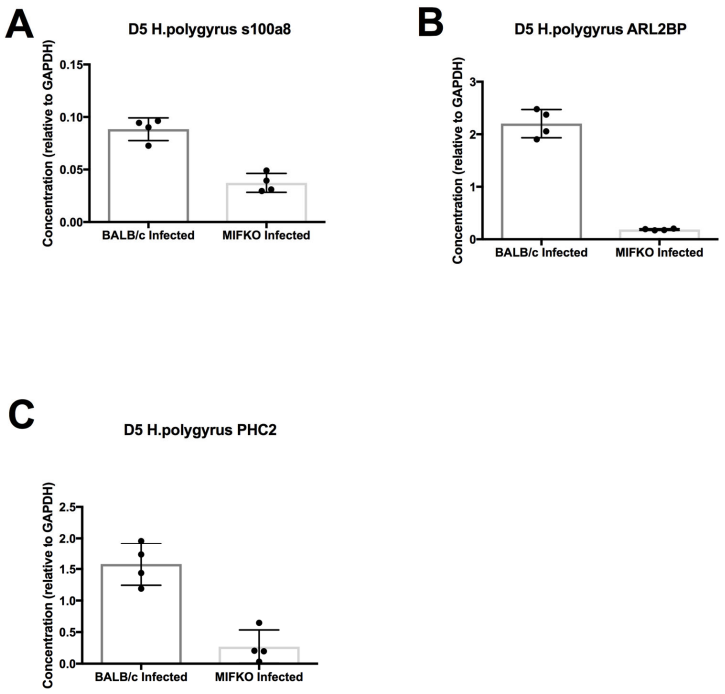

Figure 3.2.8 A-C Gene expression quantification and validation of microarray by RT-qPCR.

BALB/c and MIF$^{-/-}$ mice were infected with 200 *H.polygyrys* L3 larvae by oral gavage for 5 days. MLN was frozen in RNA later for RNA extraction and qRT-PCR.
A-C Gene expression analysis by qRT-PCR of MLN for transcription levels of *s100a8* **(A)**, *ARL2BP* **(B)** *and PHC2* **(C)**; data is representative of two experiments.

3.2.9 H. polygyrus primary and secondary infection of S100a9-/- mice

In order to further assess the role of s100a8 in *H. polygyrus* infection, we obtained mice lacking s100a9 (Manitz et al, 2003), without which s100a8 is a homodimer and functionally inactive and infected them with *H. polygyrus* in both primary and secondary infection settings. For the primary infection, both groups of mice were evaluated after 28 days. For secondary infection, we used a previously described protocol (Hewitson et al., 2011) as outlined in Fig3.2.9A. Unexpectedly, the s100a9-/- mice were better at expelling primary infections, with worm counts at day 28 being 43 in the s100a9-/- mouse compared to 118 in the BL/6 mice (Fig3.2.9B). Furthermore, there was no difference in the ability of the S100a9-deficient mice to expel the secondary challenge infection (Fig3.2.9B,C). Overall, these data demonstrate that the s100a8/9 complex is not required for immunity against *H. polygyrus* infection.

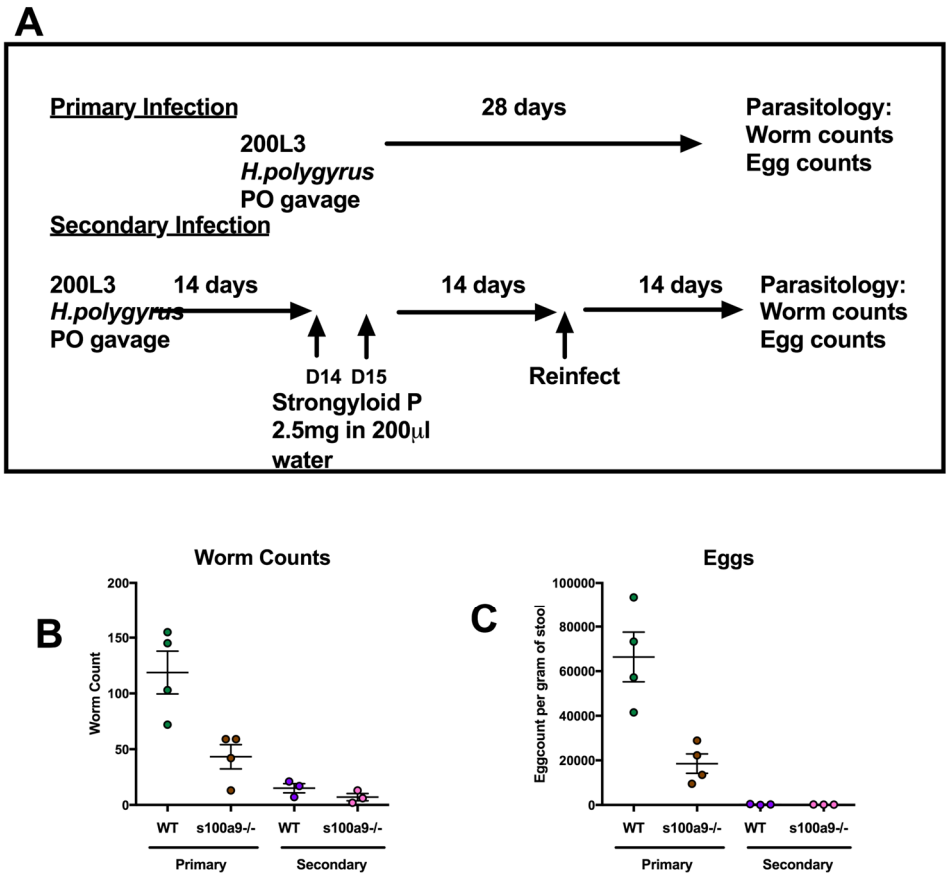

Figure 3.2.9 s100a8/9 is not important in worm expulsion in primary or secondary infection with *H.polygyrus*.

s100a9$^{-/-}$ mice and wild type BL/6 mice were infected with 200 L3 *H.polygyrus* by oral gavage

A. Schematic of experimental design for primary and secondary infections to assess the importance of s100a8 in *H.polygyrus* expulsion. In primary infection, the mice are infected for 28 days. Analysis of egg and worm counts at d28 p.i. In secondary infections, at d14 following a primary infection with 200L3 *H.Polygyrus*, BL/6 and S100a9-/- mice are administered 2.5mg of pyrantel embonate in 200µl of water. At d14 of reinfection the mice were reinfected for 14 days. Worm and egg counts were enumerated at d14 p.i.

B-C. Adult worm **(B)** and egg **(C)** counts enumerated in wild type and s100a9$^{-/-}$ mice during a course of primary and secondary infection. Experiment performed once. Contributions: mice obtained from Dr R.Gray (Edinburgh).

3.2.10 STAT3 and STAT6 phosphorylation studies in bone marrow derived macrophages

STAT6 is the transcription factor activated by IL4Rα ligation, and is essential for expulsion of intestinal helminths such as *N. brasiliensis* (Kaplan et al., 1996; Urban et al., 1998). Both IL-4 and IL-13 activate the IL4Rα-STAT6 signalling pathway. On binding of IL-4 or IL-13 to IL-4Rα, STAT6 is phosphorylated, dimerises and then translocates to the nucleus. P-STAT6 then promotes the expression of the master regulator of Type 2 cyokines, GATA3(Maier et al., 2012). STAT6 also directly drives polarisation of macrophages to the M2 phenotype secreting factors Arg1, RELMα and Ym1(Jang and Nair, 2013). Evidence exists to support STAT6 independent TH2 signaling(Ouyang et al., 2000). More recently, STAT3 may have a role in M2 activation: in myeloid-derived suppressor cells STAT3 was found to regulate Arginase-1(Vasquez-Dunddel et al., 2013).

To investigate if MIF affects STAT6/3 phosphorylation leading to reduced alternative activation of macrophages shown *in vitro* (Prieto-Lafuente et al., 2009) and by these experiments in Fig3.2.2 B, we attempted to assess the kinetics of STAT6 phosphorylation. Day 7 bone marrow derived macrophages were stimulated with ligands IL-4 for STAT6 and IL-10 for STAT3 for 30 minutes and measured the phosphorylation of STAT6/3 between BALB/c and MIF-deficient bone marrow derived macrophages. We found that early STAT6 phosphorylation kinetics was not altered in the MIF deficient mice. From 0-30 minutes, phosphorylation of STAT6 occurred equally in the bone marrow macrophages of MIF deficient and wild type mice (Fig3.2.10 B).

We assessed STAT3 phosphorylation kinetics using the ligand IL-10. We found that the MIF deficient bone marrow macrophages were as able to phosphorylate STAT3 as BALB/c macrophages (Fig3.10 B). There may however, be subtle differences in the kinetics of STAT3 which cannot be

measured by simple phosphorylation studies such as nuclear localisation and retention which is the function of ARL2BP (Muromoto et al., 2008).

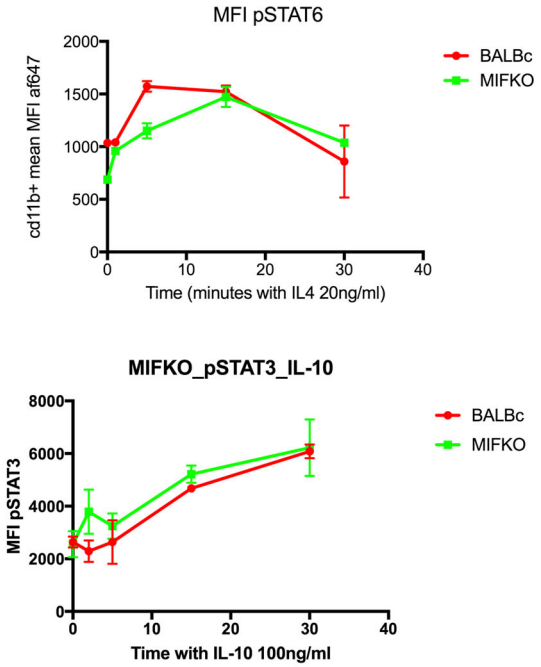

Figure 3.2.10 MIF-deficient bone marrow derived macrophages have no deficit in early phosphorylation of STAT6 or STAT3.

Bone marrow derived macrophages were differentiated for 7 days in cDMEM with 20% L929 (M-CSF source). These were then stimulated up to 40 minutes with IL-4 for phosphorylation of STAT6 and IL-6 or IL-10 for phosphorylation of STAT3.
A. BALB/c and MIF$^{-/-}$ stimulated with 20ng/ml of IL-4-MFI of pSTAT6 quantified. Experiment has been repeated 2 times
B. BALB/c and MIF$^{-/-}$ stimulated with 100ng/ml of IL-10-MFI of pSTAT3 quantified.

Experiment has been performed once.

3.3 Discussion: MIF in *H.polygyrus*

Helminths classically induce macrophages of the M2 phenotype: these are classically Arg1, RELMα and YM1 (Allen and Sutherland, 2014). These alternatively activated macrophages are correlated with increased resistance to infection (Filbey et al., 2014). Curiously, MIF derived from mouse (and parasite derived MIF homologues) synergises with IL-4 increasing the production of these three molecules (Prieto-Lafuente et al., 2009) although the exact mechanism by which this occurs is yet to be determined.

In secondary immunity, the AAM product Arginase-1 was found to be important in eliciting memory Th2 responses (Anthony et al., 2006). In *N. brasiliensis* infection Arginase-1 was found to induce intestinal smooth muscle contraction resulting in worm expulsion (Anthony et al., 2006; Assis et al., 2014; Zhao et al., 2008). We found that the BALB/c mouse was able to elicit a strong AAM response, but this was impaired in the MIF-deficient mouse during an *H.polygyrus* infection, this may explain part of the susceptibility in the MIF-deficient mouse system (Anthony et al., 2006).

A notable feature was severely impaired eosinophilia in the MIF-deficient mouse. Eosinophils are responsive to IL-5 from ILC2s and Th2 cells. Some authors have reported that eosinophils directly bind helminths *in vitro* (Shin et al., 2001), and IL-5$^{-/-}$ mouse had higher worm burdens in secondary infection during *N.brasiliensis* infection (Knott et al., 2007). At D6 of infection, the MIF-deficient mouse had fewer eosinophils. Eosinophils have a clear relationship to worm resistance in *N.brasiliensis* infection. However, this is not the case for every parasite, and may well depend very much on timing and background strain of the mouse(Allen and Sutherland, 2014).

Th2 cell responses examined by Dr K.Filbey previously, and were found to be sufficient in the MIF deficient mice, we therefore examined the role of T-

regulatory cells. There was no defect observed in the T regulatory cell recruitment to the MLN. There were higher numbers but not percentages of $CD4^+$ $Foxp3^+$ cells at D28 in BALB/c mice when compared to the MIF-deficient mice (Fig 3.4D); therefore MIF-deficient mice have a proportionately appropriate $Foxp3^+$ response to *H.polygyrus* infection.

There was no observed defect in HES specific antibody responses suggesting that antibody immune mechanisms were in tact. Therefore MIF seems less important in adaptive processes than innate processes.

MIF is known to affect MAP kinase signalling downstream, however, previous work in our lab suggests that MIF also results in IL4Ra upregulation in bone marrow derived macrophages(Prieto-Lafuente et al., 2009). We were therefore, interested in the ability of MIF to affect downstream IL4Ra-STAT6 signalling. Experiments utilised bone marrow derived macrophages to explore if MIF affects STAT6 signalling, as BMDM can be alternatively activated by MIF. We found that MIF adequately induces phosphorylation of STAT6 in BMDMs, indicating that the effect of MIF on Type 2 immunity is likely not via interfering with the IL4Ra-STAT6 signalling cascade. We also explored STAT3 as a novel pathway that affects TH2 signalling, and found no difference in the phosphorylation of STAT3. As ARL2BP was reported to be important in STAT3 nuclear retention, we also assessed nuclear STAT3 localisation at extended time points with an imaging flow cytometer (data not shown). We found no difference in the ability of the MIF-deficient macrophages to localise STAT3.

A gene array was used to compare whole duodenum from BALB/c and MIF-deficient mice infected for 3 and 7 days with naïve duodenum from BALB/c and MIF-deficient mice. The rationale for conducting this microarray was to look for novel genes that may be involved downstream of the MIF deficient phenotype, that may help explain susceptibility. The analysis has highlighted

some interesting genes that have not previously been known to be associated with MIF or resistance to helminth infection.

S100a8/9 are described as danger-associated molecular patterns (DAMPs) and promote inflammation. They are part of the s100 calgranulin family. They form a heterodimer or calprotectin and are expressed by neutrophils and monocytes. They are 45% of all cytosolic proteins in neutrophils, and are important in neutrophil exocytosis traps. The protein is normally released from activated or necrotic neutrophils. TLR4 and RAGE are potential receptors (Schiopu and Cotoi, 2013). The role that s100a9 has in myeloid cells is unclear, as S100a9-/- had normal mature phagocytes. We found that S100a8 was upregulated in the BALB/c mouse compared to the MIF-deficent mouse (Fig3.8A). We assessed s100a8 deficiency using an s100a9 deficient mouse (which is functionally deficient in s100a8 as both the molecules found a heterodimer). Whilst the s100a8 deficient mouse seemed more effective at expelling a primary infection, there was no difference in the immunity secondary infection. The mice that we used were in the process of being back crossed onto a C57BL/6 background and therefore may have harboured some of the features of their original strain. The greater immunity exhibited by the s100a8 deficient mice therefore may be because of background immunity differences rather than being due to s100a8 deficiency. In secondary infection, however, all strains are effective at expelling the parasites. There were no difference in immunity secondary infection, therefore the difference observed in primary infection may be related to adifference in background genetics (Fig 3.9).

ARL2BP is an ADP ribosylation factor like 2 binding protein: it has been found to be important for nuclear retention of STAT 3. Therefore, we assessed expression of ARL2BP in the mesenteric lymph nodes of BALB/c

versus MIF-deficient mice. We found that ARL2BP was upregulated in the BALB/c mouse but not the MIF-deficient infected mouse. Assessment of ARL2BP suggests that STAT3 may be the mechanism by which MIF is capable of amplifying Type 2 responses. No differences in phosphorylation of STAT3 were noted between BALB/c and MIF-deficient bone marrow macrophages.

PHC2 is a polycomb protein involved in histone acetylation and may be involved in epigenetic regulation. PHC2 forms part of the polycomb group that is involved in specification of anterior-posterior (A-P) polarity by regulating the Hox cluster genes. PHC2 mutants have abnormalities of skeletal development and premature sensence of mouse fibroblasts.(Isono et al., 2005) PHC2 was found to be upregulated in the BALB/c infected mice but not the MIF-deficient infected mice. The link between MIF and PHC2 in immunodeficiency is also very interesting and worthy of subsequent follow up.

Further work may involve assessing the role of ARL2BP and PHC2 in the context of helminths infection. Although we undertook a microarray of whole tissue, this does not give in-depth information with regards to the differences in cell specific responses, therefore future experiments may involve isolating particular cellular populations in wild type and MIF-deficient mice, and assessing the gene responses within specific cellular populations. We had started to assess differences in signalling in the MIF-deficient and wild type macrophages. Although there was no difference in the phosphorylation of STAT3 in the MIF-deficient and wild type macrophages, we could have assessed nuclear translocation of STAT3 (As ARL2BP has been shown to be important in STAT3 nuclear translocation (Muromoto et al., 2008)). Although, we have looked at the cellular immune responses, it is clear from the *H.polygyrus* model that the main mechanism of gut helminths expulsion occurs via the epithelium- and we use the *N.brasiliensis* model in the next chapter to explore the epithelial cells responses.

Chapter 4- Impact of MIF deficiency on *N.brasiliensis* infection

4.1 INTRODUCTION

The previous chapter demonstrated that MIF is important for polarisation of macrophages to the alternatively activated phenotype by way of production of Arg-1, RELMα and Ym1. In addition, MIF-deficient mice show reduced eosinophilia in response to *H.polygyrus* infection suggesting a deficiency in the innate immune compartment.

Nippostrongylus brasiliensis is a nematode whose primary host is the rat, but is able to infect a variety of rodent species. It is less adapted to completing its life cycle in the mouse and thus rapidly expelled in comparison to *H.polygyrus*. This makes *N.brasiliensis* an excellent model organism to study the innate immune system of the mouse. Recent findings made using this parasite include the discovery of innate lymphoid cells type-2 (ILC2) (Fallon et al., 2006). The release of ILC2-derived IL-13 results in a weep and sweep (Anthony et al., 2007) model of parasite expulsion: the epithelial cells weep fluid into the lumen and increased peristalsis and epithelial cell turnover (Cliffe et al., 2005) results in physical expulsion of the parasite, underlining the importance of ILC2-epithelial cell crosstalk for resistance to this parasite (Gerbe and Jay, 2016). The epithelial responses (the effectors of helminths expulsion) have been best characterised in *Nippostrongylus brasiliensis*, therefore this helminth has been chosen to explore the effect of MIF on the epithelial cell response.

The lung is an important priming site for immunity to *N. brasiliensis* infection (Harvie et al., 2010). *N. brasiliensis* has a larval stage that migrates to the lung (which is absent in *H. polygyrus*), therefore allowing us to explore the importance of MIF in lung type 2 immune responses to helminths.

Mechanisms by which immunity may occur are not completely discerned. Recent data has demonstrated the role of lung neutrophils in priming long lived effector macrophages which result in expulsion of adult worms from the gut (Chen et al., 2014). Therefore, by studying *N. brasiliensis,* we can analyse the role of MIF in the two complementary settings of the lung and the gut.

Whilst comprehensive literature on MIF in type-1 immunity (Calandra and Roger, 2003) is available, the function of MIF in type-2 associated immunopathology and its effect on the epithelium is largely unknown. Comparisons of data presented in chapter 3 on MIF functions during *H.polygyrus* infection with obtained results using the *N.brasiliensis* model will allow us to assess if the effect of MIF on anti-helminth immunity is generalizable.

This chapter focuses on the impact of MIF on *N.brasiliensis*-induced immunopathology and delineates the immune mediators function in innate and epithelial cell responses. Different immune-interventions are presented as well, including experiments involving the MIF-inhibitor 4IPP and IL-25 cytokine-rescue setups.

4.2 RESULTS

4.2.1 Expulsion of *N.brasiliensis* is impaired in MIF-deficient mice.

First, differences in parasitological outcomes in the absence of MIF were assessed. BALB/c and MIF deficient mice were infected with the mouse strain of *N.brasiliensis* at an inoculum of 250 L3 and small intestines were harvested to enumerate adult worm counts at d6 post infection (p.i.). In addition, daily egg counts were performed in a separate set of experiments from d6 until d10 (Fig 4.2.1A). The immunological analyses were predominantly performed at d6 post infection. Interestingly, worm counts obtained at d6 post infection demonstrate that MIF-deficient mice are unable to expel adult *N.brasiliensis* infection unlike the wild-type mice which, as previously shown (Maizels and Yazdanbakhsh, 2003), efficiently expel the worm at this time point (Fig 4.2.1B). This result is further supported by time course experiments monitoring egg counts over d6 to d10 p.i. (Fig 4.2.1C) showing that the MIF-deficiency results in increased egg burden throughout the course of the experiment, whereas wild-type animals are able to clear the infection by day 10 (Fig 4.2.1C).

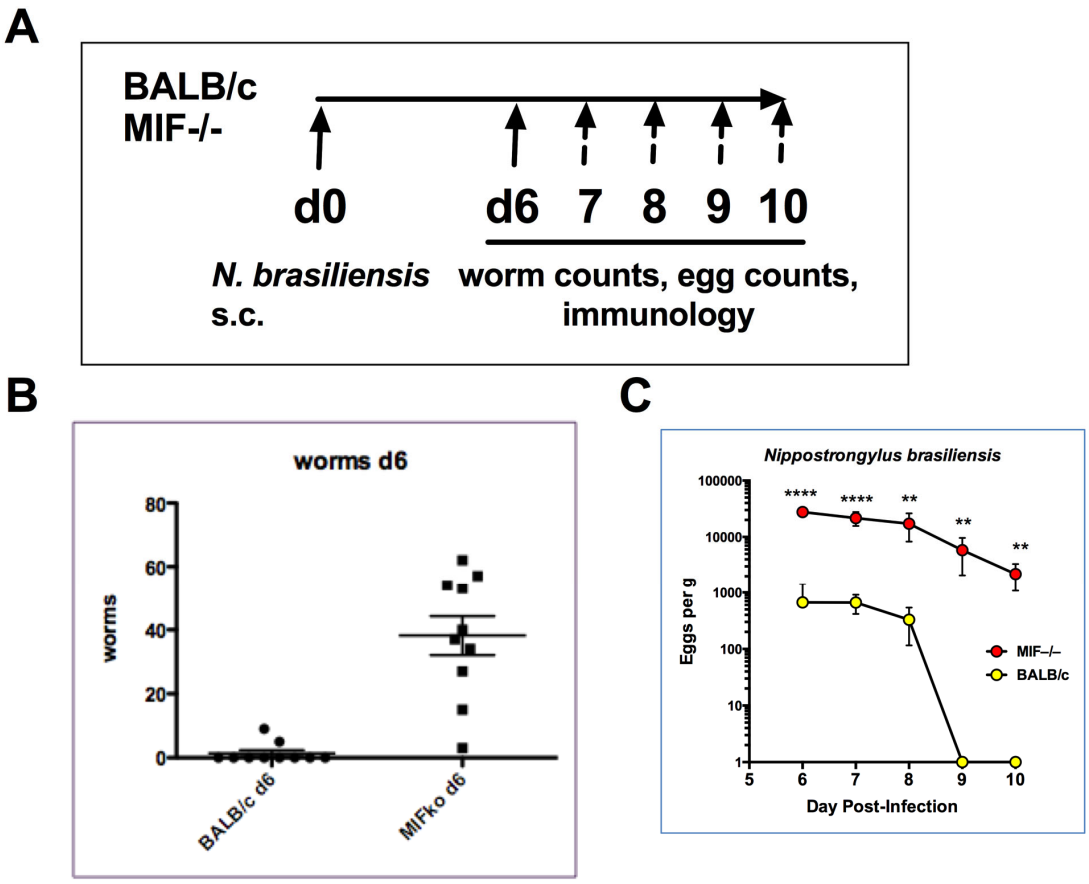

Figure 4.2. 1 Impaired expulsion of *N.brasiliensis* by MIF deficient mice

(A) Schematic of experimental design: BALB/c and MIF-/- were infected with 250 L3 *N.brasiliensis* by s.c. injection. Small intestinal worm counts were enumerated on d6 and fecal egg counts performed from d6 until d10. **(B)** Adult *N. brasiliensis* nematodes counted at d6. **(C)** Faecal egg burdens between d6-d10. Data are representative of 3 independent experiments, statistically analysed by one-way ANOVA and corrected for multiple comparisons by a Sidak's test. * $p<0.05$, ** $p<0.01$, *** $p<0.001$. Experiments performed by Mrs Yvonne Harcus, senior laboratory technician.

4.2.2 The total inflammatory response to *N. brasiliensis* is impaired in MIF-deficient mice.

As MIF has been shown to induce inflammation in the context of type-1 immunity in several models of infection, we aimed to assess the function of MIF in the type-2 inflammatory response induced following *N. brasiliensis* infection. By day 6 of infection, inflammatory cells have accumulated in the airway lumen (Fig 4.2.2A), peritoneal cavity (Fig 4.2.2B) and the MLN (Fig 4.2.2C) of BALB/c mice. This inflammatory response is impaired in MIF-deficient mice as demonstrated by total cell counts obtained at the respective sites. The increase in cell count observed in the BAL of BALB/c mice during *N. brasiliensis* infection (BAL cell count is 0.1 x 10^6 cells in naïve and 0.5 x 10^6 cells in infected mice at d6 p.i.), was not observed in the MIF-deficient mice (cell count in the naïve mice and infected mice remains at 0.15 x 10^6) (Fig 4.2.2A). The cell count in the peritoneal cavity of BALB/c mice augments during infection from a baseline of 3.8 x 10^6 cells to 3.79 x 10^6 cells. MIF-deficiency induced a decline in baseline PEC cells to 1.7 x 10^6 during immune homeostasis, which increased to 2.1 x 10^6 at d6 after *N.brasiliensis* infection (Fig 4.2.2B). A decreased number of cells at baseline was also detected in the MLN of MIF-deficient naïve mice compared to BALB/c mice (7.3 vs. 2.9 x 10^6 total cells respectively). *N. brasiliensis* infection increased the total cell number of the MLN to 10.5 x 10^6 cells in BALB/c mice. This increase was significantly attenuated in MIF-/- mice (4.8 x 10^6 cells).

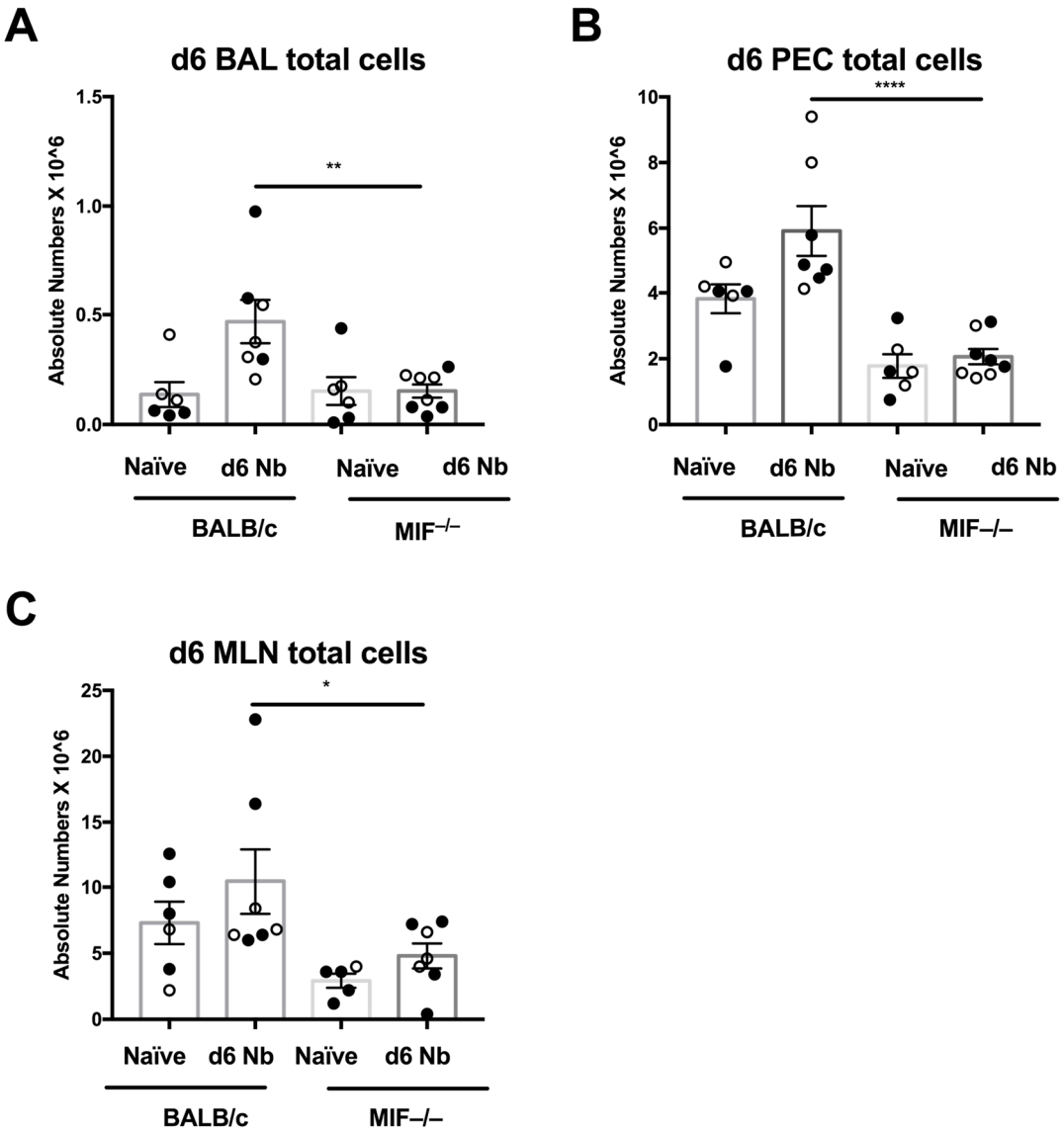

Figure 4.2. 2 A-C: Impaired inflammation in response to *N.brasiliensis* by MIF-deficient mice.

BALB/c and MIF-/- mice were infected with 400 L3 *N.brasiliensis* larvae by s.c. injection for 6 days. Cell counts of bronchoalveolar lavage (BAL) **(A)** and peritoneal exudate cells (PEC) (**B**) performed using an automated cell counter (cellometer). Manual cell counting was performed to enumerate total immune cells of the MLN (**C**). Data pooled from two independent experiments, represented as shaded and unshaded circles. Data was analysed by one-way ANOVA and corrected for multiple comparisons by a Sidak's test. * $p<0.05$, ** $p<0.01$, *** $p<0.001$. Contributions: preparation of lung and BAL by Dr S. Loeser.

4.2.3 MIF gene expression is upregulated in eosinophils and macrophages during *N.brasiliensis* infection

MIF is expressed at several mucosal immune sites by most immune cells and many mucosal tissue sites (Calandra and Roger, 2003). MIF can also be stored intracellularly in the cytoplasm and released as required. In order to assess whether MIF expression varies in the context of *N brasiliensis* infection, four major cell populations from within the peritoneal cavity were sorted by fluorescence-activated cell sorting (FACS) to assess their transcription of MIF at day 6 of infection compared to naïve cells. We found that eosinophils (Fig 4.2.3A) and macrophages (Fig 4.2.3B) significantly up-regulate the production of MIF during *N.brasiliensis* infection (30 and 140 fold over naïve respectively). Previous literature has shown that MIF is stored and released from macrophages upon inflammatory stimulation (LPS) (Calandra et al., 1994) and that human eosinophils when stimulated *in vitro* with phorbol myristate acetate release MIF (Rossi et al., 1998). MIF has also been shown to be expressed in T cells upon stimulation with glucocorticoid (Leng et al., 2009). In our experiment, we found that sorted $CD19^+$ B (Fig 4.2.3C) and $CD4^+$ T cells (Fig 4.2.3D) do not significantly upregulate the transcription of *Mif* in response to *N.brasiliensis* infection. At immune homeostasis T cells showed a higher baseline expression of MIF in comparison to the different sorted cell populations.

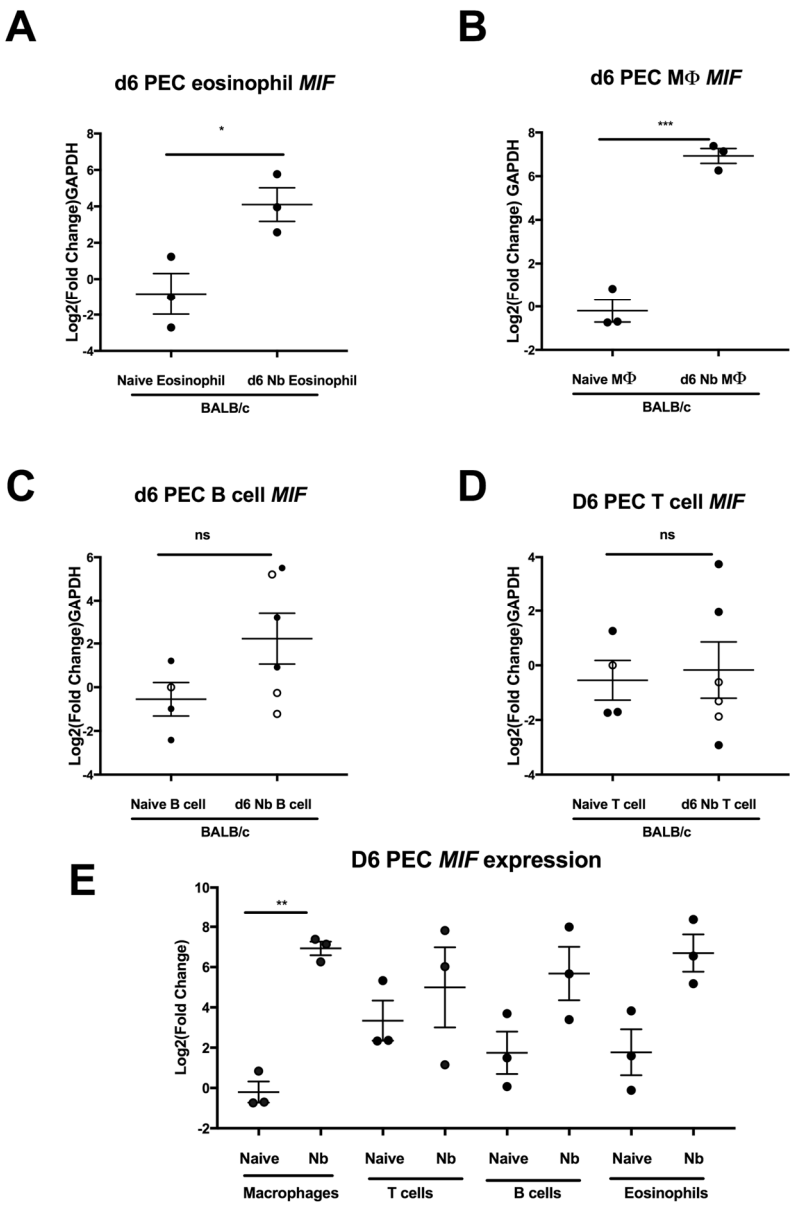

Figure 4.2. 3 A-E *Mif* gene expression is significantly upregulated in eosinophils and macrophages during *N.brasiliensis* infection

BALB/c mice were infected with 400 L3 *N.brasiliensis* s.c. for 6 days and peritoneal exudate cells (PEC) were harvested and sorted by fluorescence-activated cell sorting (FACS) for consecutive gene expression analyses by qRT-PCR. *MIF* gene expression by sorted Siglec F+ eosinophils **(A),** F4/80+ CD11b+ MΠ **(B),** CD19+ CD4- cells B cells (**C)** and CD19- CD4+ cells T cells **(D)** from naive and infected mice. *Mif* gene expression analysed comparing MΠ, eosinophlls, T and B cells. Graphs **A, B** are representative of two individually performed experiments, **C-D** show pooled data from two individually performed experiments. Graph **E** was performed once. Data from different experiments represented as shaded and unshaded circles. Statistical analysis was performed using an unpaired students T test. * = p<0.05, ** = p<0.01, *** p<0.001. Contributions: Electronic sorting of cell populations performed by Dr M. White.

4.2.4 MIF-deficiency results in reduced numbers of CD4⁺ T cells and concentrations of type-2 cytokines.

Despite MIF not being upregulated in CD4⁺ T cells during infection, we assessed if MIF influences CD4⁺ T cell proliferation or migration. To assess the ability of mice deficient of MIF to mount a type-2 immune response during *N.brasiliensis* comparable to WT mice, MLN tissue and peritoneal lavage fluid was harvested from mice at d6 p.i. Single cells prepared from MLN tissue were consecutively analysed for the presence of Th2 cells by flow cytometry and type-2 cytokine secretion into the peritoneal cavity was quantified by ELISA. It became evident that MLNs of BALB/c mice have a higher percentage of CD4⁺ T cells compared to MIF-deficient mice (Fig 4.2.4A), both at baseline (59% vs. 46%) and following *N.brasiliensis* infection (56% vs. 46%). The total counts of CD4⁺ T cells in BALB/c mice increased from an average of 3.4 x 10^6 cells to 8.9 x 10^6 cells when nematode-infected, whereas the increase in total CD4⁺ T cells induced by the helminth was significantly attenuated in MIF-deficient mice (BALB/c Nb vs. MIF-/- Nb: 8.9 x 10^6 cells vs. 1.6 x 10^6 cells) (Fig 4.2.4B). As the total numbers of MLN cells are also augmented in the BALB/c mouse (see Fig 4.2.2C), there is an overall 5-fold difference in total MLN CD4⁺ T cells between the two genotypes (Fig 4.2.4B).

As the percentage and number of CD4+ T-cells is reduced in MIF-/- mice, also during infection, we analysed in addition if these cells are defective in polarising into Th2 cells. When analysed for expression of the type-2 specific transcription factor GATA3, a similar slight but not significant increase in the percentages of CD4⁺ T cells expressing this protein (Fig 4.2.4 C) was detected in MLN harvested from both genotypes infected with *N.brasiliensis*, confirming that MIF-deficient CD4+ T cell are competent in polarising into Th2 cells. However, the total numbers of Th2 cells (GATA3⁺ CD4⁺) are significantly decreased in the infected MIF-/- MLN when compared to the wild-type BALB/c MLN (3.6 x 10^4 versus 22 x 10^4 respectively) (Fig 4.2.4 D), due to the attenuated level of total immune cells in the MLN induced by MIF deficiency, presented in Fig. 4.2.2C.

To ascertain if the type 2 cytokine responses *in vivo* reflected the total $CD4^+$ T cell profile, fluid was collected from the peritoneal cavity and assayed for levels of soluble type-2 cytokines as shown in Fig 4.2.4 E-G. There was, correspondingly, an increased production of IL-4 (Fig. 4.2.4E), IL-5 (Fig. 4.2.4F) and IL-13 (Fig. 4.2.4G) in the peritoneal lavage fluid of *N.brasiliensis* infected wild type mice, which was absent in MIF-deficient mice.

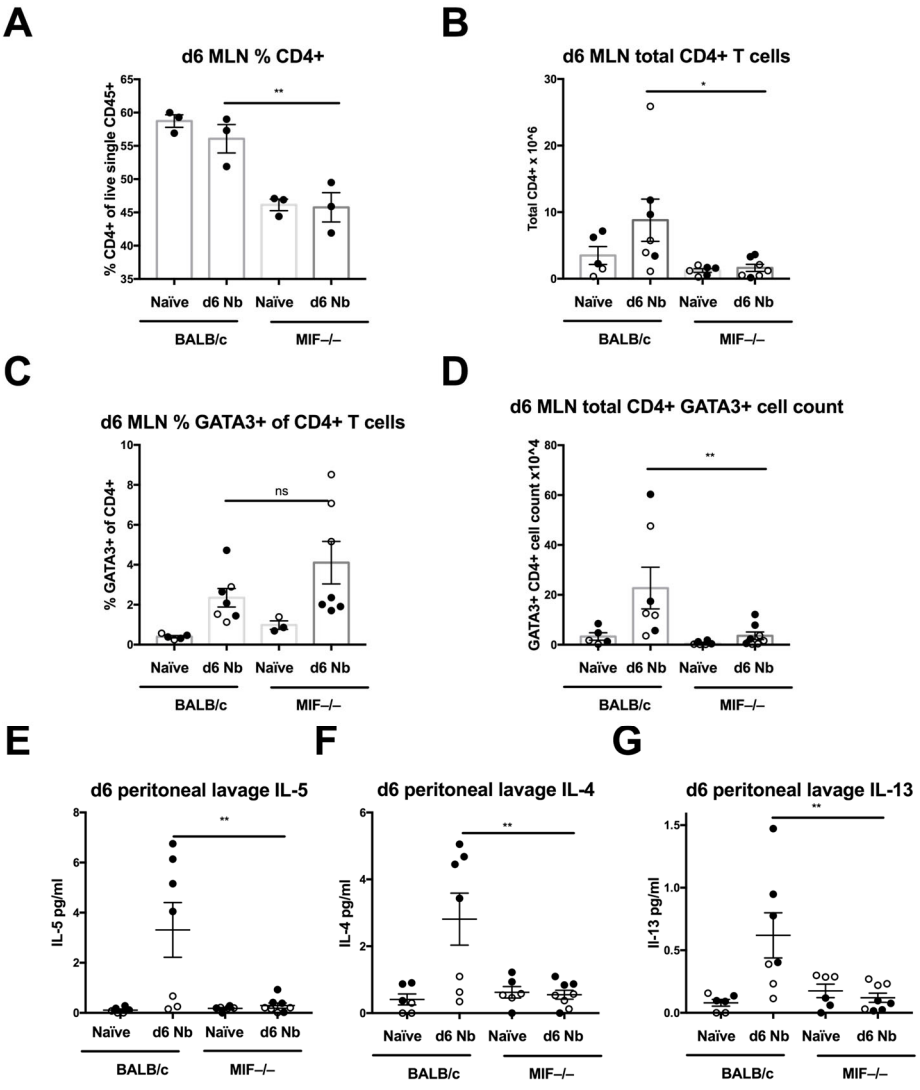

Figure 4.2. 4 A-G: MIF-deficient mice have reduced T cells and T cell cytokines but the ability of T cells to polarise remains intact.

BALB/c and MIF-/- mice were infected with 250-400 L3 *N. brasiliensis* larvae s.c. and sacrificed at d6 p.i. MLN tissue was harvested and processed for flow cytometric analyses and peritoneal lavage fluid frozen. (A) Percentage of CD4+ T cells of MLN total CD45+ immune cells. (B) Total MLN CD4+ T cells. Percentage of MLN GATA3+ TH2 cells of CD4+ T cells (C) and total number of MLN GATA3+ CD4 cells (D). Cytokine concentrations of IL-4 (E), IL-5 (F) and IL-13 (G) were measured by cytometric bead array (CBA). Data pooled from two experiments. Data presented in Graph A are representative of two individually performed experiments, B-G show pooled data from two individually performed experiments. Data from pooled experiments represented as shaded and unshaded circles. Data was analysed by parametric one-way ANOVA, and corrected for multiple comparisons by a Sidak's test (A, B) or Kruskal-Wallis test (C, D). * $p<0.05$, ** $p<0.01$, *** $p<0.001$. Contributions: experimental preparation with Dr S. Loeser.

4.2.5 MIF-deficient mice have impaired innate lymphoid cell responses

Type-2 cytokines are secreted cells other than $CD4^+$ TH2 cells during *N.brasiliensis* infection. It is now clear that a population of innate immune cells resemble an important part of the type-2 immune response by their capacity to secrete type-2 cytokines in an antigen-independent manner. Release of IL-13 by ILC2s in response to *N. brasiliensis* infection was shown to effectively result in expulsion of the worm (Neill et al., 2010). We therefore assessed the ILC2 response at d6 p.i. with 250-400 L3 in the MLN of both wild-type BALB/c and MIF-deficient mice. Significant numbers of ILCs at d6 p.i. were detected in the MLN, but not in the BAL or the PEC (data not shown).

The ILC population was defined as $CD45^+$ cells that are negative for CD4 and lineage markers CD3, Ly6C/G, CD11b, CD45R/B220, TER-119; but positive for ICOS. ILC2s were classified as ILCs that are positive for the type-2 transcription factor GATA3. We found that MIF-deficient mice showed a significantly reduced percentage (Fig. 4.2.5A) and total numbers (Fig. 4.2.5B) of ILCs in the MLN at d6 after *N.brasiliensis* infection. Due to the nematode infection, the percentage of total ILCs in the MLN increased from 0.17% of total live $CD45^+$ cells to 0.59% in wild-type BALB/c mice. This increased migration or proliferation of ILCs to the MLN during infection is absent when mice are MIF deficient, where the percentage of ILCs in the MLN remains below 0.04% during infection (Fig 4.2.5A). Correspondingly, the numbers of ILCs were found to be significantly higher (70 fold) in infected BALB/c mice when compared to infected MIF-deficient mice (BALB/c Nb: 0.08 x 10^6 ILCs vs. MIF-/- Nb: 0.0011 x 10^6 ILCs) (Fig 4.2.5B).

Next, the present ILC population was further analysed for expression of the type-2 transcription factor $GATA3^+$ to identify ILC2 cells. An elevated percentage of ILC2 cells was detected in *N.brasilliensis* infected BALB/c mice when compared to uninfected mice. When compared to MIF-deficient mice, the percentage of MLN ILC2 cells mounted during infection was significantly higher

in wild-type BALB/c mice (0.55% vs. 0.03% respectively) (Fig 4.2.5C). This result was also reflected by calculated ILC2 total cells of the MLN, where mean numbers of ILC2s in the BALB/c infected mice were 0.08 x 10^6 cells and in MIF-deficient mice 0.0001 x 10^6 cells (Fig 4.2.5 D).

The dot plots demonstrating the difference in ILCs are shown in Fig 4.2.5E and (WT) and 4.2.5F (MIF-deficient mice). These have been pregated for the live, single CD45+ and CD4- cells and demonstrate that the ICOS+ and Lin- population is expanded in the wild-type but not MIF-/- mice.

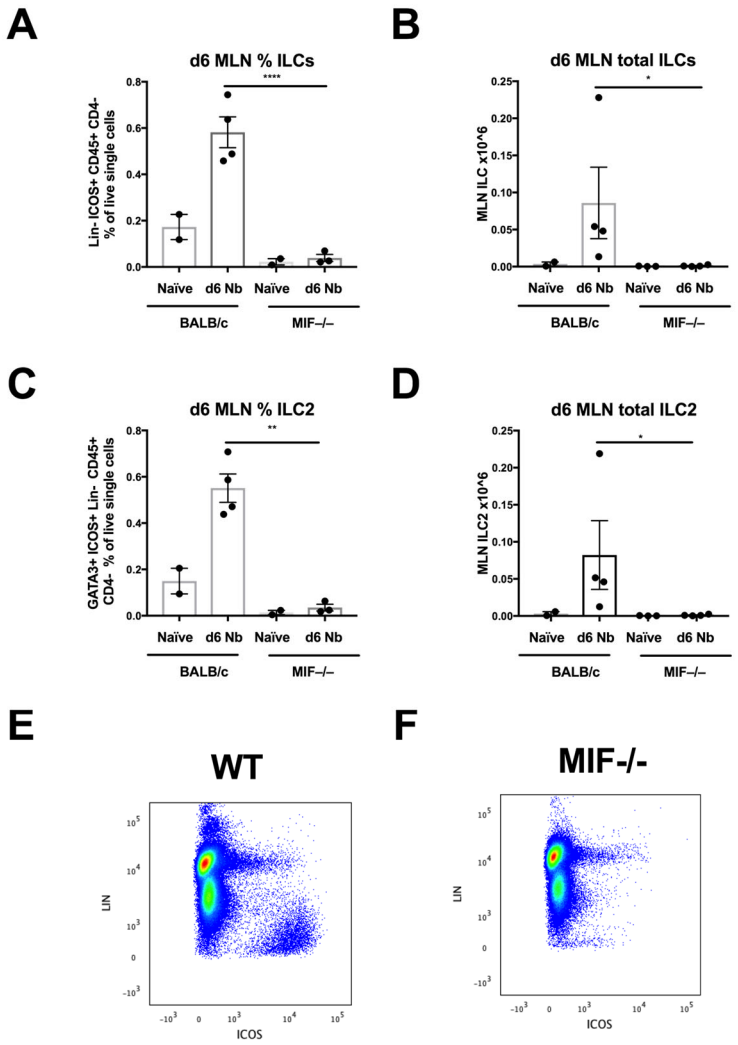

Figure 4.2.5 A-F: MIF-deficiency abrogates innate lymphoid cell responses

BALB/c and MIF-/- mice were infected with 250 L3 *N. brasiliensis* larvae s.c. and sacrificed at d6 p.i.. MLN tissue was harvested and processed for flow cytometric analyses. **(A)** Percentage and (**B)** total number of CD45+ CD4- Lin- ICOS+ ILCs in MLN. **(C)** Percentage and (**D)** total number of GATA3+ ILCs (ILC2s) in MLN. Dot plot demonstrating ILCs of WT **(E)** and MIF-/- **(F)** mice at d6 p.i. All data are representative of two individually performed experiments. Data was statistically analysed by one-way ANOVA. Data in **A.** corrected for multiple comparisons by a Sidak's test. Data presented in graphs **B, C, D** was analysed using the non-parametric one-way ANOVA Kruskal-Wallis test.* $p<0.05$, ** $p<0.01$, *** $p<0.001$. Contributions: experimental preparation with Dr S.Loeser.

4.2.6 MIF-deficient mice have impaired type 2 alternative activation and eosinophil responses

ILC2 cells are crucial orchestrators of the anti-helminth type-2 response. They are an early source of type-2 cytokines which drives alternative macrophage polarisation (Filbey et al., 2018), however, MIF may directly affect macrophages (Prieto-Lafuente et al., 2009).

Alternatively activated macrophages accumulate during helminth infection and secrete products Arg-1, RELMα and Ym1. Macrophages and their products are important in the anti-helminth immune responses. Clodronate depletion of macrophages and arginase inhibition abrogates the Th2 memory responses (Anthony et al., 2006). RELMα inhibits type 2 inflammatory responses(Chen et al., 2016; Nair et al., 2009). Ym1 is the dominant chitin like protein in the lung, and overexpression of Ym1 results in a reduced worm burden (Allen and Sutherland, 2014). Previous work in our lab had demonstrated the ability of MIF to directly affect bone marrow macrophages: MIF and IL-4 synergise to increase the production of Ym-1, RELMα and Arg-1 (Prieto-Lafuente et al., 2009).

We assessed intracellular expression of RELMα and YM1 in peritoneal exudate $CD11b^+$ $F4/80^+$ macrophages infection and found that the MIF-deficient mice had impaired intracellular production of these two proteins (Fig 4.2.6 A,C) at D6 of *N.brasiliensis*. The BALB/c and MIF-deficient naïve mice had a similar amount of intracellular RELMα (17 and 14% respectively) whereas the percentage of $RELMα^+$ macrophages in the peritoneal cavity after 6 days of *N.brasiliensis* increased to 87% in the BALB/c infected mice compared to only 43% in the MIF-deficient mice (Fig 4.2.6A). The percentage of Ym1 positive macrophages increased from 0% to 11% in BALB/c infected mice, but YM-1 was not produced by peritoneal MIF-deficient Mϕ even after infection (Fig 4.6C). The peritoneal protein concentration measured by ELISA was also a

significantly reduced for RELMα (Fig 4.2.6B) and YM1 (Fig 4.2.6D) in MIF-/- mice at d6 p.i.

In addition to alternative macrophage polarisation, *N. brasiliensis* infection is associated with a marked eosinophilia, which we evaluated in MIF-deficient mice. At day 6 following infection, the percentage of SiglecF$^+$ eosinophils in the BALB/c mice increased from 0.5 to 4.3% of the total live, single peritoneal exudate cells. In the MIF-deficient mice, the increase was also present to a lesser degree from 0.9 to 2% (Fig 4.2.6 E). The total numbers of eosinophils in the PEC of D6 *N.brasiliensis* infected BALB/c mice was 30 x 10^4 cells whereas this was 13 x 10^4 in MIF-deficient infected mice (Fig 4.2.6F).

The lung is also a site where ILCs and M2 macrophages work together during *N.brasiliensis* infection(Bouchery et al., 2015), therefore we looked at alternative activation in the lung environment. MIF deficient mice had reduced percentages of RELMα$^+$ macrophages in both the lung (Fig. 4.2.6.F) and the BAL (Fig 4.6G), correspondingly, the level of RELMα protein in the BAL of the BALB/c mice was 1.5 time the value in the MIF-deficient mice (Fig 4.2.6 H). 13% of the BALB/c lung alveolar macrophages are positive for RELMα, however, only 7% of the MIF-deficient macrophages are positive for RELMα (Fig. 4.2.6F). In the BAL, 15% of the alveolar macrophages were positive for RELMα of BALB/c mice and this was 12% of the alveolar macrophages in the BALB/c mice.

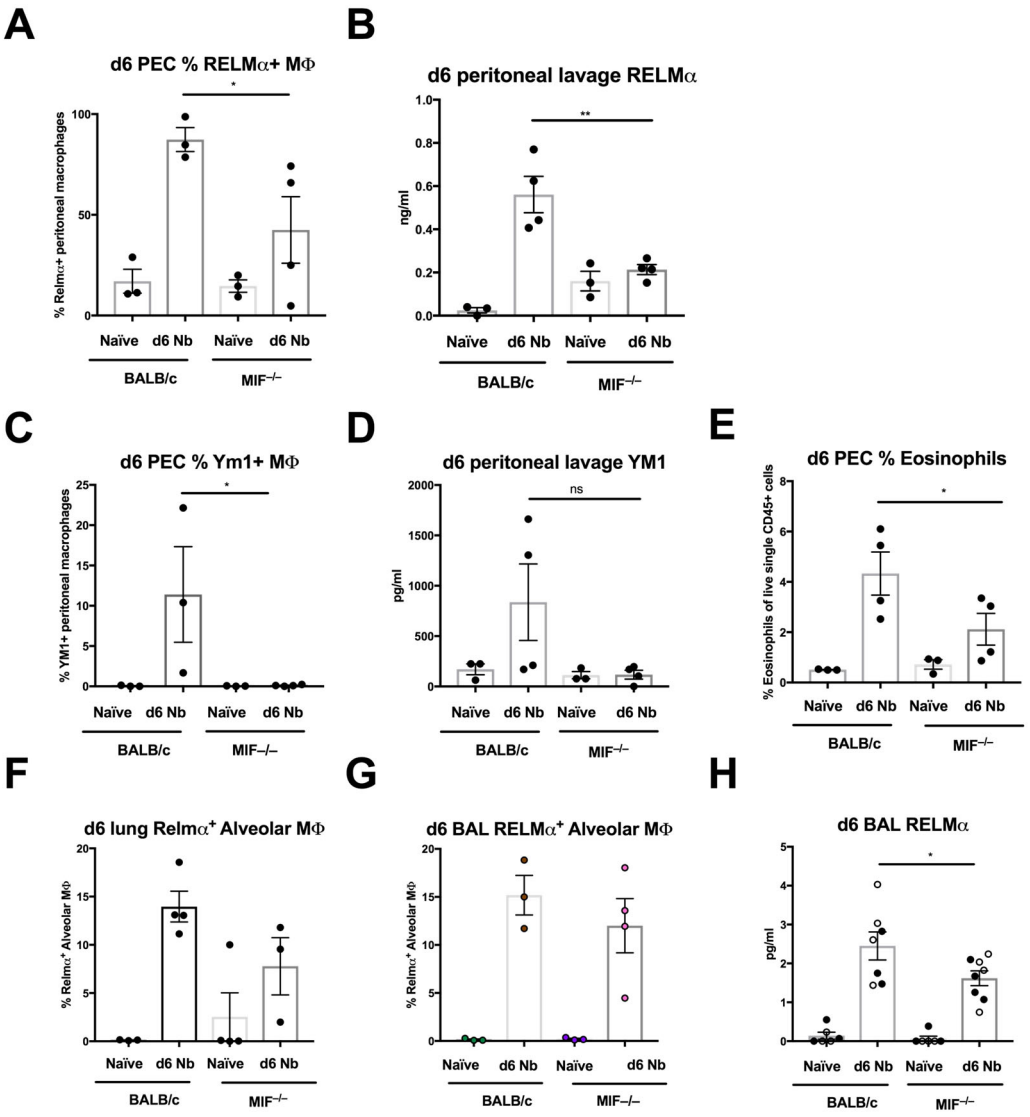

Figure 4.2.6 A-H: MIF-deficient mice have deficient type 2 alternative activation and eosinophil responses in the peritoneal cavity during *N.brasiliensis* infection.

BALB/c and MIF-/- mice were infected with 400 *N. brasiliensis* L3 larvae s.c., PEC, BAL and lung were analysed by flow cytometry at d6 p.i and peritoneal lavage fluid was frozen. (A) Percentage of RELMα+ Mϕ (CD11b+ F4/80+) and RELMα concentration (B) in collected peritoneal lavage fluid. (C) Percentage YM-1+ Mϕ of peritoneal exudate cells (PEC) and (D) concentration of YM-1 in peritoneal lavage fluid. (E) Percentage of Siglec F+ eosinophils in PEC. Percentages of Alveolar Mϕ (CD11c+ CD11b- Siglec-F+) in lung homogenate (F) and BAL (G) that are RELMα+. ELISA measurement of RELMα protein levels in BAL fluid(H). Data presented in graphs (A, C, E) are representative of two experiments, (B, D, F, G) are representative of one experiment and data presented in (H) pooled from two experiments. Data from pooled experiments represented as shaded and unshaded circles. All data analysed by one-way ANOVA, and corrected for multiple

comparisons by a Sidak's test. Contributions: lung and BAL preparation by Dr S.Loeser.

4.2.7 MIF deficient mice do not have a defect in neutrophilis at an early time point.

We examined cell changes in the lung at an earlier time point (D3), as in *N.brasiliensis*, neutrophil infiltration is associated with the acute lung injury between 18-72 hours post infection when the L3 are transforming to L4 larvae in the lung. We found no difference in the numbers of $CD11b^+$ $Ly6G^+$ neutrophils in the BAL (Fig 4.7M) or the lung (Fig4.7N), although it could be that these neutrophils were functionally altered in some way. The differential counts in both MIF-deficient mice and wild type mice was broadly similar at D3 of infection for the alveolar macrophages and eosinophils also (Fig 4. E,F, I, J).

By D6 of infection, the numbers of cells in the BAL increases 3 fold in the BALB/c mice but remains similar in naïve and infected MIF-deficient mice (Fig 4.2.7 C). In the lung, there is a trend towards higher cell counts in the BALB/c infected mice, which have 16 x 10^6 cells in total, but the MIF-deficient mice have 112 x 10^6 cells (Fig 4.2.7D) but the difference does not reach statistical significance. The fold change differences are 1.5 and 1.3 comparing naïve and infected BALB/c and MIF-deficient mice respectively (Fig 4.2.7D).

We therefore found the absolute numbers of alveolar macrophages (Fig.4.2.7G, H), eosinophils (Fig4.2.7D,G) in the lung and the BAL, and the neutrophils in the BAL were increased at D6 of infection (Fig1.18H). At day 6 of infection the number of alveolar macrophages in the BAL had risen from 0.04 to 0.21, however in the MIF-deficient mice this number had changed from 0.1 to 0.04 x 10 ^ 6 cells (Fig 4.2.7G). In the lung, at day 6 of infection the number of alveolar macrophages in the BALB/c mice was 1.2 x 10^6 but only 0.4 x 10^6 in the MIF-deficient mice (Fig 4.2.7F). The fold change was 1.5 and 1.1 from naïve to infected mice in BALB/c and MIF-deficient mice respectively. The eosinophils in the BAL was 6.2 x 10^4 cells in BALB/c mice but was 2.8 x 10^4 cells in MIF-

deficient mice. The difference was not statistically significant. The numbers of $Cd11b^+$ $Ly6G^+$ neutrophils in the BAL of BALB/c mice at D6 of infection rose to 1.9 x 10^6 in BALB/c mice but was only 0.2 x 10^4 in MIF-deficient mice (Fig 4.2.7N).

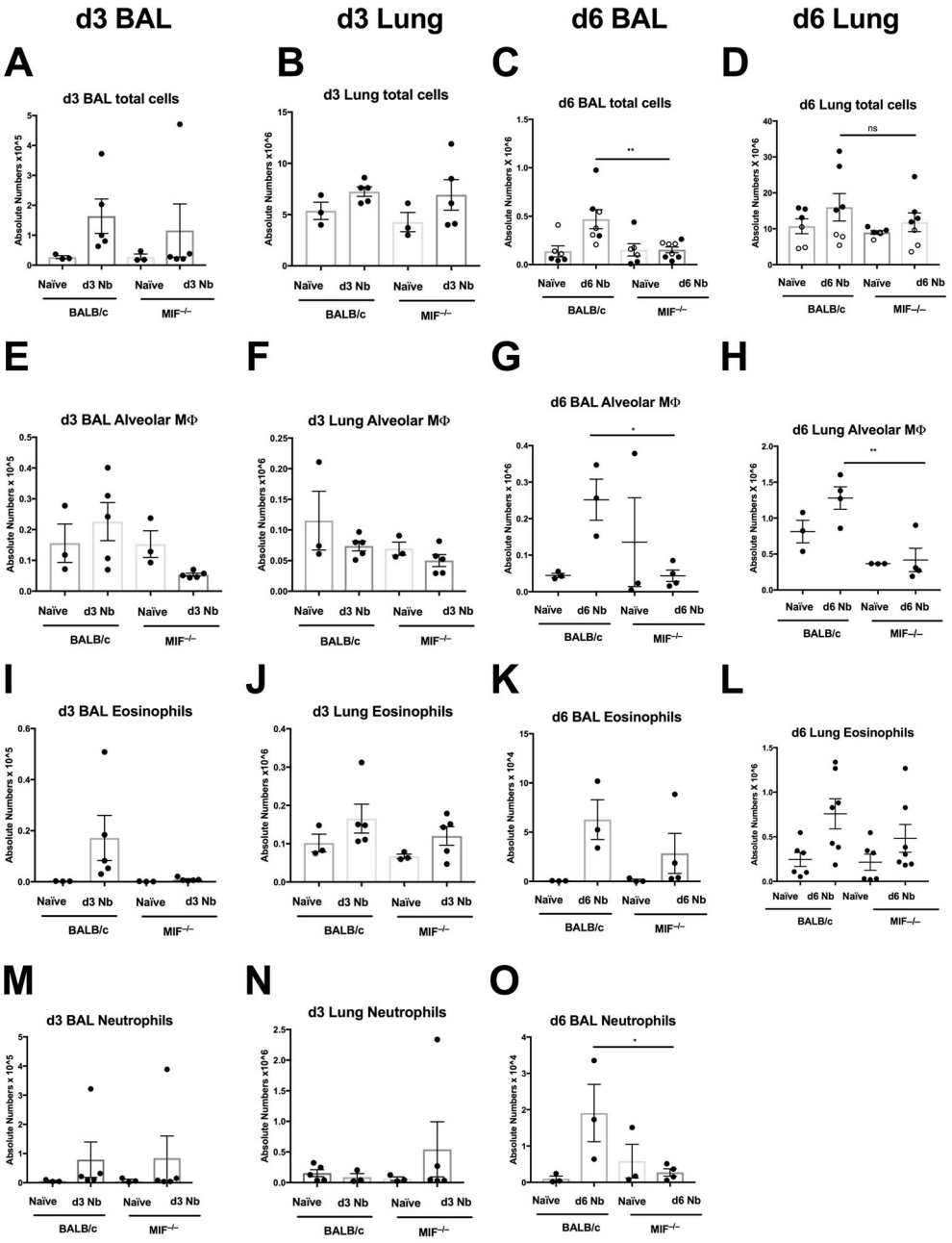

Figure 4.2.7 A-O: MIF-deficient mice do not have a defect in the neutrophil response at D3, but have reduced alveolar macrophages and eosinophils at D6 of infection

BALB/c and MIF$^{-/-}$ mice were infected with 400 *N. brasiliensis* L3 larvae s.c. BAL and Lung are analysed by flow cytometry at d6 p.i. Numbers of cells in BAL **(A)** and lung **(B)** at d3 of infection; numbers of cells in the BAL **(C)** and lung **(D)** at d6 of infection. Numbers of CD11c+ CD11b^{-} SigF+ AMs in BAL **(E)** and lung **(F)** at D3 of infection. Numbers of AMs in the BAL **(G)** and lung **(H)** at D6 of infection. Numbers of CD11c- CD11b+SigF+ eosinophils in BAL **(I)** and lung **(J)** at d3 of infection; number of eosinophils in BAL **(K)** and lung **(L)** at d6 of infecction. Numbers of CD11b+ Ly6G+ neutrophils in BAL **(M)** and lung **(N)** at d3 of infection; numbers of neutrophils in the BAL **(O)** at d6 of infection. Contributions: lung and BAL prep by Dr S.Loeser.

4.2.8 MIF-deficient mice have impaired type-2 epithelial responses to infection

In Fig 4.2.5 we demonstrate that the MIF-deficient mice had a deficit in ILCs. Tuft cells in the epithelium have recently been shown to expand rapidly in response to intestinal helminths infection, releasing IL-25 as an alarmin that activates innate lymphoid cells to initiate worm expulsion. We therefore examined tuft cell responses in MIF-deficient mice, mostly by immunohistochemistry utilising an antibody targeting the tuft cell specific marker DCLK1 (double cortin like kinase-1).

Sections of small intestine harvested from mice infected with *N. brasiliensis* for 6 days were stained for the tuft cell-specific marker DCLK1. The average tuft cell number per crypt/villus axis was subsequently calculated (Fig. 4.2.8A). Comparing representative light microscopy images acquired for all experimental groups (Fig. 4.2.8B), it became evident that wild-type mice infected with *N.brasiliensis* show tuft cell hyperplasia, a feature lacking in infected MIF deficient mice. DCLK1+ epithelial cells had proliferated in the intestine of infected BALB/c mice, reaching approximately 16 fold higher numbers compared to naïve BALB/c intestine. During infection, induced expansion of the tuft cell number was significantly augmented in the wild-type mice compared to MIF-/- mice, where the fold change from naïve was marginal at 2.5 times the number of DCLK1+ epithelial cells per crypt/villus axis (Fig 4.2.8B). Correspondingly the gene expression level of *IL-25* in the proximal small intestine of BALB/c infected mice was significantly (2 fold) greater than the levels transcribed in the MIF-deficient mice when infected with the nematode (Fig 4.2.8C).

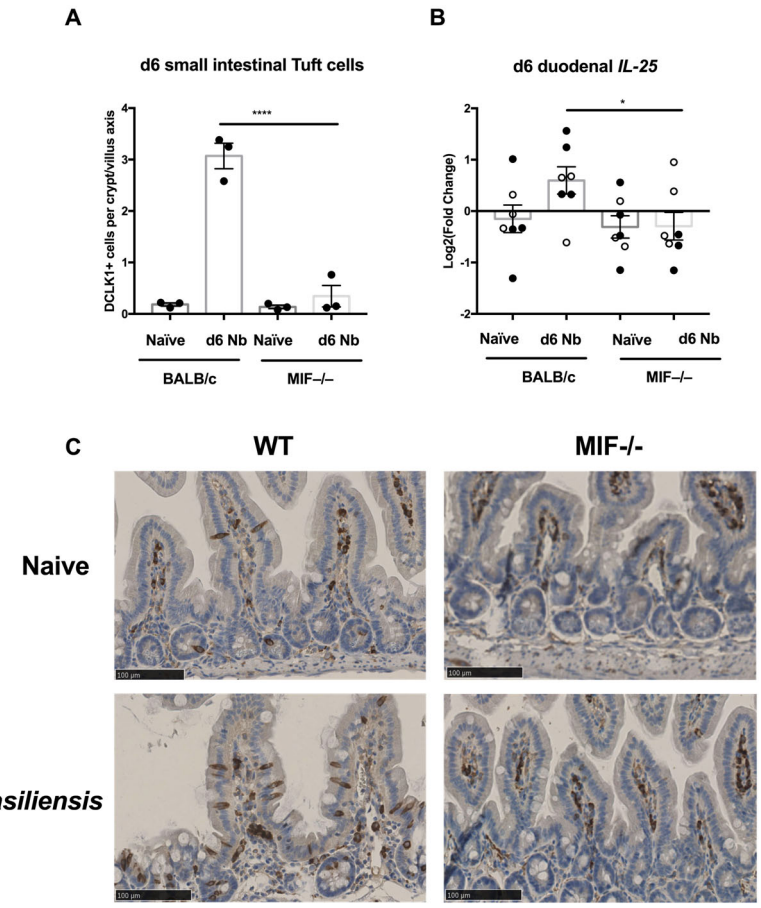

Figure 4.2.8 A-C: MIF-deficient mice have impaired Type 2 intestinal tuft cell responses.

BALB/c and MIF$^{-/-}$ mice were infected with 400 *N. brasiliensis* L3 larvae s.c.; small intestinal tissue was fixed in 10% NBF at 4°C overnight and then paraffin embedded. Sections of small intestine were consequently stained for DCLK1 at d6 p.i. **(A)** Quantification of number of DCLK1 positive cells as an average count for 100 crypt/villus axis, representative of three experiments. **(B)** Gene expression analysis by qPCR of proximal duodenum to assess transcription levels of *IL-24.* Data pooled from two experiments represented as shaded and unshaded circles. **(C)** Representative light microscopy images showing epithelial DCLK1^{+} (tuft) cells in uninfected and infected BALB/c and MIF$^{-/-}$ mice. Scale bar equals 100µm. Data analysed by one way ANOVA, and corrected for multiple comparisons using a Sidak's multiple comparison test. * $p<0.05$, ** $p<0.01$, *** $p<0.001$. Contributions: Dr F Gerbe (Jay lab, Montpellier) performed DCLK1 stainings.

4.2.9 MIF-deficient mice have reduced goblet cell hyperplasia and RELMß expression

Tuft cell-derived IL-25 commences a positive feedback loop within the intestine by recruiting innate lymphoid cells that secrete IL-4/13 further amplifying the tuft cell response, goblet cell and tuft cell hyperplasia and eventual expulsion(Gerbe et al., 2016). We therefore next examined goblet cell responses in the MIF-deficient mice.

The small intestinal epithelium of mice infected with *N.brasiliensis* for 6 days was Periodic Acid-Schiff (PAS) stained to enumerate goblet cells. Notably hyperplasia was evident in wild-type mice but limited in the MIF-deficient hosts (Fig. 4.9A). The numbers of goblet cells per villus increased from 8 to 16 in infected BALB/c mice, whereas the goblet cell number in the MIF-deficient mice increased only fractionally from 10 to 11 goblet cells per villus. Therefore there was approximately 1.5 times greater numbers of goblet cells in the BALB/c infected mice compared to the MIF deficient mouse. Similar sections were also stained for RELMß protein, which was found to be highly expressed in infected wild-type but absent from MIF-deficient mice (Fig 4.2.9 B). There was over a hundred fold difference in the BALB/c RELMß protein counts when comparing infected BALB/ and MIF-deficient small intestinal epithelium (BALB/c infected mice had RELMß count per crypt villus axis of 4.7 but in the MIF infected mice this was only 0.04). The level of *RETLNB* (RELMß) gene expression in the proximal small intestinal tissue was then assessed, and was 13 fold higher in the BALB/c infected mice compared to MIF-deficient infected mice (Fig 4.2.9 C). Representative images of intestinal tissue stained for RELMß protein from naive and infected wild-type and MIF-deficient mice are presented in Fig 4.2.9 D.

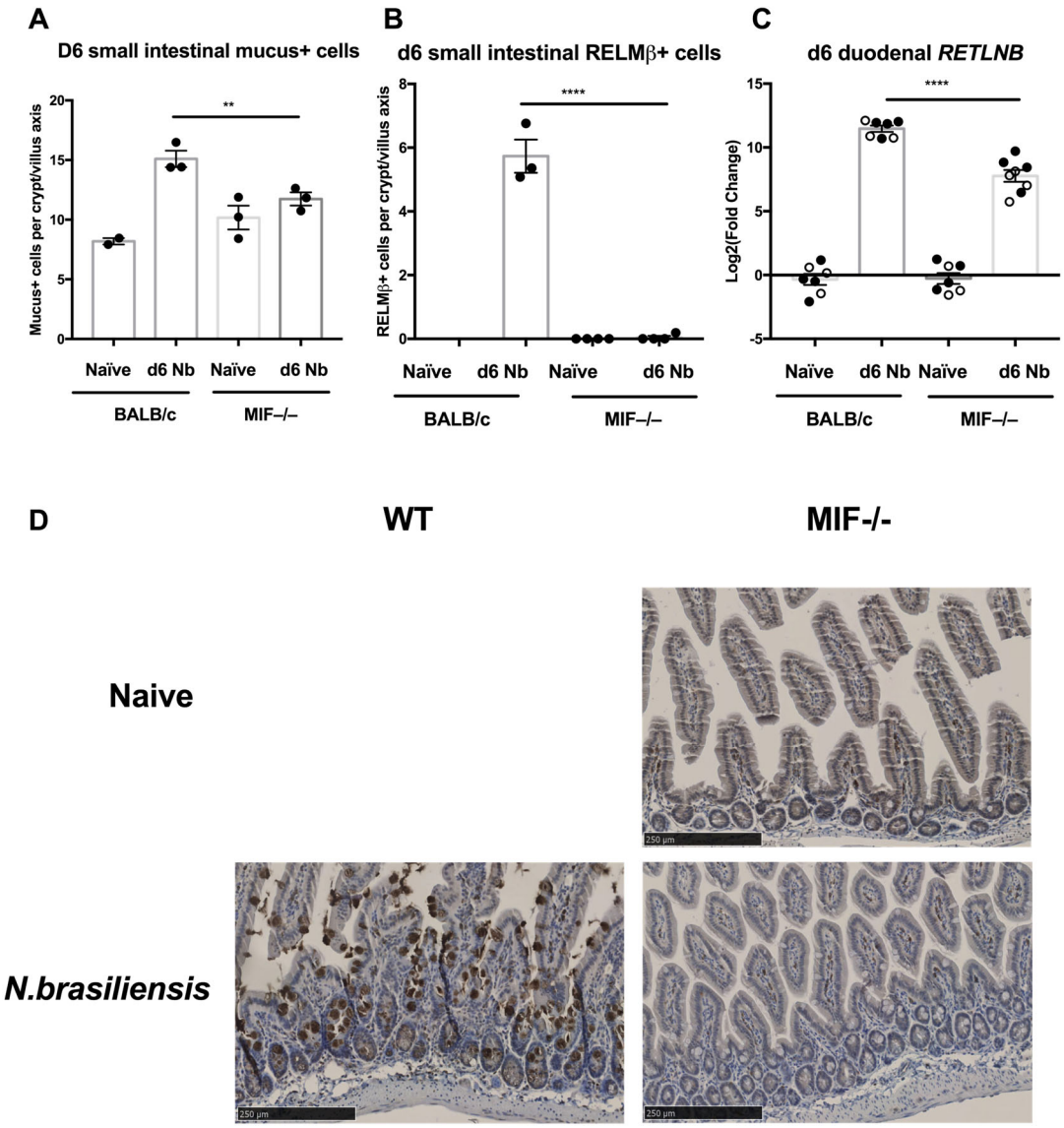

Figure 4.2.9 A-D MIF-deficient mice have impaired goblet cell hyperplasia, RELMβ production and *RETLNB* (RELMβ) gene expression in the small intestine.

BALB/c and MIF$^{-/-}$ mice were infected with 400 *N. brasiliensis* L3 larvae s.c.. Small intestine was harvested at d6 p.i., fixed in 10% NBF at 4°C overnight and paraffin embedded. Cut sections were stained for RELMβ. Duodenum was frozen in RNA later for RNA extraction and qRT-PCR **A** Quantification of number of mucus+ goblet cells per villus (100 crypt villus/axes counted per section); performed once. **B** Average number of RELMβ^{+} cells per crypt/villus axis (100 crypt/villus axis assessed per section), representative of three experiments. **C** Gene expression analysis by qRT-PCR of proximal duodenum for transcription levels of *RETLNB* (RELMβ)*;* data from pooled experiments represented as shaded and unshaded circles. **D** Representative light microscopy images of small intestinal sections stained for RELMβ in BALB/c and MIF$^{-/-}$ naive and infected mice. Scale bar equals 100µm. Data analysed by one way ANOVA, and corrected for multiple errors by a Sidak's multiple comparison test. * $p<0.05$, ** $p<0.01$, *** $p<0.001$. Contributions: Dr F Gerbe (Jay lab, Montpellier) performed RELMβ stainings. Some qRT-PCR performed by Ms N.Britton.

4.2.10 MIF-deficient mice have impared type-2 intestinal immune responses within the lymphoid compartment

We next assessed protein expression of the transcription factor GATA3, who controls gene expression of type-2 cytokines in both ILC2s and Th2 cells. Therefore, differences in cell numbers positive for the protein GATA3 in the intestinal tissue suggests changes in ILC2 and/or Th2 cell numbers. When light microscopy images of intestinal sections stained for GATA3 protein were assessed (Fig 4.2.10A), we found infected MIF-deficient mice (mean of 2.3 GATA3+ cells/villus) to have significantly reduced numbers of cells expressing GATA3 within the intestinal epithelium compared to wild-type mice infected with *N.brasiliensis* (mean of 12 GATA3+ cells/villus) (Fig 4.10A). Concomitant, gene expression of the transcription factor *Gata3* in harvested duodenal tissue from *N.brasiliensis* infected MIF deficient mice was only marginally increased compared to the respective naïve control group and significant attenuated when compared to infected wild-type mice (Fig 4.2.10B). In line with the reduced type-2 immune profile and diminished peritoneal eosinophilia (see Fig. 4.2.6E) in infected MIF-/- mice we also observed significantly dampened induction of *IL-5* gene expression in *N.brasiliensis* infected MIF-deficient animals (Fig 4.2.10C) when compared to the infected BALB/c group. These data indicated that there is a greatly reduced accumulation of either or both TH2 and ILC2s in the lamina propria of the intestine, in parallel with reductions shown by the flow cytometry of mesenteric lymph node cells (Fig 4.2.4-5).

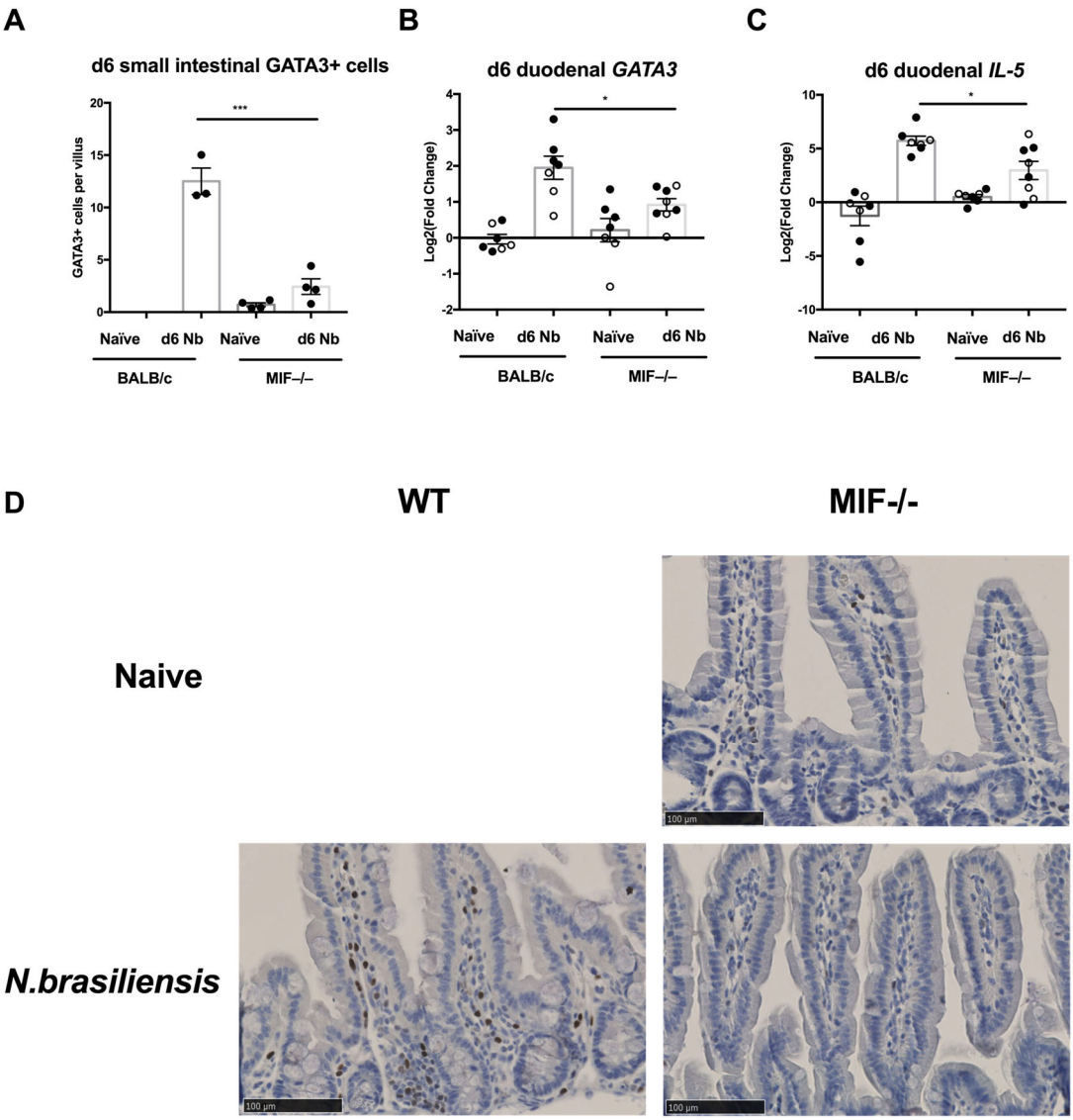

Figure 4.2.10 A-D: MIF-deficient mice have impaired Type 2 intestinal responses

BALB/c and MIF$^{-/-}$ mice were s.c. infected with 400 *N. brasiliensis* L3 larvae for 6 days: Sections cut of paraffin-embedded small intestine were stained for GATA3 by immunohistochemistry (**A-B**). **(A)** Quantification of number of GATA3 positive cells per villus as an average of 100 counts was performed. Data representative of two experiments. qRT-PCR of proximal duodenum was performed to assess transcription levels of *Gata3* **(B)** and *IL-5* **(C)**. 2 experiments pooled and shown in filled and shaded circles. **(D**) Representative light microscopy images of small intestinal sections stained for GATA3. Scale bar equals 100 µm. Data analysed by one way ANOVA, and corrected for multiple errors by a Sidak's multiple comparison test. * $p<0.05$, ** $p<0.01$, *** $p<0.001$. Contributions: Dr F Gerbe (Jay lab, Montpellier) performed GATA3 stainings. Some qRT-PCR performed by Ms N.Britton.

4.2.11-12 IL-25 rescues the immunological responses in the MIF-deficient mouse

IL-25 is produced by eosinophils (Terrier et al., 2010), basophils, mast cells and by epithelial cells (Oliphant et al., 2011). However, the most important source of IL-25 is the tuft cell. Mice that lack Pou domain class 2, transcription factor 3 (Pou2f3) are deficient in the production of IL-25 and in helminth expulsion (Gerbe and Jay, 2016). This suggests that the most important physiological source of IL-25 is the epithelial tuft cell. IL-25 produced by tuft cells and has been found to be an important epithelial cell alarmin in the response to *N. brasiliensis* and results in upregulation of ILCs (Fallon et al., 2006; Gerbe et al., 2016; Zhao et al., 2010). In this setting, IL-25 acts upstream, or independently of, IL-13 because administration of exogenous IL-25 is unable to rescue expulsion of *N. brasiliensis* in a IL-13-deficient mouse (Zhao et al., 2010). In addition, experiments in IL-25R chimeric mice demonstrate that loss of IL-25R in the haematopoetic compartment results in failure to expel *H. polygyrus* (Smith et al, unpublished results). We therefore explored whether exogenous IL-25 is able to rescue the phenotype of the MIF-deficient mouse.

Two groups of BALB/c and MIF-deficient mice were infected with *N.brasiliensis* L3 larvae and sacrificed at d6 p.i., one of these groups was administered rIL-25 i.p. daily from d1-5 of infection (Fig4.2.11A) while the other group was administered PBS i.p. (vehicle) daily from D1-5. At day 6 p.i., both groups were compared to assess the ability of rIL-25 to rescue the immunological phenotype of the MIF-deficient mouse.

The numbers of Lin^- $CD4^-$ $ICOS^+$ ILCs (Fig 4.2.12A) and $GATA3^+$ ILCs (ILC2s) (Fig 4.2.12B) is rescued with the administration of rIL-25. The percentage of ILCs in the MLN in BALB/c mice increases from 0.011 to 0.09 and 0.5% in naïve, *N.brasiliensis* treated mice, and *N.brasiliensis* treated mice given rIL-25. In MIF-deficient mice, the percentage of ILCs in the MLN is 0.018% in naive

mice, and rises to 0.03% and 1.67% in *N.brasiliensis* treated mice and *N.brasiliensis* treated mice given rIL-25. The percentage of MLN that are ILCs rises almost 8 fold in the BALB/c mice on infection, but only 2 fold in MIF deficient mice on infection which is similar to the data presented in 5.5. It is clear that administering MIF deficient mice rIL-25 results in restoration of the percentage of ILCs. This number similarly increases for ILC2s (Fig 5.2.12B). The number of T cells is not affected by the administration of rIL-25 at d6 of *N. brasiliensis* infection (Fig 4.2.12C).

The cellularity of the peritoneal exudate cells was increased with the administration of rIL-25. The number of cells in the peritoneal cavity recovered at d6 p.i. was 3.78 x 10^6 in *N.brasiliensis* infected mice to 17 x 10^6 in *N.brasiliensis* mice given rIL-25 (Fig4.2.12D). This was however less obvious in the MIF-deficient mice with cell counts increasing from 1.2 x 10^6 to 3.4 x 10^6 in MIF-deficient mice infected with *N.brasiliensis* and infected mice additionally given rIL-25 respectively. We looked at the peritoneal exudate cell $CD11b^+$ $F4/80^+$ macrophages (Fig 4.2.12E). We found that giving rIL-25 increased the percentage of RELMα+ macrophages in the peritoneal cavity from 46 to 78% in the wild type BALB/c mouse. In addition, administration of rIL-25 rescued the numbers of RELMα+ macrophages in MIF-deficient mice (the percentage of positive macrophages increased from 9% and 7% in naïve and *N.brasiliensis* infected mice to 93% in *N.brasiliensis* infected mice given rIL-25). We also found that administration of rIL-25 for five days increased the percentage of Siglec-F^+ eosinophils in the peritoneal cavity in BALB/c mice, and rescued the numbers of eosinophils in the MIF-deficient mouse. The percentage of eosinophils in BALB/c mice rose from 9 to 12 to 27% in naïve, *N.brasiliensis* infected and infected mice given rIL-25 respectively. This rescue of eosinophils was noted in the MIF deficient mice also (This rose from 4.8 to 8.9 to 26% of the peritoneal exudate cell population in naïve, *N.brasiliensis* infected and *N.brasiliensis* infected mice given rIL-25 respectively).

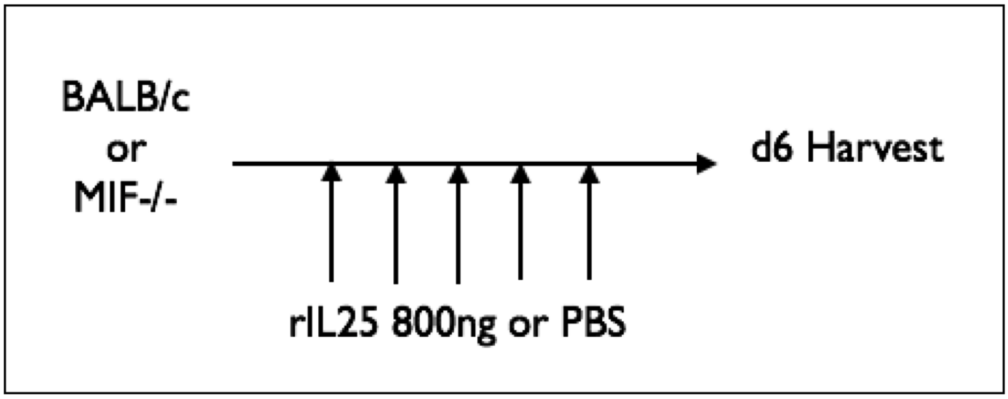

Figure 4.2.11 rIL-25 is able to rescue the epithelial cell phenotype in the MIF-deficient mouse.

A. Schematic of experimental design to administer recombinant IL-25 to a group of infected mice.Two groups of BALB/c and MIF$^{-/-}$ mice were infected with 250-400 *N. brasiliensis* L3 larvae s.c. on d0. One of the infected groups of BALB/c and MIF$^{-/-}$ mice were also administered rIL-25 800ng in 200µl PBS, the other group were given control (200µL PBS was instilled) i.p. on d1-5. These were compared to naive BALB/c and MIF$^{-/-}$ mice. Tissue was harvested on d6. Data analysed by one way ANOVA, and corrected for Multiple errors by a Sidak's multiple comparison test. For all panels, * = $p<0.05$, ** = $p<0.01$, *** $p<0.001$.

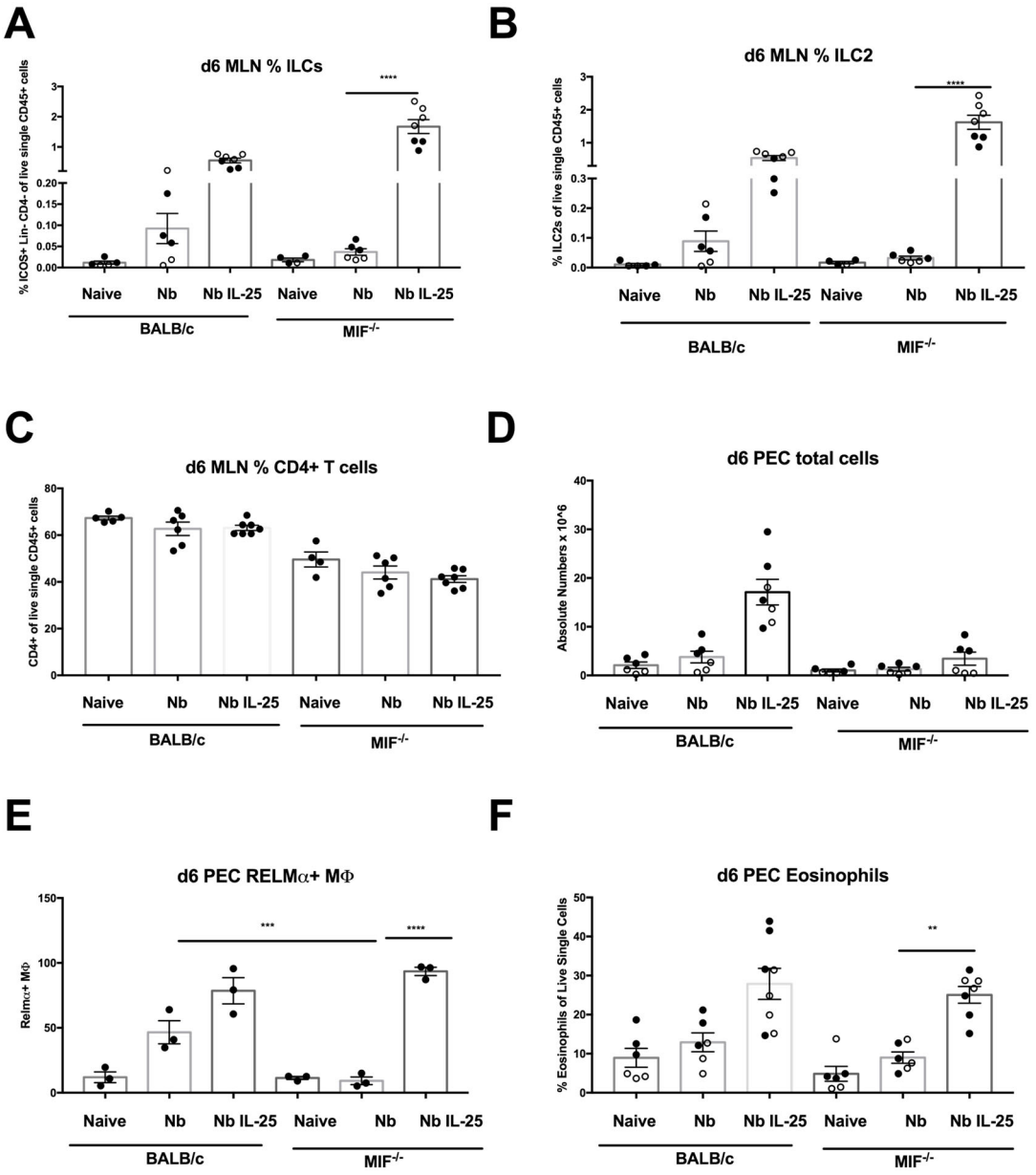

Figure 4.2.12 A-F: MLN ILC, peritoneal M2 and eosinophil responses are rescued with administration of recombinant IL-25.

BALB/c and MIF$^{-/-}$ mice were infected with 400-250 *N. brasiliensis* L3 larvae s.c for six days. Two infected groups were rescued with rIL-25, tissue harvested on D6
Flow cytometry for **(A)** percentage ICOS^{+} Lin^{-} CD4^{-} ILCs, **(B)** percentage of GATA3^{+} ILCs, **(C)** percentage CD4^{+} T cells, **(D)** Total PEC cell count, **(E)** percentage CD11b^{+} F4/80^{+} positive for RELMα **(F)** percentage SiglecF^{+} eosinophils at d6 of infection. Data pooled from two experiments combined. Data analysed by one way ANOVA, and corrected for Multiple errors by a Sidak's multiple comparison test. For all panels, * = $p<0.05$, ** = $p<0.01$, *** $p<0.001$. Contributions: sample preparation Dr S.Loeser.

4.2.13 IL-25 rescues the epithelial cell responses in the MIF-deficient mouse

We quantified the DCLK1 positive events in the small intestine of the BALB/c and MIF-deficient mice that were rescued with rIL-25. We found that administering rIL-25 increased marginally the numbers of DCLK1 positive cells per crypt/villus axis in the small intestine of BALB/c mice (from 0.2 in naïve, to 4.2 in *N.brasiliensis* infected mice and 6.19 in *N.brasiliensis* infected mice which were also administered rIL-25). The number of DCLK1$^+$ events rose from 0.1 in naïve, to 0.2 in *N.brasiliensis* infected mice to a complete rescue of the phenotype to 6.1 DCLK1$^+$ cells per crypt villus axis in MIF-deficient mice infected with *N.brasiliensis* and given rIL-25 (Fig 5.2.13 A).

Similarily this is the case with the GATA3$^+$ counts. Mean GATA3$^+$ counts per villus increased from 1.15 to 8.5 and 10.2 in BALB/c naïve, *N.brasiliensis* infected mice and *N.brasiliensis* infected mice given rIL-25. In the MIF-deficient mice, there was rescue of the GATA3$^+$ counts per villus with the administration of rIL-25. The average GATA3$^+$ counts per villus rose from 0.77 to 2.27 and 11.87 in MIF-deficient naïve, *N.brasiliensis* infected mice and *N.brasiliensis* infected mice given rIL-25 (Fig 5.2.13B). In keeping with this the level of mRNA transcription of *Gata3* (Fig 5.2.13C) and IL-5 (Fig 5.2.13 D) are rescued with the administration of rIL-25 in the MIF-deficient mice given rIL-25 to the levels observed in BALB/c mice that were infected with *N.brasiliensis*.

Administration of rIL-25 also rescued the production of RELMβ protein in MIF-deficient infected mice to levels observed in BALB/c mice infected with *N.brasiliensis* (5.68 RELMβ$^+$ cells per crypt villus axis in the MIF-deficient mice given rIL-25 compared to 5.75 RELMβ$^+$ cells per crypt/villus axis in the BALB/c mice infected with *N.brasiliensis*).

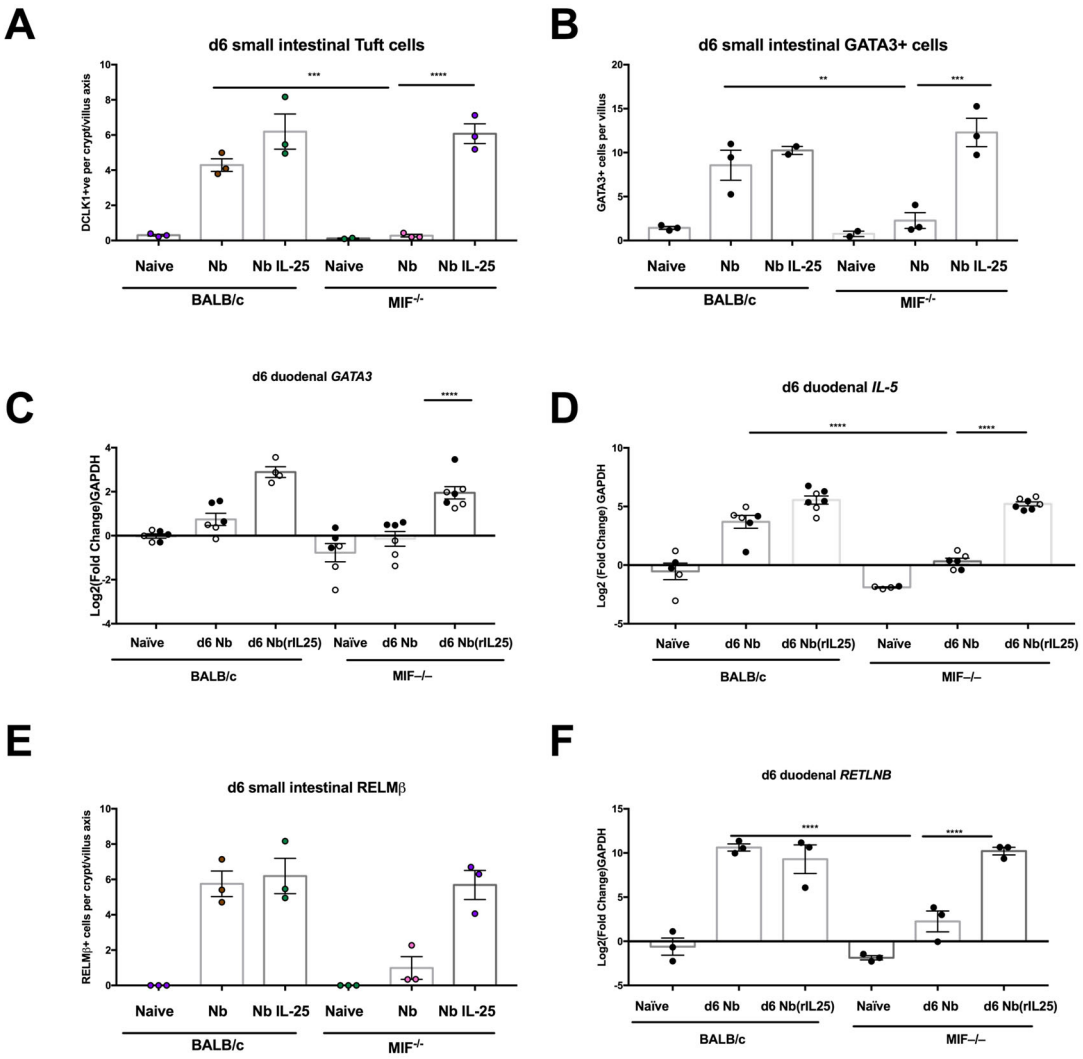

Figure 4.2.13 A-F Duodenal GATA3 and RELMb are rescued with administration of recombinant IL-25 in MIF-deficient mice.

BALB/c and MIF$^{-/-}$ mice were infected with 400-250 *N. brasiliensis* L3 larvae s.c for six days. Two infected groups were rescued with rIL-25, tissue harvested on D6
(**A)** Average of 100 small intestinal DCLK1 counts per villus axis - representative of two experiments (BALB/c Nb IL-25 performed once)
(B) Average of 100 small intestinal GATA3 counts per villus - performed once only
qPCR for duodenal *GATA3* **(C)** and *IL-5* **(D)** transcription.
Data representative of 2 experiments **(E)** Average of 100 small intestinal RELMβ counts per villus axis - representative of two experiments (BALB/c Nb IL-25 performed once).
(F) Duodenal *RETLNB* gene expression by qRT-PCR (representative of two experiments)
Data analysed by one-way ANOVA, and corrected for multiple errors by a Sidak's multiple comparison test. For all panels, * = $p<0.05$, ** = $p<0.01$, *** $p<0.001$. Contributions: Dr F Gerbe (Jay lab, Montpellier) performed DCLK1 RELMβ and GATA3 stainings. Some qRT-PCR performed by Ms N.Britton.

4.2.14 4-IPP- MIF inhibitor replicates the phenotype of the MIF-deficient mouse

There have been several reports of the role of MIF during organogenesis (Kobayashi et al., 1999), and neonatal development (Bernhagen et al., 2007). Therefore in order to assess the effect of acute deficiency of MIF on the immune systemSo far we have utilised knockout mice and we wished to verify the results utilising, 4-IPP, an inhibitor of MIF which covalently modifies MIF (Winner et al., 2008) on BALB/c mice. We administered 50µg of 4-IPP i.p. in DMSO as a solubilising agent at d0, 2 and 4 in wild-type BALB/c mice which were infected with *N.brasiliensis*. Comparisons were made against three other groups: a naïve control group, a group that was infected with *N.brasiliensis* only and a group given DMSO vehicle without 4-IPP on D0, 2 and 4 along with the infection (Fig 4.2.14 A).

Parasitology performed by Ms Yvonne Harcus, demonstrated that administration of 4-IPP increased the worm and egg burden in *N.brasiliensis* infection (data not shown). We found that 4-IPP is able to replicate the MIF-deficient phenotype when examining DCLK1$^+$ cells in the small intestinal epithelium (Fig 4.2.14B). We found that mice given DMSO and infected with *N.brasiliensis* had an average DCLK1$^+$ count of 4.34 per crypt villus axis, mice given 4-IPP in DMSO had a reduced average DCLK1$^+$ count of 0.92 per crypt villus axis (Fig 4.2.14B). In addition the percentage of ICOS+ CD4- Lin- ILCs reduced from 0.18% to 0.06% of the MLN from the DMSO to the 4-IPP in DMSO respectively. There was a similar reduction in the population of ILC2 (Fig 4.2.14D).

There was also a mean reduction of 2.6 in the transcription of *RETLNB* in the duodenum in the mice administered 4-IPP when compared to DMSO, although high variance precluded this effect reaching statistical significance (Fig 4.2.14E).

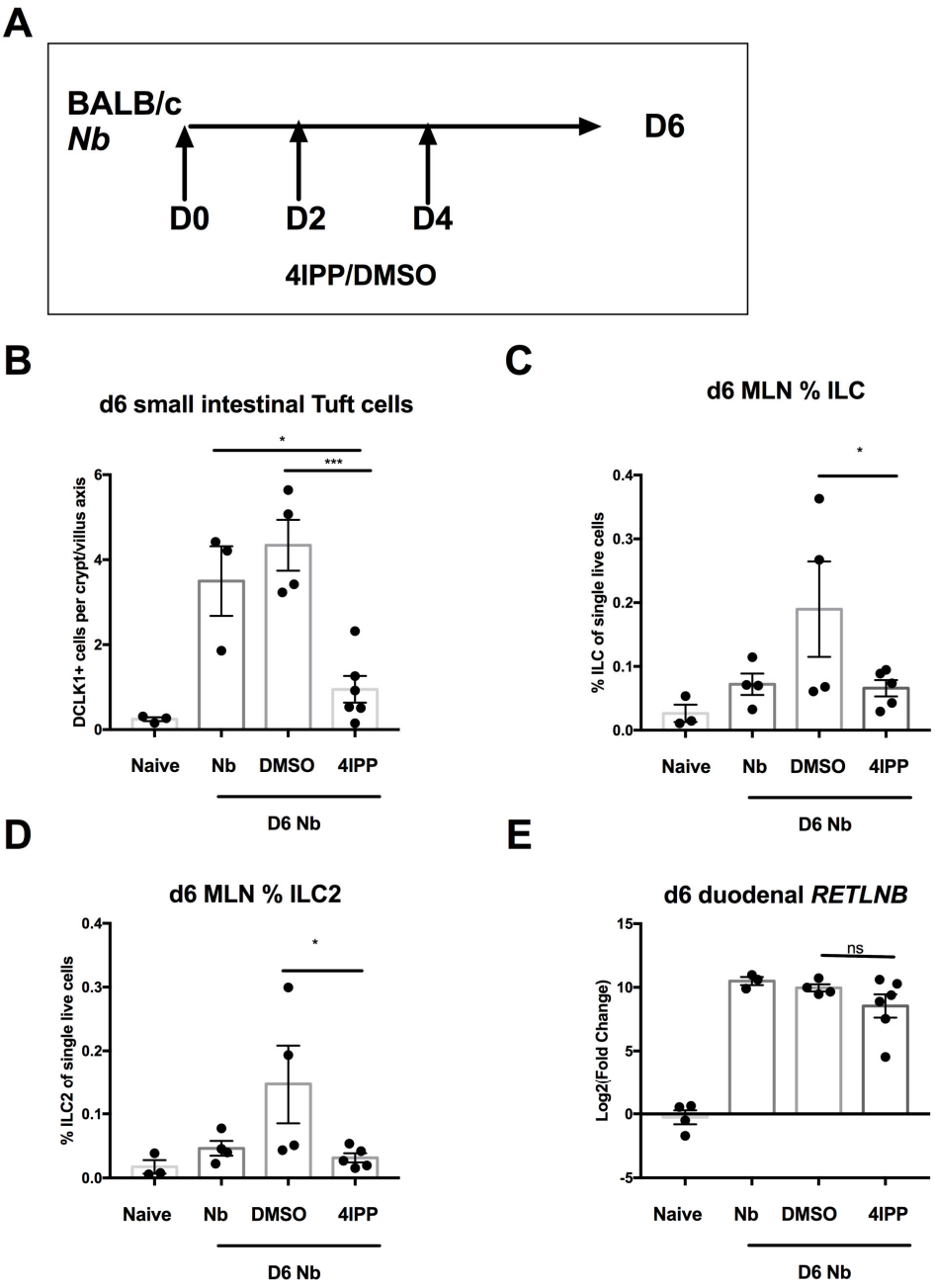

Figure 4.2.14 A-E 4-IPP, a small molecule inhibitor of MMIF can replicate ILC and epithelial tuft cell phenotype.

(A) Experimental schematic: BALB/c mice were infected with 400 *N. brasiliensis* L3 larvae for 6 days. d0,2,4 mice were administered 1mg 4IPP in 50µl DMSO or 50µl DMSO vehicle i.p. **(B)** Quantification of DCLK1^{+} cells in average of 100 crypt villus axes. Flow cytometry for percentage of ICOS^{+} Lin^{-} CD4^{-} ILCs **(C)** and percentage of GATA3^{+} ILCs (ILC2) **(D)** in MLN. **(E)** Gene expression analysis by qRT-PCR for *RETLNB* transcription. Data in **B,C,D** representative of two experiments, data in **D** performed once.. Data analysed by one way ANOVA, and corrected for multiple errors by a Sidak's multiple comparison test. For all panels, * = p<0.05, ** = p<0.01, *** p<0.001. Contributions: Dr F Gerbe (Jay lab, Montpellier) performed DCLK1 RELMβ and GATA3 stainings.

4.2.15 MIF given intravenously is not able to rescue the phenotype of the MIF-deficient mouse

We attempted to rescue the MIF-deficient phenotype by administering rMIF at a dose of 5µg i.v on d-1, 0, 2 and 4 of *N.brasiliensis* infection in MIF-deficient mice and compared parasitological responses to a MIF-deficient control group which only received *N.brasiliensis* infection. We found that MIF does not rescue the ability of the MIF-deficient mice in expelling *N.brasiliensis* infection. In fact there was a heavier worm burden in the MIF-deficient mouse given *rMIF* (Fig4.2.15A-B).

We administered *MIF* IL-13 i.v. to assess its ability to amplifying the response of *IL-13*, as previously we have reported the ability of *MIF* to synergise with *IL-4* in bone marrow macrophages (Prieto-Lafuente et al., 2009). We therefore injected wild type BALB/c mice with 200µg of recombinant *IL-13* on D2-5 and MIF on D1,3 and 5. We found a small but non-significant rise in the number of DCLK1 positive cells in the small intestine on administering MIF i.v. (Fig 4.2.14D). MIF did not affect the ability of rIL-13 to induce DCLK1 positive cells in the intestine.

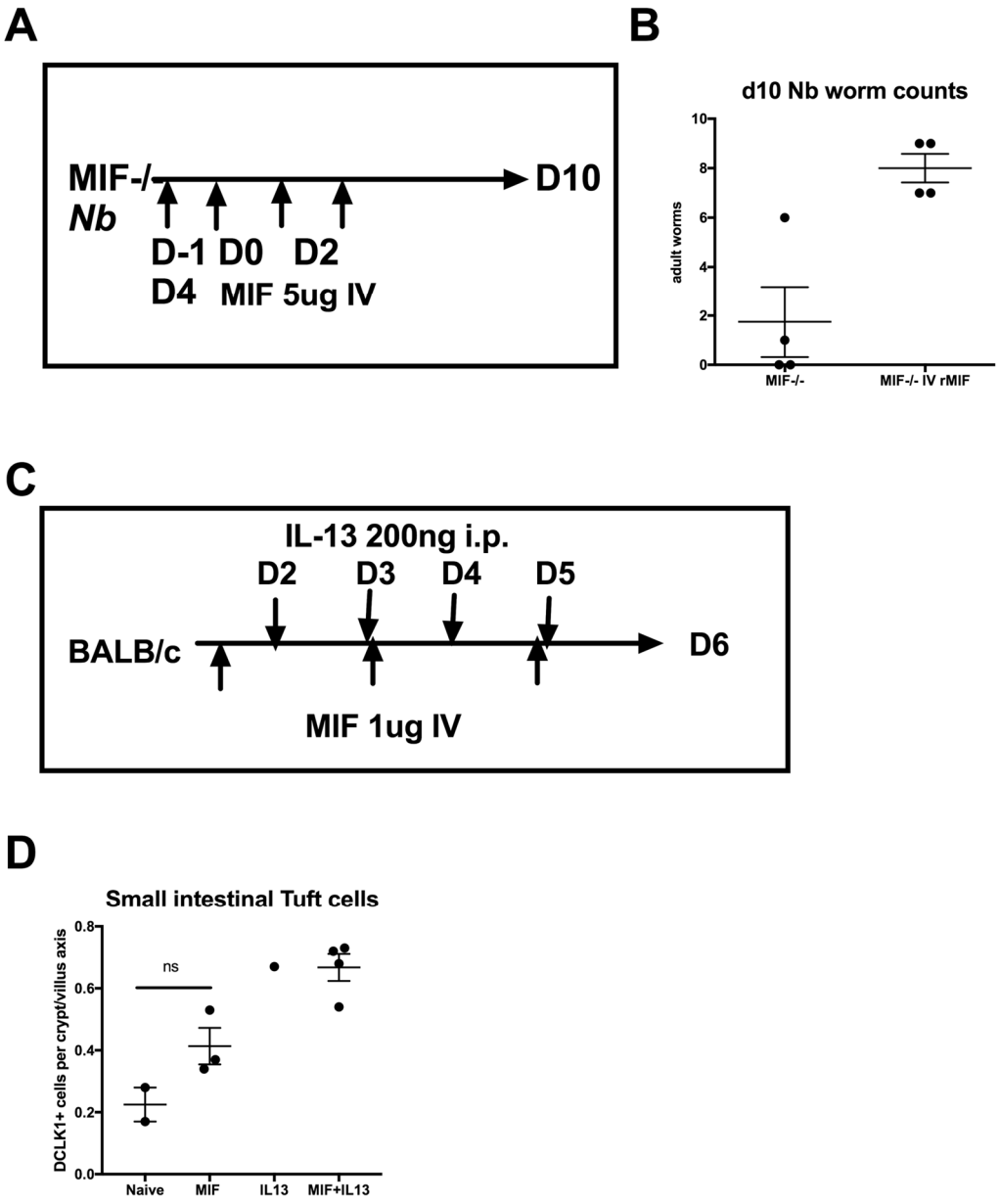

Figure 4.2.15 A-D MIF IV does not rescue parasitology or cellular phenotype in the small intestine

(A) Experimental schematic of rescue with IV MIF: MIF$^{-/-}$ were injected with 5µg of rMIF IV on d-1, 0, 2 and 4 and infected with 250L3 *N.brasiliensis* infection at d0. Parasitology was obtained at d10. These were compared to a MIF$^{-/-}$ control group that were infected with 250L3 *N.brasiliensis* only. This experiment was performed once.
(B) Worm counts obtained at d10 of *N.brasiliensis* infection in MIF$^{-/-}$ mice and MIF$^{-/-}$ mice administered rMIF. **(C)** Experimental schematic attempt at inducing epithelial cell responses in BALB/c mice were injected with MIF IV and IL-13 200ng on d2-5 i.p.- parrafin embedded sections were stained for DCLK1. This experiment was performed once. (**D**) Quantification of average DCLK1^{+} cells per crypt villus axis . Data from one experiment, analysed by one way ANOVA, and corrected for multiple errors by a Sidak's test. For all panels, * = p<0.05, ** = p<0.01, *** p<0.001. Contribuitons: IVs performed by Dr M.White

4.2.16 Expression of MIF receptors in the peritoneal cavity and mesenteric lymph node

CXCR2 expression occurs on immune cells, epithelial cells and endothelial cells (Stadtmann and Zarbock, 2012). CXCR4 is expressed immune cells including T cells and endothelial cells (Chatterjee et al., 2014). CD74 is the invariant chain and is generally expressed in cells that have MHC2. We assessed the expression of MIF receptors CD74, CXCR4 and CXCR2 expression on immune cells in the peritoneal cavity to identify cells that may be involved in driving the effects of MIF on cellular recruitment. BALB/c mice infected with *N.brasiliensis* were assessed on the expression of the receptors for $CD11b^+$ $F4/80^+$ macrophages, $CD11b^+$ Siglec-F^+ eosinophils (in the peritoneum) and Lin^- $CD4^-$ $ICOS^+$ ILCs (in the MLN).

Approximately 25% of the peritoneal cavity $CD11b^+$ $F4/80^+$ macrophages were positive for CXCR2, CXCR4 and 100% for CD74 (Fig 4.2.16 A-C). Additionally, we found that peritoneal $CD11b^+$ Siglec-F^+ eosinophils did not express CXCR2, CXCR4 or CD74 (4.2.16 D-F). We found no difference in the levels of expression between infected and naïve mice (data not shown).

The ILC population of the MLN expressed CXCR4 (Fig 4.2.16 H) but not CXCR2 (Fig 4.2.16 G) or CD74 (Fig 4.2.16 I). Almost all of the ILCs were positive for CXCR4 expression. As there are very few ILCs in naïve mice, it was not possible to compare naïve and infected mice.

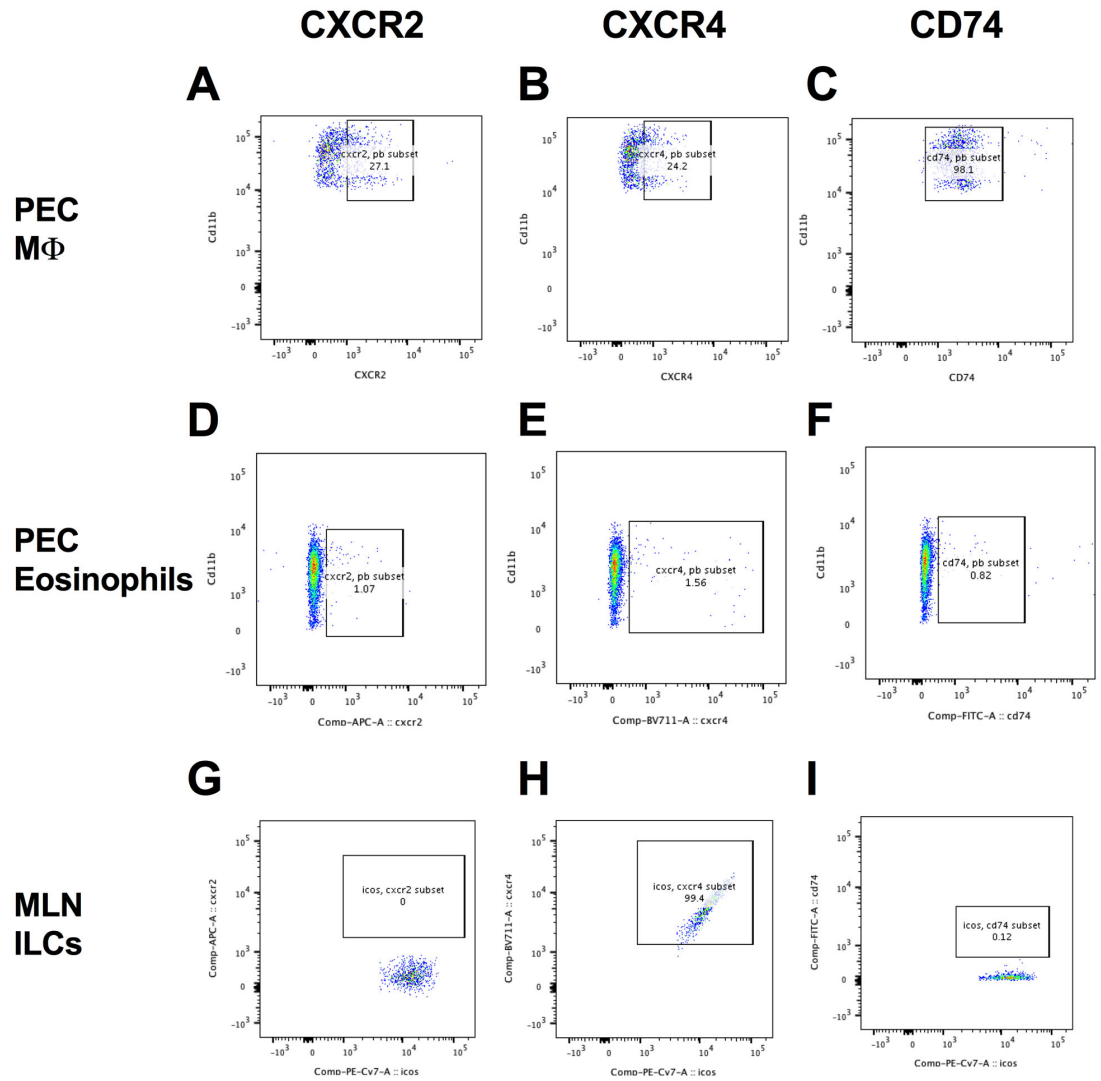

Figure 4.2.16 A-I MLN and Peritoneal exudate cell receptor expression at d6 of *N.brasiliensis* infection.

BALB/c mice infected with *N.brasiliensis* for 6 days. Peritoneal exudate cells and mesenteric lymph node were prepared for flow cytometric analysis. Markers to deterimine cell types in PEC were CD11b, SigF, F4/80. In the MLN ILCs were determined by a combination of Lin, ICOS, CD4, CD45. These were co-stained with markers for CXCR2, CXCR4 and CD74 to determine which cells produced these receptors during *N.brasiliensis* infection. **A-C.** PEC Macrophage expression of CXCR2 **(A)**, CXCR4 **(B)** and CD74 **(C)** from BALB/c infected with Nb 250L3. **D-F** PEC Eosinophil expression of CXCR2 **(D)**, CXCR4 **(E)** and CD74 **(F)** from BALB/c infected with Nb 250L3. **G-I** MLN ILC expression of CXCR2 **(G)**, CXCR4 **(H)** and CD74 **(I)** from BALB/c infected with Nb 250L3.

4.3 DISCUSSION

The effect of MIF in type 2 immunity have been explored in chapters 4 and 5 of this thesis. MIF is a chemokine that results in cellular recruitment to sites of infection (Calandra et al., 1994). First and foremost, MIF affects cellular recruitment, as noted in *N.brasiliensis* model in the lung, BAL, peritoneal lavage and MLN. This has been replicated in the peritoneal lavage of the *H.polygyrus* model also.

Secondly the absence of MIF affects the recruitment of early innate lymphoid cells namely ILCs and TH2 cells. There is a paucity of TH2 cytokines IL-4, IL-5 and IL-13 in the MIF deficient model at d6 of infection. The hypothesised receptors of MIF are CXCR2, CXCR4 and CD74 (which acts as a co-receptor for CXCR2) (Bernhagen et al., 2007). ILCs in the mesenteric lymph nodes are shown to express CXCR4 but not CXCR2, so could be directly affected by MIF. There are also a reduced number of GATA3 positive cells in the lamina propria of the MIF-deficient mouse (although without further staining it will not be possible to say if these are ILCs or TH2 cells but from the flow cytometric data –it is likely to be a reduction in both types of cells). The cells responsible for early TH2 cytokines are by far the ILCs. ILCs proliferate at the site of infection producing IL-5 which results in eosinophilia (Filbey et al., 2018), and IL-13 which commences the epithelial cell responses in the gut resulting in weep and sweep of the intestinal contents (Grencis, 2015). They migrate to the appropriate site of infection and respond to IL-25. This then starts the epithelial cell feedback loop as describe by Gerbe and colleagues(Gerbe et al., 2016). IL-25 recruits ILCs that produce TH2 cytokines that stimulate further tuft cell hyperplasia.

Thirdly, MIF may directly act on macrophages and eosinophils. Previous data demonstrated that MIF synergised with IL-4 to induce the alternative activation of bone marrow derived macrophages in isolation of other cell populations (Prieto-Lafuente et al., 2009). We show that the MIF deficient

mouse has reduced percentage of alternatively activated macrophages, and reduced eosinophilia in the peritoneal cavity after infection. Peritoneal macrophages have been shown to express CXCR2, CXCR4 and CD74 and therefore, there is the potential for MIF to directly influence the macrophage activation status, although the signalling mechanisms are unknown. Previous data has shown MIF to promote eosinophil chemotaxis in vitro (de Souza et al., 2015). Within the MIF-deficient mouse, though, it is likely the alternative activation is aided by the increased production of IL-4 and 13 from the ILCs and T cells in the wild type mouse. MIF has also been shown to

Fourthly, MIF is associated with a strong Type 2 epithelial cell phenotype- and is required for optimal upregulation of tuft cells, goblet cell hyperplasia, and RELMβ production. The data demonstrate a failure of the MIF deficient mouse to expand a suite of Type 2 cells - ILC2s, TH2s, eosinophils and M2 macrophages - during a helminth infection. This is however, likely due to the relative deficiency in cytokines IL-13 and IL-4. Thus, tuft cells in MIF-deficient organioids are equally able to proliferate when IL-4/IL-13 is added to the media. Dr C.Drurey has also shown in an organoid model, that rMIF on its own or with the addition of IL-13/4 did not affect $DCLK1^{+}$ intestinal tuft cell proliferation in wild type organoids (unpublished data). This suggests that there is no deficit in the ability of epithelial cells to respond, but there is a deficit in the overall amount of cytokine required to initiate a Type 2 epithelial cell response.

And finally this immunological phenotype is rescuable by administration of rIL-25, a cytokine known to up-regulate the ILC population, but which also has an effect in the myeloid and eosinophil compartment early in infection. IL-25 receptor chimera experiments have shown that it is the immune compartment that is responsive to rIL-25 (Katie Smith unpublished). The administration of rIL-25 results in recruitment of the ILC, TH2 cells and other type 2 immune cells. This then restarts the positive feedback circuit (Gerbe et al., 2016) that is required to initiate tuft cell proliferation in the MIF deficient

mouse. The fact that we can rescue the MIF deficient phenotype suggests that the machinery for a type 2 response is intact- and this is supported by the fact that STAT6 phosphorylation and signalling is intact. This may also explain the surprising fact that MIF is not rescuable by administration the cytokine IV, and in fact the administration of MIF results in failure of expulsion of parasites.

MIF is blocked in its biological action by 4-IPP. This inhibitor results in reduced ILCs, eosinophils and alternative macrophage activation. The epithelium of the 4-IPP treated mice demonstrates reduced $DCLK1^{+}$ intestinal tuft cells, and in addition, has a higher burden of *N.brasiliensis* worm

This data has been summarised in the schematic shown in Fig 5.16.

Further experiments will need to explore which of the immune cells are directly influenced by MIF, such as in ILC in vitro culture models. Work has been undertaken assessing the effect of MIF in organoid systems, which suggest that MIF affects the epithelial responses indirectly (by resulting in a diminished amount of IL-13/4 being produced).

5.3.1 MIF Schematic

Based on the data presented we have attempted to formulate this into a schematic describing the way MIF functions to accelerate Type 2 immune responses (Fig 5.3.1). Effectively the most important source of IL-25 is the epithelial tuft cell, these result in the accumulation of IL-25 responsive cells such as ILCs which produce IL-13 and forms part of a positive feedback loop (in blue). MIF is produced by the epithelium (Haber et al., 2017) (but also by other immune cells) in response to helminths infections. This leads to the recruitment of the IL-25 responsive cells including ILCs, which produce IL-13 and reinforce

the positive feeback loop. In the absence of MIF, there is not enough IL-13 to adequately stimulate IL-25 production in the epithelium. MIF acts via putative MIF receptors on macrophages, ILCs etc. Those receptors that were found to be expressed by flow cytometry are depicted schematically in the diagram below.

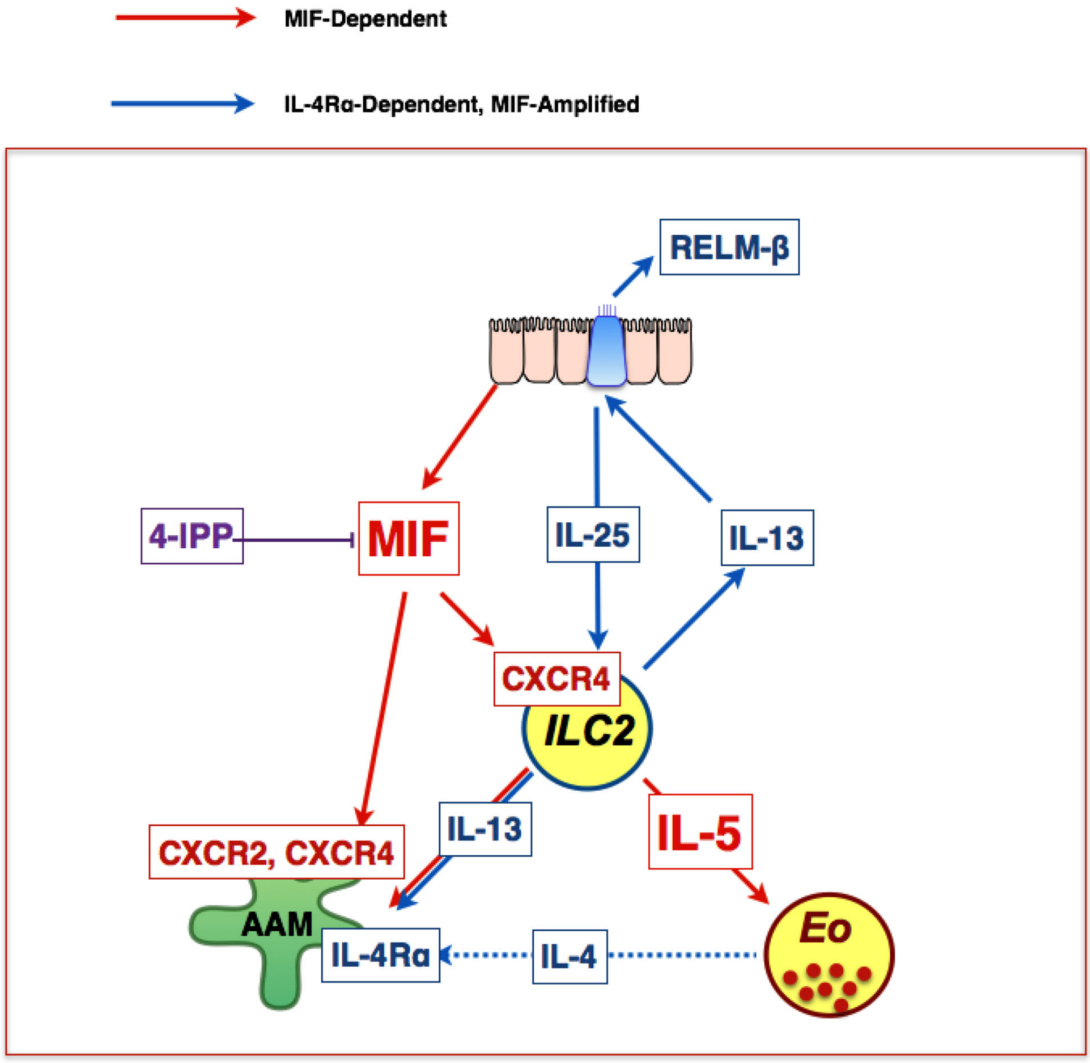

Figure 4.3.1 MIF schematic- role of MIF in type 2 immunity

A summary schematic figure demonstrating the effect of MIF on the various cell types of the immune system and the receptors potentially used by MIF to elicit Type 2 immune responses in the epithelium.

Chapter 5- Role of CXCR2 in helminths infections

5.1 Introduction

Chemokine receptors are present on leucocytes and are exposed to multiple chemokines, this leads to activation of intracellular signalling cascades and integrin binding to counter-receptors. The resulting process mediates adhesion to the endothelium and extravasation or transmigration. The chemokine receptors are part of the G-protein coupled receptor family.

CXCR4 and CXCR2 are two chemokine receptors which also bind MIF (Calandra and Roger, 2003). The ligand for CXCR4 is CXCL12 (Walenkamp et al., 2017). The known ligands for CXCR2 are CXCL1, 2, 3, 5, 6, 7 and 8, the most potent being CXCL8 which is only expressed in humans (Stadtmann and Zarbock, 2012). Binding of CXCR2 to its ligand results in activation of G protein, which dissociates into two subunits, the Gα-subunit and the Gβγ, to activate different signalling molecules. The Gβγ mediates signal transduction by interacting with other proteins including phosphatidylinositol-3-kinases (PI3K) (Hur and Kim, 2002). Downstream effects of PI3K mobilisation include activation of ERK 1 and 2 phosphorylation (Stadtmann and Zarbock, 2012), (Raghuwanshi et al., 2012).

CXCR2 and CD74 are part of a receptor complex and are responsible for monocyte arrest in areas of inflamed endothelium in response to MIF; MIF also mediates arrest of CXCR4 expressing T cells (Bernhagen et al., 2007). CXCR2 normally binds the cognate ligand CXCL8 via an N-terminal Glu-Leu-Arg (ELR) motif. MIF expresses a pseudo-ELR motif (two nonadjacent but appropriately spaced residues (Asp and Arg)) that mimicks the ELR chemokines (Blucala, 2012). CXCR2 binds the pseudo-ELR motif of MIF (Weber et al., 2008). Expression of the ligand CXCL12 results in arrest of

CXCR4 expressing cells, however, MIF has also been shown to be the ligand for CXCR4 (Bernhagen et al., 2007).

CXCR2 is expressed on neutrophils and is essential for neutrophil egress from the bone marrow (Eash et al., 2010). In the context of a helminth infection, neutrophils produce type 2 products such as RELMα and YM1(Allen and Sutherland, 2014); in addition, neutrophils and macrophages have been reported to function sequentially to clear *N. brasiliensi*s and generate immunity to secondary infection with *H. polygyrus* (Chen et al., 2014).

Recently, myeloid derived suppressor cells (MDSCs) have also been found to express CXCR2 (Katoh et al., 2013; Zhang et al., 2017). CXCR2 deficient mice have attenuated tumorigenesis in a DSS model and adoptive transfer of CXCR2-expressing MDSCs restores tumorigenesis (Katoh et al., 2013). Myeloid derived suppressor cells encompass two different populations: polymorphonuclear MDSCs (PMN-MDSCs) that are similar to neutrophils, and monocytic MDSCs (M-MDSCs) which are similar to monocytes. The M-MDSCs are $CD11b^{+}Ly6G^{-}Ly6C^{hi}$ cells with low side scatter and PMN-MDSCs are $CD11b^{+}Ly6G^{+}Ly6C^{lo}$ cells with high side scatter (Bronte et al., 2016). Additional markers can differentiate between MDSCs and typical neutrophils/monocytes such as s100a9 (Zhao et al., 2012). The functional ability of MDSCs to supress immune cell is an important defining feature that can be measured by several assays, including inhibition of cytotoxic T lymphocyte activity (Bronte et al., 2016).

Following on from the previous chapters, where we explore the effect of MIF deficiency, we chose to explore CXCR2, because is a known ligand for MIF (Bernhagen et al., 2007) and because of the known importance of CXCR2 in immune cells but particularly neutrophils (Eash et al., 2010) and myeloid derived suppressor cells. We therefore chose to explore if we could replicate the MIF-deficient phenotype in a CXCR2 receptor knock out mouse model.

5.2 Results

5.2.1 CXCR2-deficient mice expel *N. brasiliensis* within 7 days

We assessed the parasitological responses of the CXCR2-deficient mice in comparison to those of wildtype mice in expelling *N. brasiliensis* parasites. A schematic of the experimental design is shown in Fig 5.2.1A, and all subsequent in vivo data was analysed at day 7 post infection. However, at D7 of infection, we found that both the wildtype and CXCR2-deficient mice had expelled their worm burdens completely.

Cell populations were recovered from BAL, lung, peritoneum and MLN of CXCR2-/-, CXCR2-/+ and CXCR2+/+ mice at D7 of infection with 250 L3 larvae of *N. brasiliensis*. There was an overall trend to reduced cell numbers in the lung (Fig 5.2.1 B) and BAL (Fig 5.2.1 C) of the CXCR2-deficient mice when compared to heterozygous and wildtype mice but this did not reach significance.

The CXCR2-deficient mice have reduced total cell numbers in the peritoneal lavage; less than half of that found in heterozygous and wildtype mice (Fig 5.2.1D). CXCR2-deficient mice had an average of 3.42 x 10^6 cells, with CXCR2 heterozygous mice and wildtype mice having 8.9 x 10^6 and 8.6 x 10^6 cells respectively (Fig5.2.1D). There was an overall trend to reduced cells in the CXCR2-deficient mice in the MLN (Fig 5.2.1E), but again this did not reach significance.

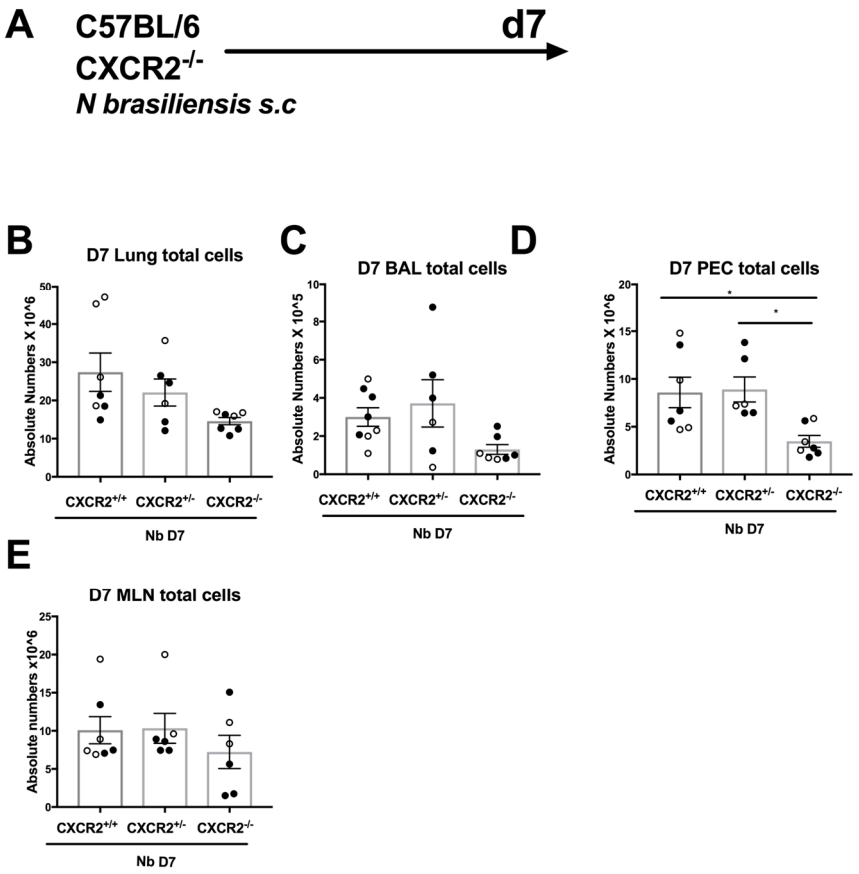

Figure 5.2.1 Inflammation in response to *N.brasiliensis* by CXCR2-deficient mice.

A BL/6, CXCR2$^{-/-}$ and CXCR2$^{-/+}$ mice were infected with 250 *N brasiliensis* L3 larvae for 7 days; Cell counts obtained by Nexelecom cellometer for Peritoneal Exudate Cells and BAL (**C,D)** and manual cell counting of Lung and MLN (**B,E)**. Data pooled from two experiments, the two experiments are depicted as solid and open circles respectively Data analysed by one-way ANOVA, and corrected for multiple comparisons by a Sidak's test. For all panels, * = p<0.05, ** = p<0.01, *** p<0.001. Contributions: experimental prep with Dr S. Loeser, mice obtained from Prof Graham.

5.2.2-3 Alternative activation of macrophages is impaired in response to *N. brasiliensis* in the lung of CXCR2-deficient mice.

The lung markers CD11b, F4/80, CD11c, Siglec F were used to differentiate lung alveolar macrophages ($CD11c^{hi}$ $SiglecF^{hi}$ $CD11b^{-}$) or AM, from interstitial macrophages ($CD11c^{-}$ $CD11b^{+}$ $F4/80^{+}$) or CM, and eosinophils ($CD11c^{int}$ Siglec F^{hi}). These markers were costained with intracellular marker RELMα for identification of the alternative activation/M2 phenotype. From this flow cytometry analysis, CXCR2-deficient mice had a trend towards a higher percentage of alveolar and interstitial macrophages in total lung single cell suspensions (Fig5.2.2 A,B), although their absolute numbers are comparable in all groups (Fig 5.2.2 C,D). Strikingly, however, there was greatly reduced expression of the M2 marker RELMα in CXCR2-deficient animals compared to wildtype or heterozygous mice (Fig5.2.3 E, F). In the case of alveolar macrophages, approximately 12% are $RELM\alpha^{+}$ in the CXCR2-deficient mice, whereas in the heterozygote and wildtype animals some 46% of AMs expressed this M2 marker. An even starker difference was seen among interstitial macrophages, with approximately 2% of cells from the CXCR2-deficient mice positive for RELMα, whereas 20% of heterozygote and 17 % of wildtype IMs were $RELM\alpha^{+}$ at D7 of *N. brasiliensis* infection.

The expression of M2 products in the lung was further assessed by PCR for Arginase-1 and Ym1 (Chil3) as well as RELMα. There was a trend toward reduced transcription of *Arginase 1* which was more than 2-fold lower than the wild-type level (Fig 5.2.3 A) but showing high variance, this did not reach statistical significance. RELMα expression was also reduced in the CXCR2-deficient mice (Fig 5.2.3 B) by 12-fold and 8-fold compared to the heterozygotes and wildtype mice respectively. For YM1 the CXCR2 deficient mice had an even more marked 27- and 37-fold reduction *Chil3* mRNA compared to heterozygotes and wildtype mice (Fig 5.2.3C)

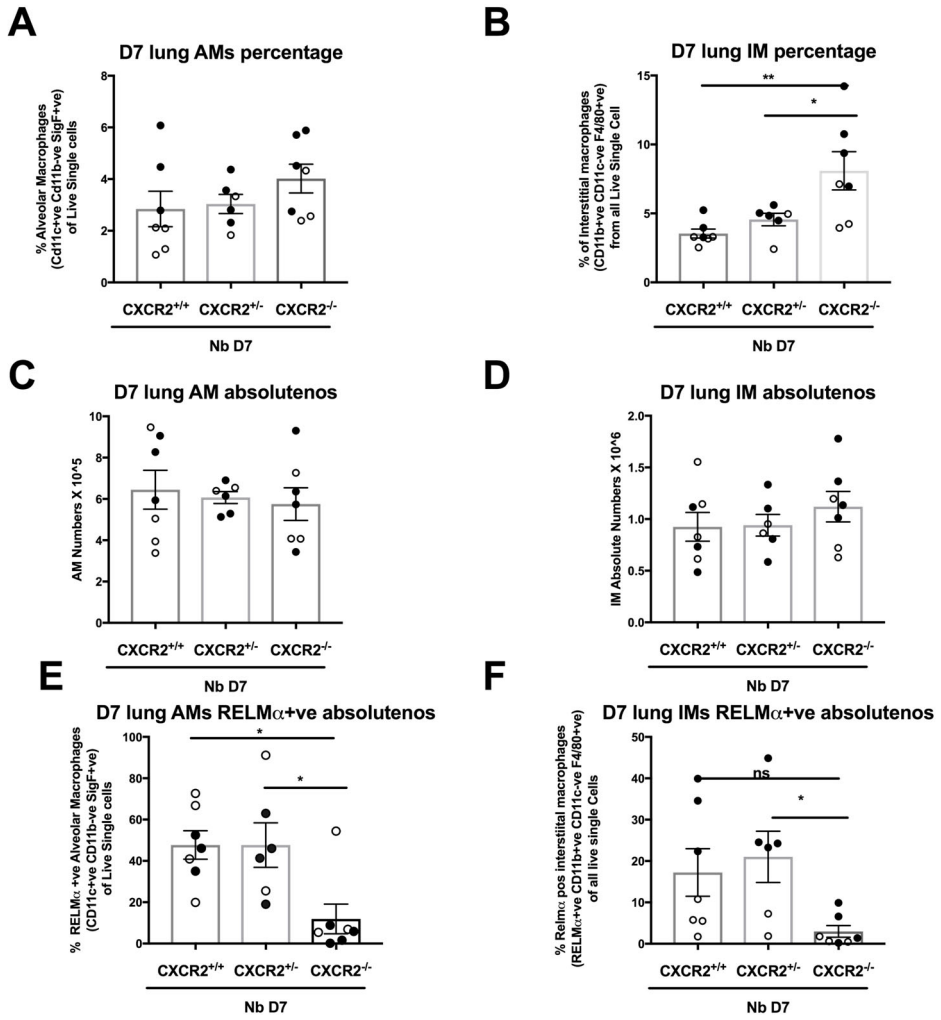

Figure 5.2.2 Alternative activation of lung macrophages is impaired in *N.brasiliensis* infection of CXCR2-deficient mice

B6 mice, CXCR2$^{-/-}$ and CXCR2$^{+/-}$ were infected with 250 *N. brasiliensis* L3 larvae at d0. Lung tissue taken at d7 p.i and digested for analysis by flow cytometry. Data from two experiments, depicted as solid and open circles respectively. **(A)** Alveolar macrophage (AM);**(B)** Interstitial macrophage percentages **(C)** Alveolar macrophage; **(D)** interstitial macrophage total numbers; (**E)** Percentage RELMα positive AMs; **(F)** Percentage RELMα positive IMs. For all panels, * = p<0.05, ** = p<0.01, *** p<0.001. Contributions: experimental prep with Dr S. Loeser, mice obtained from Prof Graham.

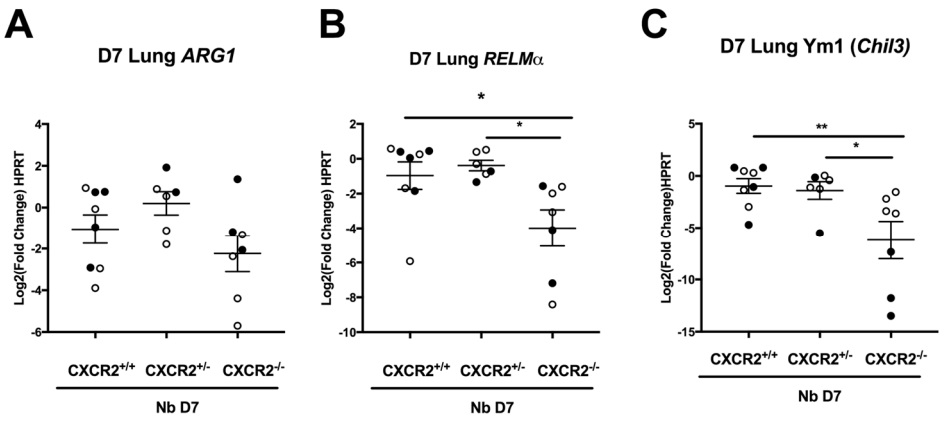

Figure 5.2.3 Alternative activation of lung macrophages is impaired in response to *N.brasiliensis* in CXCR2-deficient mice

B6 mice, CXCR2$^{-/-}$ and CXCR2$^{+/-}$ were infected with 250 *N. brasiliensis* L3 larvae d0. At d7 post infection, lung tissue was taken for gene expression analysis by qPCR. Data pooled from two experiments depicted as solid and open circles respectively. Gene expression in lung homogenate tissue for *ARG1* **(A)**, *RELMα* **(B)** and YM1 (Chil3)**(C)**. Data analysed by one-way ANOVA, and corrected for multiple comparisons by a Sidak's test. For all panels, * = p<0.05, ** = p<0.01, *** p<0.001. Contributions: experimental prep with Dr S. Loeser, mice obtained from Prof Graham.

5.2.4-5 CXCR2-deficient mice have reduced airway eosinophila in response to *N. brasiliensis*

N. brasiliensis infection provokes significant airway eosinophilia (Coyle et al., 1998). Notably, CXCR2 is also expressed on human eosinophils on priming with IL-5 (Heath et al., 1997), while CXCR2-deficient mice, after exposure to the fungus *Aspergillus fumigatus,* demonstrated markedly reduced eosinophila, and production of type 2 cytokines (Schuh et al., 2002). We therefore examined eosinophil numbers in tissues of *N. brasiliensis*-infected wildtype and CXCR2-deficient mice.

We observed a profound reduction of eosinophilia in the lungs of CXCR2 deficient mice, compared to both heterozygote and wildtype mice, in terms of both percentage (Fig 5.2.4A) and absolute numbers (Fig 5.2.4B). Thus, at D7 of *N. brasiliensis* infection, the CXCR2-deficient mice had only 4% of all live single cells consisting of eosinophils in the lung at D7 of *N. brasiliensis* infection, compared to 21% and 19% in the heterozygote and wildtype animals. In contrast, lung neutrophils increased proportionately in the CXCR2-deficient mice at D7 (Fig5.2.4C) and there was a similar trend for increased absolute numbers that did not attain statistical significance (Fig 5.2.4 D).

Analysis of cells in the BAL fluids revealed a picture similar to the lung. Thus, there is an increase in the percentage of alveolar macrophages, reaching 36% in CXCR2-deficient mice compared to only 16 and 10% in the BAL of heterozygotes and wildtype mice (Fig 5.2.5A). Similar differences were seen as trends in absolute AM numbers (Fig 5.2.5 B). Significantly, there is a sharp reduction in expression of RELMα within the AM population (Fig 5.2.5C). Moreover, the percentage of eosinophils in the BAL at D7 of *N. brasiliensis* infection was 15% in the CXCR2 deficient mice, but 63 and 62% in the heterozygotes and the wildtype mice (Fig 5.2.5D).

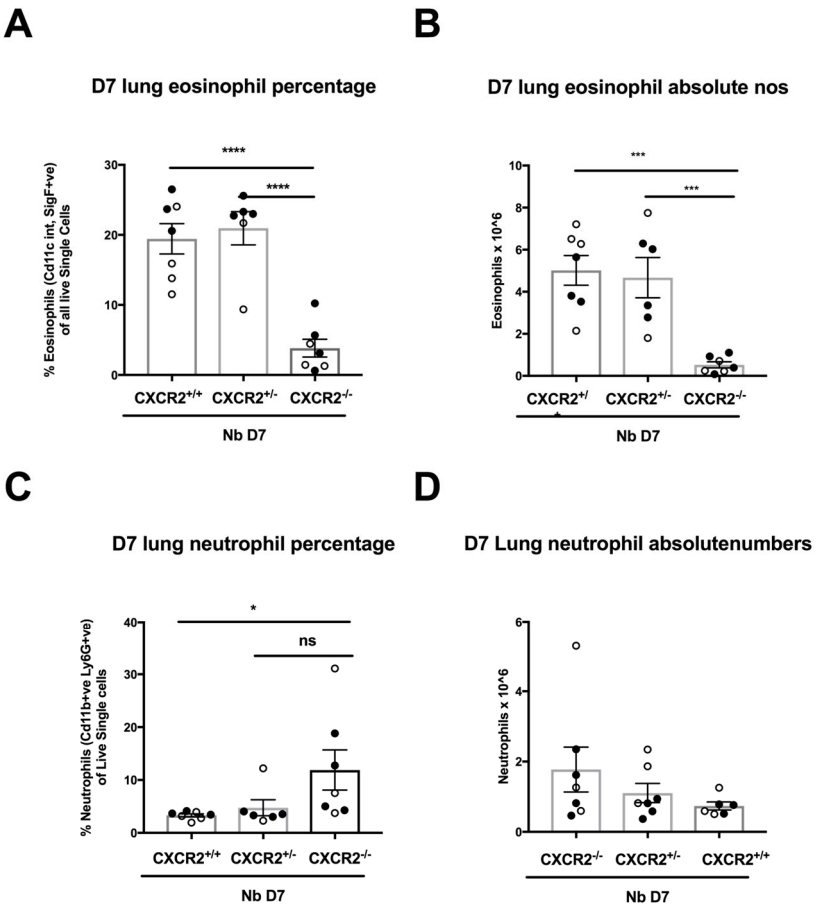

Figure 5.2.4 CXCR2 deficient mice have fewer eosinophils in lung after *N.brasiliensis* infection

BL/6 mice, CXCR2-/- and CXCR2+/- were infected with 250 *N. brasiliensis* L3 larvae. Digestion performed of lung tissue at d7 post infection for analysis by flow cytometry. A represent eosinophil percentage and total cell numbers in the lung. C,D represent neutrophil percentage and total cell numbers in the lung.All data is pooled from two experiments; the two experiments are depicted as solid and open circles respectively. Data analysed by one-way ANOVA, and corrected for multiple comparisons by a Sidak's test. For all panels, * = $p<0.05$, ** = $p<0.01$, *** $p<0.001$. Contributions: experimental prep with Dr S. Loeser, mice obtained from Prof Graham.

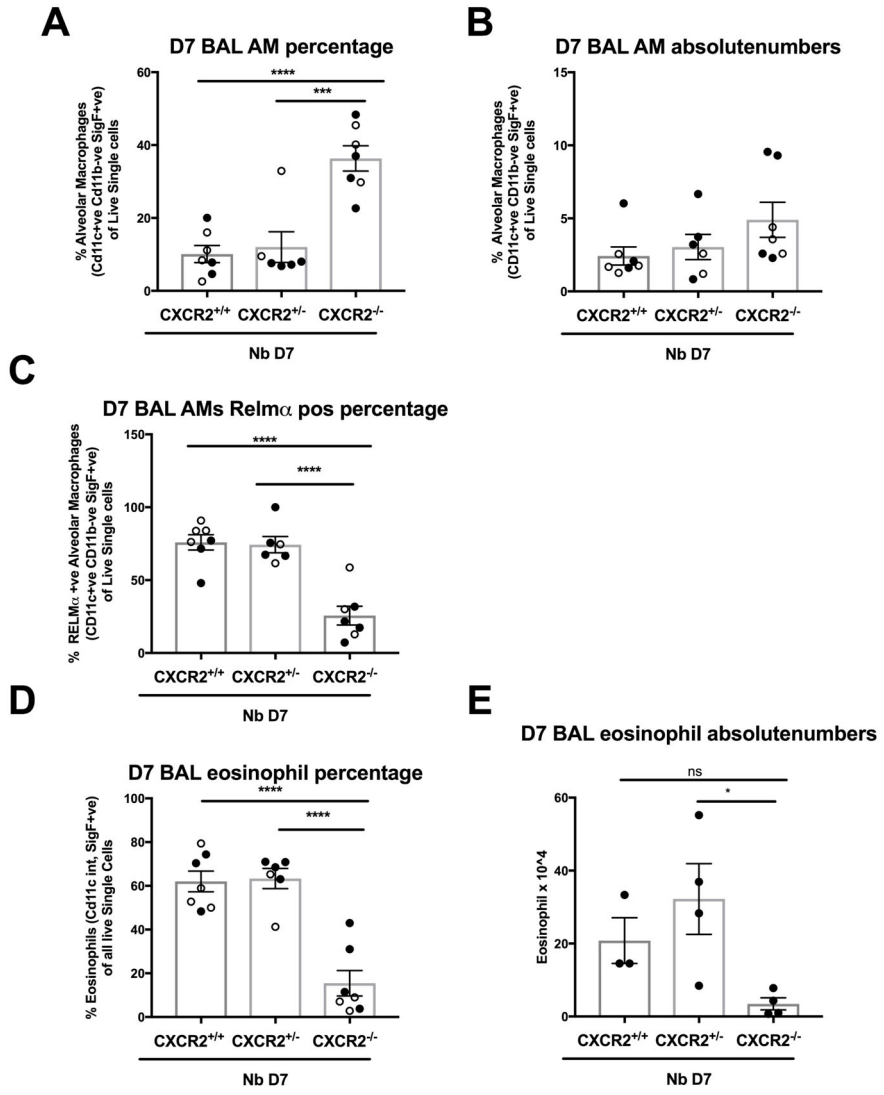

Figure 5.2.5 CXCR2-deficient mice have fewer eosinophils and alternatively activated macrophages in the BAL after *N.brasiliensis* infection.

BL6 mice, CXCR2$^{-/-}$ and CXCR2$^{+/-}$ were infected with 250 *N. brasiliensis* L3 larvae D0. Digestion performed of lung tissue at d7 post infection for analysis by flow cytometry. Data demonstrates percentage alveolar macrophage (AM) **(A)**; total cell numbers of AMs **(B)**; percentage of RELMα positive AMs **(C)**; percentage of eosinophils **(D)** and total numbers of eosinophils **(E)**. Data pooled from two experiments and are depicted as solid and open circles respectively. Data analysed by one-way ANOVA, and corrected for multipe comparisons by a Sidak's test. For all panels, * = $p<0.05$, ** = $p<0.01$, *** $p<0.001$. Contributions: experimental prep with Dr S. Loeser, mice obtained from Prof Graham.

5.2.6 CXCR2-deficient mice have reduced TH2 cytokines and reduced percentage of GATA3 positive T cells

The T cell profile of wild-type and CXCR2-deficient mice was then examined. The overall percentage of T cells in the lung of infected mice is only slightly affected by the absence of CXCR2 (Fig 5.2.6A). However, in contrast, the percentage of T cells which express GATA3 is reduced in the CXCR2-deficient mice (Fig 5.2.6B) at only ~7%, compared to ~35% in the heterozygotes and wildtype mice. Cytokines were measured by cytokine bead arrays for the TH2 cytokines IL-4, 5 and 13. There was approximately a 7-fold increase in the amount of IL-4 (Fig 5.2.6C,D) and over a 5-fold increase in the amount of IL-13 (Fig 5.2.6E) in the BAL of heterozygotes and wildtype mice when compared to CXCR2 deficient mice.

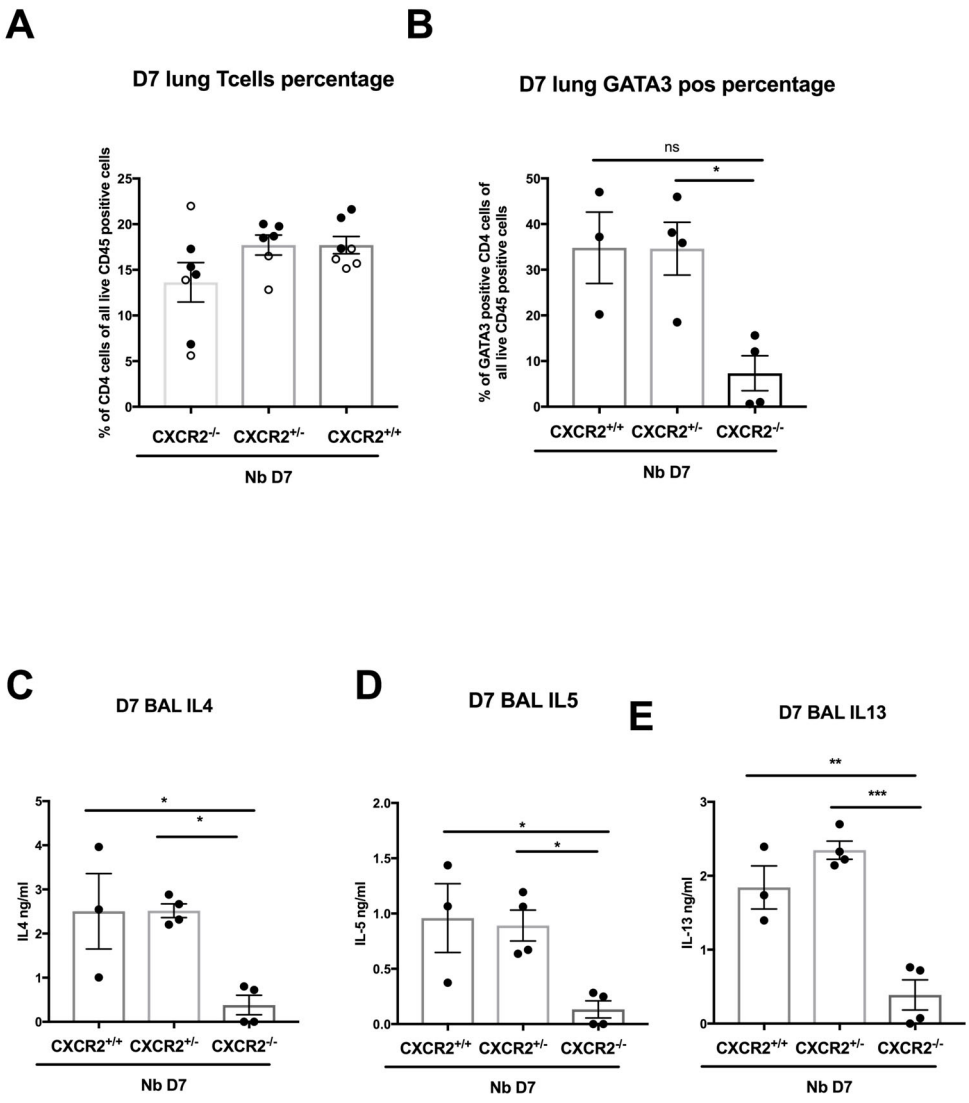

Figure 5.2. 6 TH2 responses in the lung are impaired in the CXCR2-deficient mice

BL/6, CXCR2$^{-/-}$ and CXCR2$^{-/+}$ mice were infected with 250 *N. brasiliensis* L3 larvae for 7 days. Digestion performed of lung tissue at d7 post infection for analysis by flow cytometry, BAL fluid frozen for CBA. Percentage of T cells of all live single CD45+ve cells **(A)**; Percentage of T cells that are positive for GATA3 **(B)**; measured levels of IL4 (**C**), IL5 **(D)** and IL13 **(E)** in the BAL fluid by CBA. Data from two experiments depicted as solid and open circles respectively **(A,B)** Data from one experiment **(C-E)**.
Data analysed by one-way ANOVA, and corrected for multiple comparisons by a Sidak's test. For all panels, * = p<0.05, ** = p<0.01, *** p<0.001. Contributions: experimental prep with Dr S. Loeser, mice obtained from Prof Graham.

5.2.7 CXCR2-deficient mice have reduced ILCs in the Lung

Finally, the percentage of ILCs within the infected lung was found to be 0.4% in the CXCR2-deficient mice, but reached 0.8-0.9 % in the heterozygotes and wildtype mice (Fig 5.2.7A). The subset expressing GATA3 and thus designated as ILC2 cells, were even more profoundly deficient in the absence of CXCR2 (Fig 5.7B). Fig 5.7 C and D present flow plots of lung cells gated on Lin vs ICOS, with fewer Lin^{-} $ICOS^{+}$ cells in the CXCR2-deficient mice versus wildtype mice.

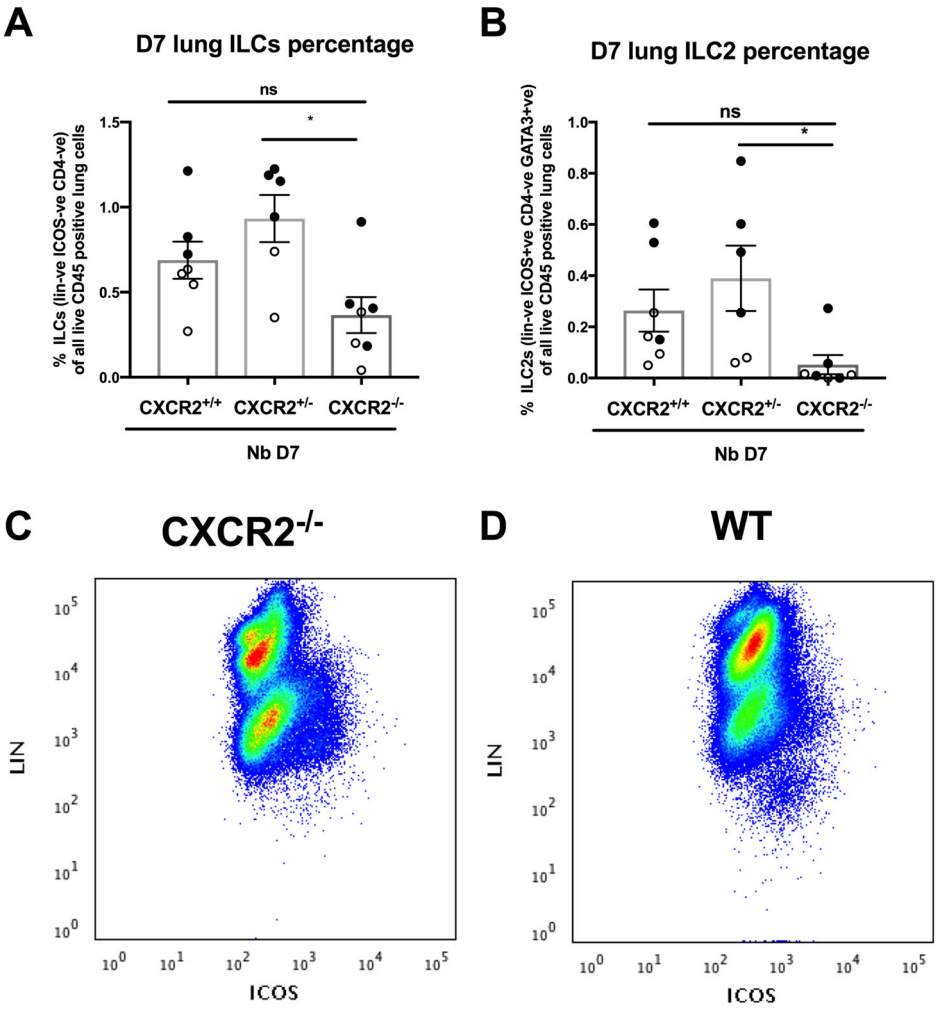

Figure 5.2.7 ILC response is impaired in CXCR2-deficient mice

BL/6, CXCR2-/- and CXCR2-/+ mice were infected with 250 *N. brasiliensis* L3 larvae for 7 days. Digestion performed of lung tissue at d7 post infection for analysis by flow cytometry. Analysis of percentage ILCs **(A)** and percentage ILC2s **(B)** of all live $CD45^+$ cells in lung. Dot plots of Lin vs ICOS in CXCR2-/- **(C)** and BL/6 **(D)** mice. Data in A, B Data from two experiments depicted as solid and open circles respectively **(A, B)**. Data analysed by one-way ANOVA, and corrected for multiple comparisons by a Sidak's test. For all panels, * = $p<0.05$, ** = $p<0.01$, *** $p<0.001$. Contributions: experimental prep with Dr S. Loeser, mice obtained from Professor Graham.

5.2.8 CXCR2-deficient mice have partially diminished alternative activation of macrophages in the peritoneum

In the peritoneal cavity, *N. brasiliensis* induces a strong alternatively activated macrophage response as seen in chapter 5. As the phenotype in the lung of CXCR2-deficient mice shows reduced polarisation of macrophages to an M2 phenotype, we assessed if this was true in the peritoneal cavity, in which macrophage numbers were similar in all genotypes (Fig 5.2.8 A). Surprisingly, the CXCR2-deficient mouse was able to polarise peritoneal macrophages to produce M2 products RELMα (Fig 5.2.8B) and Ym1 (Fig 5.2.8C), although RELMα expression was reduced around 50% compared to the wildtype and heterozygotes. Further evidence that the CXCR2-deficient phenotype is less penetrant in the peritoneal cavity came from eosinophil numbers, which were only slightly reduced in the CXCR2-deficient homozygotes (Fig 5.2.8D).

The transcription of M2 products in whole duodenal tissue was also assessed. While arginase expression was little different, RELMα and Ym1 levels showed some degree of reduction, although insufficient to attain statistical significance. Hence, the effects of CXCR2 deficiency appear to be more marked in the lung than at other sites.

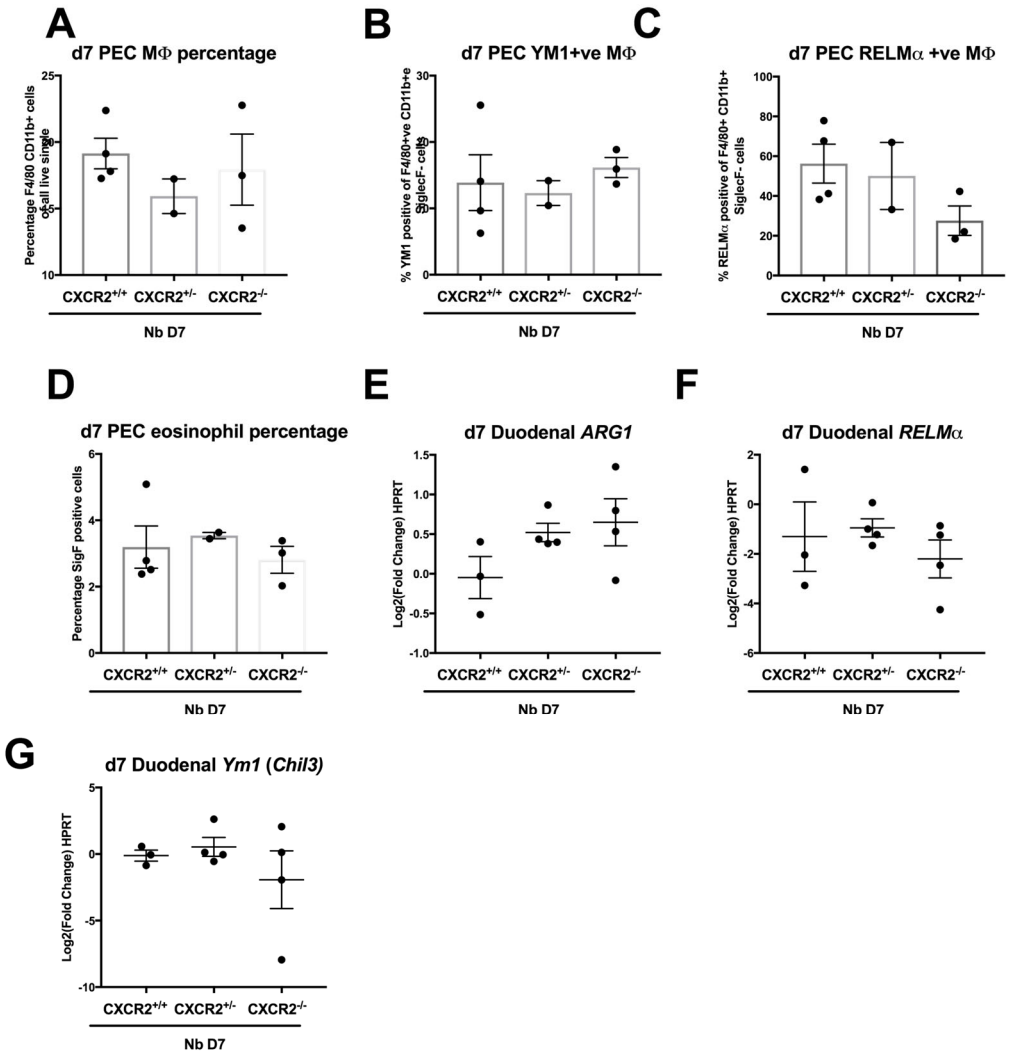

Figure 5.2.8 M2 responses in the peritoneum and gut are intact in CXCR2-deficient mice

BL/6, CXCR2$^{-/-}$ and CXCR2$^{-/+}$ mice were infected with 250 *N. brasiliensis* L3 larvae for 7 days. Peritoneal exudate cells were taken for flow cytometry and duodenum taken for qPCR at d7 p.i. Percentage of CD11b^{+} F4/80^{+} macrophages in the peritoneal cavity **(A)**; percentage of peritoneal macrophages positive for YM1 **(B)** and RELMα **(C)**; percentage of SiglecF^{+} eosinophils **(D)**. Gene expression quantification by qPCR for *ARG1* **(E)**, *RELMα* **(F)** and *YM1/ Chil3*(**G**). Data analysed by one-way ANOVA, and corrected for multiple comparisons by a Sidak's test. For all panels, * = p<0.05, ** = p<0.01, *** p<0.001. Contributions: experimental prep with Dr S. Loeser, mice obtained from Prof Graham.

5.2.9 CXCR2-deficient mice have intact Type 2 epithelial cell responses

To assess if the CXCR2-deficient mice have a similar epithelial cell phenotype as the MIF-deficient mice, we stained the intestine for DCLK1, a marker for tuft cells in the intestine. We quantified the number of DCLK1 positive cells per villus (average of 100 villi) and found no significant difference between the CXCR2-deficient and the wildtype or heterozygous mice (Fig 5.2.9D).

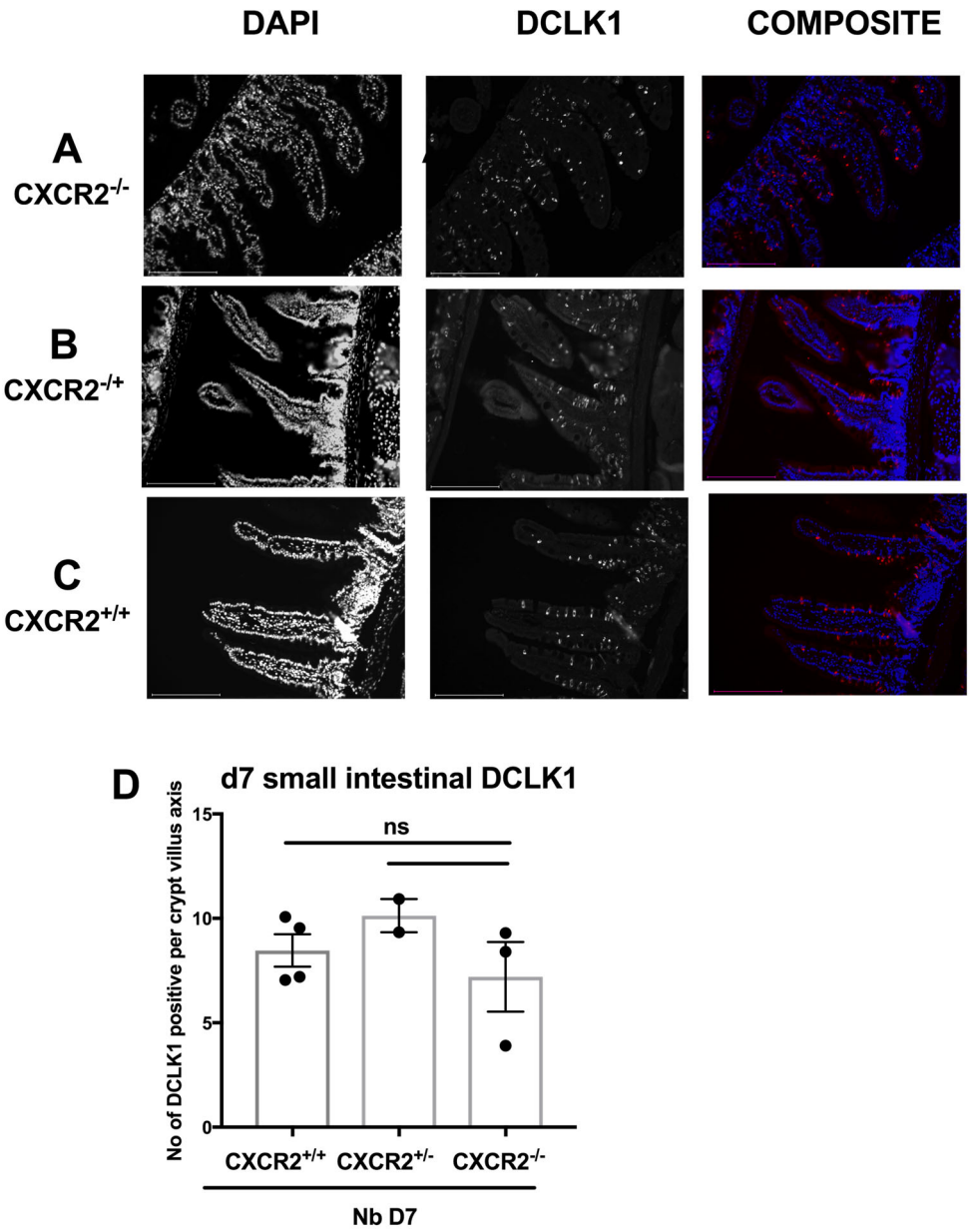

Figure 5.2.9 CXCR2-deficient mice have retained type 2 epithelial cell responses

B6 mice, CXCR2$^{-/-}$ and CXCR2$^{+/-}$ were infected with 250 *N. brasiliensis* L3 larvae D0. Tissue taken at day 7 and paraffin embedded for analysis. From left to right staining for DAPI, DCLK1 and merged images for the following groups: CXCR2$^{-/-}$ **(A)**, CXCR2$^{-/+}$ **(B),** B6 **(C)**. Scale bar is 200μM. DCLK1 positive cells counts per crypt villus axis (taken of an average of 100 crypt/villus axes) in small intestine at day 7 p.i. **(D)**. Data from one experiment. Contributions: experimental prep with Dr S. Loeser, mice obtained from Prof Graham.

5.2.10 CXCR2-expression on immune cells in the lung

To identify which cells express CXCR2 in the lung, we stained cells for surface CXCR2 expression. We found that CXCR2 was expressed highly on neutrophils and eosinophils. There was very little expression on T cells and macrophages. It is therefore likely that CXCR2 mediates its effect on the lung macrophages through an intermediate cell type such as the neutrophil or the eosinophil (Fig 5.2.10). This experiment was performed on one occasion only, and would have to be repeated using CXCR2 deficient mice as negative controls in order to verify the result.

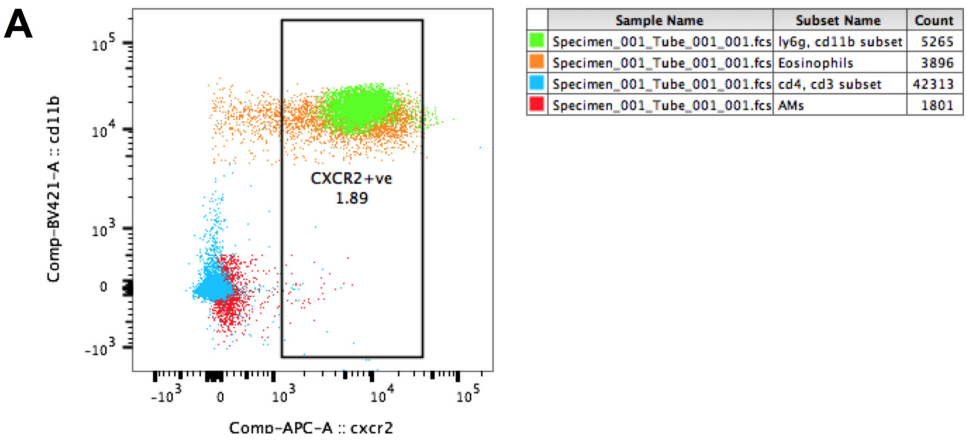

Figure 5.2.10 CXCR2 expression in lung occurs predominantly in neutrophils and eosinophils.

(A) Cells were harvested from the lung and gated using CD11b, Siglec F, CD3, CD4, Ly6G to determine populations of alveolar macrophages, neutrophils, T cells and eosinophils. These were superimposed onto a plot of CD11b versus CXCR2, to demonstrate the expression of CXCR2 in the various populations within the lung. CXCR2 expression is represented in green for neutrophils, orange for eosinophils, blue for T cells and red for alveolar macrophages. Data obtained from one experiment.

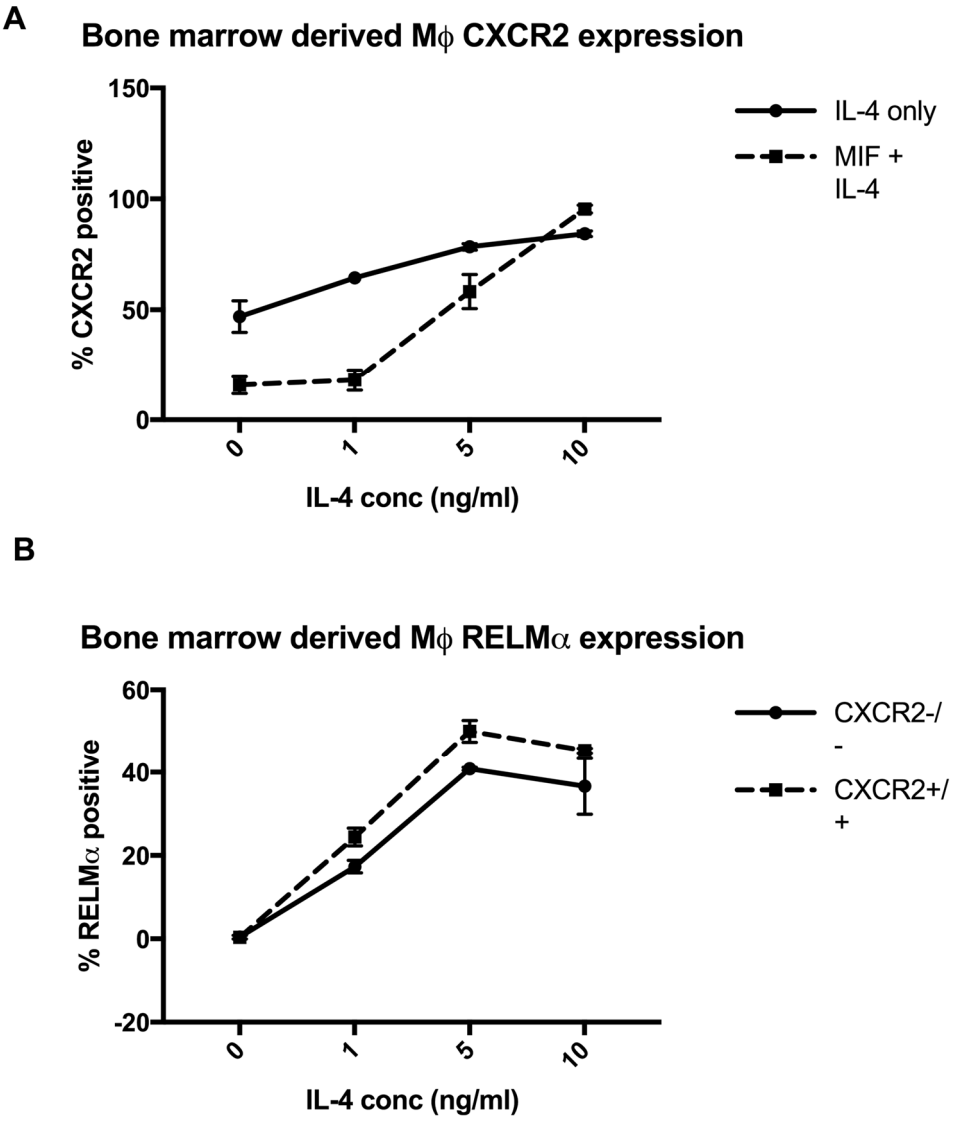

Figure 5.2.11 CXCR2 expression on bone marrow macrophages

(A) d7 Bone marrow derived macrophages (BMDMs) from 6-8 week BL/6 mice grown to 7 days old with L929 supernatant for M-CSF. D7 macrophages stimulated with different concentrations of rIL4 (10ng/ml) and rMIF (1µg/ml). These are analysed for CXCR2 expression by flow cytometry. Data from one experiment. (**B**) Flow cytometry in $CXCR2^{-/-}$ and BL/6 BMDMs grown to 7 days and stimulated for 24 hours with different concentrations of rIL-4 for 24 hours, before staining for intracellular RELMα. Data from one experiment.

5.2.11 CXCR2-expression on bone marrow derived macrophages

In order to assess if the effect of CXCR2 deficiency directly affects the ability of macrophages to produce alternatively activated products in response to a type 2 stimulus, we looked at CXCR2 expression in bone marrow derived macrophages grown for 7 days in L929 media as a source of M-CSF and stimulated with IL-4 or MIF. MIF reduces the expression of CXCR2, and IL-4 treatment upregulates CXCR2 expression but also rescues it from MIF reduction (Fig 5.2.11A). In order to assess if a type 2 stimulus has a direct effect on the macrophage population, we grew, and then stimulated wildtype and CXCR2 deficient bone marrow derived macrophages with IL-4 and MIF for 24 hours. We stained the macrophages with F4/80 and CD11b along with intracellular RELMα. We found that the CXCR2 macrophages produced slightly less RELMα, but there was no intrinsic inability of the CXCR2 deficient cells to make RELMα (Fig 5.2.11 B).

5.3 Discussion

In this chapter, we report that the absence of CXCR2 in the context of an *N. brasiliensis* infection results in a predominant phenotype in the lung. Similar to the MIF-deficient mice, there is a deficiency of eosinophils, M2 macrophages, and ILC2s. However, whilst the MIF-deficient mice have a reduction in the numbers of tuft cells and reduced alternative activation of macrophages, there is no difference in the number of tuft cells in the intestine

of infected CXCR2 deficient mice, and only limited changes in M2 cells in the peritoneal lavage.

In the lung, CXCR2 is expressed on $CD11b^+$ $Ly6G^+$ neutrophils and on $CD11b^+$ $SiglecF^+$ eosinophils but is absent from alveolar macrophages and T cells (Fig 5.10A). At this time, we have not assessed whether interstitial macrophages may express CXCR2, but based on the data now available it is likely that the effect of the MIF-CXCR2 interaction in the lung is mediated via neutrophils.

CXCR2 is highly expressed on neutrophils. Classically, neutrophils are known to mediate type 1 innate immune responses, but more recently have been found to facilitate type 2 immune responses during helminth infections. For example, in an *N. brasiliensis* infection, Chen et al (Chen et al., 2014) depleted neutrophils by injecting antibody to neutrophil surface antigen lymphocyte antigen 6 complex, locus G (Ly6G). Depletion of neutrophils during the primary phase of infection resulted in delayed worm expulsion in a secondary infection but not primary infection. Neutrophils may mediate an effector macrophage population. A group of naïve mice undergoing a primary *N.brasiliensis* infection were transferred fluorescent electronically sorted macrophages from the lung of mice that had neutrophils depleted and another group given macrophages from mice that had neutrophils. The naïve mice that were adoptively transferred macrophages from mice that had neutrophils during primary infection had less worms in the gut at day 5 post infection when compared to mice given compared macrophages from the lung of mice that had the neutrophils depleted with Ly6G antibody. Depletion of neutrophils indirectly affected macrophages by reducing the M2 phenotypic markers Arg1 and Ym1(Chen et al., 2014). It could therefore be that a neutrophil defect is responsible for the observed deficiency of M2 macrophage polarisation in CXCR2-deficient mice.

MIF has been shown to interact with CXCR2 on aorto-endothelial cells (Bernhagen et al., 2007). Our in vitro data further suggests that the surface expression of CXCR2 can be modified by MIF, raising the possibility that this constitutes a negative feedback loop. Interestingly we found CXCR2 to be upregulated with IL-4 on bone marrow derived macrophages, and that the absence of CXCR2 has a modest but measurable effect on the expression of RELMα in bone marrow derived macrophages. Taken together, these findings suggest that CXCR2 may also directly affect macrophage populations at sites where it is expressed, such as the peritoneum, and may thus be directly important in Type 2 macrophage immune responses.

As MIF is not the only ligand for CXCR2, and MIF also utilises CXCR4 as a receptor (Bernhagen et al., 2007), there may be confounders in the phenotype observed. This may account for the difference we see in the penetrance of MIF and CXCR2 deficiency, as the absence of MIF results in a generalised impairment of Type 2 responses that extends to the gut, while the requirement for CXCR2 is much more evident in the lung. Despite this, the published evidence that MIF signals through CXCR2 and the new data from this study argue strongly that the MIF-CXCR2 interaction is responsible, either directly or indirectly, for the development of a Type 2 immune response within the lung innate cell compartment.

Futher work may involve assessing the interaction of MIF with CXCR4 in the context of helminth infections. However, the CXCR4 deficient mouse is a lethal phenotype, therefore this analysis may only be possible using pharmacological CXCR4 inhibitors, which can have off target effects. Although there are striking immunological differences, there were no differences in parasitology at D7, and this would have to be repeated in a time course experiment to verify that there is no difference in expulsion. If, however, there is truly no difference in the ability of the CXCR2 mouse to expel *N. brasiliensis* it is suggestive that MIF operates independently of CXCR2 in the gut. as the proliferation of tuft cells was equal in the CXCR2

sufficient and deficient mouse. The CXCR2 deficient phenotype resulted in a TH2 deficiency in the lung, but not in the gut. In contrast, the MIF-deficient phenotype results in a TH2 deficiency in both the lung and the gut. The MIF-CXCR2 interaction may be important in the lung phenotype, however, CXCR2 is also vital for neutrophil recruitment to the lung and this may be the true reason for the CXCR2 phenotype. This will be explored in the lab through neutrophil depletion experiments in the future but is beyond the scope of this thesis.

Chapter 6: Helminth modulation of colitis

6.1 Introduction to Helminth modulation of colitis

6.1.1 Inflammatory bowel diseases

Ulcerative Colitis (UC) and Crohn's disease (CD) are both inflammatory bowel diseases (IBD) resulting in significant long term morbidity and mortality (Molodecky et al., 2012). Potent anti-TNF treatments are available, however, contraindications, primary non-response, loss of response and intolerance occur often. Consequently, IBD is associated with a high economic impact not only from hospitalisation and surgery but also loss of productivity at work (van der Valk et al., 2014). In adults, the incidence has risen to 24.3/100000/yr for UC and 12.7/100000/yr for CD in Europe (Molodecky et al., 2012). There is strong epidemiological evidence of the role of the environment in IBD phenotype. In the case for CD, there is an almost two-fold increase risk in smokers and previous appendectomy increases risk of CD. There is also an inverse association between IBD and number of siblings, large family size, and exposure to pets. The hygiene hypothesis (Strachan, 1989) proposed that early-life microbial infections modulated immune responses away from inappropriate hyperactivity; more recently this has broadened to recognise that parasites are very effective at dampening immune reactivity of their host (Maizels et al., 2014). For example, as parasitic infections have decreased, human autoimmune disease incidence has risen, suggesting a role of parasites in modulating inflammatory diseases (Hotez et al., 2008).

6.1.2 Helminth modulation of inflammatory disease

Colitis can be induced in a variety of different models. These include models that are due to gene defects (such as IL-10, MUC2 & MDR1 deficient mice), models that disrupt the epithelial barrier (DSS), innate anti-CD40 colitis and the T cell dependant colitis models (Kiesler et al., 2015). In each of these models, authors have demonstrated the effectiveness of helminth infections, in reducing disease severity scores and inflammatory cytokine production, as well as improving histological inflammation (**Table 6.1.1**).

6.1.2.1 Effect of helminths exposure in colitis models- *H.polygyrus*

Mice infected with *Heligmosomoides polygyrus* L3 larvae orally showed both reduced severity of TNBS colitis and increased mucosal resistance (Sutton et al., 2008a) while the same parasite also protected against TNBS colitis in C57BL/6 mice (Setiawan et al., 2007a). *H.polygyrus* supressed inflammatory responses in an IL-10-/- model of colitis (Elliott et al., 2004). In an IL-10-/-T cell and piroxicam model of colitis (where mice were reconstituted with IL-10-/- T cells and a week later administered piroxicam in their feed for two weeks to induce colitis) transfer of intestinal DCs from *H.polygyrus* infected mice protected animals from IBD (Blum et al., 2012). In this model, protection was associated with Foxp3$^+$ Tregs, as this subset when isolated from the mesenteric lymph node of *H. polygyrus* infected mice and adoptively transferred into RAG-/- animals conferred protection from piroxicam colitis, whereas Foxp3$^+$ Tregs from uninfected animals did not (Blum et al., 2012; Hang et al., 2013). Furthermore, in an OVA-specific colitis model (RAG-/- mice reconstituted with ova specific T cells and IL-10-/- T cells then given piroxicam) protected mice from intestinal inflammation by inducing Foxp3$^+$ Tregs (Leung et al., 2012). In a T cell transfer model of colitis, CD4$^+$ and

$CD8^+$ T cells were also required for worm induced protection (Metwali et al., 2006). Furthermore, adoptive transfer of dendritic cells from *H. polygyrus* infected mice in a RAG-/- T cell transfer model improved histological inflammation: these DCs were able to block OVA induced cytokine secretion in vitro (Blum et al., 2012). In another study, short-term *H. polygyrus* infection as far as the 4^{th} larval stage also improved disease score and histopathology in DSS colitis (Donskow-Łysoniewska et al., 2012).

6.1.2.2 Effect of helminths exposure in colitis models- *H.diminuta*

Other investigations testing live parasite infections included the cestode *Hymenolepis diminuta* which improved clinical scores and histopathology in a DNBS model of colitis. Infection of STAT6-/- mice did not affect colitis score or MPO activity suggesting that the protective effect is dependant on STAT6 (Hunter et al., 2005a). Anti-IL-10 blocking antibodies (Hunter et al., 2005a), as well as clodronate macrophage depletion (Hunter et al., 2010b) reduced the effects of *H diminuta*. In addition, IL-22-/- mice have less severe DNBS induced colitis and had greater protection of the colitis phenotype when infected with *H.diminuta*. This was associated with IL-25 upregulation ; neutralisation of IL-25 in IL-22-/- restored susceptibility (Reyes et al., 2016a).

6.1.2.3 Effect of helminths exposure in colitis models- *Schistosoma*

Transcutaneous infection of rats with *S.mansoni* resulted in improved histological scores in a TNBS model of colitis. *S.mansoni* infection was associated with increased IL-4, IL-5, IL-10 and smooth muscle contractility (Moreels et al., 2004). Mice infected with *S.mansoni* were also resistant to DSS-induced colitis which is associated with increased lamina propria macrophage infiltration (Smith et al., 2007).

Schistosome trematode parasites also have protective effects. *Schistosoma mansoni* eggs also reduce the severity of experimental colitis (Elliott et al., 2003) in a TNBS model. In this model, Tregs were found to be increased in spleens of egg-treated mice compared to those subjected to TNBS alone

(Mo et al., 2007). Exposure of mice to *S. japonicum* eggs also resulted in reduced idiopathic bacterial transfer (measured by culture of blood, liver, spleen and mesenteric lymph node to identify micro-organisms) during TNBS colitis (Zhao et al., 2009).

6.1.2.4 Effect of helminths exposure in colitis models- *Trichinella spiralis*

Two laboratories found that *Trichinella spiralis* infection could ameliorate DNBS colitis (Khan et al., 2002; Zhao et al., 2013).

6.1.2.5 Human infection models

Deliberate human infection with helminths has been performed to assess it as a potential treatment for gut inflammatory conditions. *Trichuris trichiura* has been used successfully to alleviate active ulcerative colitis in one case report, this was associated with increase IL-22 production (Broadhurst et al., 2010). This is an unusual report of someone who had chosen to self medicate with *T.suis* ova rather than conventional medical treatment during a flare, and remained in remission for 3 years, before re-infecting himself for a subsequent flare. It suggests the potential of helminths for treatment of colitis. On a much wider scale, the therapeutic potential of the related pig parasite *Trichuris suis* has been tested in two large scale clinical trials; however, a high placebo response rate obscured any treatment difference (Croft et al., 2012; Elliott and Weinstock, 2017; Fleming and Weinstock, 2015).

Macaques with idiopathic chronic diarrhoea (a serious cause of mortality in juvenile rhesus macaques) demonstrate a similar pathology to human IBD. Macaques were administered *T.trichiura* ova and faecal consistency scores were much improved and associated with increased mucosal $CD4^+$ T cells producing IL-4 (Broadhurst et al., 2012). Although the safety profile of *T. suis* is favourable, ethical and practical considerations are likely to preclude wider

use of live worm infections, however, the potential remains that worm-derived products may be effective future therapies.

Model	Detail	Suppression	Reference
Heligmosomoides polygyrus			
TNBS colitis	BALB/c d10 infection, d4 colitis	Histopathology, IFN-γ and TNF	(Sutton et al., 2008b)
TNBS colitis	C57BL/6 d14 infection, d4 colitis	Histopathology	(Setiawan et al., 2007b)
IL-10-deficient colitis	C57BL/6 piroxicam-induced	Histopathology, IFN-γ and IL-12	(Elliott et al., 2004)
RAG transfer model	IL-10-/- T cells + piroxicam	Histopathology, IFN-γ and IL-17	(Blum et al., 2012; Hang et al., 2013; Hang et al., 2010)
OVA-specific colitis	OVA-specific T cells and oral OVA	Histopathology, IFN-γ and IL-17	(Leung et al., 2012)
RAG transfer model	IL-10-/- T cells + piroxicam	Histopathology	(Metwali et al., 2006)
DSS colitis	BALB/c mice, up to 18 days	Weight loss and faecal blood	(Donskow-Łysoniewska et al., 2012)
Hymenolepis diminuta			
DNBS colitis	Infection 8 days prior to DNBS	Clinical score, histopathology and	(Hunter et al., 2005b)
DNBS colitis	Infection 8 days prior to DNBS	Myeloperoxidase	(Hunter et al., 2010b)
DNBS colitis	Infection 8 days prior to DNBS	Protection IL-25 dependent	(Reyes et al., 2016a)
Schistosoma japonicum* and *S. mansoni			
TNBS colitis	Rats infected with *Sm* 7 days prior to TNBS	Histopathology and myelo-peroxidase	(Moreels et al., 2004)
DSS colitis	*Mice* infected with *Sm* 8 weeks prior to DSS	Weight loss, colon shortening, disease activity index	(Smith et al., 2007)
TNBS colitis	Mice exposed to *Sm* eggs	Histopathology, IFN-γ and mortality	(Elliott et al., 2003)
TNBS colitis	Mice exposed to *Sj* eggs	Histopathology, IFN-γ	(Mo et al., 2007)
TNBS colitis	Mice exposed to *Sj* eggs (freeze-thawed)	Histopathology, IFN-γ and bacterial translocation	(Zhao et al., 2009)
Trichinella spiralis			
DNBS colitis	Infection 21 days prior to DNBS	Histopathology, IL-12 and myeloperoxidase	(Khan et al., 2002)
DNBS colitis	Infection 21 days after DNBS	Histopathology, myeloperoxidase and mortality	(Zhao et al., 2013)

Table 6.1.1 Effects of helminth infection or exposure on intestinal inflammation in rodent models, adapted from Varyani et al, 2017.

6.1.2.6 Modulation of autoimmune diseases and IBD through parasite-derived products

Several groups have found that helminth Excretory/Secretory (ES) products and specific helminth derived molecules can supress immune-mediated inflammatory diseases and allergy (Johnston et al., 2009; McSorley et al., 2013; Shepherd et al., 2015; Wu et al., 2017).

6.1.2.7 Parasite extracts and excretory secretory products

Crude extract from *Ancylostoma* (Cançado et al., 2011; Ferreira et al., 2013) and *Trichinella spiralis* (Motomura et al., 2009; Yang et al., 2014) protected from TNBS and DSS induced colitis. *Shistosoma mansoni* extract (Ruyssers et al., 2009) improved a TNBS and a T cell cell transfer model of colitis (Heylen et al., 2014).

6.1.2.8 Specific parasite molecules

To date, a range of parasite proteins have been shown to reduce disease activity in a variety of mouse IBD models (**Table 6.1.2**).

Anisakis simplex recombinant macrophage migration inhibitory factor (As-MIF) (Cho et al., 2011), *B.malayi* cystatin (rBMCys), B.malayi abundant larval transcript protein (rBMALT2) (Khatri et al., 2015a; Khatri et al., 2015b), *Clonorichis sinensis* Type 1 cystatin (CsStefin-1) (Jang et al., 2011a) and *Toxascaris leonina* galectin (Kim et al., 2010b) improved disease activity scores in a DSS model of colitis. *Brugia malayi* cytoplasmic asparaginyl-tRNA synthetase (rBMAsnRS) (Kron et al., 2013) improved a T cell model of colitis. S mansoni glutathione S-transferse (P28GST) and *S.japonicum* cystatin (Wang et al., 2016) improved TNBS colitis in rats (Driss et al., 2016). In colitis models, our group have also tested whether *H.polygyrus* ES

products (HES) can ameliorate pathology with encouraging results in T cell transfer colitis (unpublished data)

The effect of parasite proteins is found not only in IBD, but also other auto-immune diseases and in allergy. Our group have discovered a *H. polygyrus* TGF-β mimic (*Hp*TGM) capable of inducing mouse and human FoxP3 T regulatory cells, and reducing inflammation *in vivo* in a skin allograft model (Johnston et al., 2017). ES-62 from *Acanthocheilonema viteae* inhibits TLR-dependent inflammation in a variety of settings (Harnett et al., 2010). More recently, it has been reported in an Alternaria model of asthma, *H.polygyrus* Alarmin Release Inhibitor (HpARI) interferes in the IL-33 release pathway and eosinophil accumulation (Osbourn et al., 2017).

One mechanism by which some helminth products reduce disease activity is immune deviation to a Type 2 response. Another outcome was seen following administration of recombinant cystatin from *Schistosoma japonicium* (rSjcystatin), which induced $Foxp3^+$ T regulatory cells and improved disease activity scores in a TNBS model of colitis (Wang et al., 2016). In the case of *Ancylostoma caninum* adult excretory secretory products (AcES), protection from DSS-induced colitis appeared to be through induction of IL-4 and IL-10 double positive T cells and alternatively activated macrophage products (Ferreira et al., 2013).

IL-10 production is known to be important in ameliorating colitis severity (Zigmond et al., 2014): As-MIF has also been shown to induce upregulation of IL-10 in intestinal epithelial cells and CsStefin-1 was shown to increase IL-10 production in the large intestine, and of the IL-10 positive population there was an increase in the percentage of $F4/80^+$ cells in this population (Jang et al., 2011b). Protection by P28GST (a schistosome enzymatic protein, the 28-kDa glutathione S-transferase) was dependent on eosinophil infiltration, and the effect was lost in IL-5-/- mice (Driss et al., 2016). Dendritic cells pulsed with *H. diminuta* antigen were also successfully transferred to treat DNBS colitis (Matisz et al., 2015). Adoptive transfer of *H. diminuta*-stimulated

myeloid populations, which induced T cell IL-10 production, resulted in an attenuated colitis (Reyes et al., 2016b)

Molecules	Detail	Suppression	Reference
Cestodes			
Hymenolepis diminuta extract	DNBS induced colitis	Clinical and histopathological score, (IL-10 and IL-4 levels increased in splenocytes)	(Matisz et al., 2015)
H. diminuta antigen	DNBS colitis in mice	Histopathology and Disease activity score suppression	(Reyes et al., 2016b)
Nematode Extracts and ES			
Ancylostoma caninum ES	DSS colitis in BALB/c mice	Histopathology, cytokines, myeloperoxidase	(Cançado et al., 2011)
A. caninum ES	DSS colitis	Histopathology, cytokines, weight loss	(Ferreira et al., 2013)
A. caninum soluble proteins	TNBS colitis in Swiss mice	Histopathology, MPO	(Ruyssers et al., 2009)
Trichinella spiralis larval extract	DNBS colitis in C57BL/6 mice	Histopathology, MPO, IL-1β respons; raised TGF-β, IL-13	(Motomura et al., 2009)
Nematode Proteins			
Anisakis simplex MIF homologue	DSS colitis in C57BL/6 mice	Disease Activity Index, Weight Loss	(Cho et al., 2011)
Brugia malayi asparaginyl-tRNA synthase	T cell transfer model	Histopathology	(Kron et al., 2013)
B. malayi Cystatin	DSS colitis in BALB/c mice	Disease Activity Score, Histopathology	(Khatri et al., 2015a)
B. malayi ALT 2 protein	DSS colitis	Disease activity score, myeloperoxidase activity	(Khatri et al., 2015b)
Toxascaris leonina Galectin	DSS colitis in C57BL/6 mice	Disease Activity Index, Weight Loss; raised TGF-β, IL-10	(Kim et al., 2010a)
Trematode Extracts			
Schistosoma mansoni soluble proteins	TNBS colitis in Swiss mice	Histopathology, MPO, IFNγ response	(Ruyssers et al., 2009)
S. mansoni soluble extract	T cell transfer model	Clinical disesase score, colonoscopy, myeloperoxidase	(Heylen et al., 2014)
Trematode Proteins			
Clonorchis sinensis cystatin	DSS colitis in C57BL/6 mice	Disease Activity Index	(Jang et al., 2011a)
S. mansoni 28-kDA glutathione S-transferase (P28GST)	TNBS colitis in rats	Reduced clinical and histological scores, 50% reduction in colonic Myeloprexoidase	(Driss et al., 2016)
Schistosoma japonicum cystatin	TNBS colitis in BALB/c mice	Histology, Cytokine responses	(Wang et al., 2016)

Table 6.1.2 Helminth Products and Proteins in Intestinal Inflammation in rodent models- adapted from Varyani et al, 2017.

6.1.3 Innate immunity and colitis models

Two important innate cell types in colitis are macrophages and innate lymphoid cells. Although colitis is largely T cell mediated, alterations in innate cell populations can result in a worsening phenotype of colitis. Moreover, macrophages lacking IL-10R are intrinsically pro-inflammatory and cause spontaneous colitis in mice, while paediatric patients with mutations in the IL-10 receptor have more pro-inflammatory macrophages and an IBD like phenotype (Shouval et al., 2014; Zigmond et al., 2014). Another important gene locus is NOD2, as the odds ratio for a carrier of two susceptibility alleles of NOD2 is 17.1 for Crohn's disease (95% CI 10.7-27.2) (Economou et al., 2004) and this gene is highly expressed in macrophages (Forrest et al., 2014). DNBS colitis in BALB/c mice was ameliorated with *H.diminuta* infection and this effect was associated with increased colonic expression of RELMα, ARG1 and CD14. On depleting the macrophages with clodronate, this protective effect was diminished. In T cell transfer models, depletion of macrophages by administration of a saporin-conjugated anti-CD11b antibody results less severe colitis (Kanai et al., 2006). Transfer of alternatively activated (polarised with IL-4/13) but not classically activated (polarised with IFNY) macrophages ameliorated colitis (Hunter et al., 2010a).

Innate lymphoid cells (ILCs) are a family of lymphocytes that express subunits of cytokine receptors including IL2a (CD25) and IL-7RA (CD127) but unlike adaptive T and B cells they do not express antigen receptors and are not antigen-specific (Eberl et al., 2015; McKenzie et al., 2014). The ILC family includes NK cells and a non-cytotoxic family: ILC1, 2 and 3 including Lti cells. These are defined in both mice and humans by their differential expression of transcription factors and cytokines: ILC1 express Tbet and produce IFNγ and TNF. ILC2 express GATA3 and produce Th2 associated cytokines and initiate immune responses to helminths.

Depleting total ILC population by administration of an anti Thy-1 antibody in RAG-/- mice (which lack the recombination activating gene 1- and do not have mature B and T cells) results in improvement of inflammation in colitis and typhilitis scores (Buonocore et al., 2010).

ILC1s accumulate in the terminal ileum of patients with Crohn's' disease (Bernink et al. 2013). A population of IL13Ra1^{+} c-Kit^{+} cells which impair MMP synthesis has been found in Crohn's disease (Bailey et al. 2012) although further work needs to be undertaken in order to assess if these are truly ILC2s. The role of ILC2s has not been completely elucidated in humans (Goldberg et al., 2015). In a *Helicobacter hepaticus* RAG-/- model of colitis, the mice develop diarrhoea, ranging from watery to bloody, with ulceration from caecum to colon (Shomer et al., 1998). ILC3s (Thy1^{+} Rorgt^{+} SCA1^{+} cells) in the *Helicobacter hepaticus* RAG-/- model of colitis produce IL-23 mediated gut inflammation (Buonocore et al., 2010).

A follow up study (between 7 to 39 years) found no increase in susceptibility to particular diseases in patients who lacked ILCs (Vely et al., 2016), however, the study was small (18 patients) and longer follow up may be required. Despite the limited evidence available on how human ILCs impact disease, they remain an attractive target for drugs as they are present at mucosal sites and are therefore able to respond quickly to epithelial alarmins.

6.1.4 Rationale for anti-CD40 antibody model of colitis

The anti-CD40 antibody colitis model is mediated by activated cells of the innate immune system, using a protocol adapted from Uhlig et al 2006 (Uhlig et al., 2006). In this model, 200µg of anti-CD40 antibody is injected intraperitoneally into a RAG-/- mouse.

CD40^{+} antigen presenting cells (APCs) interact with CD4^{+}CD40L^{+} T cells. This CD40L-CD40 interaction leads to activation of the CD40^{+} APCs and

results in a feedback loop that activates APCs and T cells (van Kooten and Banchereau, 2000). Anti-CD40 stimulation in APCs of RAG-/- mice results in a global phenotype of weight loss and diarrhoea (Uhlig et al., 2006). The colon of mice given this antibody demonstrated epithelial cell damage, leucocyte infiltration, and goblet cell depletion. There is activation of the innate immune cell $CD11c^+$ dendritic cells. Serum TNFα, IL-6 and IL-12p70 were increased in the CD40 antibody treated group, and antibody against TNFα can rescue the phenotype. This model has been utilised to investigate the role of $IL23^+$ ILCs in innate colitis (Buonocore et al., 2010), and the NF-kB protein c-Rel which regulates inflammatory ILC1s (Visekruna et al., 2015).

Both innate (Dendritic Cells) and adaptive components (T Regulatory cells) of the immune system are modulated by HES which consists of over 350 proteins including a TGF-β mimic (Hewitson et al., 2011). As we have demonstrated the role of HES in modulating T cell transfer colitis (unpublished data), we explored the anti-CD40 RAG-/- model as a means of assessing *in vivo* the ability of helminth excretory/secretory products and helminth-derived proteins to modulate the innate immune response in an autoimmune setting such as IBD.

6.2 Results

6.2.1 HES does not significantly ameliorate body weight loss or colitis scores in the anti-CD40 model of colitis

Fig 6.2.1A demonstrates the model utilised to evaluate the effect of HES in an anti CD40 disease model. On D0, two groups of RAG-/- mice were given 200 µg of anti-CD40 antibody and one group received isotype control rat IgG. One of the groups given the anti-CD40 antibody was also administered HES i.p. daily from d1-5, the other group was instilled with 200µl of PBS i.p. as control. Daily evaluations of weight and colitis score were recorded. The experiment would be terminated if any of the mice lost over 25% of the body weight.

Fig 6.2.1.B and 6.2.1.C demonstrate no significant difference in the colitis score obtained when we attempted to rescue the CD40 model with HES, although there was marginally less disease in the HES recipients. This is in contrast to unpublished data available in the Maizels group that shows HES is capable of significantly modifying a T cell-mediated colitis.

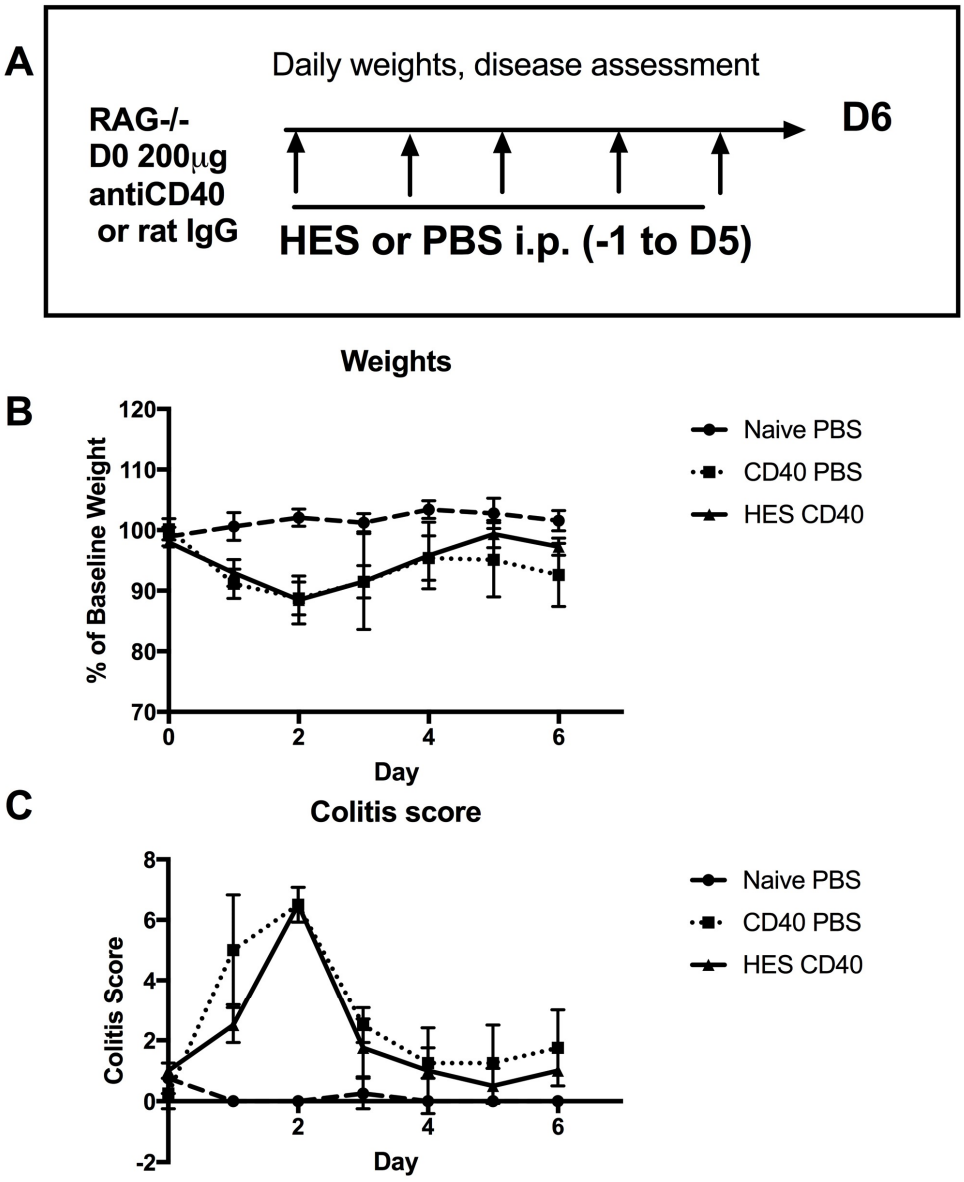

Figure 6.2.1 HES does not affect the body weight and colitis score in anti-CD40 model of colitis

(A) Schematic of experimental design assessing the ability of *Heligmosomoides polygyrus* excretory secretory product (HES) to modify the phenotype of the anti-CD40 model. Experiment consisted of three groups of mice (n=4). **Group 1** Naïve mice adminstered 200μg of rat IgG isotype control and 200ul of PBS i.p. from d-1 to 5; **Group 2** mice administered 200μg of anti-CD40 antibody i.p. at D0 and 200μl PBS i.p. daily from d-1 to 5; **Group 3** administered 200μg of anti-CD40 antibody i.p. at D0 and D0 10μg of HES in 200μl PBS from d-1 to 5.Daily weights **(B)** and colitis score **(C)** was recorded. Data is representative of two experiments. Points represent mean colitis scores with error bars representing standard deviations. Data analysed by a one way ANOVA.

6.2.2 HES results in reduced inflammatory infiltrate in the anti-CD40 antibody colitis model.

The major feature noted was the effect of HES on total cell numbers and especially macrophages in the peritoneal cavity exudate cells (Fig 6.2.2 A-C). Administration of HES resulted in a global reduction of inflammatory cell infiltrate in the peritoneal cavity when compared to the treatment with anti-CD40 antibody only (Fig 6.2.2.A). The total cell count in the peritoneal cavity was reduced in mice treated with HES and anti-CD40 antibody from 50.4 x 10^5 in anti-CD40 treated mice to 8.85 x 10^5 in HES and anti-CD40 antibody treated mice. In order to assess the innate cell macrophages, eosinophil and neutrophil populations were stained the peritoneal cavity cells with CD11b, F4/80, SigF and Ly6G. The percentage of $CD11b^+$ $F4/80^+$ macrophages is reduced with HES treatment in an anti-CD40 antibody model from 62% of the cells in the peritoneal cavity being $CD11b^+$ $F4/80^+$ cells (in the CD40 group) to 12% in the HES-CD40 group (Fig 6.2.2 B). Similarly, the absolute numbers of $CD11b^+$ $F4/80^+$ cells were reduced with 31 x 10^5 cells in CD40 colitis to only 1.4 x 10^5 cells in HES-CD40 colitis (Fig 6.2.2 C). The percentage of $SigF^+$ eosinophils is reduced in the peritoneal cavity from 24% in naïve mice to 3 and 4% in CD40 colitis and HES-CD40 colitis groups respectively (Fig 6.2.2D). Similarly, the numbers of eosinophils reduced from naïve 6.8 x 10^5 to 1.6 x 10^5 in CD40 colitis and 0.4 x 10^5 in HES-CD40 colitis (Fig 6.2 E). There was no statistical difference in the percentage or number of eosinophils between the CD40 and HES-CD40 groups (Fig 6.2 D,E). The percentage of $CD11b^+$ $Ly6G^+$ neutrophils rose from 1.4% in naïve mice to 10% in CD40 colitis and 20% in HES-CD40 colitis, although the difference between the CD40 colitis and HES-CD40 colitis groups were not statistically significant (Fig 6.2.2F). The numbers of $CD11b^+$ $Ly6G^+$ neutrophils was 0.002 x 10^5 cells in the naïve group, 0.06 x 10^5 cells in the CD40 treated group and 0.009 x 10^5 in the HES-CD40 treated group.

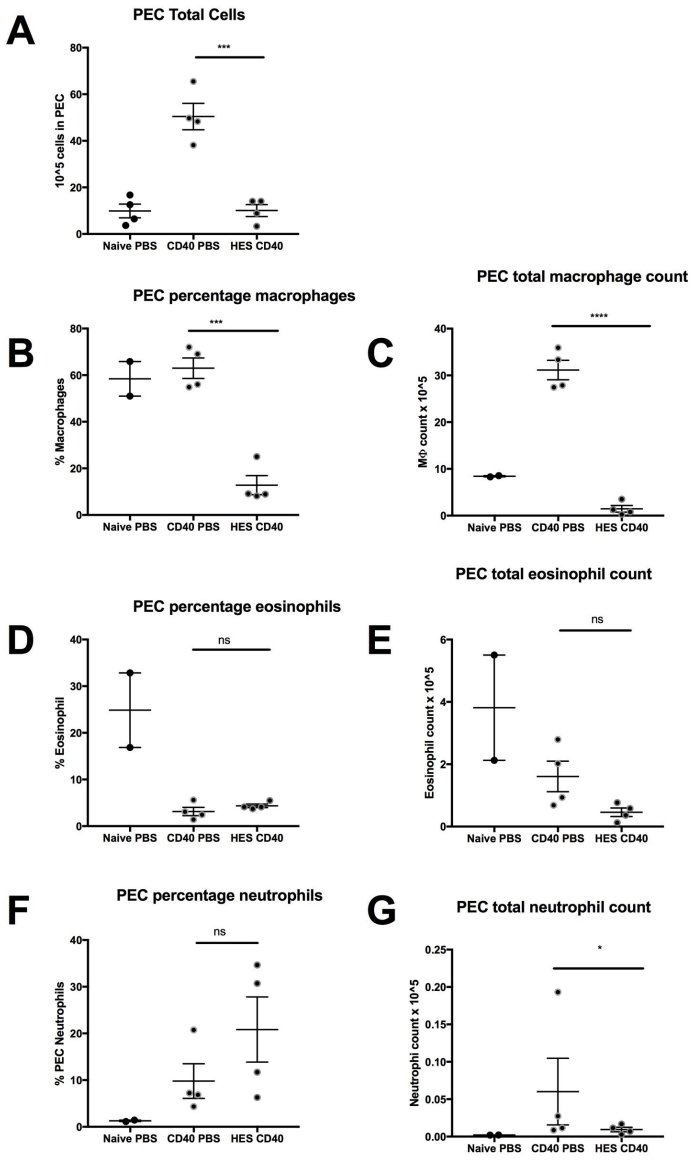

Figure 6.2.2 HES reduces the infiltration of inflammatory cells in anti-CD40 antibody colitis

(A) Total cell count of peritoneal exudate cells obtained at d6 of anti-CD40 colitis model (details of experimental design in Fig 6.1A). Peritoneal exudate cells at d6 stained for CD11b, F4/80, Siglec F and Ly6G**.** Percentage **(B)** and total numbers **(C)** of $CD11b^+$ $F4/80^+$ macrophages in peritoneal exudate cell lavage. Percentage **(D),** and total numbers of **(E)** $CD11b^+$ $Siglec\text{-}F^+$ eosinophils in lavage at d6 p.i. Percentage **(F)**, and total numbers of **(G)** $CD11b^+$ $Ly6G^+$ neutrophils in lavage fluid at d6 p.i. Experiment performed once, data represents mean with SEM. Data analysed by one way ANOVA, and corrected for multiple errors by a Sidak's test. For all panels, * = $p<0.05$, ** = $p<0.01$, *** $p<0.001$.

6.2.3 HES upregulates the production of Arg1 in peritoneal lavage exudate cells

We assessed the transcription of anti-inflammatory cytokine IL-10 and pro-inflammatory cytokine IFNγ in the peritoneal exudate cells and found no difference between the CD40 and the HES-CD40 groups (Fig 6.2.3 A,B). Next, we looked at the balance of M2 products which have been shown in other models to be affected by the administration of parasite products resulting in a type 2 macrophage phenotype. There was no difference in the transcriptional expression of RELMα between the CD40 and the HES-CD40 groups (Fig 6.2.3C), however, the level of ARG1 was upregulated in the HES-CD40 group when compared to the CD40 group. This result is inconsistent with other markers RELMα (which showed no difference in transcription in the peritoneal exudate cells (Fig 6.2.3C) or in the level of protein in the peritoneal lavage fluid (Fig 6.2.3E) or YM1 (which showed no difference in the level of protein in the peritoneal lavage fluid with HES treatment) (Fig 6.2.3 F). Presumably these proteins have been released by the macrophages before they disappeared.

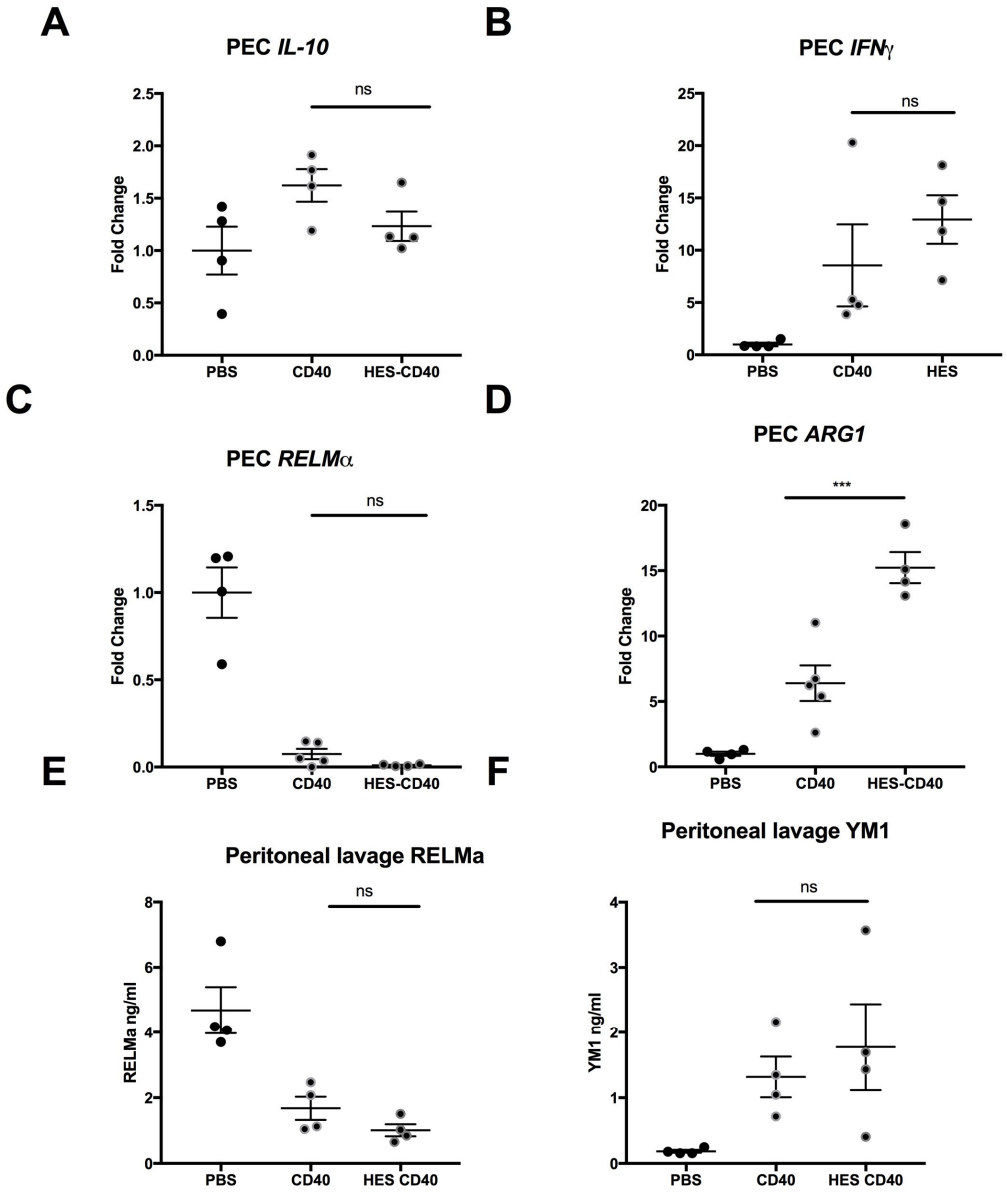

Figure 6.2.3 HES upregulates the production of Arg1 in peritoneal lavage exudate cells.

Peritoneal lavage cells taken at day 6 of an anti CD40 colitis model (experimental schematic Fig6.1A). Gene expression analysis by qRT-PCR of peritoneal exudate cells for *IL-10* **(A)**, *IFNγ* **(B)** *RELMα* **(C)** and *ARG1* **(D)** at D6. Protein levels of RELMα (**E**) and YM1 **(F)** in lavage fluid. Experiment performed once. Data analysed by one way ANOVA, and corrected for multiple errors by a Sidak's test. For all panels, * = $p<0.05$, ** = $p<0.01$, *** $p<0.001$.

6.2.4 HES does not affect the histology score in an anti-CD40 colitis model

Sections of colonic tissue were assessed to obtain global histopathology scores for each mouse, performed by Dr Derakashan (Consultant pathologist at QEUH, Glasgow). He was blinded to the treatment groups and crosschecked the score with a second histopathologist. There was no significant difference in colon histology scores between groups which were administered HES versus those given the anti-CD40 antibody only (Fig6.2.4.A), although overall scores were lower in 2 of the 4 animals receiving HES. There were only two animals in the anti-CD40 group only as one of the samples had not been processed by accident. Figures 6.2.4.B-D illustrates colon samples stained with H&E from naïve mice (B), and mice with either anti-CD40 antibody alone (C) or anti-CD40 antibody with HES (D).

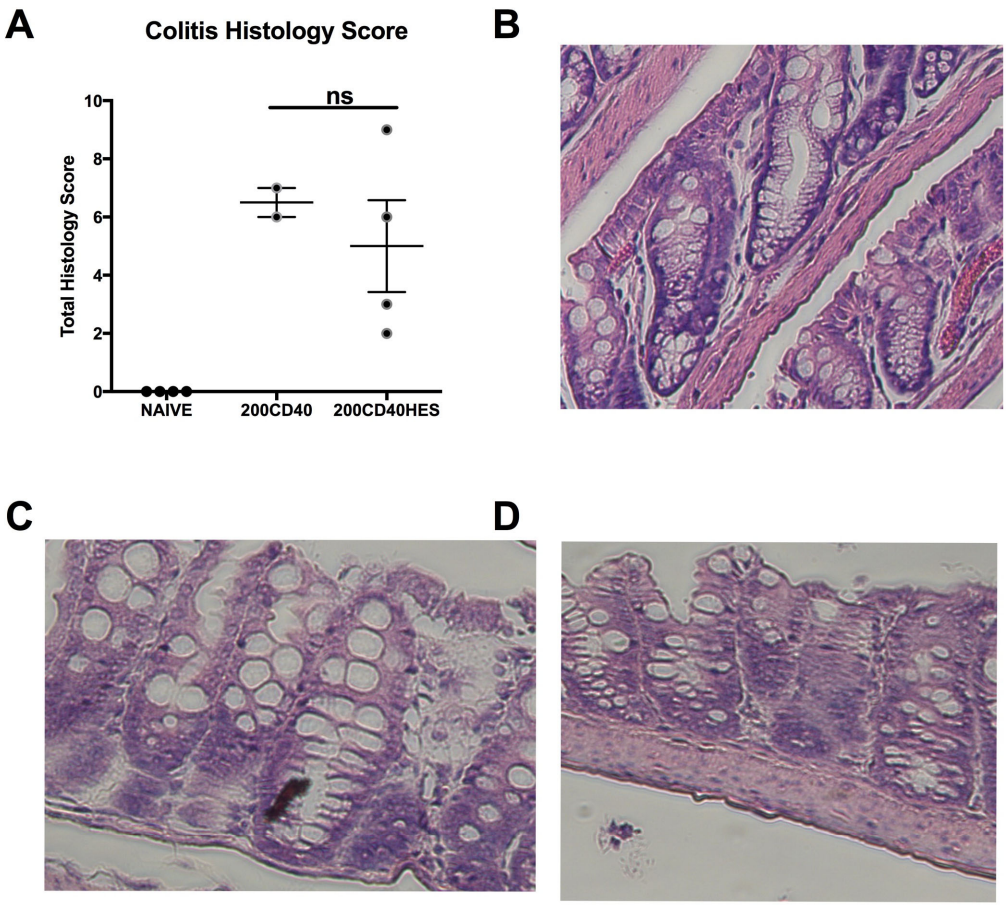

Figure 6.2.4 HES does not affect the colitis histology score in anti-CD40 model of colitis

(A) HES colitis score performed by two histopathologists blinded to the underlying treatment. Score calculated based on following parameters: degree of crypt loss, ulceration, crypt abscesses, goblet cell loss, mucosal and submucosal inflammatory infiltrate. Histology score developed by Dr D J Smyth and Professor M Arends (University of Edinburgh). H&E staining of colonic tissue of Naive **(B)** CD40 **(C)** and HES CD40 **(D)** colitis models. Data analysed by one way ANOVA, and corrected for multiple errors by a Sidak's test. For all panels, * = $p<0.05$, ** = $p<0.01$, *** $p<0.001$.

6.3 Discussion

The data presented in this Chapter suggest that HES does not have a significant effect on the disease score in a model of innate-mediated colitis driven by anti-CD40 antibody. This conclusion is in contrast to previous data from our laboratory suggesting that HES is able to ameliorate colitis in a T cell transfer model. However, it had also been found that HES has variable effects in another, acute, model of colitis provoked by DSS (Smyth, unpublished data).

Both the anti-CD40 and DSS models of colitis can be categorised as innate forms of colitis. DSS causes extensive epithelial damage, resulting in a colitis phenotype in SCID mice. Similarly, anti-CD40 is injected into RAG mice (without T and B cells), and therefore allows us to assess the innate components of the immune system. Another contrast with the T cell transfer model is the severity of disease: with the anti-CD40-treated mice losing 20% body weight in the first four days of disease, compared to approximately 10% over three weeks in a T cell transfer model.

We chose to use the peritoneal lavage as a readout, as we placed the colon in paraffin for H&E staining. Although we saw a reduction in the cellular infiltration in the peritoneal cavity and upregulation of Arginase 1 transcription, this may not in itself have been enough to alter the acute severe pathology seen in DSS and the anti CD40. The loss of macrophages following infection is widely acknowledged to occur in many pathology models and has been attributed to adherence to tissues, increased cell death or emigration to draining lymph nodes (Davies et al., 2013). As there is an overall loss of the macrophages in the peritoneal lavage, the arginase here may have been produced by other cell types e.g. neutrophils.

Potentially HES has a role in a more chronic model of inflammation such as the T cell transfer model, given that HES treated mice had reduced colon

histology scores and disease activity scores (D.Smyth unpublished results). HES has been recognised to induce Foxp3^{+} T regulatory cells (Grainger et al., 2010). In context of innate cells, HES has been shown to down-modulate IL-12 production in both DCs (Kemter et al, unpublished data) and macrophages (Coakley et al., 2017). Despite the potential of HES to modulate these key cell types in vivo, the pathology induced in the DSS model may be too acute for HES to have a measurable impact. This model was tested to investigate the effect of HES on innate cell activation and pathogenesis, but the results were not promising enough to explore further. The anti-CD40 antibody was also produced in house, and batch variation in potency resulted in several unexpected deaths, making further work not possible. In addition, a longer-term goal would be to transfer innate cell types in an attempt to rescue colitis. However, with the widespread activation of macrophages and DCs by the anti-CD40 antibody, the possibility remained that transferred cells would also undergo activation by residual antibody; therefore we felt it best to conclude this part of the study as it stands. Potential future work in the more promising T cell transfer model of colitis, may involve adoptive transfer experiments, which will assess the effector cells that are involved in HES induced immunomodulation. Furthermore, as the lab has now produced recombinant proteins such as the TGF-beta mimick (Johnston et al., 2017).

Final Conclusion

In Gastrointestinal immunity models, the immune mechanisms that are protective in colitis and result in expulsion of helminths is highly influenced by macrophage populations. It was therefore of interest when MIF was found to influence anti-helminth immunity.

MIF was the first cytokine to be discovered in the 1960s (Bloom and Bennett, 1966; David, 1966), as being important in delayed-type hypersensitivity reactions and has been investigated in several TH1 models of inflammatory disease (Calandra and Roger, 2003). MIF is highly conserved between humans and mice, with proteins sharing >90% amino acid identify (Calandra and Roger, 2003). Homologues of MIF have also been found in filarial helminths(Pastrana et al., 1998). Neutralising MIF results in protection from septic shock (Calandra et al., 2000). Polymorphisms in the MIF gene are associated with autoimmune diseases of the liver (Assis et al., 2014). MIF is produced by epithelial cells (Haber et al., 2017), but also at many other mucosal immune sites and by immune cells (Calandra and Roger, 2003). Here we have shown that MIF is upregulated in macrophages during *N.brasiliensis* infection.

From our data, a model has been developed in which MIF initiates inflammation in helminth infections predominantly via recruitment of innate lymphoid cells. Evidence to support this hypothesis includes the observation that the numbers of ILCs are approximately 15 fold higher in wild-type mice than in MIF-deficient mice (Fig 3.5A). This leads to a reduction in the production of GATA3-dependent cytokines IL-4, IL-5 and IL-13. Although there is also an reduction in the T cell population in the mesenteric lymph nodes of MIF-deficient mice, published data demonstrates the innate cell IL-13 is important for the combined epithelial cell responses that expel *N. brasiliensis* that we observe in mouse models (Oeser et al., 2015; Voehringer et al., 2006).

ILCs were first described in RAG-/- mice as being IL-25 responsive cells that expelled *N. brasiliensis* by producing IL-13 (Fallon et al., 2006). The ILCs proliferated in this model and effectively led to the expulsion of *N.brasiliensis* in RAG-/- mice which lack T cells, therefore they are likely the predominant source of the IL-13 required to expel the parasite in this model. Indeed, we can administer IL-25 to the MIF-deficient mouse and effectively rescue the complete immunological and epithelial phenotype.

ILCs have also been demonstrated to be the source of IL-5 required to drive initial eosinophilia (Nussbaum et al., 2013). The MIF-deficient mouse has been previously reported to lack eosinophils (de Souza et al., 2015; Falcone et al., 2001; Magalhaes et al., 2009; Yoshihisa et al., 2011). However, eosinophils do not seem to be required for primary immunity to *N. brasiliensis* (Knott et al., 2007), and hence in this context represent a marker of the changes in innate cell populations induced, directly or indirectly, by MIF.

The experiments reported here are the first to describe the innate lymphoid and epithelial cell phenotypes of the MIF-deficient mouse, in which there is a deficiency of tuft cell hyperplasia, RELMβ production, goblet cell hyperplasia and *IL-25*. Studies have previously demonstrated that reduced RELMβ production (Herbert et al., 2009) or failure of tuft cell hyperplasia (Gerbe et al., 2016) can individually impair *N.brasiliensis* expulsion. A lack of *IL-13* in itself reduces the “weep-and-sweep” (Anthony et al., 2007)phenomenon required to expel helminths. A compromised epithelial response is the most likely explanation for impaired *N.brasiliensis* expulsion in the MIF-deficient mouse, but was not known if MIF acted directly on the epithelial cell or the immune cell populations. Data by Dr Claire Druery (Postdoctoral Scientist, Maizels’ lab) demonstrated that MIF-deficient organoids were as able as wild type organoids to respond to IL-4/13 to upregulate tuft cells production. This impolies that the underlying defect is in the total IL4/13 produced.

While this work was under way, Damle et al (Damle et al., 2017) reported that MIF-deficient C57BL/6 mice was in fact better able to expel *N. brasiliensis*, with increased cellularity and higher amounts of IL-13 production. It is difficult to account for this disparity, in view of the profound phenotype observed here including disruption of the essential epithelial cell response, and the effects in both the *H. polygyrus* and *N. brasiliensis* models of infection in BALB/c mice. Even in secondary infection with *H. polygyrus*, MIF-deficient mice are unable to mount an effective immune response, indicative of a robust phenotype. In addition, other laboratories have also reported that MIF is required for a protective Th2 response in models such as *Taenia craciceps* (Rodriguez-Sosa et al., 2003) and *Schistosoma japonicum* , so that at this point the reason for the discrepant report by Damle et al is not resolved.

MIF deficient macrophages have been previously studied in the context of Type 1 immune responses, in which they are unable to mount an adequate TNFα response to infections with mycobacteria (Das et al., 2013), *Toxoplasma gondii*.and *Leishmania major* (Juttner et al., 1998). One explanation for this is that MIF-deficient macrophages are hypo-responsive to LPS, and perhaps other TLR ligands (Roger et al., 2001). Whilst most of the studies documented a reduction in cytokine production in the MIF-deficient mouse (or where antibodies were given to MIF), these were conducted prior to the knowledge of innate lymphoid cells.

Subsequently, the suggestion that MIF may also be important in a Type 2 context was prompted by the discovery that MIF synergises with IL-4 to upregulate Arginase production in bone marrow macrophages (Buck et al.; Prieto-Lafuente et al., 2009; Yaddanapudi et al., 2013). Data reported here confirm that MIF is important in polarisation of Type 2 macrophages in both *H. polygyrus* and *N. brasiliensis* infections. This may be direct or through the effect of innate lymphoid cells cytokine production. There is also a direct

effect of MIF on macrophages, and previous data suggested this was through IL4Rα (Prieto-Lafuente et al., 2009). However, our data shows that the downstream pathway (phosphorylation of STAT6) is unaffected. As yet there may be other contributing transcription factors important in Type 2 polarisation, which have not yet been discovered, and may have an influence on the ability of MIF to initiate Type 2 macrophage polarisation.

MIF has also been shown to be important in development, However, it was shown that in wild-type mice, the MIF inhibitor 4-IPP is able to replicate the MIF-deficient phenotype as seen in reduced ILC responses, and reduced DCLK1 expression in the epithelium. These data suggest that MIF plays an active role in the response to infection, and the absence of MIF signalling within the mature immune system results in the immunological phenotype of the MIF-deficient mouse.

The receptors for MIF have been described as a combination of CXCR2,4 and CD74 (Bernhagen et al., 2007; Kraemer et al., 2011). Most of the literature has focused on the interaction of CXCR2 and MIF that initiates ERK signalling downstream(Das et al., 2013). There is also strong evidence of CXCR4 being important in monocyte arrest mediated by MIF. Inhibition of CXCR4 or its receptor results in greater numbers of *L. sigmodontis* (Bouchery et al., 2012).

Global deletion of the CXCR4 gene has an embryonic lethal phenotype, but it was possible to assess the phenotype of the CXCR2-deficient mouse in the context of an *N.brasiliensis* infection. CXCR2 is expressed on neutrophils(Eash et al., 2010) and tumor macrophages.(Katoh et al., 2013) MIF, however, is not the only ligand for CXCR2, and is in fact one of many. Infection of CXCR2 deficient mice led to a lung dominant phenotype of reduced alternative activation of macrophages, reduced ILCs and reduced

cytokines IL-4,-5 and -13 in the bronchoalveolar lavage. Taking into account the known expression profile of CXCR2, it seems likely that these effects of MIF in the lung act through an intermediary cell such as the neutrophil. Indeed, neutrophils are known to prime effector M2 macrophage development in the setting of helminth infection (Chen et al., 2014; Sutherland et al., 2014).

Interestingly, however, there was no similar phenotype observed in the intestinal tracts of CXCR2-deficient mice. This suggests that MIF interaction with CXCR2 is not required for the epithelial cell responses that are compromised in the MIF-deficient mouse. In many ways, these conclusions reflect the multi-faceted role of MIF, interacting with different cell types and tissues through different receptors and pathways. In both the lung and the gut, MIF can now be identified as an important cytokine for recruitment of ILCs, although in the lung this appears to be an indirect effect through CXCR4 receptor-positive third party cells. In the gut, however, impairment of MIF mediated ILC recruitment underpins defective epithelial cell responses and thereby leads to the failure of helminth expulsion. In both tissues, further investigation of the role(s) of MIF is likely to uncover further key interactions for effective immunity.

Key novel findings that have advanced the field

- This is the first study that identifies the role of MIF in Innate Lymphoid Cell proliferation and TH2 polarisation.
- It identifies MIF as a highly context specific cytokine- amplifying multiple type 2 immune cell pathways in the context of helminth infection
- MIF has its primary action on immune cells, either or both ILC2 and Th2, and in its absence, the lack of Type 2 cytokines results in a compromised epithelial cell phenotype.
- MIF acts upstream of the feed-forward loop which expands IL-25 production in response to IL-13.

A summary figure of the above points is given below

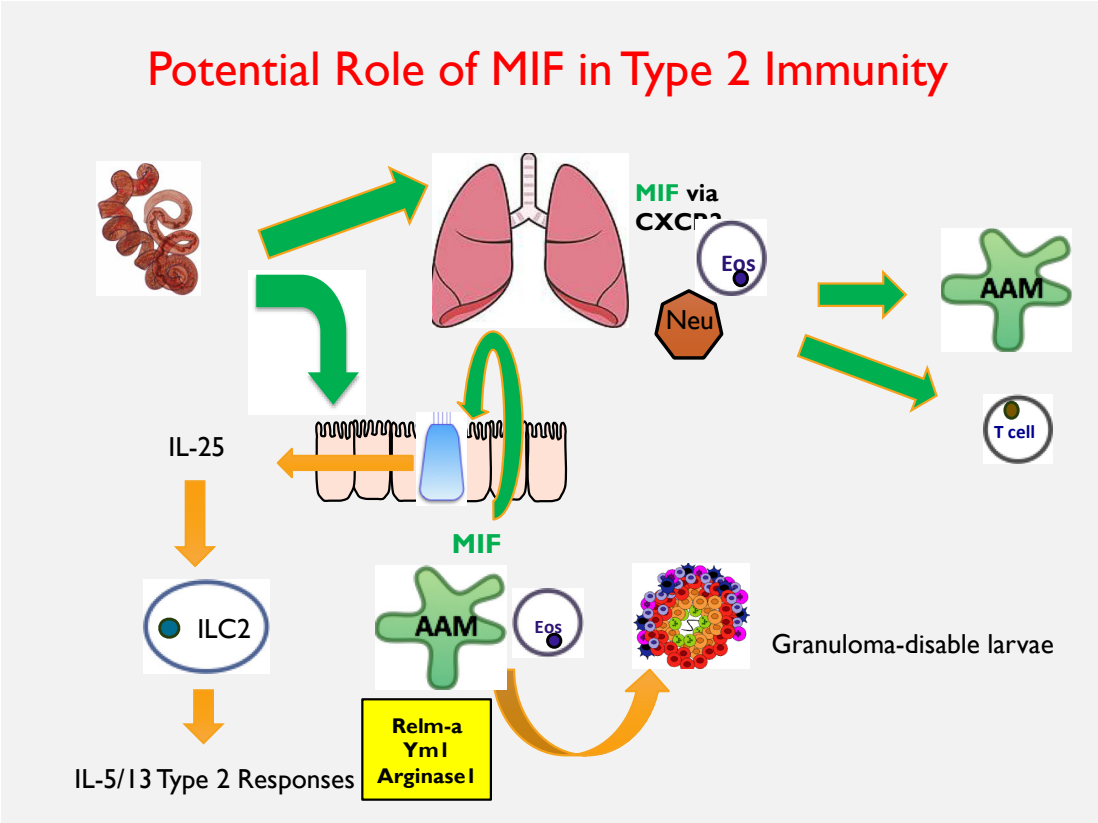

Figure 7.1 A summary of the potential role of MIF in the lung versus the gut. A more comprehensive schematic of the role of MIF in the epithelium is presented in chapter 4.

New questions arisen from data and future directions:

We propose that ILCs are the main initiators of the MIF response- this is because the MIF response occurs early (prior to when a TH2 response is known to develop). ILC *in vitro* cultures with and without MIF may help assess this question. If indeed ILCs do proliferate with the addition of MIF in vitro, then RNA Sequencing may identify downstream genes altered on exposure to MIF.

There is a clear rescue of the IL-25 phenotype with MIF. A greater clarification of how MIF and IL-25 interact is vital. Therefore further experiments involving addition of MIF to IL-25R deficient mice may help address if MIF is upstream or downstream of IL-25. IL-25 was felt to act predominantly on ILCs, however, we have discovered an ILC independent effect of IL-25 (Smith et al., 2018), it may also be that MIF is pleiotropic and has effects on multiple cells, as has been discovered to be the case of IL-25.

Further research needs to be performed to drill down the exact cell types that are important in MIF, the downstream cytokines (which can include IL-25), and MIF's interactions with its own ligands such as CXCR4. Further work may also assess the microbial interactions with MIF, and the role of dendritic cells. This will be the focus of further work in the Maizels' laboratory, but is beyond the scope of a 3 year PhD thesis.

References

(2016). Worldwide trends in diabetes since 1980: a pooled analysis of 751 population-based studies with 4·4 million participants. Lancet (London, England) *387*, 1513-1530.
Allen, J.E., and Sutherland, T.E. (2014). Host protective roles of type 2 immunity: parasite killing and tissue repair, flip sides of the same coin. Seminars in immunology *26*, 329-340.
Allen, J.E., Sutherland, T.E., and Ruckerl, D. (2015). IL-17 and neutrophils: unexpected players in the type 2 immune response. Current opinion in immunology *34*, 99-106.
Anthony, R.M., Rutitzky, L.I., Urban, J.F., Jr., Stadecker, M.J., and Gause, W.C. (2007). Protective immune mechanisms in helminth infection. Nature reviews. Immunology *7*, 975-987.
Anthony, R.M., Urban, J.F., Jr., Alem, F., Hamed, H.A., Rozo, C.T., Boucher, J.L., Van Rooijen, N., and Gause, W.C. (2006). Memory T(H)2 cells induce alternatively activated macrophages to mediate protection against nematode parasites. Nature medicine *12*, 955-960.
Artis, D., Wang, M.L., Keilbaugh, S.A., He, W., Brenes, M., Swain, G.P., Knight, P.A., Donaldson, D.D., Lazar, M.A., Miller, H.R.*, et al.* (2004). RELMbeta/FIZZ2 is a goblet cell-specific immune-effector molecule in the gastrointestinal tract. Proceedings of the National Academy of Sciences of the United States of America *101*, 13596-13600.
Assis, D.N., Leng, L., Du, X., Zhang, C.K., Grieb, G., Merk, M., Garcia, A.B., McCrann, C., Chapiro, J., Meinhardt, A.*, et al.* (2014). The role of macrophage migration inhibitory factor in autoimmune liver disease. Hepatology (Baltimore, Md.) *59*, 580-591.
Bain, C.C., and Mowat, A.M. (2014). Macrophages in intestinal homeostasis and inflammation. Immunological reviews *260*, 102-117.
Bancroft, A.J., McKenzie, A.N., and Grencis, R.K. (1998). A critical role for IL-13 in resistance to intestinal nematode infection. Journal of immunology (Baltimore, Md. : 1950) *160*, 3453-3461.
Bansemir, A.D., and Sukhdeo, M.V. (2001). Intestinal distribution of worms and host ingesta in Nippostrongylus brasiliensis. The Journal of parasitology *87*, 1470-1472.
Barron, L., Smith, A.M., El Kasmi, K.C., Qualls, J.E., Huang, X., Cheever, A., Borthwick, L.A., Wilson, M.S., Murray, P.J., and Wynn, T.A. (2013). Role of arginase 1 from myeloid cells in th2-dominated lung inflammation. PloS one *8*, e61961.
Bernhagen, J., Calandra, T., and Bucala, R. (1998). Regulation of the immune response by macrophage migration inhibitory factor: biological and structural features. Journal of molecular medicine (Berlin, Germany) *76*, 151-161.
Bernhagen, J., Krohn, R., Lue, H., Gregory, J.L., Zernecke, A., Koenen, R.R., Dewor, M., Georgiev, I., Schober, A., Leng, L.*, et al.* (2007). MIF is a noncognate ligand of

CXC chemokine receptors in inflammatory and atherogenic cell recruitment. Nature medicine *13*, 587-596.
Bernink, J.H., Peters, C.P., Munneke, M., te Velde, A.A., Meijer, S.L., Weijer, K., Hreggvidsdottir, H.S., Heinsbroek, S.E., Legrand, N., Buskens, C.J.*, et al.* (2013). Human type 1 innate lymphoid cells accumulate in inflamed mucosal tissues. Nature immunology *14*, 221-229.
Betts, C.J., and Else, K.J. (1999). Mast cells, eosinophils and antibody-mediated cellular cytotoxicity are not critical in resistance to Trichuris muris. Parasite immunology *21*, 45-52.
Bezencon, C., Furholz, A., Raymond, F., Mansourian, R., Metairon, S., Le Coutre, J., and Damak, S. (2008). Murine intestinal cells expressing Trpm5 are mostly brush cells and express markers of neuronal and inflammatory cells. The Journal of comparative neurology *509*, 514-525.
Bloom, B.R., and Bennett, B. (1966). Mechanism of a reaction in vitro associated with delayed-type hypersensitivity. Science (New York, N.Y.) *153*, 80-82.
Blum, A.M., Hang, L., Setiawan, T., Urban, J.P., Stoyanoff, K.M., Leung, J., and Weinstock, J.V. (2012). HELIGMOSOMOIDES BAKERI INDUCES TOLEROGENIC DENDRITIC CELLS THAT BLOCK COLITIS AND PREVENT ANTIGEN-SPECIFIC GUT T CELL RESPONSES. J Immunol *189*, 2512-2520.
Bonne-Annee, S., Kerepesi, L.A., Hess, J.A., O'Connell, A.E., Lok, J.B., Nolan, T.J., and Abraham, D. (2013). Human and mouse macrophages collaborate with neutrophils to kill larval Strongyloides stercoralis. Infection and immunity *81*, 3346-3355.
Bouchery, T., Denece, G., Attout, T., Ehrhardt, K., Lhermitte-Vallarino, N., Hachet-Haas, M., Galzi, J.L., Brotin, E., Bachelerie, F., Gavotte, L.*, et al.* (2012). The chemokine CXCL12 is essential for the clearance of the filaria Litomosoides sigmodontis in resistant mice. PloS one *7*, e34971.
Bouchery, T., Kyle, R., Camberis, M., Shepherd, A., Filbey, K., Smith, A., Harvie, M., Painter, G., Johnston, K., Ferguson, P.*, et al.* (2015). ILC2s and T cells cooperate to ensure maintenance of M2 macrophages for lung immunity against hookworms. Nature Communications *6*, 6970.
Bouchery, T., Kyle, R., Ronchese, F., and Le Gros, G. (2014). The Differentiation of CD4(+) T-Helper Cell Subsets in the Context of Helminth Parasite Infection. Frontiers in immunology *5*, 487.
Bozza, M., Satoskar, A.R., Lin, G., Lu, B., Humbles, A.A., Gerard, C., and David, J.R. (1999). Targeted disruption of migration inhibitory factor gene reveals its critical role in sepsis. The Journal of experimental medicine *189*, 341-346.
Broadhurst, M.J., Ardeshir, A., Kanwar, B., Mirpuri, J., Gundra, U.M., Leung, J.M., Wiens, K.E., Vujkovic-Cvijin, I., Kim, C.C., Yarovinsky, F.*, et al.* (2012). Therapeutic helminth infection of macaques with idiopathic chronic diarrhea alters the inflammatory signature and mucosal microbiota of the colon. PLoS pathogens *8*, e1003000.
Broadhurst, M.J., Leung, J.M., Kashyap, V., McCune, J.M., Mahadevan, U., McKerrow, J.H., and Loke, P. (2010). IL-22+ CD4+ T cells are associated with therapeutic trichuris trichiura infection in an ulcerative colitis patient. Science translational medicine *2*, 60ra88.

Bronte, V., Brandau, S., Chen, S.H., Colombo, M.P., Frey, A.B., Greten, T.F., Mandruzzato, S., Murray, P.J., Ochoa, A., Ostrand-Rosenberg, S.*, et al.* (2016). Recommendations for myeloid-derived suppressor cell nomenclature and characterization standards. Nature Communications *7*, 12150.
Bucala, R. (2012). The Mif Handbook (World Scientific).
Buck, A.H., Coakley, G., Simbari, F., McSorley, H.J., Quintana, J.F., Le Bihan, T., Kumar, S., Abreu-Goodger, C., Lear, M., Harcus, Y.*, et al.* Exosomes secreted by nematode parasites transfer small RNAs to mammalian cells and modulate innate immunity. Nature Communications *5*.
Buonocore, S., Ahern, P.P., Uhlig, H.H., Ivanov, II, Littman, D.R., Maloy, K.J., and Powrie, F. (2010). Innate lymphoid cells drive interleukin-23-dependent innate intestinal pathology. Nature *464*, 1371-1375.
Cadman, E.T., Thysse, K.A., Bearder, S., Cheung, A.Y., Johnston, A.C., Lee, J.J., and Lawrence, R.A. (2014). Eosinophils are important for protection, immunoregulation and pathology during infection with nematode microfilariae. PLoS pathogens *10*, e1003988.
Calandra, T., Bernhagen, J., Mitchell, R.A., and Bucala, R. (1994). The macrophage is an important and previously unrecognized source of macrophage migration inhibitory factor. The Journal of experimental medicine *179*, 1895-1902.
Calandra, T., Echtenacher, B., Roy, D.L., Pugin, J., Metz, C.N., Hultner, L., Heumann, D., Mannel, D., Bucala, R., and Glauser, M.P. (2000). Protection from septic shock by neutralization of macrophage migration inhibitory factor. Nature medicine *6*, 164-170.
Calandra, T., and Roger, T. (2003). Macrophage migration inhibitory factor: a regulator of innate immunity. Nature reviews. Immunology *3*, 791-800.
Camberis, M., Le Gros, G., and Urban, J., Jr. (2003). Animal model of Nippostrongylus brasiliensis and Heligmosomoides polygyrus. Current protocols in immunology *Chapter 19*, Unit 19.12.
Canavan, J.B., Scotta, C., Vossenkamper, A., Goldberg, R., Elder, M.J., Shoval, I., Marks, E., Stolarczyk, E., Lo, J.W., Powell, N.*, et al.* (2016). Developing in vitro expanded CD45RA+ regulatory T cells as an adoptive cell therapy for Crohn's disease. Gut *65*, 584-594.
Cançado, G.G., Fiuza, J.A., de Paiva, N.C., Lemos, L.D., Ricci, N.D., Gazzinelli-Guimarães, P.H., Martins, V.G., Bartholomeu, D.C., Negrão-Correa, D.A., Carneiro, C.M., and Fujiwara, R.T. (2011). Hookworm products ameliorate dextran sodium sulfate-induced colitis in BALB/c mice. Inflamm Bowel Dis *17*, 2275-2286.
Cardoso, V., Chesne, J., Ribeiro, H., Garcia-Cassani, B., Carvalho, T., Bouchery, T., Shah, K., Barbosa-Morais, N.L., Harris, N., and Veiga-Fernandes, H. (2017). Neuronal regulation of type 2 innate lymphoid cells via neuromedin U. Nature *549*, 277-281.
Cayrol, C., and Girard, J.P. (2018). Interleukin-33 (IL-33): A nuclear cytokine from the IL-1 family. Immunological reviews *281*, 154-168.
Chatterjee, S., Behnam Azad, B., and Nimmagadda, S. (2014). The intricate role of CXCR4 in cancer. Advances in cancer research *124*, 31-82.
Chen, C.Y., Lee, J.B., Liu, B., Ohta, S., Wang, P.Y., Kartashov, A.V., Mugge, L., Abonia, J.P., Barski, A., Izuhara, K.*, et al.* (2015). Induction of Interleukin-9-Producing

Mucosal Mast Cells Promotes Susceptibility to IgE-Mediated Experimental Food Allergy. Immunity *43*, 788-802.
Chen, F., Wu, W., Millman, A., Craft, J.F., Chen, E., Patel, N., Boucher, J.L., Urban, J.F., Kim, C.C., and Gause, W.C. (2014). Neutrophils prime a long-lived effector macrophage phenotype that mediates accelerated helminth expulsion. Nature immunology *15*, 938-946.
Chen, G., Wang, S.H., Jang, J.C., Odegaard, J.I., and Nair, M.G. (2016). Comparison of RELMalpha and RELMbeta Single- and Double-Gene-Deficient Mice Reveals that RELMalpha Expression Dictates Inflammation and Worm Expulsion in Hookworm Infection. Infection and immunity *84*, 1100-1111.
Cho, M.K., Lee, C.H., and Yu, H.S. (2011). Amelioration of intestinal colitis by macrophage migration inhibitory factor isolated from intestinal parasites through toll-like receptor 2. Parasite Immunol *33*, 265-275.
Chuang, T.Y., Chang, H.T., Chung, K.P., Cheng, H.S., Liu, C.Y., Liu, Y.C., Huang, H.H., Chou, T.C., Chang, B.L., Lee, M.R.*, et al.* (2014). High levels of serum macrophage migration inhibitory factor and interleukin 10 are associated with a rapidly fatal outcome in patients with severe sepsis. International journal of infectious diseases : IJID : official publication of the International Society for Infectious Diseases *20*, 13-17.
Cliffe, L.J., Humphreys, N.E., Lane, T.E., Potten, C.S., Booth, C., and Grencis, R.K. (2005). Accelerated intestinal epithelial cell turnover: a new mechanism of parasite expulsion. Science (New York, N.Y.) *308*, 1463-1465.
Coakley, G., McCaskill, J.L., Borger, J.G., Simbari, F., Robertson, E., Millar, M., Harcus, Y., McSorley, H.J., Maizels, R.M., and Buck, A.H. (2017). Extracellular Vesicles from a Helminth Parasite Suppress Macrophage Activation and Constitute an Effective Vaccine for Protective Immunity. Cell reports *19*, 1545-1557.
Cook, P.C., Jones, L.H., Jenkins, S.J., Wynn, T.A., Allen, J.E., and MacDonald, A.S. (2012). Alternatively activated dendritic cells regulate CD4+ T-cell polarization in vitro and in vivo. Proceedings of the National Academy of Sciences of the United States of America *109*, 9977-9982.
Coyle, A.J., Kohler, G., Tsuyuki, S., Brombacher, F., and Kopf, M. (1998). Eosinophils are not required to induce airway hyperresponsiveness after nematode infection. European journal of immunology *28*, 2640-2647.
Croft, A.M., Bager, P., and Kumar, S. (2012). Helminth therapy (worms) for allergic rhinitis. The Cochrane database of systematic reviews, Cd009238.
Damle, S.R., Martin, R.K., Cross, J.V., and Conrad, D.H. (2017). Macrophage migration inhibitory factor deficiency enhances immune response to Nippostrongylus brasiliensis. Mucosal immunology *10*, 205-214.
Das, R., Koo, M.S., Kim, B.H., Jacob, S.T., Subbian, S., Yao, J., Leng, L., Levy, R., Murchison, C., Burman, W.J.*, et al.* (2013). Macrophage migration inhibitory factor (MIF) is a critical mediator of the innate immune response to Mycobacterium tuberculosis. Proceedings of the National Academy of Sciences of the United States of America *110*, E2997-3006.

David, J.R. (1966). Delayed hypersensitivity in vitro: its mediation by cell-free substances formed by lymphoid cell-antigen interaction. Proceedings of the National Academy of Sciences of the United States of America *56*, 72-77.
Davies, L.C., Rosas, M., Jenkins, S.J., Liao, C.T., Scurr, M.J., Brombacher, F., Fraser, D.J., Allen, J.E., Jones, S.A., and Taylor, P.R. (2013). Distinct bone marrow-derived and tissue-resident macrophage lineages proliferate at key stages during inflammation. Nature Communications *4*, 1886.
de Souza, H.S., Tortori, C.A., Lintomen, L., Figueiredo, R.T., Bernardazzi, C., Leng, L., Bucala, R., Madi, K., Buongusto, F., Elia, C.C*., et al.* (2015). Macrophage migration inhibitory factor promotes eosinophil accumulation and tissue remodeling in eosinophilic esophagitis. Mucosal immunology *8*, 1154-1165.
Desreumaux, P., Foussat, A., Allez, M., Beaugerie, L., Hebuterne, X., Bouhnik, Y., Nachury, M., Brun, V., Bastian, H., Belmonte, N*., et al.* (2012). Safety and efficacy of antigen-specific regulatory T-cell therapy for patients with refractory Crohn's disease. Gastroenterology *143*, 1207-1217.e1201-1202.
Donskow-Łysoniewska, K., Majewski, P., Brodaczewska, K., Jowicka, K., and Doligalska, M. (2012). *Heligmosmoides polygyrus* fourth stages induce protection against DSS-induced colitis and change opioid expression in the intestine. Parasite Immunol *34*, 536-546.
Driss, V., El Nady, M., Delbeke, M., Rousseaux, C., Dubuquoy, C., Sarazin, A., Gatault, S., Dendooven, A., Riveau, G., Colombel, J.F*., et al.* (2016). The schistosome glutathione S-transferase P28GST, a unique helminth protein, prevents intestinal inflammation in experimental colitis through a Th2-type response with mucosal eosinophils. Mucosal immunology *9*, 322-335.
Eash, K.J., Greenbaum, A.M., Gopalan, P.K., and Link, D.C. (2010). CXCR2 and CXCR4 antagonistically regulate neutrophil trafficking from murine bone marrow. The Journal of clinical investigation *120*, 2423-2431.
Eberl, G., Colonna, M., Di Santo, J.P., and McKenzie, A.N. (2015). Innate lymphoid cells. Innate lymphoid cells: a new paradigm in immunology. Science (New York, N.Y.) *348*, aaa6566.
Economou, M., Trikalinos, T.A., Loizou, K.T., Tsianos, E.V., and Ioannidis, J.P. (2004). Differential effects of NOD2 variants on Crohn's disease risk and phenotype in diverse populations: a metaanalysis. The American journal of gastroenterology *99*, 2393-2404.
Elliott, D.E., Li, J., Blum, A., Metwali, A., Qadir, K., Urban, J.F., Jr., and Weinstock, J.V. (2003). Exposure to schistosome eggs protects mice from TNBS-induced colitis. Am J Physiol Gastrointest Liver Physiol *284*, G385-391.
Elliott, D.E., Setiawan, T., Metwali, A., Blum, A., Urban, J.F., Jr., and Weinstock, J.V. (2004). *Heligmosomoides polygyrus* inhibits established colitis in IL-10-deficient mice. European Journal of Immunology *34*, 2690-2698.
Elliott, D.E., and Weinstock, J.V. (2017). Nematodes and human therapeutic trials for inflammatory disease. Parasite immunology *39*.
Esser-von Bieren, J., Mosconi, I., Guiet, R., Piersgilli, A., Volpe, B., Chen, F., Gause, W.C., Seitz, A., Verbeek, J.S., and Harris, N.L. (2013). Antibodies Trap Tissue

Migrating Helminth Larvae and Prevent Tissue Damage by Driving IL-4Rα-Independent Alternative Differentiation of Macrophages. PLoS pathogens *9*.
Falcone, F.H., Loke, P., Zang, X., MacDonald, A.S., Maizels, R.M., and Allen, J.E. (2001). A Brugia malayi homolog of macrophage migration inhibitory factor reveals an important link between macrophages and eosinophil recruitment during nematode infection. Journal of immunology (Baltimore, Md. : 1950) *167*, 5348-5354.
Fallon, P.G., Ballantyne, S.J., Mangan, N.E., Barlow, J.L., Dasvarma, A., Hewett, D.R., McIlgorm, A., Jolin, H.E., and McKenzie, A.N. (2006). Identification of an interleukin (IL)-25-dependent cell population that provides IL-4, IL-5, and IL-13 at the onset of helminth expulsion. The Journal of experimental medicine *203*, 1105-1116.
Faulkner, H., Humphreys, N., Renauld, J.C., Van Snick, J., and Grencis, R. (1997). Interleukin-9 is involved in host protective immunity to intestinal nematode infection. European journal of immunology *27*, 2536-2540.
Ferreira, I., Smyth, D., Gaze, S., Aziz, A., Giacomin, P., Ruyssers, N., Artis, D., Laha, T., Navarro, S., Loukas, A., and McSorley, H.J. (2013). Hookworm excretory/secretory products induce interleukin-4 (IL-4)+ IL-10+ CD4+ T cell responses and suppress pathology in a mouse model of colitis. Infection and immunity *81*, 2104-2111.
Filbey, K., Bouchery, T., and Le Gros, G. (2018). The role of ILC2 in hookworm infection. Parasite immunology *40*.
Filbey, K.J., Grainger, J.R., Smith, K.A., Boon, L., van Rooijen, N., Harcus, Y., Jenkins, S., Hewitson, J.P., and Maizels, R.M. (2014). Innate and adaptive type 2 immune cell responses in genetically controlled resistance to intestinal helminth infection. Immunology and Cell Biology *92*, 436-448.
Finney, C.A.M., Taylor, M.D., Wilson, M.S., and Maizels, R.M. (2007). Expansion and activation of CD4+CD25+ regulatory T cells in Heligmosomoides polygyrus infection. European journal of immunology *37*, 1874-1886.
Fleming, J.O., and Weinstock, J.V. (2015). Clinical trials of helminth therapy in autoimmune diseases: rationale and findings. Parasite immunology *37*, 277-292.
Forgue-Lafitte, M.E., Fabiani, B., Levy, P.P., Maurin, N., Flejou, J.F., and Bara, J. (2007). Abnormal expression of M1/MUC5AC mucin in distal colon of patients with diverticulitis, ulcerative colitis and cancer. International journal of cancer *121*, 1543-1549.
Forrest, A.R., Kawaji, H., Rehli, M., Baillie, J.K., de Hoon, M.J., Haberle, V., Lassmann, T., Kulakovskiy, I.V., Lizio, M., Itoh, M.*, et al.* (2014). A promoter-level mammalian expression atlas. Nature *507*, 462-470.
Fujino, S., Andoh, A., Bamba, S., Ogawa, A., Hata, K., Araki, Y., Bamba, T., and Fujiyama, Y. (2003). Increased expression of interleukin 17 in inflammatory bowel disease. Gut *52*, 65-70.
Gao, Y., Nish, S.A., Jiang, R., Hou, L., Licona-Limon, P., Weinstein, J.S., Zhao, H., and Medzhitov, R. (2013). Control of T helper 2 responses by transcription factor IRF4-dependent dendritic cells. Immunity *39*, 722-732.
Gause, W.C., Wynn, T.A., and Allen, J.E. (2013). Type 2 immunity and wound healing: evolutionary refinement of adaptive immunity by helminths. Nature reviews. Immunology *13*, 607-614.

Gerbe, F., and Jay, P. (2016). Intestinal tuft cells: epithelial sentinels linking luminal cues to the immune system. Mucosal immunology *9*, 1353-1359.
Gerbe, F., Sidot, E., Smyth, D.J., Ohmoto, M., Matsumoto, I., Dardalhon, V., Cesses, P., Garnier, L., Pouzolles, M., Brulin, B.*, et al.* (2016). Intestinal epithelial tuft cells initiate type 2 mucosal immunity to helminth parasites. Nature *529*, 226-230.
Goldberg, R., Prescott, N., Lord, G.M., MacDonald, T.T., and Powell, N. (2015). The unusual suspects--innate lymphoid cells as novel therapeutic targets in IBD. Nature reviews. Gastroenterology & hepatology *12*, 271-283.
Grainger, J.R., Smith, K.A., Hewitson, J.P., McSorley, H.J., Harcus, Y., Filbey, K.J., Finney, C.A., Greenwood, E.J., Knox, D.P., Wilson, M.S.*, et al.* (2010). Helminth secretions induce de novo T cell Foxp3 expression and regulatory function through the TGF-β pathway. The Journal of experimental medicine *207*, 2331-2341.
Greenwald, R.J., Urban, J.F., Ekkens, M.J., Chen, S., Nguyen, D., Fang, H., Finkelman, F.D., Sharpe, A.H., and Gause, W.C. (1999). B7-2 is required for the progression but not the initiation of the type 2 immune response to a gastrointestinal nematode parasite. Journal of immunology (Baltimore, Md. : 1950) *162*, 4133-4139.
Grencis, R.K. (2015). Immunity to helminths: resistance, regulation, and susceptibility to gastrointestinal nematodes. Annual review of immunology *33*, 201-225.
Grencis, R.K., and Worthington, J.J. (2016). Tuft Cells: A New Flavor in Innate Epithelial Immunity. Trends in parasitology *32*, 583-585.
Gutcher, I., and Becher, B. (2007). APC-derived cytokines and T cell polarization in autoimmune inflammation. The Journal of clinical investigation *117*, 1119-1127.
Haber, A.L., Biton, M., Rogel, N., Herbst, R.H., Shekhar, K., Smillie, C., Burgin, G., Delorey, T.M., Howitt, M.R., Katz, Y.*, et al.* (2017). A single-cell survey of the small intestinal epithelium. Nature *551*, 333-339.
Hams, E., Armstrong, M.E., Barlow, J.L., Saunders, S.P., Schwartz, C., Cooke, G., Fahy, R.J., Crotty, T.B., Hirani, N., Flynn, R.J.*, et al.* (2014). IL-25 and type 2 innate lymphoid cells induce pulmonary fibrosis. Proceedings of the National Academy of Sciences of the United States of America *111*, 367-372.
Hang, L., Blum, A.M., Setiawan, T., Urban, J.P., Jr., Stoyanoff, K.M., and Weinstock, J.V. (2013). Heligmosomoides polygyrus bakeri infection activates colonic Foxp3+ T cells enhancing their capacity to prevent colitis. Journal of immunology (Baltimore, Md. : 1950) *191*, 1927-1934.
Hang, L., Setiawan, T., Blum, A.M., Urban, J., Stoyanoff, K., Arihiro, S., Reinecker, H.C., and Weinstock, J.V. (2010). *Heligmosomoides polygyrus* infection can inhibit colitis through direct interaction with innate immunity. J Immunol *185*, 3184-3189.
Harnett, M.M., Melendez, A.J., and Harnett, W. (2010). The therapeutic potential of the filarial nematode-derived immunodulator, ES-62 in inflammatory disease. Clinical and Experimental Immunology *159*, 256-267.
Harris, N., and Gause, W.C. (2011). To B or not to B: B cells and the Th2-type immune response to helminths. Trends in immunology *32*, 80-88.
Harris, N.L., and Loke, P. (2017). Recent Advances in Type-2-Cell-Mediated Immunity: Insights from Helminth Infection. Immunity *47*, 1024-1036.

Harvie, M., Camberis, M., Tang, S.C., Delahunt, B., Paul, W., and Le Gros, G. (2010). The Lung Is an Important Site for Priming CD4 T-Cell-Mediated Protective Immunity against Gastrointestinal Helminth Parasites ▿ ‡. Infection and immunity *78*, 3753-3762.
Hasnain, S.Z., Evans, C.M., Roy, M., Gallagher, A.L., Kindrachuk, K.N., Barron, L., Dickey, B.F., Wilson, M.S., Wynn, T.A., Grencis, R.K., and Thornton, D.J. (2011). Muc5ac: a critical component mediating the rejection of enteric nematodes. The Journal of experimental medicine *208*, 893-900.
Hasnain, S.Z., Wang, H., Ghia, J., Haq, N., Deng, Y., Velcich, A., Grencis, R.K., Thornton, D.J., and Khan, W.I. (2010). Mucin Gene Deficiency in Mice Impairs Host Resistance to an Enteric Parasitic Infection. Gastroenterology *138*, 1763-1771.e1765.
Heath, H., Qin, S., Rao, P., Wu, L., LaRosa, G., Kassam, N., Ponath, P.D., and Mackay, C.R. (1997). Chemokine receptor usage by human eosinophils. The importance of CCR3 demonstrated using an antagonistic monoclonal antibody. The Journal of clinical investigation *99*, 178-184.
Herbert, D.R., Yang, J.Q., Hogan, S.P., Groschwitz, K., Khodoun, M., Munitz, A., Orekov, T., Perkins, C., Wang, Q., Brombacher, F*., et al.* (2009). Intestinal epithelial cell secretion of RELM-beta protects against gastrointestinal worm infection. The Journal of experimental medicine *206*, 2947-2957.
Herndon, F.J., and Kayes, S.G. (1992). Depletion of eosinophils by anti-IL-5 monoclonal antibody treatment of mice infected with Trichinella spiralis does not alter parasite burden or immunologic resistance to reinfection. Journal of immunology (Baltimore, Md. : 1950) *149*, 3642-3647.
Hewitson, J.P., Filbey, K.J., Esser-von Bieren, J., Camberis, M., Schwartz, C., Murray, J., Reynolds, L.A., Blair, N., Robertson, E., Harcus, Y*., et al.* (2015). Concerted activity of IgG1 antibodies and IL-4/IL-25-dependent effector cells trap helminth larvae in the tissues following vaccination with defined secreted antigens, providing sterile immunity to challenge infection. PLoS pathogens *11*, e1004676.
Hewitson, J.P., Filbey, K.J., Grainger, J.R., Dowle, A.A., Pearson, M., Murray, J., Harcus, Y., and Maizels, R.M. (2011a). Heligmosomoides polygyrus elicits a dominant non-protective antibody response directed against restricted glycan and peptide epitopes. Journal of immunology (Baltimore, Md. : 1950) *187*, 4764-4777.
Hewitson, J.P., Harcus, Y., Murray, J., van Agtmaal, M., Filbey, K.J., Grainger, J.R., Bridgett, S., Blaxter, M.L., Ashton, P.D., Ashford, D*., et al.* (2011b). Proteomic analysis of secretory products from the model gastrointestinal nematode Heligmosomoides polygyrus reveals dominance of Venom Allergen-Like (VAL) proteins. Journal of proteomics *74*, 1573-1594.
Heylen, M., Ruyssers, N.E., De Man, J.G., Timmermans, J.P., Pelckmans, P.A., Moreels, T.G., and De Winter, B.Y. (2014). Worm Proteins of Schistosoma mansoni Reduce the Severity of Experimental Chronic Colitis in Mice by Suppressing Colonic Proinflammatory Immune Responses. PLoS One *9*, e110002.
Hotez, P.J., Brindley, P.J., Bethony, J.M., King, C.H., Pearce, E.J., and Jacobson, J. (2008). Helminth infections: the great neglected tropical diseases. The Journal of clinical investigation *118*, 1311-1321.

Hoyler, T., Klose, C.S., Souabni, A., Turqueti-Neves, A., Pfeifer, D., Rawlins, E.L., Voehringer, D., Busslinger, M., and Diefenbach, A. (2012). The transcription factor GATA-3 controls cell fate and maintenance of type 2 innate lymphoid cells. Immunity *37*, 634-648.
Humphreys, N.E., Xu, D., Hepworth, M.R., Liew, F.Y., and Grencis, R.K. (2008). IL-33, a potent inducer of adaptive immunity to intestinal nematodes. Journal of immunology (Baltimore, Md. : 1950) *180*, 2443-2449.
Hung, L.Y., Lewkowich, I.P., Dawson, L.A., Downey, J., Yang, Y., Smith, D.E., and Herbert, D.R. (2013). IL-33 drives biphasic IL-13 production for noncanonical Type 2 immunity against hookworms. Proceedings of the National Academy of Sciences of the United States of America *110*, 282-287.
Hunter, M.M., Wang, A., Hirota, C.L., and McKay, D.M. (2005a). Neutralizing anti-IL-10 antibody blocks the protective effect of tapeworm infection in a murine model of chemically induced colitis. Journal of immunology (Baltimore, Md. : 1950) *174*, 7368-7375.
Hunter, M.M., Wang, A., Hirota, C.L., and McKay, D.M. (2005b). Neutralizing anti-IL-10 antibody blocks the protective effect of tapeworm infection in a murine model of chemically induced colitis. J Immunol *174*, 7368-7375.
Hunter, M.M., Wang, A., Parhar, K.S., Johnston, M.J., Van Rooijen, N., Beck, P.L., and McKay, D.M. (2010a). In vitro-derived alternatively activated macrophages reduce colonic inflammation in mice. Gastroenterology *138*, 1395-1405.
Hunter, M.M., Wang, A., Parhar, K.S., Johnston, M.J.G., Van Rooijen, N., Beck, P.L., and McKay, D.M. (2010b). *In vitro*-derived alternatively activated macrophages reduce colonic inflammation in mice. Gastroenterology *138*, 1395-1405.
Hur, E.M., and Kim, K.T. (2002). G protein-coupled receptor signalling and cross-talk: achieving rapidity and specificity. Cellular signalling *14*, 397-405.
Isono, K., Fujimura, Y., Shinga, J., Yamaki, M., J, O.W., Takihara, Y., Murahashi, Y., Takada, Y., Mizutani-Koseki, Y., and Koseki, H. (2005). Mammalian Polyhomeotic Homologues Phc2 and Phc1 Act in Synergy To Mediate Polycomb Repression of Hox Genes. Molecular and Cellular Biology *25*, 6694-6706.
Jackson-Jones, L.H., Ruckerl, D., Svedberg, F., Duncan, S., Maizels, R.M., Sutherland, T.E., Jenkins, S.J., McSorley, H.J., Benezech, C., MacDonald, A.S., and Allen, J.E. (2016). IL-33 delivery induces serous cavity macrophage proliferation independent of interleukin-4 receptor alpha. European journal of immunology *46*, 2311-2321.
Jang, J.C., and Nair, M.G. (2013). Alternatively Activated Macrophages Revisited: New Insights into the Regulation of Immunity, Inflammation and Metabolic Function following Parasite Infection. Current immunology reviews *9*, 147-156.
Jang, S.W., Cho, M.K., Park, M.K., Kang, S.A., Na, B.-K., Ahn, S.C., Kim, D.-H., and Yu, H.S. (2011a). Parasitic helminth cystatin inhibits DSS-induced intestinal inflammation via IL-10^{+}F4/80^{+} macrophage recruitment. Korean J Parasitol *49*, 245-254.
Jang, S.W., Cho, M.K., Park, M.K., Kang, S.A., Na, B.K., Ahn, S.C., Kim, D.H., and Yu, H.S. (2011b). Parasitic helminth cystatin inhibits DSS-induced intestinal inflammation via IL-10(+)F4/80(+) macrophage recruitment. The Korean journal of parasitology *49*, 245-254.

Jarvi, O., and Keyrilainen, O. (1956). On the cellular structures of the epithelial invasions in the glandular stomach of mice caused by intramural application of 20-methylcholantren. Acta pathologica et microbiologica Scandinavica. Supplement *39*, 72-73.
Jenkins, S.J., Ruckerl, D., Thomas, G.D., Hewitson, J.P., Duncan, S., Brombacher, F., Maizels, R.M., Hume, D.A., and Allen, J.E. (2013). IL-4 directly signals tissue-resident macrophages to proliferate beyond homeostatic levels controlled by CSF-1. The Journal of experimental medicine *210*, 2477-2491.
Joeris, T., Muller-Luda, K., Agace, W.W., and Mowat, A.M. (2017). Diversity and functions of intestinal mononuclear phagocytes. Mucosal immunology *10*, 845-864.
Johnston, C.J.C., Robertson, E., Harcus, Y., Grainger, J.R., Coakley, G., Smyth, D.J., McSorley, H.J., and Maizels, R. (2015). Cultivation of Heligmosomoides Polygyrus: An Immunomodulatory Nematode Parasite and its Secreted Products. Journal of Visualized Experiments : JoVE.
Johnston, C.J.C., Smyth, D.J., Kodali, R.B., White, M.P.J., Harcus, Y., Filbey, K.J., Hewitson, J.P., Hinck, C.S., Ivens, A., Kemter, A.M*., et al.* (2017). A structurally distinct TGF-β mimic from an intestinal helminth parasite potently induces regulatory T cells. Nature Communications *8*.
Johnston, M.J., MacDonald, J.A., and McKay, D.M. (2009). Parasitic helminths: a pharmacopeia of anti-inflammatory molecules. Parasitology *136*, 125-147.
Juttner, S., Bernhagen, J., Metz, C.N., Rollinghoff, M., Bucala, R., and Gessner, A. (1998). Migration inhibitory factor induces killing of Leishmania major by macrophages: dependence on reactive nitrogen intermediates and endogenous TNF-alpha. Journal of immunology (Baltimore, Md. : 1950) *161*, 2383-2390.
Kanai, T., Uraushihara, K., Totsuka, T., Nemoto, Y., Fujii, R., Kawamura, T., Makita, S., Sawada, D., Yagita, H., Okumura, K., and Watanabe, M. (2006). Ameliorating effect of saporin-conjugated anti-CD11b monoclonal antibody in a murine T-cell-mediated chronic colitis. Journal of gastroenterology and hepatology *21*, 1136-1142.
Kaplan, M.H., Schindler, U., Smiley, S.T., and Grusby, M.J. (1996). Stat6 is required for mediating responses to IL-4 and for development of Th2 cells. Immunity *4*, 313-319.
Katoh, H., Wang, D., Daikoku, T., Sun, H., Dey, S.K., and Dubois, R.N. (2013). CXCR2-expressing myeloid-derived suppressor cells are essential to promote colitis-associated tumorigenesis. Cancer cell *24*, 631-644.
Khan, W.I., Blennerhasset, P.A., Varghese, A.K., Chowdhury, S.K., Omsted, P., Deng, Y., and Collins, S.M. (2002). Intestinal nematode infection ameliorates experimental colitis in mice. Infect Immun *70*, 5931-5937.
Khatri, V., Amdare, N., Tarnekar, A., Goswami, K., and Reddy, M.V. (2015a). Brugia malayi cystatin therapeutically ameliorates dextran sulfate sodium-induced colitis in mice. J Dig Dis *16*, 585-594.
Khatri, V., Amdare, N., Yadav, R.S., Tarnekar, A., Goswami, K., and Reddy, M.V. (2015b). Brugia malayi abundant larval transcript 2 protein treatment attenuates experimentally-induced colitis in mice. Indian J Exp Biol *53*, 732-739.

Kiesler, P., Fuss, I.J., and Strober, W. (2015). Experimental Models of Inflammatory Bowel Diseases. Cellular and molecular gastroenterology and hepatology *1*, 154-170.
Kim, B.S., Siracusa, M.C., Saenz, S.A., Noti, M., Monticelli, L.A., Sonnenberg, G.F., Hepworth, M.R., Van Voorhees, A.S., Comeau, M.R., and Artis, D. (2013). TSLP elicits IL-33-independent innate lymphoid cell responses to promote skin inflammation. Science translational medicine *5*, 170ra116.
Kim, J.Y., Cho, M.K., Choi, S.H., Lee, K.H., Ahn, S.C., Kim, D.-H., and Yu, H.S. (2010a). Inhibition of dextran sulfate sodium (DSS)-induced intestinal inflammation via enhanced IL-10 and TGF-β production by galectin-9 homologues isolated from intestinal parasites. Mol Biochem Parasitol *174*, 53-61.
Kim, J.Y., Cho, M.K., Choi, S.H., Lee, K.H., Ahn, S.C., Kim, D.H., and Yu, H.S. (2010b). Inhibition of dextran sulfate sodium (DSS)-induced intestinal inflammation via enhanced IL-10 and TGF-beta production by galectin-9 homologues isolated from intestinal parasites. Molecular and biochemical parasitology *174*, 53-61.
Kim, M.J., Kim, W.S., Kim, D.O., Byun, J.E., Huy, H., Lee, S.Y., Song, H.Y., Park, Y.J., Kim, T.D., Yoon, S.R*., et al.* (2017). Macrophage migration inhibitory factor interacts with thioredoxin-interacting protein and induces NF-kappaB activity. Cellular signalling *34*, 110-120.
Kim, Y.S., and Ho, S.B. (2010). Intestinal Goblet Cells and Mucins in Health and Disease: Recent Insights and Progress. Current Gastroenterology Reports *12*, 319-330.
Klose, C.S.N., Mahlakoiv, T., Moeller, J.B., Rankin, L.C., Flamar, A.L., Kabata, H., Monticelli, L.A., Moriyama, S., Putzel, G.G., Rakhilin, N*., et al.* (2017). The neuropeptide neuromedin U stimulates innate lymphoid cells and type 2 inflammation. Nature *549*, 282-286.
Knott, M.L., Matthaei, K.I., Giacomin, P.R., Wang, H., Foster, P.S., and Dent, L.A. (2007). Impaired resistance in early secondary Nippostrongylus brasiliensis infections in mice with defective eosinophilopoeisis. International journal for parasitology *37*, 1367-1378.
Kobayashi, S., Satomura, K., Levsky, J.M., Sreenath, T., Wistow, G.J., Semba, I., Shum, L., Slavkin, H.C., and Kulkarni, A.B. (1999). Expression pattern of macrophage migration inhibitory factor during embryogenesis. Mechanisms of development *84*, 153-156.
Koebernick, H., Grode, L., David, J.R., Rohde, W., Rolph, M.S., Mittrucker, H.W., and Kaufmann, S.H. (2002). Macrophage migration inhibitory factor (MIF) plays a pivotal role in immunity against Salmonella typhimurium. Proceedings of the National Academy of Sciences of the United States of America *99*, 13681-13686.
Koyama, K., Tamauchi, H., and Ito, Y. (1995). The role of CD4+ and CD8+ T cells in protective immunity to the murine nematode parasite Trichuris muris. Parasite immunology *17*, 161-165.
Kozak, C.A., Adamson, M.C., Buckler, C.E., Segovia, L., Paralkar, V., and Wistow, G. (1995). Genomic cloning of mouse MIF (macrophage inhibitory factor) and genetic mapping of the human and mouse expressed gene and nine mouse pseudogenes. Genomics *27*, 405-411.

Kraemer, S., Lue, H., Zernecke, A., Kapurniotu, A., Andreetto, E., Frank, R., Lennartz, B., Weber, C., and Bernhagen, J. (2011). MIF-chemokine receptor interactions in atherogenesis are dependent on an N-loop-based 2-site binding mechanism. FASEB journal : official publication of the Federation of American Societies for Experimental Biology *25*, 894-906.
Kron, M.A., Metwali, A., Vodanovic-Jankovic, S., and Elliott, D. (2013). Nematode asparaginyl-tRNA synthetase resolves intestinal inflammation in mice with T-cell transfer colitis. Clin Vaccine Immunol *20*, 276-281.
Lee, G.R., Fields, P.E., and Flavell, R.A. (2001). Regulation of IL-4 gene expression by distal regulatory elements and GATA-3 at the chromatin level. Immunity *14*, 447-459.
Leng, L., Metz, C.N., Fang, Y., Xu, J., Donnelly, S., Baugh, J., Delohery, T., Chen, Y., Mitchell, R.A., and Bucala, R. (2003). MIF signal transduction initiated by binding to CD74. The Journal of experimental medicine *197*, 1467-1476.
Leng, L., Wang, W., Roger, T., Merk, M., Wuttke, M., Calandra, T., and Bucala, R. (2009). Glucocorticoid-induced MIF Expression by Human CEM T cells. Cytokine *48*, 177-185.
Leung, J., Hang, L., Blum, A., Setiawan, T., Stoyanoff, K., and Weinstock, J. (2012). *Heligmosomoides polygyrus* abrogates antigen-specific gut injury in a murine model of inflammatory bowel disease. Inflamm Bowel Dis.
Licona-Limon, P., Henao-Mejia, J., Temann, A.U., Gagliani, N., Licona-Limon, I., Ishigame, H., Hao, L., Herbert, D.R., and Flavell, R.A. (2013). Th9 Cells Drive Host Immunity against Gastrointestinal Worm Infection. Immunity *39*, 744-757.
Liu, Q., Kreider, T., Bowdridge, S., Liu, Z., Song, Y., Gaydo, A.G., Urban, J.F., and Gause, W.C. (2010). B Cells Have Distinct Roles in Host Protection against Different Nematode Parasites. Journal of immunology (Baltimore, Md. : 1950) *184*, 5213-5223.
Liu, Y.J., Soumelis, V., Watanabe, N., Ito, T., Wang, Y.H., Malefyt Rde, W., Omori, M., Zhou, B., and Ziegler, S.F. (2007). TSLP: an epithelial cell cytokine that regulates T cell differentiation by conditioning dendritic cell maturation. Annual review of immunology *25*, 193-219.
Loser, S., and Maizels, R.M. (2018). Immunology: The Neuronal Pathway to Mucosal Immunity. Current biology : CB *28*, R33-r36.
Lue, H., Kapurniotu, A., Fingerle-Rowson, G., Roger, T., Leng, L., Thiele, M., Calandra, T., Bucala, R., and Bernhagen, J. (2006). Rapid and transient activation of the ERK MAPK signalling pathway by macrophage migration inhibitory factor (MIF) and dependence on JAB1/CSN5 and Src kinase activity. Cellular signalling *18*, 688-703.
MacDonald, A.S., and Maizels, R.M. (2008). Alarming dendritic cells for Th2 induction. The Journal of experimental medicine *205*, 13-17.
Magalhaes, E.S., Paiva, C.N., Souza, H.S., Pyrrho, A.S., Mourao-Sa, D., Figueiredo, R.T., Vieira-de-Abreu, A., Dutra, H.S., Silveira, M.S., Gaspar-Elsas, M.I.*, et al.* (2009). Macrophage migration inhibitory factor is critical to interleukin-5-driven eosinophilopoiesis and tissue eosinophilia triggered by Schistosoma mansoni infection. FASEB journal : official publication of the Federation of American Societies for Experimental Biology *23*, 1262-1271.

Maier, E., Duschl, A., and Horejs-Hoeck, J. (2012). STAT6-dependent and -independent mechanisms in Th2 polarization. European journal of immunology *42*, 2827-2833.
Maizels, R.M., and McSorley, H.J. (2016). Regulation of the host immune system by helminth parasites. The Journal of allergy and clinical immunology *138*, 666-675.
Maizels, R.M., McSorley, H.J., and Smyth, D.J. (2014). Helminths in the hygiene hypothesis: sooner or later? Clinical and Experimental Immunology *177*, 38-46.
Maizels, R.M., and Yazdanbakhsh, M. (2003). Immune regulation by helminth parasites: cellular and molecular mechanisms. Nature reviews. Immunology *3*, 733-744.
Marsland, B.J., Kurrer, M., Reissmann, R., Harris, N.L., and Kopf, M. (2008). Nippostrongylus brasiliensis infection leads to the development of emphysema associated with the induction of alternatively activated macrophages. European journal of immunology *38*, 479-488.
Martinez Rodriguez, N.R., Eloi, M.D., Huynh, A., Dominguez, T., Lam, A.H.C., Carcamo-Molina, D., Naser, Z., Desharnais, R., Salzman, N.H., and Porter, E. (2012). Expansion of Paneth Cell Population in Response to Enteric Salmonella enterica Serovar Typhimurium Infection. Infection and immunity *80*, 266-275.
Massacand, J.C., Stettler, R.C., Meier, R., Humphreys, N.E., Grencis, R.K., Marsland, B.J., and Harris, N.L. (2009). Helminth products bypass the need for TSLP in Th2 immune responses by directly modulating dendritic cell function. Proceedings of the National Academy of Sciences of the United States of America *106*, 13968-13973.
Matisz, C.E., Leung, G., Reyes, J.L., Wang, A., Sharkey, K.A., and McKay, D.M. (2015). Adoptive transfer of helminth antigen-pulsed dendritic cells protects against the development of experimental colitis in mice. European journal of immunology *45*, 3126-3139.
Mayer, J.U., Demiri, M., Agace, W.W., MacDonald, A.S., Svensson-Frej, M., and Milling, S.W. (2017). Different populations of CD11b(+) dendritic cells drive Th2 responses in the small intestine and colon. Nature Communications *8*, 15820.
McCoy, K.D., Stoel, M., Stettler, R., Merky, P., Fink, K., Senn, B.M., Schaer, C., Massacand, J., Odermatt, B., Oettgen, H.C*., et al.* (2008). Polyclonal and specific antibodies mediate protective immunity against enteric helminth infection. Cell host & microbe *4*, 362-373.
McDermott, J.R., Bartram, R.E., Knight, P.A., Miller, H.R., Garrod, D.R., and Grencis, R.K. (2003). Mast cells disrupt epithelial barrier function during enteric nematode infection. Proceedings of the National Academy of Sciences of the United States of America *100*, 7761-7766.
McKenzie, A.N.J., Spits, H., and Eberl, G. (2014). Innate lymphoid cells in inflammation and immunity. Immunity *41*, 366-374.
McSorley, H.J., Harcus, Y.M., Murray, J., Taylor, M.D., and Maizels, R.M. (2008). Expansion of Foxp3+ regulatory T cells in mice infected with the filarial parasite Brugia malayi. Journal of immunology (Baltimore, Md. : 1950) *181*, 6456-6466.
McSorley, H.J., Hewitson, J.P., and Maizels, R.M. (2013). Immunomodulation by helminth parasites: defining mechanisms and mediators. International journal for parasitology *43*, 301-310.

Metwali, A., Setiawan, T., Blum, A.M., Urban, J., Elliott, D.E., Hang, L., and Weinstock, J.V. (2006). Induction of $CD8^+$ regulatory T cells in the intestine by *Heligmosomoides polygyrus* infection. Am J Physiol Gastrointest Liver Physiol *291*, G253-259.
Minutti, C.M., Drube, S., Blair, N., Schwartz, C., McCrae, J.C., McKenzie, A.N., Kamradt, T., Mokry, M., Coffer, P.J., Sibilia, M.*, et al.* (2017a). Epidermal Growth Factor Receptor Expression Licenses Type-2 Helper T Cells to Function in a T Cell Receptor-Independent Fashion. Immunity *47*, 710-722.e716.
Minutti, C.M., Jackson-Jones, L.H., Garcia-Fojeda, B., Knipper, J.A., Sutherland, T.E., Logan, N., Ringqvist, E., Guillamat-Prats, R., Ferenbach, D.A., Artigas, A.*, et al.* (2017b). Local amplifiers of IL-4Ralpha-mediated macrophage activation promote repair in lung and liver. Science (New York, N.Y.) *356*, 1076-1080.
Mo, H.M., Liu, W.Q., Lei, J.H., Cheng, Y.L., Wang, C.Z., and Li, Y.L. (2007). Schistosoma japonicum eggs modulate the activity of CD4+ CD25+ Tregs and prevent development of colitis in mice. Exp Parasitol *116*, 385-389.
Molodecky, N.A., Soon, I.S., Rabi, D.M., Ghali, W.A., Ferris, M., Chernoff, G., Benchimol, E.I., Panaccione, R., Ghosh, S., Barkema, H.W., and Kaplan, G.G. (2012). Increasing incidence and prevalence of the inflammatory bowel diseases with time, based on systematic review. Gastroenterology *142*, 46-54.e42; quiz e30.
Mombaerts, P., Iacomini, J., Johnson, R.S., Herrup, K., Tonegawa, S., and Papaioannou, V.E. (1992). RAG-1-deficient mice have no mature B and T lymphocytes. Cell *68*, 869-877.
Monticelli, L.A., Sonnenberg, G.F., Abt, M.C., Alenghat, T., Ziegler, C.G., Doering, T.A., Angelosanto, J.M., Laidlaw, B.J., Yang, C.Y., Sathaliyawala, T.*, et al.* (2011). Innate lymphoid cells promote lung tissue homeostasis following acute influenza virus infection. Nature immunology *12*, 1045-1054.
Moreels, T.G., Nieuwendijk, R.J., De Man, J.G., De Winter, B.Y., Herman, A.G., Van Marck, E.A., and Pelckmans, P.A. (2004). Concurrent infection with *Schistosoma mansoni* attenuates inflammation induced changes in colonic morphology, cytokine levels, and smooth muscle contractility of trinitrobenzene sulphonic acid induced colitis in rats. Gut *53*, 99-107.
Motomura, Y., Wang, H., Deng, Y., El-Sharkawy, R.T., Verdu, E.F., and Khan, W.I. (2009). Helminth antigen-based strategy to ameliorate inflammation in an experimental model of colitis. Clin Exp Immunol *155*, 88-95.
Munitz, A., Cole, E.T., Karo-Atar, D., Finkelman, F.D., and Rothenberg, M.E. (2012). Resistin-Like Molecule–α Regulates IL-13–Induced Chemokine Production but Not Allergen-Induced Airway Responses. American Journal of Respiratory Cell and Molecular Biology *46*, 703-713.
Munitz, A., Waddell, A., Seidu, L., Cole, E.T., Ahrens, R., Hogan, S.P., and Rothenberg, M.E. (2008). Resistin-like molecule alpha enhances myeloid cell activation and promotes colitis. The Journal of allergy and clinical immunology *122*, 1200-1207.e1201.
Muromoto, R., Sekine, Y., Imoto, S., Ikeda, O., Okayama, T., Sato, N., and Matsuda, T. (2008). BART is essential for nuclear retention of STAT3. International immunology *20*, 395-403.

Nair, M.G., Du, Y., Perrigoue, J.G., Zaph, C., Taylor, J.J., Goldschmidt, M., Swain, G.P., Yancopoulos, G.D., Valenzuela, D.M., Murphy, A.*, et al.* (2009). Alternatively activated macrophage-derived RELM-{alpha} is a negative regulator of type 2 inflammation in the lung. The Journal of experimental medicine *206*, 937-952.
Nair, M.G., Guild, K.J., and Artis, D. (2006). Novel effector molecules in type 2 inflammation: lessons drawn from helminth infection and allergy. Journal of immunology (Baltimore, Md. : 1950) *177*, 1393-1399.
Nair, M.G., Guild, K.J., Du, Y., Zaph, C., Yancopoulos, G.D., Valenzuela, D.M., Murphy, A., Stevens, S., Karow, M., and Artis, D. (2008). Goblet cell-derived resistin-like molecule beta augments CD4+ T cell production of IFN-gamma and infection-induced intestinal inflammation. Journal of immunology (Baltimore, Md. : 1950) *181*, 4709-4715.
Nausch, N., and Mutapi, F. (2018). Group 2 ILCs: A way of enhancing immune protection against human helminths? Parasite immunology *40*.
Neill, D.R., Wong, S.H., Bellosi, A., Flynn, R.J., Daly, M., Langford, T.K., Bucks, C., Kane, C.M., Fallon, P.G., Pannell, R.*, et al.* (2010). Nuocytes represent a new innate effector leukocyte that mediates type-2 immunity. Nature *464*, 1367-1370.
Ni, J., Wu, G.D., Albenberg, L., and Tomov, V.T. (2017). Gut microbiota and IBD: causation or correlation? Nature reviews. Gastroenterology & hepatology *14*, 573-584.
Nussbaum, J.C., Van Dyken, S.J., von Moltke, J., Cheng, L.E., Mohapatra, A., Molofsky, A.B., Thornton, E.E., Krummel, M.F., Chawla, A., Liang, H.E., and Locksley, R.M. (2013). Type 2 innate lymphoid cells control eosinophil homeostasis. Nature *502*, 245-248.
Oeser, K., Schwartz, C., and Voehringer, D. (2015). Conditional IL-4/IL-13-deficient mice reveal a critical role of innate immune cells for protective immunity against gastrointestinal helminths. Mucosal immunology *8*, 672-682.
Oliphant, C.J., Barlow, J.L., and McKenzie, A.N. (2011). Insights into the initiation of type 2 immune responses. Immunology *134*, 378-385.
Oliphant, C.J., Hwang, Y.Y., Walker, J.A., Salimi, M., Wong, S.H., Brewer, J.M., Englezakis, A., Barlow, J.L., Hams, E., Scanlon, S.T.*, et al.* (2014). MHCII-mediated dialog between group 2 innate lymphoid cells and CD4(+) T cells potentiates type 2 immunity and promotes parasitic helminth expulsion. Immunity *41*, 283-295.
Osbourn, M., Soares, D.C., Vacca, F., Cohen, E.S., Scott, I.C., Gregory, W.F., Smyth, D.J., Toivakka, M., Kemter, A.M., le Bihan, T.*, et al.* (2017a). HpARI Protein Secreted by a Helminth Parasite Suppresses Interleukin-33. Immunity *47*, 739-751.e735.
Osbourn, M., Soares, D.C., Vacca, F., Cohen, E.S., Scott, I.C., Gregory, W.F., Smyth, D.J., Toivakka, M., Kemter, A.M., le Bihan, T.*, et al.* (2017b). HpARI Protein Secreted by a Helminth Parasite Suppresses Interleukin-33. Immunity *47*, 739-751.e735.
Ouyang, W., Lohning, M., Gao, Z., Assenmacher, M., Ranganath, S., Radbruch, A., and Murphy, K.M. (2000). Stat6-independent GATA-3 autoactivation directs IL-4-independent Th2 development and commitment. Immunity *12*, 27-37.
Ouyang, W., Ranganath, S.H., Weindel, K., Bhattacharya, D., Murphy, T.L., Sha, W.C., and Murphy, K.M. (1998). Inhibition of Th1 development mediated by GATA-3 through an IL-4-independent mechanism. Immunity *9*, 745-755.

Owyang, A.M., Zaph, C., Wilson, E.H., Guild, K.J., McClanahan, T., Miller, H.R., Cua, D.J., Goldschmidt, M., Hunter, C.A., Kastelein, R.A., and Artis, D. (2006). Interleukin 25 regulates type 2 cytokine-dependent immunity and limits chronic inflammation in the gastrointestinal tract. The Journal of experimental medicine *203*, 843-849.
Pastrana, D.V., Raghavan, N., FitzGerald, P., Eisinger, S.W., Metz, C., Bucala, R., Schleimer, R.P., Bickel, C., and Scott, A.L. (1998). Filarial nematode parasites secrete a homologue of the human cytokine macrophage migration inhibitory factor. Infection and immunity *66*, 5955-5963.
Patel, N., Kreider, T., Urban, J.F., and Gause, W.C. (2009). Characterization of effector mechanisms at the host:parasite interface during the immune response to tissue-dwelling intestinal nematode parasites. International journal for parasitology *39*, 13-21.
Pelly, V.S., Kannan, Y., Coomes, S.M., Entwistle, L.J., Ruckerl, D., Seddon, B., MacDonald, A.S., McKenzie, A., and Wilson, M.S. (2016). IL-4-producing ILC2s are required for the differentiation of TH2 cells following Heligmosomoides polygyrus infection. Mucosal immunology *9*, 1407-1417.
Pentilla, I.A., Ey, P.L., Lopez, A.F., and Jenkin, C.R. (1985). Suppression of early immunity to Nematospiroides dubius in mice by selective depletion of neutrophils with monoclonal antibody. The Australian journal of experimental biology and medical science *63 (Pt 5)*, 531-543.
Pesce, J.T., Ramalingam, T.R., Mentink-Kane, M.M., Wilson, M.S., El Kasmi, K.C., Smith, A.M., Thompson, R.W., Cheever, A.W., Murray, P.J., and Wynn, T.A. (2009a). Arginase-1–Expressing Macrophages Suppress Th2 Cytokine–Driven Inflammation and Fibrosis. PLoS pathogens *5*.
Pesce, J.T., Ramalingam, T.R., Wilson, M.S., Mentink-Kane, M.M., Thompson, R.W., Cheever, A.W., Urban, J.F., and Wynn, T.A. (2009b). Retnla (Relmα/Fizz1) Suppresses Helminth-Induced Th2-Type Immunity. PLoS pathogens *5*.
Powrie, F., Leach, M.W., Mauze, S., Caddle, L.B., and Coffman, R.L. (1993). Phenotypically distinct subsets of CD4+ T cells induce or protect from chronic intestinal inflammation in C. B-17 scid mice. International immunology *5*, 1461-1471.
Price, A.E., Liang, H.E., Sullivan, B.M., Reinhardt, R.L., Eisley, C.J., Erle, D.J., and Locksley, R.M. (2010). Systemically dispersed innate IL-13-expressing cells in type 2 immunity. Proceedings of the National Academy of Sciences of the United States of America *107*, 11489-11494.
Prieto-Lafuente, L., Gregory, W.F., Allen, J.E., and Maizels, R.M. (2009). MIF homologues from a filarial nematode parasite synergize with IL-4 to induce alternative activation of host macrophages. Journal of leukocyte biology *85*, 844-854.
Pullan, R.L., Smith, J.L., Jasrasaria, R., and Brooker, S.J. (2014). Global numbers of infection and disease burden of soil transmitted helminth infections in 2010. Parasites & vectors *7*, 37.
Raghuwanshi, S.K., Su, Y., Singh, V., Hayes, K., Richmond, A., and Richardson, R.M. (2012). The chemokine receptors CXCR1 and CXCR2 couple to distinct G protein-

coupled receptor kinases to mediate and regulate leukocyte functions. Journal of immunology (Baltimore, Md. : 1950) *189*, 2824-2832.
Rausch, S., Huehn, J., Kirchhoff, D., Rzepecka, J., Schnoeller, C., Pillai, S., Loddenkemper, C., Scheffold, A., Hamann, A., Lucius, R., and Hartmann, S. (2008). Functional analysis of effector and regulatory T cells in a parasitic nematode infection. Infection and immunity *76*, 1908-1919.
Reyes, J.L., Fernando, M.R., Lopes, F., Leung, G., Mancini, N.L., Matisz, C.E., Wang, A., and McKay, D.M. (2016a). IL-22 Restrains Tapeworm-Mediated Protection against Experimental Colitis via Regulation of IL-25 Expression. PLoS Pathog *12*, e1005481.
Reyes, J.L., Lopes, F., Leung, G., Mancini, N.L., Matisz, C.E., Wang, A., Thomson, E.A., Graves, N., Gilleard, J., and McKay, D.M. (2016b). Treatment with cestode parasite antigens recruits CCR2+ myeloid cells, the adoptive transfer of which ameliorates colitis. Infection and immunity.
Reynolds, L.A., Filbey, K.J., and Maizels, R.M. (2012). Immunity to the model intestinal helminth parasite Heligmosomoides polygyrus. Seminars in immunopathology *34*, 829-846.
Rhodin, J., and Dalhamn, T. (1956). Electron microscopy of the tracheal ciliated mucosa in rat. Zeitschrift fur Zellforschung und mikroskopische Anatomie (Vienna, Austria : 1948) *44*, 345-412.
Rodriguez, P.C., Ochoa, A.C., and Al-Khami, A.A. (2017). Arginine Metabolism in Myeloid Cells Shapes Innate and Adaptive Immunity. Frontiers in immunology *8*.
Rodriguez-Sosa, M., Rosas, L.E., David, J.R., Bojalil, R., Satoskar, A.R., and Terrazas, L.I. (2003). Macrophage migration inhibitory factor plays a critical role in mediating protection against the helminth parasite Taenia crassiceps. Infection and immunity *71*, 1247-1254.
Roger, T., David, J., Glauser, M.P., and Calandra, T. (2001). MIF regulates innate immune responses through modulation of Toll-like receptor 4. Nature *414*, 920-924.
Rossi, A.G., Haslett, C., Hirani, N., Greening, A.P., Rahman, I., Metz, C.N., Bucala, R., and Donnelly, S.C. (1998). Human circulating eosinophils secrete macrophage migration inhibitory factor (MIF). Potential role in asthma. The Journal of clinical investigation *101*, 2869-2874.
Ruyssers, N.E., De Winter, B.Y., De Man, J.G., Loukas, A., Pearson, M.S., Weinstock, J.V., Van den Bossche, R.M., Martinet, W., Pelckmans, P.A., and Moreels, T.G. (2009). Therapeutic potential of helminth soluble proteins in TNBS-induced colitis in mice. Inflamm Bowel Dis *15*, 491-500.
Salas, A., and Panes, J. (2015). IBD. Regulatory T cells for treatment of Crohn's disease. Nature reviews. Gastroenterology & hepatology *12*, 315-316.
Sato, A., Uinuk-ool, T.S., Kuroda, N., Mayer, W.E., Takezaki, N., Dongak, R., Figueroa, F., Cooper, M.D., and Klein, J. (2003). Macrophage migration inhibitory factor (MIF) of jawed and jawless fishes: implications for its evolutionary origin. Developmental and comparative immunology *27*, 401-412.
Schiopu, A., and Cotoi, O.S. (2013). S100A8 and S100A9: DAMPs at the crossroads between innate immunity, traditional risk factors, and cardiovascular disease. Mediators of inflammation *2013*, 828354.

Schuh, J.M., Blease, K., and Hogaboam, C.M. (2002). CXCR2 is necessary for the development and persistence of chronic fungal asthma in mice. Journal of immunology (Baltimore, Md. : 1950) *168*, 1447-1456.
Schwartz, C., Khan, A.R., Floudas, A., Saunders, S.P., Hams, E., Rodewald, H.R., McKenzie, A.N.J., and Fallon, P.G. (2017). ILC2s regulate adaptive Th2 cell functions via PD-L1 checkpoint control. The Journal of experimental medicine *214*, 2507-2521.
Setiawan, T., Metwali, A., Blum, A.M., Ince, M.N., Urban, J.F., Jr., Elliott, D.E., and Weinstock, J.V. (2007a). Heligmosomoides polygyrus promotes regulatory T-cell cytokine production in the murine normal distal intestine. Infection and immunity *75*, 4655-4663.
Setiawan, T., Metwali, A., Blum, A.M., Ince, M.N., Urban, J.F., Jr., Elliott, D.E., and Weinstock, J.V. (2007b). *Heligmosomoides polygyrus* promotes regulatory T-cell cytokine production in the murine normal distal intestine. Infect Immun *75*, 4655-4663.
Shaw, T.N., Houston, S.A., Wemyss, K., Bridgeman, H.M., Barbera, T.A., Zangerle-Murray, T., Strangward, P., Ridley, A.J.L., Wang, P., Tamoutounour, S*., et al.* (2018). Tissue-resident macrophages in the intestine are long lived and defined by Tim-4 and CD4 expression. The Journal of experimental medicine *215*, 1507-1518.
Shepherd, C., Navarro, S., Wangchuk, P., Wilson, D., Daly, N.L., and Loukas, A. (2015). Identifying the immunomodulatory components of helminths. Parasite immunology *37*, 293-303.
Sher, A., Coffman, R.L., Hieny, S., Scott, P., and Cheever, A.W. (1990). Interleukin 5 is required for the blood and tissue eosinophilia but not granuloma formation induced by infection with Schistosoma mansoni. Proceedings of the National Academy of Sciences of the United States of America *87*, 61-65.
Shin, E.H., Osada, Y., Sagara, H., Takatsu, K., and Kojima, S. (2001). Involvement of complement and fibronectin in eosinophil-mediated damage to Nippostrongylus brasiliensis larvae. Parasite immunology *23*, 27-37.
Shomer, N.H., Dangler, C.A., Marini, R.P., and Fox, J.G. (1998). Helicobacter bilis/Helicobacter rodentium co-infection associated with diarrhea in a colony of scid mice. Laboratory animal science *48*, 455-459.
Shouval, D.S., Biswas, A., Goettel, J.A., McCann, K., Conaway, E., Redhu, N.S., Mascanfroni, I.D., Al Adham, Z., Lavoie, S., Ibourk, M*., et al.* (2014). Interleukin-10 receptor signaling in innate immune cells regulates mucosal immune tolerance and anti-inflammatory macrophage function. Immunity *40*, 706-719.
Smith, K.A., Filbey, K.J., Reynolds, L.A., Hewitson, J.P., Harcus, Y., Boon, L., Sparwasser, T., Hammerling, G., and Maizels, R.M. (2016). Low-level regulatory T-cell activity is essential for functional type-2 effector immunity to expel gastrointestinal helminths. Mucosal immunology *9*, 428-443.
Smith, K.A., Loser, S., Varyani, F., Harcus, Y., McSorley, H.J., McKenzie, A.N., and Maizels, R.M. (2018). Concerted IL-25R and IL-4Ralpha signaling drive innate type 2 effector immunity for optimal helminth expulsion. eLife *7*.
Smith, P., Mangan, N.E., Walsh, C.M., Fallon, R.E., McKenzie, A.N.J., van Rooijen, N., and Fallon, P.G. (2007). Infection with a helminth parasite prevents experimental colitis via a macrophage-mediated mechanism. J Immunol *178*, 4557-4566.

Sorobetea, D., Svensson-Frej, M., and Grencis, R. (2018). Immunity to gastrointestinal nematode infections. Mucosal immunology.
Stadtmann, A., and Zarbock, A. (2012). CXCR2: From Bench to Bedside. Frontiers in immunology *3*, 263.
Strachan, D.P. (1989). Hay fever, hygiene, and household size. BMJ : British Medical Journal *299*, 1259-1260.
Stutz, A.M., Pickart, L.A., Trifilieff, A., Baumruker, T., Prieschl-Strassmayr, E., and Woisetschlager, M. (2003). The Th2 cell cytokines IL-4 and IL-13 regulate found in inflammatory zone 1/resistin-like molecule alpha gene expression by a STAT6 and CCAAT/enhancer-binding protein-dependent mechanism. Journal of immunology (Baltimore, Md. : 1950) *170*, 1789-1796.
Sutherland, T.E., Logan, N., Rückerl, D., Humbles, A.A., Allan, S.M., Papayannopoulos, V., Stockinger, B., Maizels, R.M., and Allen, J.E. (2014). Chitinase-like proteins promote IL-17-mediated neutrophilia in a trade-off between nematode killing and host damage. Nature immunology *15*, 1116-1125.
Sutton, T.L., Zhao, A., Madden, K.B., Elfrey, J.E., Tuft, B.A., Sullivan, C.A., Urban, J.F., Jr., and Shea-Donohue, T. (2008a). Anti-Inflammatory mechanisms of enteric Heligmosomoides polygyrus infection against trinitrobenzene sulfonic acid-induced colitis in a murine model. Infect Immun *76*, 4772-4782.
Sutton, T.L., Zhao, A., Madden, K.B., Elfrey, J.E., Tuft, B.A., Sullivan, C.A., Urban, J.F., Jr., and Shea-Donohue, T. (2008b). Anti-Inflammatory mechanisms of enteric *Heligmosomoides polygyrus* infection against trinitrobenzene sulfonic acid-induced colitis in a murine model. Infect Immun *76*, 4772-4782.
Svetic, A., Madden, K.B., Zhou, X.D., Lu, P., Katona, I.M., Finkelman, F.D., Urban, J.F., Jr., and Gause, W.C. (1993). A primary intestinal helminthic infection rapidly induces a gut-associated elevation of Th2-associated cytokines and IL-3. Journal of immunology (Baltimore, Md. : 1950) *150*, 3434-3441.
Tamura, T., Tailor, P., Yamaoka, K., Kong, H.J., Tsujimura, H., O'Shea, J.J., Singh, H., and Ozato, K. (2005). IFN regulatory factor-4 and -8 govern dendritic cell subset development and their functional diversity. Journal of immunology (Baltimore, Md. : 1950) *174*, 2573-2581.
Taylor, B.C., Zaph, C., Troy, A.E., Du, Y., Guild, K.J., Comeau, M.R., and Artis, D. (2009). TSLP regulates intestinal immunity and inflammation in mouse models of helminth infection and colitis. The Journal of experimental medicine *206*, 655-667.
Taylor, M.D., van der Werf, N., and Maizels, R.M. (2012). T cells in helminth infection: the regulators and the regulated. Trends in immunology *33*, 181-189.
Terrier, B., Bieche, I., Maisonobe, T., Laurendeau, I., Rosenzwajg, M., Kahn, J.E., Diemert, M.C., Musset, L., Vidaud, M., Sene, D.*, et al.* (2010). Interleukin-25: a cytokine linking eosinophils and adaptive immunity in Churg-Strauss syndrome. Blood *116*, 4523-4531.
Turner, J.E., Morrison, P.J., Wilhelm, C., Wilson, M., Ahlfors, H., Renauld, J.C., Panzer, U., Helmby, H., and Stockinger, B. (2013). IL-9-mediated survival of type 2 innate lymphoid cells promotes damage control in helminth-induced lung inflammation. The Journal of experimental medicine *210*, 2951-2965.

Uhlig, H.H., McKenzie, B.S., Hue, S., Thompson, C., Joyce-Shaikh, B., Stepankova, R., Robinson, N., Buonocore, S., Tlaskalova-Hogenova, H., Cua, D.J., and Powrie, F. (2006). Differential activity of IL-12 and IL-23 in mucosal and systemic innate immune pathology. Immunity *25*, 309-318.
Urban, J.F., Jr., Katona, I.M., and Finkelman, F.D. (1991). Heligmosomoides polygyrus: CD4+ but not CD8+ T cells regulate the IgE response and protective immunity in mice. Experimental parasitology *73*, 500-511.
Urban, J.F., Jr., Noben-Trauth, N., Donaldson, D.D., Madden, K.B., Morris, S.C., Collins, M., and Finkelman, F.D. (1998). IL-13, IL-4Ralpha, and Stat6 are required for the expulsion of the gastrointestinal nematode parasite Nippostrongylus brasiliensis. Immunity *8*, 255-264.
Urban, J.F., Jr., Noben-Trauth, N., Schopf, L., Madden, K.B., and Finkelman, F.D. (2001). Cutting edge: IL-4 receptor expression by non-bone marrow-derived cells is required to expel gastrointestinal nematode parasites. Journal of immunology (Baltimore, Md. : 1950) *167*, 6078-6081.
Van de Velde, L.A., Subramanian, C., Smith, A.M., Barron, L., Qualls, J.E., Neale, G., Alfonso-Pecchio, A., Jackowski, S., Rock, C.O., Wynn, T.A., and Murray, P.J. (2017). T Cells Encountering Myeloid Cells Programmed for Amino Acid-dependent Immunosuppression Use Rictor/mTORC2 Protein for Proliferative Checkpoint Decisions. The Journal of biological chemistry *292*, 15-30.
van der Valk, M.E., Mangen, M.J., Leenders, M., Dijkstra, G., van Bodegraven, A.A., Fidder, H.H., de Jong, D.J., Pierik, M., van der Woude, C.J., Romberg-Camps, M.J.*, et al.* (2014). Healthcare costs of inflammatory bowel disease have shifted from hospitalisation and surgery towards anti-TNFalpha therapy: results from the COIN study. Gut *63*, 72-79.
van Kooten, C., and Banchereau, J. (2000). CD40-CD40 ligand. Journal of leukocyte biology *67*, 2-17.
Varyani, F., Fleming, J.O., and Maizels, R.M. (2017). Helminths in the gastrointestinal tract as modulators of immunity and pathology. American Journal of Physiology - Gastrointestinal and Liver Physiology *312*, G537-549.
Vasquez-Dunddel, D., Pan, F., Zeng, Q., Gorbounov, M., Albesiano, E., Fu, J., Blosser, R.L., Tam, A.J., Bruno, T., Zhang, H.*, et al.* (2013). STAT3 regulates arginase-I in myeloid-derived suppressor cells from cancer patients. The Journal of clinical investigation *123*, 1580-1589.
Vely, F., Barlogis, V., Vallentin, B., Neven, B., Piperoglou, C., Ebbo, M., Perchet, T., Petit, M., Yessaad, N., Touzot, F.*, et al.* (2016). Evidence of innate lymphoid cell redundancy in humans. Nature immunology *17*, 1291-1299.
Visekruna, A., Linnerz, T., Martinic, V., Vachharajani, N., Hartmann, S., Harb, H., Joeris, T., Pfefferle, P.I., Hofer, M.J., and Steinhoff, U. (2015). Transcription factor c-Rel plays a crucial role in driving anti-CD40-mediated innate colitis. Mucosal immunology *8*, 307-315.
Voehringer, D., Reese, T.A., Huang, X., Shinkai, K., and Locksley, R.M. (2006). Type 2 immunity is controlled by IL-4/IL-13 expression in hematopoietic non-eosinophil cells of the innate immune system. The Journal of experimental medicine *203*, 1435-1446.

von Moltke, J., Ji, M., Liang, H.E., and Locksley, R.M. (2016). Tuft-cell-derived IL-25 regulates an intestinal ILC2-epithelial response circuit. Nature *529*, 221-225.
Wagner, M., Koester, H., Deffge, C., Weinert, S., Lauf, J., Francke, A., Lee, J., Braun-Dullaeus, R.C., and Herold, J. (2014). Isolation and intravenous injection of murine bone marrow derived monocytes. Journal of Visualized Experiments : JoVE.
Walenkamp, A.M.E., Lapa, C., Herrmann, K., and Wester, H.J. (2017). CXCR4 Ligands: The Next Big Hit? Journal of nuclear medicine : official publication, Society of Nuclear Medicine *58*, 77s-82s.
Wang, S., Xie, Y., Yang, X., Wang, X., Yan, K., Zhong, Z., Wang, X., Xu, Y., Zhang, Y., Liu, F., and Shen, J. (2016). Therapeutic potential of recombinant cystatin from Schistosoma japonicum in TNBS-induced experimental colitis of mice. Parasit Vectors *9*, 6.
Weber, C., Kraemer, S., Drechsler, M., Lue, H., Koenen, R.R., Kapurniotu, A., Zernecke, A., and Bernhagen, J. (2008). Structural determinants of MIF functions in CXCR2-mediated inflammatory and atherogenic leukocyte recruitment. Proceedings of the National Academy of Sciences of the United States of America *105*, 16278-16283.
Weller, P.F., and Spencer, L.A. (2017). Functions of tissue-resident eosinophils. Nature reviews. Immunology *17*, 746-760.
Wildin, R.S., Ramsdell, F., Peake, J., Faravelli, F., Casanova, J.L., Buist, N., Levy-Lahad, E., Mazzella, M., Goulet, O., Perroni, L.*, et al.* (2001). X-linked neonatal diabetes mellitus, enteropathy and endocrinopathy syndrome is the human equivalent of mouse scurfy. Nature genetics *27*, 18-20.
Winner, M., Meier, J., Zierow, S., Rendon, B.E., Crichlow, G.V., Riggs, R., Bucala, R., Leng, L., Smith, N., Lolis, E.*, et al.* (2008). A novel, macrophage migration inhibitory factor suicide substrate inhibits motility and growth of lung cancer cells. Cancer research *68*, 7253-7257.
Wojciechowski, W., Harris, D.P., Sprague, F., Mousseau, B., Makris, M., Kusser, K., Honjo, T., Mohrs, K., Mohrs, M., Randall, T., and Lund, F.E. (2009). Cytokine-producing effector B cells regulate type 2 immunity to H. polygyrus. Immunity *30*, 421-433.
Wong, S.H., Walker, J.A., Jolin, H.E., Drynan, L.F., Hams, E., Camelo, A., Barlow, J.L., Neill, D.R., Panova, V., Koch, U.*, et al.* (2012). Transcription factor RORalpha is critical for nuocyte development. Nature immunology *13*, 229-236.
Wu, Z., Wang, L., Tang, Y., and Sun, X. (2017). Parasite-Derived Proteins for the Treatment of Allergies and Autoimmune Diseases. Frontiers in microbiology *8*, 2164.
Yaddanapudi, K., Putty, K., Rendon, B.E., Lamont, G.J., Faughn, J.D., Satoskar, A., Lasnik, A., Eaton, J.W., and Mitchell, R.A. (2013). Control of tumor-associated macrophage alternative activation by MIF. Journal of immunology (Baltimore, Md. : 1950) *190*, 2984-2993.
Yang, X., Yang, Y., Wang, Y., Zhan, B., Gu, Y., Cheng, Y., and Zhu, X. (2014). Excretory/secretory products from Trichinella spiralis adult worms ameliorate DSS-induced colitis in mice. PloS one *9*, e96454.

Yoshihisa, Y., Makino, T., Matsunaga, K., Honda, A., Norisugi, O., Abe, R., Shimizu, H., and Shimizu, T. (2011). Macrophage migration inhibitory factor is essential for eosinophil recruitment in allergen-induced skin inflammation. The Journal of investigative dermatology *131*, 925-931.
Zaiss, D.M., Yang, L., Shah, P.R., Kobie, J.J., Urban, J.F., and Mosmann, T.R. (2006). Amphiregulin, a TH2 cytokine enhancing resistance to nematodes. Science (New York, N.Y.) *314*, 1746.
Zaiss, D.M.W., Gause, W.C., Osborne, L.C., and Artis, D. (2015). Emerging functions of amphiregulin in orchestrating immunity, inflammation, and tissue repair. Immunity *42*, 216-226.
Zhang, H., Ma, L., Dong, L.Q., Shu, C., and Xu, J.L. (2013). Association of the macrophage migration inhibitory factor gene--173G/C polymorphism with inflammatory bowel disease: a meta-analysis of 4296 subjects. Gene *526*, 228-231.
Zhang, H., Ye, Y.L., Li, M.X., Ye, S.B., Huang, W.R., Cai, T.T., He, J., Peng, J.Y., Duan, T.H., Cui, J.*, et al.* (2017). CXCL2/MIF-CXCR2 signaling promotes the recruitment of myeloid-derived suppressor cells and is correlated with prognosis in bladder cancer. Oncogene *36*, 2095-2104.
Zhang, Y., Chen, L., Gao, W., Hou, X., Gu, Y., Gui, L., Huang, D., Liu, M., Ren, C., Wang, S., and Shen, J. (2012). IL-17 neutralization significantly ameliorates hepatic granulomatous inflammation and liver damage in Schistosoma japonicum infected mice. European journal of immunology *42*, 1523-1535.
Zhao, A., McDermott, J., Urban, J.F., Jr., Gause, W., Madden, K.B., Yeung, K.A., Morris, S.C., Finkelman, F.D., and Shea-Donohue, T. (2003). Dependence of IL-4, IL-13, and nematode-induced alterations in murine small intestinal smooth muscle contractility on Stat6 and enteric nerves. Journal of immunology (Baltimore, Md. : 1950) *171*, 948-954.
Zhao, A., Urban, J.F., Jr., Anthony, R.M., Sun, R., Stiltz, J., van Rooijen, N., Wynn, T.A., Gause, W.C., and Shea-Donohue, T. (2008). Th2 cytokine-induced alterations in intestinal smooth muscle function depend on alternatively activated macrophages. Gastroenterology *135*, 217-225.e211.
Zhao, A., Urban, J.F., Jr., Sun, R., Stiltz, J., Morimoto, M., Notari, L., Madden, K.B., Yang, Z., Grinchuk, V., Ramalingam, T.R.*, et al.* (2010). Critical role of IL-25 in nematode infection-induced alterations in intestinal function. Journal of immunology (Baltimore, Md. : 1950) *185*, 6921-6929.
Zhao, F., Hoechst, B., Duffy, A., Gamrekelashvili, J., Fioravanti, S., Manns, M.P., Greten, T.F., and Korangy, F. (2012). S100A9 a new marker for monocytic human myeloid-derived suppressor cells. Immunology *136*, 176-183.
Zhao, Y., Liu, M.Y., Wang, X.L., Liu, X.L., Yang, Y., Zou, H.B., Sun, S.M., Yu, L., Rosenthal, B., Shi, H.N.*, et al.* (2013). Modulation of inflammatory bowel disease in a mouse model following infection with Trichinella spiralis. Vet Parasitol *194*, 211-216.
Zhao, Y., Zhang, S., Jiang, L., Jiang, J., and Liu, H. (2009). Preventive effects of *Schistosoma japonicum* ova on trinitrobenzenesulfonic acid-induced colitis and bacterial translocation in mice. J Gastroenterol Hepatol *24*, 1775-1780.

Ziegler, S.F., and Artis, D. (2010). Sensing the outside world: TSLP regulates barrier immunity. Nature immunology *11*, 289-293.
Ziegler, S.F., Roan, F., Bell, B.D., Stoklasek, T.A., Kitajima, M., and Han, H. (2013). The biology of thymic stromal lymphopoietin (TSLP). Advances in pharmacology (San Diego, Calif.) *66*, 129-155.
Zigmond, E., Bernshtein, B., Friedlander, G., Walker, C.R., Yona, S., Kim, K.W., Brenner, O., Krauthgamer, R., Varol, C., Muller, W., and Jung, S. (2014). Macrophage-restricted interleukin-10 receptor deficiency, but not IL-10 deficiency, causes severe spontaneous colitis. Immunity *40*, 720-733.